DEVELOPMENT AND ASSESSMENT OF REDUCED ORDER POWER SYSTEM MODELS

by

MAKHETSI FLORA NTEKA

Thesis submitted in fulfilment of the requirements for the degree

Master of Technology: Electrical Engineering

in the Faculty of Engineering

at the Cape Peninsula University of Technology

Supervisor: Prof. R Tzoneva
Co-supervisor: Mr. Carl Kriger

Bellville
Date submitted: July 2013

DECLARATION

I, Makhetsi Flora Nteka, declare that the contents of this dissertation/thesis represent my own unaided work, and that the dissertation/thesis has not previously been submitted for academic examination towards any qualification. Furthermore, it represents my own opinions and not necessarily those of the Cape Peninsula University of Technology.

Signed **Date**

ABSTRACT

The demand for electrical energy has kept on increasing, thus causing power systems to be more complex and bringing the challenging problems of electrical energy generation, transmission, stability, as well as storage to be examined more thoroughly.

With the advent of high-speed computation and the desire to analyze increasingly complex behaviour in power systems, simulation techniques are gaining importance and prevalence. Nevertheless, while simulations of large, interconnected complex power systems are feasible, they remain time-consuming. Moreover, the models and parameters used in simulations are uncertain, due to measurement uncertainty, the need to represent a complex behaviour with low-order models, and the inherent changing nature of the power system.

This research explores the use of a model reduction technique and the applications of a Real-Time Digital Simulator (RTDS) to reduce the uncertainty in large-scale complex power system models. The main goal of the research is to develop a reduced order model and to investigate the applications of the RTDS simulator in reduction of large, interconnected power systems models. The first stage of the study is to build and simulate the full model of the power system using the DigSILENT and RTDS simulators. The second phase is to apply model reduction technique to the full model and to determine the parameters in the reduced-order model as well as how the process of reduction increases this model uncertainty. In the third phase the results of the model reduction technique are compared based on the results of the original model - IEEE standard benchmark models has been used. The RTDS was used for comparative purposes.

The thesis investigations use a particular model reduction technique as Coherency based Method. Though the method ideas are applicable more generally, a concrete demonstration of its principles is instructive and necessary. Further, while this particular technique is not relevant to every system, it does apply to a broad class of systems and illustrates the salient features of the proposed methodology.

The results of the thesis can be used in the development of reduced models of complex power systems, simulation in real-time during power system operation, education at universities, and research.

Keywords: IEEE benchmark models, reduced models, Coherency based Method, DigSILENT, RTDS, model uncertainty, power system stability

ACKNOWLEDGEMENTS

I wish to thank:

- The Almighty GOD, the who has helped me for the completion of this research,
- My great supervisor, Prof. Tzoneva, my co-supervisor, Mr. Kriger for their untiring guidance throughout the research, despite their busy schedules.
- Mrs Matankiso, my lovely mother and Mrs Maselimo Mona, my esteemed aunty for allowing me to embark on this course of study.
- Qelewe, Khotso, Anu, Masechaba, Kenneth, Ganesan, Ogidan, my dear friends, for their prayers towards the success of this project
- Tankiso, Mateboho, Mont'suoe, Maphakiso and Phoka, my siblings for their full support and prayers throughout the course of study.
- Dr. Apostolov, Dr. Paul, Mr Behardien, Mr Xolile, Mr Senthil, Mr Mnguni and Ms Panda, my unforgettable helpers and technical advisers, for linking me up with this great Institution and their timely and elderly advices

The financial assistance of the National Research Foundation towards this research is acknowledged. Opinions expressed in this thesis and the conclusions arrived at, are those of the author, and are not necessarily to be attributed to the National Research Foundation.

DEDICATION

This is dedicated to Almighty God, my lovely mother ‘Matankiso, my beloved nephews Majoro and Moleleki Nteka.

TABLE OF CONTENTS

LIST OF FIGURES

LIST OF TABLES

GLOSSARY

Terms/Acronyms/ Abbreviations	Definition/Explanation
Algebraic Equation	Equation in the form of a polynomial having a finite number of terms and equated to zero
Algorithm	A step -by- step procedure for solving a problem or accomplishing some end, especially by a computer
Aggregation	A process of grouping together things and considering them as a whole
Bus	Electrical wiring in general refers to insulated conductors used to carry electricity, and associated devices.
CEBTREL	Networks of Poland, Czech, Slovak Republics, and Hungary
Complex	Term that is indicating the difficulty of fully understanding of a process characterized by nonlinearities and several interacting variables
Conductor	Metals conduct electricity because electrons are free to move under the influence of an electric field. In liquid solutions, there have to be charge carriers, typically ions (molecules which exist in solution as ionized species) which can move under the influence of an electric field.
Coherency	If a group has coherence; its members can be connected or united because they share common aims, qualities, or characteristics
DISCORE	Software program which computes the distance measures and identifies coherent generators, using only flow data, machine inertias and transient reactance
Dynamic Equivalency	A simplified reduced order dynamic module can be represented by its dynamic equivalence, which represents the entire system, whilst still maintaining all the characteristic behaviour. This is a neat and great way of system simplification.
EISPACK	A software library for numerical computation of eigenvalues and eigenvectors of matrices
Electromagnetic	The ability of an electrical current to displace a magnetic field
EUROSTAG	The renowned software dedicated to the accurate simulation of the dynamics of all electric power systems
GAL RED	The software program used to perform generator bus aggregation

Generator	A machine that converts mechanical energy into electrical energy
Grid	A system of high tension cables by which electrical power is distributed throughout a region power grid, or power system.
GROUP	A clustering algorithm which determines coherent groups based on the computed coherency measure
LIMSIM	Simulation algorithm which allows the maximum and minimum coherency measure to be computed
LODRED &GALRED	Softwares package developed by Podmore and Germond in the mid 1970's and used to produce equivalents for transient stability analysis
LU Decomposition	LU Decomposition of a matrix A is a process of finding a lower triangular matrix (L) and an upper triangular matrix (U) for which A = LU
Model	A usable knowledge based on representation of the essential aspects of an existing system.
Method	The procedures and techniques characteristics, orderly arrangement of parts or steps to accomplish an end
Network	The apparatus, equipment, plant and buildings used to convey, and control the conveyance of, electricity to customers (whether wholesale or retail) excluding any connection assets.
Power System	A network when includes the point where the power is generated to transmission networks up to distribution. A system of high tension cable by which electrical power is distributed throughout a region
Protection System	A system, which includes equipment, used to protect facilities from damage due to an electrical or mechanical fault or due to certain conditions of the power system.
Real-time	Time span from present time to a few minutes ahead
SDEN	the sum of the norms of the sub-matrices of the area
SNUM	the sum of the norms of the sub-matrices of the system matrix
STOT	the sum of **SNUM** and **SDEN**
Reliability	The possibility of a system, performing its function sufficiently for the period of time intended, under the encountered operating conditions
Simulator	A machine for simulating certain environmental and other conditions for purposes of training or experimentation
Simulink	A program developed by Math Works, is a commercial tool for modelling, simulating and analyzing multi-domain dynamic systems

Stability	The quality or attribute of being firm and steadfast, reliable and balanced power system
Synchrony	A natural generalization of coherency, which requires the responses to be identical
Transient	A sudden, brief increase in current or voltage in a circuit that can damage sensitive components and instruments

AC	Alternating Current
AGC	Automatic Generator Control
ANN	Artificial Neural Network
AUEPs	Approximate Unstable Equilibrium Points
BFS	Breadth First Search
CI	Coherency Index
CIRCE	Coherent InfraRed CEnter
COI	Centre of Inertia
C T	Current Transformer
CPUT	Cape Peninsula University of Technology
CRIEPIs	Power System Analysis Tools
CUT	Capacitive Voltage Transformer
DAE	Differential Algebraic Equations
DC	Direct Current
DDL	Data Definition Language
DigSILENT	Digital Simulation and Electrical Network
DNP3	Distributed Network Protocol 3
DPL	DigSILENT Programming Language
DYNAGG	Dynamic Aggregation Algorithm
DYNEQ	Dynamic Equalizer
DYNRED	DYNamic REDuction
DSP	Digital Signal Process
ECPG	East China Power Grid
EMD	Empirical Mode Decomposition
EMF	Electro-Magnetic Force
EMT	Electro-Magnetic Transient
EPRI	Electric Power Research Institute
FACTS	Flexible AC Transmission Systems
FBST	Frequency Domain Stochastic Balanced Truncation
FDNE	Frequency Dependent Network Equivalent
GPC	Giga Processor Card
GUI	Graphical User Interface
HIL	Hardware- In-Loop
HOS	High Order System
HVAC	High Voltage Alternating Current
HVDC	High Voltage Direct Current
IEEE	Institute of Electrical and Electronic Engineers
IMF	Intrinsic Model Functions
IMSL	International Mathematics and Statistics Library
IPFLOW	Internet Protocol Flow
I/O	Input / Output
IRC	Inter-Rack Communication Card
KEPCO	Korea Electric Power Corp (system)
MATLAB	Matrix Laboratory
MFTS	Modified Full Transient Stability
MIPS	Million Instructions Per Second
MMF	Magneto-Motive Force

MPS	Model Power System
NPCC	Northeast Power Coordinating Council (system)
ODE	Ordinary Differential Equations
PC	Personal computer
PEALS	Program for Eigen Analysis of Large System
POSSIM	Power System Simulator Program
PSAPAC	Power System Analysis Package
PSASP	Power System Analysis Software Package
PSAT	Power System Analysis Toolbox
PSS/E	Power System Stability
PG & E	Pacific Gas and Electric Company system
P I	Proportional-Integral
PTDFs	Power Transfer Distribution Factors
PSCAD	Power System Computer Aided Design Software
PSO	Practical Swarm Optimization
PT	Power Transformer
PUB	Public Utility Board of Singapore
RKE	Rate of change of Kinetic Energy
RMS	Root Mean Square
RPC	Risc Processor Card
RTDS	Real-Time Digital Simulator
RSCAD	Real Time Simulation Computer Aided Design Software
ROM	Reduced Order Model
SCADA	Supervisory Control And Data Acquisition
SEL	Schweitzer Engineering Laboratories
SME	Synchronic Modal Equivalencing
SOAR	Second Order Arnoidi Algorithm for model reduction
SSI	Sustainable Sugarcane Initiative
STOT	Specific Target Organ Toxicity
SVC	Support Vector Clustering
TNA	Transient Network Analyzer
TNB	Tenanga Nasional Berhad of Malaysia
TSA	Transient Stability Analysis
VSC	Voltage Source Converter
UCPTE	Union for the Coordination of Production and Transmission of Electricity
UHVDC	Ultra High Voltage Direct Current
WAMS	Wide Area Measurement System
WECC	Western Electricity Coordinating Council (system)
WIF	Workstation Interface
3PC	Triple Processor Card

$\overline{x_i}(t)$	Consists of none of the modes in chord v
n_s	Dimension of the study group variables x_s ;
n_b	Dimension of the basis variables x_b and,
n_z	Dimension of the non relevant variables x_z
B_s	Constraint,
W	The external input directly applied to the system
$R(t)$	The vector of differential variable at time t ,
$S(t)$	The vector of algebraic variables
U_v	The chordal eigenvector
d_{ij}	The synchronic distance of the row i from the row j
a_i	The i^{th} row of U_v matrix

$\|\cdot\|$	The vector norm
$\bar{d}_{ij}$	The degree of synchrony between two generators
ϕ_{ij}	The angle between rows i and j of U_v
Y	– Shunt admittance matrix.
G	– Shunt conductance matrix.
$j\mathrm{B}$	– Shunt reactance matrix.
P_i	The active power of the generator i
jQ_i	The reactive power of the generator i
V_i	The complex voltage of node i
I_i	The complex current flowing out of the generator node i
θ	Angle of the voltages at the buses to which the generators are connected
$\bar{\delta}$	The steady state value of the angle δ
c	Any scalar
β	The voltage angles only at the load nodes.
λ	The finite eigenvalue
$\Re\{V\}$	The real component of voltages at the nodes
$\Im\{V\}$	The imaginary component of voltages at the nodes
A	The state space matrix
x	Denotes the state variable vector
U	A right eigenvector matrix
λ^T	A left eigenvector matrix
λ_E	The element of the left eigenvector
P_{ki}	The participation of the i^{th} mode on the k^{th} variable
u	Denotes eigenvectors associated with eigenvalues
u^c	Denotes the complement of the eigenvector set
δ_G	The vector of generator bus angles,
K_G	The matrix of synchronizing coefficients
Y_{ij}	The admittance of the line
V_i	The voltage at the bus i
V_j	The voltage at the bus j
Δ_u	The small perturbation in the power vector
δ_i	The rotor angle
P_{mi}	The mechanical input power
P_{ei}	The electrical output power
M_i	The inertial constant
$D_i^{'}$	The damping constant
n	The number of generators
ω_i	The rotor speed of the i th generator
f_i	The frequency of the i th generator
$\Delta\delta_i$	The change in the rotor angle
$\Delta\omega_i$	The change in the rotor speed
ΔP_{mi}	The change in mechanical input power
u_i	The i th eigenvector of the matrix A
u_{ij}	The i-th entry of u_i
a_j and b_j	The initial operating conditions coefficients.
θ_{ij}	Represents the vector angle between vectors w_i and w_j

w_i and w_j	Denote vectors.
u_k	Denotes the activity of $k-th$ state variable in the $i-th$ mode
E_i	The (constant) voltage behind transient reactance (PU)
T_{mi}	The (constant) input mechanical torque (PU)
T_{ei}	The electromagnetic torque (PU)
B_{ij}	The $(i, j)th$ entry of the susceptance matrix B
G_{ij}	The $(i, j)th$ entry of the conductance matrix G
H_i	The inertia constant (MW - s/MVA)
D_i	The damping constant (s/rad)
G_i and G_j	The sets having generators coherent with the generators j and i respectively.
L_{ij}	The relation factor
R_{ij}	The relation factor of the machine j towards the machine i
R_{ii}	The self-relation factor
R_{ik}	The relation factor for the machine k towards the machine i
μ_1, μ_2, and μ_3	The weighting coefficients for relation factor error.
Z	The variable whose transients are to be disregarded
X	The remaining variables
r	The invariable input
α_1	The stator flux linkage
α_2	The first rotor circuit flux linkage
x_d	The direct axis reactance
x'_d	The direct axis transient reactance
x'_q	The quadrature axis transient reactance
x_q	The quadrature axis reactance
τ'_{d0}	The direct axis open-circuit sub-transient time-constant
τ'_{q0}	The quadrature axis open-circuit sub-transient time-constant
τ_{d0}	The direct axis open-circuit transient time-constant
τ_{q0}	The quadrature axis open-circuit transient time-constant
E'_{d0}	The direct axis open-circuit transient terminal internal voltage
E'_{q0}	The quadrature axis open-circuit transient internal voltage
I_{q0}	The quadrature axis open-circuit transient current
I_{d0}	The direct axis open-circuit transient current
V_{q0}	The quadrature axis open-circuit transient terminal voltage
V_{d0}	The direct axis open-circuit transient terminal voltage
δ_0	The rotor angle of the generator
E'	The terminal voltage of the generator
Xl	The leakage reactance

CHAPTER ONE
INTRODUCTION

Introduction

The Electrical Energy is the life blood of any modern economy. The demand for electrical energy has kept on increasing, thus causing power system models to be more complex and bringing the challenging problems of electrical energy generation, transmission, transient study, and energy storage to be examined more thoroughly. With the advent of high-speed computation and the desire to analyze increasingly complex behaviour in power system, simulation techniques are gaining importance and prevalence. However, also simulations of large, interconnected power systems are feasible, they remain time-consuming. Models and parameters used in simulations are uncertain, due to measurement uncertainty. The need exists to represent the complex behaviour of power system models with reduced-order models using different model reduction techniques. All the power system research topics involve the study of a wide variety of power system variables with respect to time conditions. These time conditions can be described as follows;

- **Fast transient conditions:** The dimensions of the power system components are no longer negligible.
- **Slowly changing conditions:** in which a power system engineer can control the conditions with a pattern of normal variation of load over time.
- **Transient conditions:** Include electromechanical swingings of machines, and actions of main voltage and speed control of electrical machines.
- **Steady-state conditions:** All the power system engineering quantities and parameters are said to be constant throughout the observation time.

Many power system studies can be done by means of system simulations, specially using Real Time Digital Simulator (RTDS) and those time visions can be easily included in the software which leads a real-time study of power systems if the system model is reduced and enough fast processing capability is available. RTDS can resolve the power system equations quick enough to constantly generate output conditions which practically symbolize conditions in the real-world network. The necessity to explore the use of model reduction techniques to enable RTDS faster simulation process requires further research studies.

The focus of this study is to develop procedures and a technique based on Coherency reduction technique for building of a reduced-order model and to analyze the reduced model simulation results in terms of accuracy to the simulation results of

the full order model. The most accurate results can be highly recommended to the practitioners in the field of power system engineering. Moreover to research on the applications of both Real-time Simulation Computer Aided Design Software (RSCAD) and Digital Simulation and Electrical Network (DigSILENT) software environments in the process of model reduction and to do simulations of both the reduced and full order models is further investigated, in the thesis.

Section 1.1 describes both the reduced ordere model and the idea of dynamic equivalency. Awareness of the problem is presented in section 1.2 and section 1.3 constitutes problem statement. In section 1.4, research aims and objectives are decribed. Section 1.5 offers hypothesis, while sections 1.6 and 1.7 present the delimination and motivation of the reaearch respectively. Moreover, section 1.8 deals with research methodology such as literature review method, design, experiment, and description method. In sections 1.9, 1.10 and 1.11 remarks, contribution and the organization of the thesis are given respectively. Finally, section 1.12 presents the conclusions of the chapter.

1.1 Reduced order model and the idea of dynamic equivalency

A simplified reduced order dynamic model can be represented by its dynamic equivalence, which represents the entire system, whilst still maintaining all the characteristic behaviour (Guruprasada and Yeakub, 1998).This is a neat and great way of system simplification.

The procedure for the construction of a coherency-based dynamic equivalent model engages three fundamental steps: (Olivera and Massaud, 1988; Chow, 1993)

- To identify coherent generators groups;
- Dynamic aggregation of the coherent generating unit models.
- Network reduction

A good understanding of model reduction technique is relevant for studying the effect of uncertainty on it. Coherency method has been chosen as a model reduction technique, and a deep understanding of it has been established with the help of further investigations. This thesis may be of interest to anyone studying the reduced order modelling and dynamic equivalencing of the power system.

1.2 Awareness of the problem

Owing to the outsized of the existing power system network, the computational time required to simulate power system behaviour is extremely high. This simulation, especially the transient behaviour helps in planning and analysis processes.

To reduce possible damage caused by abnormality in the power system, dynamic simulation is necessary in power system design. As the transient analyses and the steady-state analysis of a power system utilize non-linear differential algebraic equations, solving the equation is computationally expensive. That is why a reduced

order model is needed for faster simulations which can be performed by using the best simulator which can produce a quick, consistent, precise, and cost effective study of power systems with compound high voltage networks. That simulator is named Real-Time Digital Simulator which is considerable for two reasons-one can do Hardware In-Loop (HIL) test and is more dynamic by running various studies with real-time simulation quickly (www.rtds.com)

Convergence errors are common during the simulations owing to the large size of the power system modelling data. The concept of reduced-order model and RTDS has been introduced to solve the above described problems. Modelling and computation of large interconnected power systems, distant monitoring and control, and save remote testing of equipments are best examples of numerous feasible functions in which RTDS simulators are advantageous (www.rtds.com).

1.3 Problem statement

The simulations of large, interconnected power systems are feasible, but they remain time-consuming. Additionally, the models and parameters used in simulations are uncertain, due to measurement uncertainty, the need to approximate complex behaviour with reduced-order models and the inherent changing nature of the power system. This research explores the use of model reduction techniques to enable the study of uncertainty in large-scale power system models.

Therefore, the procedure of Model Order Reduction engages learning the parameters of a composite dynamic model in the use for decreasing its complexity, while retaining its input – output behaviour. Due to the practical application bases, one may have to retain assured precise parameters of the large inter-connected complex system into the simple equivalent model. There are many model reduction methods which are compartable enough to detain the important characteristics of the complex system as per the demand of the practical situation (Kokotovic and Sauer, 1989).

1.4 Research aim and objectives

1.4.1 Aim

This research is aimed to develop and assess procedures and a method and algorithms based on Coherency reduction technique for building of a reduced-order model of large complex power systems and investigate on the applications of DigSILENT and RTDS in building reduced models of the power system.

1.4.2 Objectives

The objectives are as follows:

- To conduct literature review on the theory for Reduced-Order Model (ROM) development in power systems.
- To overview the existing methods for model order reduction in power systems.
- To do investigations on RTDS applications in power systems.
- To deveop the Coherency based model reduction procedures, method and algorithms.
- To incorporate DigSILENT simulation in the algorithm of the Coherency method.
- To incorporate RTDS simulation in the algorithm of the Coherency method.
- To compare the simulation results for both full and reduced model.
- To compare the reduced models accuracy of the obtained by the use of DigSILENT and RSCAD softwares.

1.5 Hypothesis

1. The reduced models built on the basis of the method of Coherency are reliable with dynamic behaviour very close to this of the full models.

2. The use of DigSILENT and RSCAD software environments as tools in the process of power system model reduction leads to production of reduced model with very close behaviour to this of the full ones.

3. The use of the RTDS allows the reduced model based simulation of the power system to be done in real-time and applied for management purposes.

1.6 Delimitation of the research

1. The proposed research is to develop and assess procedures, method and algorithms based on Coherency technique for building of a reduced order model of power system. Additionally, to investigate the applications of RTDS simulators in power systems

2. The proposed research uses three software tools which are applied for simulations and calculation during the investigation, namely:

- MATLAB;
- DigSILENT, and
- Real-Time Digital Simulator.

3. IEEE benchmark models, IEEE 14-bus and IEEE 9-bus systems are considered for model reduction purposes.

1.6.1 Assumptions

The coherency equivalent technique is based on identifying the coherent generators by comparison of the generator's rotor angle deviation during an off-line large disturbance condition. If the generator rotor angle deviation curves have highly similarity, the generators can be aggregated as one by modified the generator parameters theoretically. This means the reduction degree is mainly dependent on how many coherent generators can be found. Then, when the generators aggregated in a dynamic way, the bus bars and loads will be aggregated accordingly by equivalent impedance. Consequently, the full order power system which contents many bus bars can be represented as a reduced power system with less Bus bar number.

In order to indentify the coherent generators fast and accurately, there are four basic assumptions for simplify the elements.

1. The coherent group identification is independent on the magnitude of the disturbance. With a certain disturbance the system can be divided into several groups by linearization of the system.

2. The coherent group identification is independent on the detailed model of each generator unit model. Thus, the generator model is expressed by the second-order electromechanical model. The excitation system, driven motor and governor system are neglected.

3. Coherent group identification has negligiable effect on the load.

4. On the assumption that the reactance / resistance ratio is big enough, the active and reactive load flows can be computed independently.

5. RTDS/RSCAD simulations are faster than the DigSILENT simulations

6. Slag generator is considered as the reference generator for calculating swing curves.

7. The buses where there no generators connected can be eliminated.

8. It is possible to linearise the non-linear full model

9. Load buses can be represented by a constant admittance.

1.7 Motivation for the project development

The use of the power system models is increasing because of the high demand for electrical energy in the entire world. The operation of the large modern power system is a complicated multi-faced problem involving a large number of interrelated variables. This adds to the complexity of the problem and the no-linearity of the mathematical equations involved. These mathematical equations include quadratic as

well as trigonometric functions. Nevertheless, it is impractical to use the full model in power system studies because of their size and resultant computational effort. Developing reduced-order models, or dynamic equivalents, is an essential challenge in the study of large interconnected power systems, and it has been conducted in numerous papers (Chow et al., 1984; Troullinos et al., 1988; Troullinos and Dorsey, 1989; Chow et al., 1995; Rasmaswamy et al., 1996; Shuqiang et al., 1998; Hockenberry, 2000)

Therefore, reduced order models are used in power system studies. The investigation of large interconnected power systems is tiresome and expensive as they are normally too complex to be utilized in real-time problems. Power system studies can be performed by means of system simulations, especially using Real-Time Digital Simulator and time vision can easily be included in the software which can lead to a real-time study of power system. RTDS can resolve the power systems equations quicker enough to constantly deliver output conditions. This is the reason why the thesis intention is to do investigations on both methods for building of reduced models and RTDS, which is very important for the power system practitioners.

1.8 Research methodology

1.8.1 Literature review method

- Literature review study of different model reduction techniques.

1.8.2 Design method

- Development and assessment of procedures, methods and algorithms for reduced-order model building and strategies for using RTDS, MATLAB, and Dig SILENT software's environments.

1.8.3 Experimental method

- RTDS, IEEE Power System Model and PC are used for calculations and simulations of both full and reduced model.

1.8.4 Description method

- The power system reduced order model is described with all its specifications, characteristics and functions in power system.

1.8.5 Research statement

Reduced order model is intended to study the character and the dynamic behaviour of a complicated higher order system, and also to copy the important features of this complex system into the reduced order model.

The objectives for applying reduced order models of a higher order power system are as follows:

- Simulation process is much faster than the simulation process of the full order system;
- For improved understanding of the complexity;
- To reduce the computation difficulty;
- To decrease the hardware complexity in realization of the system;
- To impose possible controller design;
- To enable the study of uncertainty in large-scale power system models, and
- To reduce simulation times and to allow the system to be simulated multiple times in a reasonable time-frame.

In order to achieve this goal, model reduction technique was applied. There are many methods for model order reduction described in the literature references. The most used include, Synchronic Modal Equivancing (SME), Coherency based Reduction Method, and Integral Manifold Method. The Coherency based Reduction technique is applied in the thesis to give an idea how good the reduction technique is in power systems.

1.9 Remarks

The literature review shows that in order to achieve model reduction in power system, it is essential to apply the suitable appropriate model reduction technique and the linearization of the full model is the most required. Numerous researchers pointed that it is hard to take a large system model and reduce it to one that can be simulated in real-time (Xi, 2010; Liang, 2011).The literature has failed to approve the most appropriated model reduction technique in the power system engineering studies. That is why further study of applicability of the existing methods is needed.

1.10 Contribution of the Thesis

This thesis constitutes the developments and assessment of the reduced order power system models.It also involves the introduction of common power system model and the generator aggregation algorithm which is appropriate in an advanced context of distributed generation. The major results of this thesis have contribution to many fields of electrical power systems. They are:

- Load flow,
- Transient Stability, and
- Real-time opearation of the power systems

The reduced order model developed utilizing a Coherency based method provides a feasible approach to power system operation, planning, design and control.

The thesis contributions can be concisely outlined as follows:

- Development of IEEE nine bus system model. Bus admittance matrix of the model and its values were prepared and calculated and utilized in load flow analysis.
- Development of constant admittance representation of load code.
- Development of Kron's elimination algorithm.
- Development of Inertial aggregation algorithm.
- Development of decomposition based Gaussian elimination algorithm.
- Reduction of bus admittance matrix of IEEE nine bus model into six bus model.
- Development of IEEE fourteen bus system model. Bus admittance matrix of the model and its values were prepared and calculated and utilized in load flow analysis.
- Reduction of bus admittance matrix of IEEE fourteen bus model into nine bus model.
- Comparison of capabilities of DigSILENT and RSCAD to be applied in the order model reduction process.

1.11 The organization of the thesis

This research thesis structure has been structured as follows;

- Chapter 1 constitutes the introduction of the research, states the problems and aimed possible solution based on the research scope.
- Chapter 2 presents the literature review of the network reduction techniques available in the literature. This is where the comparison between the techniques, the most used network model and the most used software utilized in the literature is dealt with since 1969 till 2012.
- Chapter 3 deals with power system stability, security assessment and the brief introduction of RTDS and its application to power systems.
- Chapter 4 describes the application of coherency based method for IEEE 9-bus system using DigSILENT power factory software package.
- Chapter 5 constitutes coherency based technique applied on IEEE 9-bus system using RSCAD software package in real-time simulation environment.
- Chapter 6 deals with the application of coherency based technique on IEEE 14-bus system using DigSILENT power factory software package.
- Chapter 7 constitutes coherency based technique applied on IEEE 14-bus system using RSCAD software package in real-time simulation environment.
- Finally Chapter 8 presents the overall conclusions and the recommendations for the future research activities on this field of study.

1.12 Conclusions

In conclusions, the research is aimed at developing procedures, method and algorithms for a Coherency based reduced-order model of the large complex power systems model, using the model order reduction technique and at investigating the applications of the DigSILENT and RTDS in power systems order model reduction. Chapter one states the aim and objectives of the research in the thesis. It determines the hypothesis, assumptions and the delimitations of the research work.The document has taken a close at the applications and background of the different model order reduction techniques which have been utilized in the previous researches. The research has indicated the growing interest in terms of simulations process in power system by using RTDS simulator. Moreover model order reduction also makes simulations faster. The proposed research is finally developed a Reduced-Order Model of a complex power system model of IEEE test bench and provided the applications of RTDS in power systems. In addition, the proposed algorithm has been put on test to evaluate its accuracy.

Chapter 2 explores the review of the reduced order models in power systems.

CHAPTER TWO
REVIEW OF REDUCED ORDER POWER SYSTEM TECHNIQUES

Introduction

The order of the power system network and the progressively more harassed circumstances under which power systems drive require utilization of computers for analysis and simulation (www.ipst.org; Shojaei, 2009; Abd-Aal, 2006). Therefore the effect of economizing, or reducing the high order models of large scale power systems plays an important part in simplifying of the high dimensional and with nonlinear loads power system. Hereby reduced models are mainly needed for two reasons: fast calculation of certain characteristics and generation of macro models. The main aim is to retain some physical relationship between the full model with the one of a much smaller dimension according to the following instructions, as follows (Ramaswamy et al., 1997; Hockenbeny, 2000; Jesko, 1997; El-Arini and Fathy, 2010; Prochaska et al., 2005; Pyo et al., 2010; Shaker et. al., 2006; Stankovic´et al.,2003; Wang et al., 2008; Vasilyev and White, 2005; Marinescu et al., 2010; Chang et al., 2000; Marinescu et al., 2010; Ma and Vittal, 2012; Schmieg et al.,1992; Singh et al., 2011; Dukic and Saric, 2012; Chaniotis and Pai , 2002; Guowei, et al., 2010; Tianqi et al., 2009; Zhou et al., 2010; Agrawal et al., 2011; Ghafurian and Siving , 1982; Hiyama , 1981; Zhou et al., 2011; Alsafih and Dunn , 2010; Feng et al., 2011; Zhou et al., 2011; Chen , 2009; Nouri et al., 2013; Agrawal and Dhadbanjan, 2013)

- In the analysis carried out, the reduced model should precisely represent the original one (Agrawal and Dhadbanjan, 2013).
- If the price of developing the reduced model and doing the analysis by means of the original models are compared, the analysis of the reduced models should be the cheaper one (Chaniotis and Pai, 2005; Shaker et al., 2006; Shaker et. al., 2006; Shaker et. al., 2006; Rudnick et al., 1981; Chen , 2009).

Most of physical systems can be explained in terms of differential equations, considered as the mathematical model derived by applying special objective fundermentals or from a sequence of experiments. The mathematical modelling of networks normally delivers differential equations of higher order which are not easy to perform the analysis. Complexity measurement of the system model is considered to be a number of the first order equations used in the description (Hockenbeny, 2000; Jesko, 1997; Chen, 2009).

In power system modelling, the system order provides suggestion of how is the accuracy of the modelling of the system is. For description of the system, the higher the order, the more precise the model is. Nevertheless, in many examples, the quantity of data included in a complex network can confuse easy intelligent behaviours, that can be more effectively captured as well as shown by a network with

lesser order. This is done by approximating a higher order system (www.egr.msu.edu) to an appropriate lower order system; giving possibilities for much better understanding of the system (Hockenbeny, 2000; Jesko, 1997).Model order reduction involves studying the properties of a complex dynamic system in application for reducing its complexity, while preserving its input-output behaviour. In the practical application, one can have to preserve certain special properties of the higher order complex power system into the reduced one. There are a lot of possible captures of the important behaviours of the complex systems as per demand of the practical situation (Hockenbeny, 2000).

Section 2.1 presents the meaning of the reduced order model. In section 2.2, the following points are described:

- Chord
- Synchrony
- Coherency
- Basis generators
- Aggregation of generators

Section 2.3 deals with the problem for model order reductionformulation in Reduced Order Model (ROM). Synchronic Modal Equivalency (SME), Coherency based method, and Intrgral Manifold are discussed in sections 2.4, 2.5 and 2.6 respectifully. Moreover, section 2.7 offers non-linear Decomposition Approach while section 2.8 presents softwares applied for building the ROM. Finally section 2.9 presents the overall conclusion of the whole chapter two.

2.1 What is model order reduction?

Model order reduction is described as an achievement of approximating a higher order system to a suited less order model which has more enhanced understanding of the network. Consequently, the method of Model Order Reduction engages learning the characteristics of a complex dynamic model in order to reduce its complexity, whereas retaining its input-output performance (Brucoli et al, 1988). Practically, the transformation of the higher order complex model into new reduced order model (www.egr.msu.edu) has to preserve the system properties. There are different kinds of model reduction techniques which are flexible enough to capture the important behaviours of the complex system as per demand of the practical situation (Hockenbeny, 2000).

2.2 Why model order reduction?

Definition of important terms used in the model reduction techniques

In this field of study, one needs to understand some of the terminology used by the researchers who have done power system model reduction. Therefore, the following terms must be explained as used in the literature: Ariyo, 2013, states that, Reduced Order Model (ROM) is applicable in situations where there is no need to model the full model in details for specific reasons (Ariyo, 2013).

The reasond are (Ariyo, 2013):

- Calculation times would increase significantly, and
- Situations where it is not desirable to do the studies with the full model.

2.2.1 Chord ν

In (Ramaswamy et al., 1996), it is stated that, a chord is a subset of generators which have exactly or approximately angular variations in invariable percentage for any transition behaviour in which only the modes in ν are excited. It is called ν-synchronic or ν-coherency depending on which technique is used (Jesko, 1997; Ramaswamy et al., 1995). Briefly, (Ramaswamy, 1995) explains the chord ν of a system as a subset of modes or natural frequencies of the system (Ramaswamy, 1997).

2.2.2 Synchrony

Reference (Ramaswamy et al., 1995) constitutes it as the term used for (Singh et al.,2011) two generators(i and j) to be ν synchronic together in chord ν if there is a unique scalar constant k_{ij} in such a way that all the time t their angles $\delta_i(t)$ and $\delta_j(t)$ satisfy $\delta_i(t) = k_{ij}\delta_j(t)$ in response to every initial condition that excites only the modes in ν-synchronic set (Ramaswamy, 1995). In reference to (Marinescu et al., 2010) this is the measure of redundancy in a power system. According to reference (Ramaswamy et al., 1996), synchrony is defined in relation to a selected subset of modes of a linearised model (Jesko, 1997).

2.2.3 Coherency

Coherency of generators is the term used to describe the correspondence of generator responses after subjected to the disturbances (Ghafurian, 1979; Dukic and Saric, 2012; Ma and Vittal, 2005). On the contrary to synchrony, ν-coherency entails the exact or approximate egalitarianism of the angular variations, and the slow-coherency limits ν-coherency to have only the slowest electromechanical modes of

the power system model (Jesko, 1997; Ramaswamy et al., 1996; Ramaswamy, 1995). More, so in reference (Germond and Podmore, 1978; Dukic and Saric, 2012) they have explained it as a coherent group of generating units which oscillate with the same terminal and angular speed in a constant complicated ratio. Coherency detailed conditions are noted in references (Brucoli et.al., 1983; Caprio, 1981; Caprio, 1982; Dorsey and Schlueter, 1984; and Wu and Narasimhamurthi, 1983) for better understanding of the meaning of the coherency.

2.2.4 Basis generators in Synchronic Modal Equivalancy (SME)

A basis generator is normally a reference generator (Dukic and Saric, 2012). These are the generators used to assign every node in the system to a group, so that every node is in exactly one group and every group has exactly one basis generator (Hockenbeny, 2000).

2.2.5 Aggregation of generators in Synchronic Modal Equivalancy method

Partitioning of the whole system consists in, switching from applying the core matrix to applying the extended core matrix at the same operating point. As a result, the big concern is with the model structure of the system and use of generalized eigenanalysis, as opposed to the more familiar regular eigenanalysis. There is a need to group each load and generator with one of the basis generators such that the performance of the generator or load node is well-shown by scalar multiple of the characteristics of the basis generator (Hockenbeny, 2000; Yang et al., 2005).

First, the partitioning algorithm importantly finds one-dimensional synchrony within each group, and minimization of such synchrony between groups. The equivalencing is established on multi-dimensional synchrony. On the contrary, the partitioning algorithm searches for the single basis generator which approximately equals to a specific generator or load node and groups the generators or the load nodes with the basis generator, although the reduced system will be established on symbolizing each non-basis generator and load as a linear group of all of the basis machines in the external area. In the formation of partitioning, the study-area has not yet been discovered, so it is not obvious at the point which of the basis generators will be outside the study-area and which one(s) will be inside the study-area. Practically, under some algorithms, once the study-area is chosen, all other exterior partitions are disregarded. There is only division which is applied between the nodes of the study-area that are exterior to the study-area and the basis generators (Hockenbeny, 2000; Yang et al., 2005). Moreover, another radically dissimilar idea would be to utilize the

local modes to do the partitioning. Normally, this initiative is maybe not practicable but the reduced model requests to preserve the modes local to the (www.pserc.wisc.edu) study-area and the extensive modes of the network. Nevertheless, it is possible that a specific local node dominates for the preferred event and has high degree of partitioning with another node or generator that is grouped external to the study-area (Hockenbeny, 2000; Yang et al., 2005).Secondly, partitioning algorithm presupposes that the desired number of partitions is already known. Obviously, partitioning a system into four groups instead of five groups will have to be the same.

The third and last note is the connectivity of the groups. Each group must be connected which means one could travel along lines in the system from any node in a group to any other node in the same group while only traversing nodes within the same group. For the reason that this connectivity worsens, the number of new lines and current injectors in the equivalent may maximize, thus leads to the less of a reduction (Yang et al., 2005).

Reduced order model is intended to study the nature and the dynamic response of a complex higher order system and (www.egr.msu.edu) also to preserve the important features of this complex system (Schlueter and Ahn, 1979; Cai and Wu, 1986; Chen, 2009).

The reasons for using reduced order models of higher order linear systems are as follows (www.egr.msu.edu):

- Simulation process is much faster than the simulation process of the full order system;
- For greater realization of the complexity;
- To reduce the computation complexity;
- To decrease the hardware complexity in understanding of the system;
- To make possible controller design;
- To enable the study of uncertainty in large-scale power system models, and
- Reduction of simulation times and to allow the system to be simulated multiple times in a reasonable time-frame (El-Arini and Fathy, 2010; Prochaska et al., 2005; Lei et al., 2002; Lihong, 2005; Lee, 2009; Dukic and Saric, 2012; Trudnowski, 1994; Chen, 2009).

This chapter reviews publications period of 45 years from 1968 until 2013. Figure (2.1) depicts graphical comparison on number of publications per year.

For the analysis of the bar-chart in Figure (2.1), from 1968 to 1982, the publication number increasing and then dropping from years 1983 -1985. In the year 1987 only one paper was published. Seven papers were published then four papers were published from 1989 – 1992. The number of published papers is fluctuating between 1993 and 1997. In 1998 it increases to eight papers, then drop to three in 1999 and

2000. From the year 2001, it is increasing gradually until the year 2007 where it decreased to three papers. By the years, 2008, 2010, and 2011 it seems to have the highest number of published papers, while both in 2012 and in 2013 only three papers are published. Appendix H presents the MATLAB code for generationg Figure (2.1).

There are many methods for model order reduction described in the literature. The existing methods, problem formation, standard steps, used software, developed models and the real-time based simulations are presented in Table 2.1 The most used method include Synchronic Modal Equivancing (SME) method, Slow Coherency Reduction (SCR) method, and Integral Manifold (IM) method. These are reviewed in this chapter in order to compare and analyze their characteristics. The theses (Nath, 1985) and (Wang, 1997) contain extra explanation of synchrony, SME, multi-dimensional synchrony, as well as preliminary explorations related to the essential process of identifying dynamic equivalents (Smith et al., 1976). References (Price at el., 1975; Ibrahim et al., 1976; Trudnowski, 1994; Yu and El-Sharkawi, 1981; Djukanovic et al., 1992; Ganapati et al., 1996; Wehenkel, 1995; and Arredondo, 1999) presented different methods of identifying equivalents. What has been considered in this chapter as criteria for comparison of the reviewed methods are: problem formation, algorithms of each method, type of the model used, software used, and whether Real-Time simulation has been used, Table 2.1.

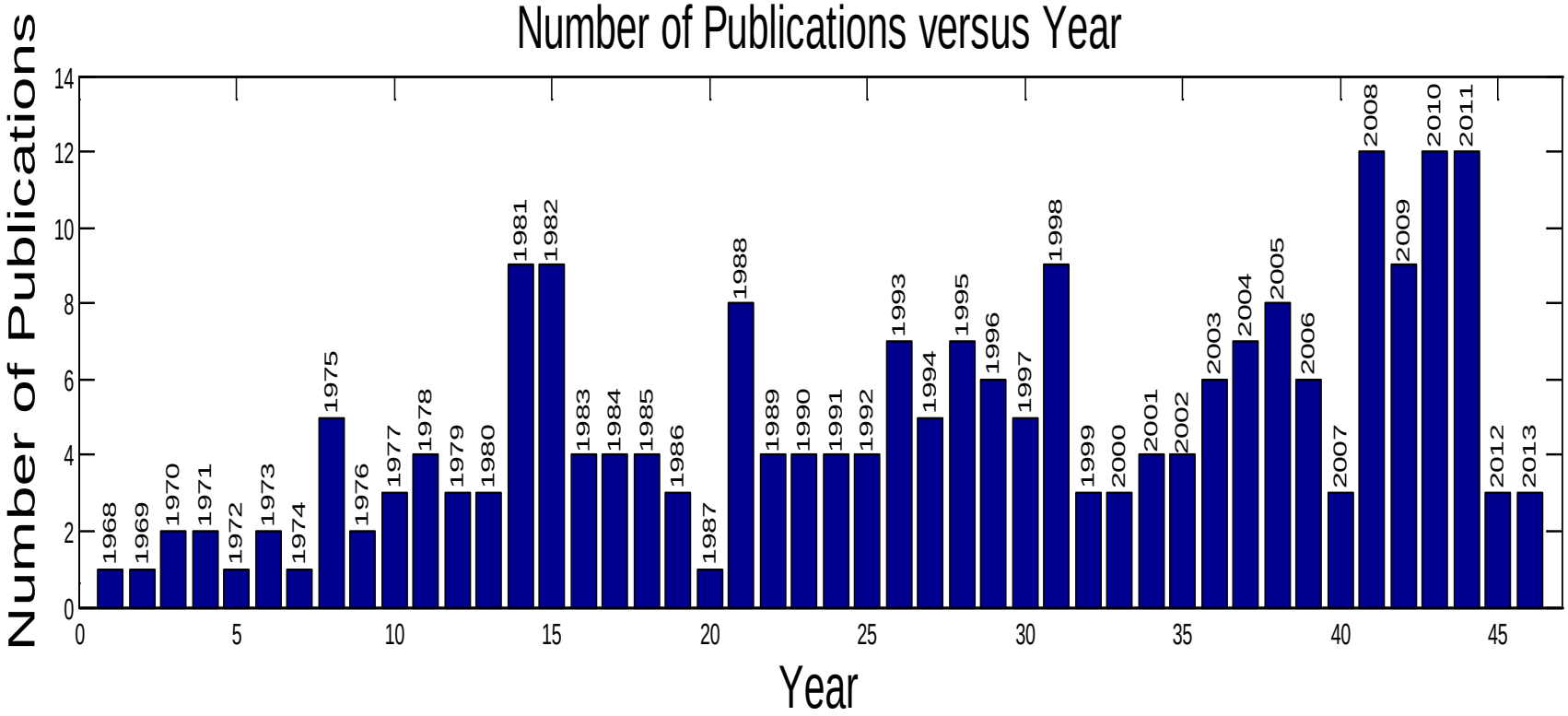

Figure 2. 1: Number of publications versus years

Table 2. 1: Methods, models, algorithms, software, and system used comparison

Paper	Method used	System model	Algorithm	Software used	System used
(Ramaswamy et al., 1997) (Jesko ,1997), (Ramaswamy et al., 1996) (Ramaswamy et al., 1995) (Ramaswamy et al., 1994) (Ramaswamy ,1995)	SME	Swing Equation Model	1.Form detailed nonlinear model and determine its nominal operating point 2. Linearise the detailed model about the operating point. 3. Obtain a simple linearised model of the undamped swing dynamics. 4. Select a good chord, find basis generators and form synchronic group. 5. Select a study group. 6. Impose synchrony-derived structure on the full model. 7. Obtain the form of SME equivalent. 8. Compute the modal correction.	EUROSTAG AND MATLAB	1. France-Spain power system; **83** buses, **23** generators and **476** state variables. 2. New England Model; **10** Generators and **39**-Buses.
(Hockenberry , 2000)	SME	Differential Algebraic Equation	1. Linearization of the original power system model. 2. Ideal simplified model for generator partitioning development. 3. Simplified model extraction and load partitioning. 4. Chord and basis generator selection. 5. Partitioning the system. 6. Study area selection. 7. Generator equivalencing. 8. Network reduction.	EUROSTAG AND MATLAB	**3-** Generators, **9-** Buses, **15**- Lines (b) **7-** Generators, **15-** Buses, **16-** Lines. (c) **262**-Generators, **93**2-Buses, **670**-Lines.
(Chow et al., 1984)	A Sparsity-Based Technique	Linearised electromechanical model	1 .Decide on the desired number of coherent generators.(To simplify the computation, first transform the A matrix into a symmetric Matrix). 2. Perform Gaussian elimination with complete Pivoting (www.pserc.org) to find the set of most linearly Independent number of coherent generators. 3. Compute L form using the LU decomposition of number of coherent generators computed from step 2. 4. Approximate L such that, if the largest positive entry in the i-th row of L is the j-th entry, then the (i,j)-th entry of Lg is 1 and all the other entries in the i-th row iare 0 (www.research.att.com) .	EISPACK	(a) Texas 175-Generators, 1326-buses, 2115-lines. (b) WSCC 411-Generators, 1750-buses, 2800-lines. From U. S Power Systems
(Lawler and Schlueter , 1982)	The RMS Coherency Measure Computational Algorithm	Linearised system model	1. The first step is to show that the expected value of symmetric matrix, evaluated for the probabilistic modal disturbance, is equal to a sum of symmetric matrices for coherent generators evaluated for a particular sequence of deterministic disturbances. The sequence of vectors can be represented as a sequence of deterministic step disturbances in mechanical powers where each generator is in turn, subjected to a disturbance proportional to its inertia. 2. The second step is to show that for each disturbance, in the modal	EPRI	3- Generators, 6-buses, 6-lines

			disturbance sequence, the corresponding symmetric matrix can be determined by the steady state response of the generator rotor angles to the disturbance. 3. Evaluate the steady state deviations in generator angles, corresponding to each disturbance in the modal disturbance sequence. 4. To show that the steady state response of the generator angles to the disturbance can be computed directly from the steady state deviations in generator angles network equations without knowledge of the inertia and synchronous torque matrix. 5. Ensure that, linear algebraic constraints on the generator rotor motions are satisfied at any point in time. The disturbance therefore introduces an excess of Mk units of mechanical power into the system model. 6. Since the deviations in real power generations sum to zero, one row of the network equations is redundant and can be deleted.		
(Ishchenko et al., 2008)	Balanced Truncation Method	Non-Linear state-space model.	1. Linearization of the system model. 2. Define the operating point on the load flow results. 3. Obtain linearised state-space equations in additional form. 4. Introduce the disturbance to the system. 5. Transform the system to a balanced form. 6. Evaluate the Hankel Singular values of the generators. 7. Apply singular perturbation to make accurate responses of the reduced system.		Distribution network with DG **4**- Generators, **11**- Buses, **6**- Lines
(Nath et al., 1985)	Weak coupling factor Approach	Linearised system model	**2n1** is the state of the machines of the first subsystem **2n2** is the state of the machines of the second subsystem S is the coupling factor. **SNUM** is the sum of the norms of the sub matrices of system matrix **SDEN** is the sum of the norms of the sub matrices of the shaded area in Fig.2: System matrix of the paper. **STOT** is the sum of SNUM and SDEN 1. Read the system data of an n-generator System. 2. Form the linearised system matrix. 3. Compute the norms of the sub-matrices 4. Sum up all the norms obtained in step 3 and let this sum be **STOT.** 5. Consider a division of the total system into two subsystems with the first subsystem containing an arbitrarily chosen generator i , so that **nl=l.** The second subsystem contains the remaining **n2=n-1** generators. 6. Initialize the minimum value of the coupling factor to be as minimum value as the value of **STOT.** 7. For the predetermined system division, compute the coupling factor, **S=S (nl)**.		50- generators system

			8. Check whether **S (nl)'<Smin,** if less do step 9, or else do step 10. 9. Reset **Smin=S (nl)** and store corresponding generator number in array L, i.e. **L(nl)=i.** 10. Repeat steps 7 and 8 for all the remaining generators by replacing generator **'i in** the first subsystem with any one generator out of the remaining **n2** generators. Then from step 9 we can identify the generator **L (nl)** for which the minimum value of the coupling factor was recorded. Print **Smin** and **L (nl).** 11. Now consider a total system partition into two subsystems in which the first subsystem consists of generators **L(1), L(2),...L(nl**) that were identified in step 10 together with an arbitrarily selected generator **i'**. 12. Go to Step 6 if **nl<n** and stop if **nl=n.**		
(Winkelman et al., 1981)	Slow Coherency	Nonlinear Model	1a. Computation of basis generators for the slow subspace of matrix A. 2. Gaussian elimination of basis generators matrix **V** 3. Computation of grouping matrix **L** 4. Approximation of dichotomic matrix **Ld** by grouping matrix **L**	EISPACK	NPCC test System, 48 generators
(Joo et al., 2004)	Coherency identification algorithm.		1. Choose the number of coherent groups (Joo et al., 2004). 2. Obtain Matrix A by Linearizing system equations about the initial operating point (Joo et al., 2004). 3. Identification of models which are mostly influenced by state variables. Coherency grouping based on chosen modes. 4. Formation of a normalized row vectors. 5. Randomly form an initial centroid vector at the selected group. 6. Find the closest centroid vector to each vector (Joo et al., 2004). 7. Update the centroid vector. 8. Stop if there is no more reassignment of any generator from one group to another (Joo et al., 2004).	DYNRED, MATLAB, EPRI AND ETMSP	**4**- Generator **11**- Bus and **177**- Generator **779**- Bases System
(Joo et al., 2004)	Slow Coherency (inertial aggregation algorithm)	Classical generator model	1 Compute the voltages of the machine internal nodes (Joo et al., 2004); 2 Create the artificial bus "**p**" (Joo et al., 2004); 3 Add new lines to connect buses "**a**" and "**b**" to bus "**p**" (Joo et al., 2004); 4 Aggregate generator model (Joo et al., 2004); 5 Create a new terminal bus "**q**" (Joo et al., 2004); 6 Adjust generation on buses "**a**", "**b** and "**q**" (Joo et al., 2004).	MATLAB	4-Generators, 11-bus system.
(Nababhushana , and Veeramanju, 1998)	Growing Self Organizing Feature Maps	Power System network admittance matrix	1. The network is a rectangular grid A of the size $k \times m$ units. 2. Choose an input pattern from the training set and find the nearest localized unit and adapt the unit and its neighbors. 3. Insertion of new units: perform a specified number of iterations and determine the unit with largest resource value. 4. Stop the growth process when no unit share more than 36 signal	Not specified	62- Generators, 1000- bus, system.

(Shuqiang et al., 1998)	Fuzzy – C Means	Linearised Power System Model	1. Read the data of the power system. 2. Calculate the admittance matrix reduced to internal nodes of the generators and the synchronizing torque coefficient matrix, form the linearised system state matrix **A.** 3. Form the similarity matrix R 4. Form the fuzzy equivalence relation matrix **R2** 5. Give the coherent coefficient ξ and form the clustering matrix. 6. Recognize the coherent groups. 7. Aggregate the coherent groups into corresponding equivalent generators and form the reduced-order state equation. 8. Calculate the inter-area mode eigenvalues. 9. Reorder the state matrix of the power system according to the coherent groups and form the sub-state matrices. 10. From the sub-state matrices formed in step 9, calculate the local mode eigenvalues.		New England test system, **10** generators, **39** buses and **46** lines
(Gacic et al.,1998)	Epsilon Decomposition	Linear Differential Equations	1. Obtain the matrix $\mathrm{A} = \lfloor a_{ji} \rfloor$, and the value of parameter $\varepsilon \geq \mathrm{O}$. where ε is the specified tolerance. 2. All elements satisfying $\lfloor a_{ji} \rfloor \leq \varepsilon$. 3. Set all elements in step.2 to 0. 4. Permute the resultant matrix into a block diagonal form. 5. All the variables in the same block have to be robustly coupled (Liu, 2009).	Not specified	**(a) NPCC** system with **48** generators and **140** buses, (b) **IEEE 118** bus system with **20** generators
(Haque and Rahim , 1988)	(Slow Coherency)Taylor Series Expansion	Linear Differential Equations	1. Assume a 3-phase fault on a certain bus to be cleared at time t_1 . 2. Obtain relative rotor angles of all generators through Taylor series expansion at t_1 . 3. For each pair of generators in the external system, check for all the criterias and identify all coherent pairs. 4. Identify the coherent group using the criteria that all possible generator pairs in a coherent group are also coherent.		(a) CICRE system **7** -generators **11 -**buses. (b) Bangladesh system **I 1-** generators **33-** buses. (c)New England system **10-** generators **39-** buses. (d) **IEEE** test system **20-** generators **I18-** buses. (e) Iowa system **17**- generators 163-buses.

(Troullinos and Dorsey, 1989)	State-Space Point Of View based on the singular value of the balanced system	State-Space Equations	1. Calculate the matrix of the original system, such that, the size of this matrix is **(N-1)** x **(N-1),** where **N** is the number of generators in the system. Additionally, it can be obtained with simple computational iterations. Therefore, the matrix can be computed for systems that contain as many as 400 or 500 generators or more (www.pserc.org). 2. Calculate the RMS coherency measures using the matrix obtained in step 1. 3. Reduce the system size to approximately 150 to 180 generators by grouping the most coherent generators as determined by the RMS coherency measure. 4. Apply the balanced realizations algorithm to the reduced system. 5. Calculate the singular values of the transformed system. 6. Continue the reduction based on the singular values of balanced system.	Not specified	(a) **240**-generators, **2500** -bus system (b) New England System **10-** generators **39-** buses (c) **254**- generator model of Southern Company and its neighbors
(Chow et al., 1995)	Inertial Aggregation	Linear Internal Node Voltage Equations	1. Computing the voltages of the machine internal nodes. 2. Creating common bus. 3. Adding new lines to connect the buses. 4. Generator aggregation. 5. Creation of another bus. 6. Adjusting generation on the certain buses.	EPRI DYNRED	NPCC **48-** Generators system.
(Troullinos et al., 1988)	Modal- Coherency Method	Linearised steady state model	1. Linearise the model about the steady-state operating point. 2. Assume that the ratio of damping to the inertia is the same for all the generators. 3. Apply a particular disturbance on the system to produce relative inter-generator coherency measure between every pair of generators using global ranking table. 4. Compute the aggregation process to obtain a single equivalent generator. 5. Eliminate the modes of the generators associated with the very coherent generators. 6. Obtain the reduced order model.	Not specified	Southern Company System (a) **86** generator model (b) **254** generators, **2500** buses
(Pai and Adgaonkar, 1979)	Time Domain Simulation	Swing equation of the rotor	**1. Identification of generation of coherent generator group.** The coherency identification technique is based on the fact that some generators tend to swing together following a disturbance in the multi-machine power systems (Yang et al., 2005). **2. Aggregation of generators in the group.** The generators in a group can be aggregated to an equivalent generator, while the generator buses are lumped together to form an equivalent bus. The aggregation of coherent generator buses is based on the Zhukov's method in which each terminal bus is connected through an ideal transformer with complex turns ratio to the equivalent bus (Yang et al., 2005).. **3. Reduction of the network.**	NETOMAC, PSS/E	ECPG System, **2055**-Buses, **2896**-Lines, **469**-Generators, and **874**- Loads.

			The topological reduction method is done by eliminating the selected load buses by performing Gauss elimination operation on the admittance matrix of the external system (Yang et al., 2005).		
(Ourari et al., 2003)	Topological reduction method	Admittance Matrix of power system	1. Perform Time domain simulation with fault applied in the study system (Yang et al., 2005). 2. Determine the coherent generators. 3. Lump the coherent generators in each group into an equivalent generator using the following procedure (Yang et al., 2005): - Rearranging the second row of Admittance Matrix. - Obtain current equation of the retained buses (Yang et al., 2005). - The admittance matrix corresponds to a reduced equivalent network that consists of the retained buses and the equivalent branches linking them (Yang et al., 2005).	PSS/E	The East China Power Grid (ECPG) **2055**-buses, **2896** -branches, **469**-Generators and **874** loads.
(Lee and Schweppe, 1973)	Slow coherency based on Distance Measures (Admittance Distance and Reflection Distance)	Non-Linear swing equations	1. All generators except those in the Inner Circle are marked as eligible. 2. Search for the highest transfer admittance between eligible generators, and the two generators at both ends temporarily become a new group. 3. Calculate Coherency Criteria r1, r2 and r3. If any of the criteria is not satisfied, go to step 6. 4. Among the rest of the eligible generators, find the one which gives the maximum value of r2 if it becomes a member of the group and which meets all the criteria. Include it as a member of the group. If none is found, go to step 7. 5. If all eligible generators are exhausted in step 4, mark the new coherent group as non-eligible and do step 2. Or else go to step 4. 6. Search for the next highest transfer admittance between eligible generators and form a new group. Go to step 3. 7. A new coherent group is found. Mark the generators as non-eligible for further consideration. Go to step 2.	DISCORE program	System consisting of **128**- buses, **253**-lines and **31**-generators.
(Abdul , 2006)	Simple Equivalent	Linear State Matrix Model Of Power Systems	1. Compute the voltages at the nodes. 2. Partition the system into two areas: a Study-area and an External-area (www.pserc.wisc.edu) 3. Obtain the passive network model and the total inertia of the generators (www.pserc.wisc.edu). 4. The two areas must be connected by a boundary bus. 5. Perform system configurations in the study area. 6. The mathematical formulation of equivalent (Abdul, 2006). (Generators which swing together can be lumped together to obtain an equivalent generato) . 7. Network reduction.	Not specified	1.New England 39-bus, 10-generator system 2. IEEE 162-Bus, 17-Generator System

(Wang and Vttal, 2004)	Minimal Cut-set based on tuning indices and Load rich islands	Power Flow equations	1. Based on the Tuning Indices, find the reasonable cut sets for all the generator groups (www.pserc.org). 2. Determine the load rich islands (www.certs.lbl.gov). 3. Consider all those generators in load rich islands as one group, and find out the minimal cut sets for this aggregated group with minimal net flow, which indicates the aggregated islands. 4. Assume that once the minimal cut set for the aggregated group is acquired the optimal cut set for these individual groups can always be found (www.certs.lbl.gov). 5 Calculate the load-generation imbalance within the aggregated islands (www.certs.lbl.gov). 6. Taking other criteria considering restoration into account; based on appropriate priority indices, the islanding procedure can be re-run again with the estimation of the load-generation imbalance within each island (www.certs.lbl.gov).	DYNRED PSAPAC	WECC **179**-Bus, **29**-Generator test system.
(Vittal et al., 1998)	Method of normal forms	Linear System	1. Calculate the Linear Participation Factors. 2. Calculate the second order Participation Factors. 3. Determine the Nonlinear Interaction Index and the associated procedure to determine the critical modes. 4. Determine the Nonlinear Dominance Index. 5. Determine a suitable post disturbance balanced point after the loss of the system. 6. Conduct time simulations on the full model. 7. Indication of the presence of the modes identified in the analysis. 8. The analysis indicates that there is considerable nonlinear interaction between the fundamental modes of oscillation. 9. The generator grouping is established using the nonlinear interactions and the analysis from the method of normal forms.	ETMSP	Manitoba Hydro, 300 -generators and 5000-buses.
(Lim, 2003)	Slow Coherency	Swing Equations for generator	**1. Coherency Identification** - Introduce a disturbance on the system. - Obtain responses of the rotor angles due to the disturbance. - Identify the coherent generators groups by comparing the identical responses of the rotor angles. **2. Generator Aggregation** - Simplify coherent generator groups into single equivalent generator using classical aggregation 3. **Network Reduction** - Obtain the reduced equivalent system using Radial Network Reduction or Loop Network Reduction procedures. The rotor speed and the acceleration of the generator are used to measure the coherency between generators (www.innovexpo.itee.uq.edu.au).	MATLAB Power System Tools Box and EPRI DYNRED.	2-Generators, 4 - Buses System 4 – Generators, 13 -Buses System 16 – Generators, 68- Buses System

(Joo et al., 2001)	Slow Coherency	Swing Equations for Generator	1. Choose the number of coherent groups (Joo et al., 2001). 2. Construct the matrix A from the linearised swing equations. 3. Form a normalized row vector which represents the modal response of generators (Joo et al., 2001) 4. Randomly form a centroid vector. 5. Find the closest centroid vector of each vector by computing the closeness measures between two vectors (Joo et al., 2001). 6. Assign the generator 'i' to the k-th group. 7. In the j-th iteration, update the centroid vector by computing the means of all vectors in the group and normalize it (Joo et al., 2001). 8: Stop if the results from step 7 are accurate. Else do Step 5 and repeat the algorithm (Joo et al., 2001).	The MATLAB Power System Toolbox	The system consists of **48** generators, **140**Buses and **233** transmission lines.
(Hsu and Wu, 1991)	Slow Coherency	Linearised Swing Equations	**1. Coherency Identification** -Integration technique using bilinear transformation to evaluate linearised swing equations. - Elimination of load buses using Gaussian elimination **2. Generator Aggregation** Applying time domain approach using coefficient matrix matching and frequency domain using transfer function matching **3. Network Reduction** Apply current sink reduction technique.	Not specified	Taiwan Power system network 16- Generators, 202- buses, 241-lines.
(Artenstein and Giusto, 2008)	Slow Coherency	Nonlinear Differential Equations and a set of Nonlinear Algebraic Equations	**1. Initial equilibrium point** **-**The equivalent model is computed for an equilibrium point which is obtained by running the load flow module of the PSAT program. **2. Number of coherent areas** -The system can be divided in an arbitrary number of coherent areas or clusters. This number is an important design tool since the performance of the equivalent model depends directly on it. **3. Identification of coherent machines** **-**The identifications of the groups of coherent generators is done through the analysis of the mode shapes such as right eigenvectors, corresponding to each one of the lowest natural frequencies. **4. Equivalent machines** **-**the reduction of the size of the model is done by the creation of equivalent generators which substitute the set of original generators. **5. Coherent area aggregation** **-The following conditions must be considered to select the number of coherent areas** (www.manchesteruniversitypress.co.uk); ▪ The number of coherent areas must be small, for the reason that a relevant reduction of the size of the network can be achieved.	MATLAB with the help of the PSAT	Uruguayan power system 200 -generators, 1800 -buses.

			▪ The reduced model must have a good accuracy. **6. Equivalent network** **-** The substitution of the individual generators in each cluster by the equivalent generator.		
(Krishnaparandhama et al., 1981)	Slow Coherency	Swing Equations for Generator	1. Read in bus data and make bus admittance matrix. 2. Read in bus data. Eliminate load buses and obtain the admittance matrix of the retained network with only generators. 3. Consider a pair of generators in the external system. 4. Compute Coherency Index (CI) of each generator 5. Comparison of the values of CI. If is greater, redo step 6. Or else do step 9. 6. Identify generators having greater value of CI. 7. Provide some tolerance for the approximation. 8. Obtain the value of CI. If greater than the specified tolerance value, go to step 9. 9. If all the pairs of generators in the external area are tested for coherency, go to step 10. Otherwise, consider the next pair generators and go to step 4. 10. Identify the coherent groups of generators from the print out of the coherent pairs in step 8. Obtain the coherent groups. 11. Replace each coherent group by an equivalent generator on the basis of power invariance condition. 12. Obtain the equivalent admittance matrix (Ma, 2012).	Not specified	**12**- Generators, **19**-buses, and **33**- Line System.
(yamagishi and Komami, 2008)	Y-connection method	Power flow equations	**1. Network Aggregation** **-**Preserve original power flow results. -Preserve limits of voltage, transient, and dynamic stability. **2. Aggregation** **-**Observe transient impedance of the subsystem. -Preserve loads stability. **3. Application to loop system.** -This is done by using heuristic cut-and-try procedures. **4. Aggregation of Generating units.** -Generator Aggregation -Exciter aggregation, by making an equivalent weighted average for frequency responses. **5. Aggregation of (Power System Stability) PSS** **6. Aggregation of speed Governor.**	Transient Stability Analysis tool of CPAT (CRIEPI's Power System Analysis Tools)	33- Generators, 31- loads System.
(Izugbunam et al., 2011)	Slow Coherency	Rotor Dynamic Equation	1 Input data for machines with more than 30% Power variation. 2. Perform electrical proximity test to choose coherent generators candidates. 3. Perform the Inertia index for generators check for the coherent group candidates. 4. Evaluate the fault on Damping index for generators, check for	Not Specified	16- generators, 49- bus 330KV Nigeria Power System

			coherent groups. 5. Re-evaluate Post fault γ-index, check for coherent groups. Otherwise, Choose another pair of machines for coherency check and go to step 4. 6. Repeat step 4 after step 5. 7. Coherent generator identification. 8. Construction of dynamic equivalents of coherent generator pairs. 9. Reintegration of the aggregated generators with the rest of system machines.		
(Eduardo Pires de Souza, 2008)	Slow Coherency	Admittance matrix *Y*	1. Apply a disturbance to the system. 2. Run a linear simulation period of 5 seconds. 3. Obtain coherency measure (**C**) in Hertz. 4. Obtain the corresponding coherency quality index. 5. Compute the electrical proximity measure index in percentage for the generators. 6. Obtain coherent generator groups utilizing the index obtained in step5. 7. Eliminate all the buses except generator buses. 8. Reduce the nodal matrix using a sparsity programming and bi-factorization technique on sub-matrix	Not Specified	(a) New England system 10 generators 39-buses, and 46 - lines (b) Brazilian system 133- generators 2808- buses, and 3989-Lines
(Wang and Chang, 1994)	Artificial Neural Network	Power system motion of generators equation	1. Read system data, fault is applied, fault condition, and the number of Study generators. 2. Build the pre-fault, fault-on, and post-fault admittance matrices. 3. Compute the input set of the external generators. 4. Produce the first cluster. 5. Read the input pattern vectors. 6. Read the $i-_{th}$ input set and calculate the Euclidean distance 7. Find the minimum Euclidean distance to the existing clusters, 8. Create a new cluster center if the Euclidean distance in greater than vigilance parameter. 9. If a set of vector changes from the old one to the new one, then modify its coordinates. 10. Repeat Step 6-Step 9 until all the patterns have been compared with the existing clusters; 11. If the clustering process has converged, end; otherwise, return to Step 5.		1.The 10-machine New England system, 2. 34-generators Tai power system
(Senroy, 2008)	Hilbert-Huang Transform	Distorted Signal Equation	1. Identify local maxima and minima of distorted signal 2. Perform cubic spline interpolation between the maxima and the minima to obtain upper and lower envelopes 3. Compute mean of the two envelopes 4. Elimination of the new distorted computation	IPFLOW program in PSAPAC	www.eece.ksu.edu 6- machines 21-buses System.

			5. New distorted wave form is an Intrinsic Mode Functions (IMF) if the number of local extreme of new distorted wave form is equal to or differs from the number of zero crossings by one, and the average of new distorted wave form is zero. If new distorted wave form is not an IMF, then repeat steps 1–4 replacing old distorted wave form by a new distorted wave form until the other new distorted wave form obtained satisfies the conditions of being an IMF. 6. Compute the residue, now the reduced model is obtained.		
(El-Arini and Fathy, 2011) (El-Arini and Fathy, 2010) (Ma and Vittal, 2011) (Wang et al., 2007)	Fuzzy C-Means Clustering	Linear Swing Equation (curves)	1. Construct fuzzy matrix from the coherency measure. 2. Select number of clusters and initialize membership matrix. 3. Start new iterative procedure. 4. Calculate Clusters centres. 5. Compute distances between generators and clusters centres. 6. Update membership matrix. 7. Differentiate between membership matrices less than convergent tolerance of reaching specified iterative time. 8. If step 7 is obtained, go to step 9. Or else redo step 4. 9. Compare convergent matrix. If it is not within tolerance, do step 10. Or else do step 11. 10. Compute the final sampling. If it is not equivalent to the specified value of the sampling instant, go to step 3. Or else, do step 11. 11. Defuzzify membership matrix.	Not specified	(a) A Six-Generator System example from paper **(Wang et al., 2007)** (b) Taipower 23-generator 85-bus System **(El-Arini and Fathy, 2011)** (c)16-generators, 68-buses. (d) IEEE system 20-Generators, 118-Bus **(El-Arini and Fathy, 2010)** IEEE, 5- Generators 14-Bus, system. **(Ma and Vittal, 2011)** The test system comprises 10 generators, 39 buses and 46 lines Taipower 23-generator 85-bus system
(Lei et al., 2002)	Gauss-Newton approach and coherency of the	Linear Active and Reactive Power equations.	1. Identification of coherent generators (Yang et al., 2005), 2. Aggregation of coherent generators (Yang et al., 2005), 3. Construction of a passive network,	NETOMAC	(a) Hydropower stations in an Asian 500 kV grid

	generators.		4. Determination of parameters of aggregated equivalent generators and corresponding equivalent controllers		of the power pool containing about 100 Generators. (b)UCTE/CENTREL, Machines 400, Nodes 2000, Branches 6700
(Pyo et al., 2010)	PAM (Partitioning Around Medoids) algorithm	Dynamic model of generators.	**1. Introduce a fault to the system**. -The rotor angle information obtained from the nonlinear time simulation results and is put into a tabular form in this procedure **2. Define the coherency of each generator** (Pyo et al., 2010)**.** -The initial value of the objective function should be calculated using the generator set. **3. Calculate dissimilarity Index table.** - The swing curves of each generator are to be obtained from nonlinear time simulation response using PSS/E since the system consists of nonlinear models. 2. Build initial generator set M. 3. Swap test between generators of the set M and non medoid set (Pyo et al., 2010). **4. Perform clustering of each generator using optimal medoids set.** **5. Accomplish aggregations of each generator groups**. - Join the buses - Aggregation of the static model of generators and loads - Aggregation of the dynamic model of generators - Aggregation of the control units 6. **Then, network reduction is performed** using static reduction method, such as Ward-PV equivalencing (Pyo et al., 2010).	PSS/E	IEEE 39-Bus system
(Shaker et al., 2006)	Frequency- domain stochastic balanced truncation (FBST)	State-space model	1 Find the left spectral factor. 2. Apply inner-outer factorization and find the left spectral factor $\psi_{(s)}$. 3. Complete the frequency domain controllability Gramain of the (A, B, C,D) system within a frequency bound $[w_1,w_2]$ (www.ijcas.com) 4. Compute frequency domain observability (www.ijcas.com). 5. Find similarity transformation T for stochastically balancing and balance the system stochastically www.ijcas.com). 6. Eliminate the state related to the longest set of the singular values and find reduced system matrices ($A_rB_rC_rD_r$) www.ijcas.com).		CD player Benchmark example
(Lee, 2009)	H∞ control based on dynamic reduction	Dynamic model of generator	1. Linearizing the power system at operating point. 2. Perform simulation for a disturbance on the system. 3. Partition the system. 4. Perform transient stability analysis for disturbances on the system. 5. Calculate the relation indices of generators	PSS	Korea Electric Power Corporation **1095**-Bus **217**-Generators

			6. Select a number reductions group of generators according to the circumstance of the analysis. 7. Dynamic reduction of the generators can be performed using the relation index.		**1705**-Lines
(Stankovic´ et al.,2003)	Artificial Neural Network	Differential-Algebraic Equations (DAEs)	1. Change of the system state. 2. Initial data segment determination. 3. Restore missing measurement. 4. State reduction using Nonlinear Principal components method (bottle-neck ANN) 5. State prediction: To approximate the vector field of the corresponding system of differential equations (recurrent ANN) 6. Prediction system behaviour: Bottle-neck ANN and recurrent ANN outputs are used to predict system behaviour 7. Now, the reduced model is obtained.	DYNRED	WSCC Test system, 46-Nodes, 19-Generators, and 123-Dimensional state vectors.
(Yan and Lam, 1999)	L_2 optical algorithm	Linear time-Invariant system	1. Select a balanced realization of the full-order model and initial projection Matrix. 2. Solve the ODE or the recursive equation with projection Matrix as the starting point to get a suboptimal reduced order model. 3. Construct an induced realization from the current full- order realization and the reduced order realization. 4. If the direct transaction of the induced realization achieves the same cost as the reduced- order model or is unstable, stop; otherwise, go back to step 2 with the induced realization. 5. Obtain the reduced system by using balanced truncation technique.	Not specified	Not specified
(Nath et al.,1985)	Coherency Based System Decomposition	Linearised System Model	1. Read the system data of an n- generator system. 2. Form the linearised system matrix A. 3. Compute the norms of the sub-matrices. 4. Sum up all the norms obtained in 3 and let this sum be Specific Target Organ Toxicity (STOT). 5. Divide the system in two subsystems. 6. Initialize the minimum value of the coupling factor to be S min = STOT. 7. Compute the coupling factor. 8. Check whether the coupling factor is less, go to 9. 9. Reset step 6 and store corresponding machines number in array. 10. Repeat 7 and 8 for all the remaining generators, then from step 9. 11. Identify the generators for which the minimum value of the coupling factor was recorded. 12. Total system partition into subsystems.	UNIVAD 1100/10 digital computer	North region of India 50- Generators 185- buses 180-Lines
(Mallem and	Synchrony-based	Linear state-	1. Synchrony classes	EUROSTAG	European

Marinescu 2010)	border equivalent s method	space Equation	- Generalize slowest modes of the system and work with a specific class modes of interest. This class modes of interest of synchronous generators are the generators which are nearly called class modes of interest only if the changing of their internal angles area approximately equal for any disturbance in which only the modes of interest are excited. 2. Choice of the chord by applying; - Inter-area modes - Border synchrony balanced chord 3. Aggregation of the reduced model 4 Computation of the correction factors		power system **1000**- Generators **6000-** Buses
(Ishchenko et al., 2006)	Balanced Truncations Algorithm	Linear dynamical system in state space form.	1. Find a non singular constant matrix 2. Perform similarity transformation of the system matrices. - The state variables and system matrices are modified, while the inputs and outputs stay the same. 3. Obtain the system in a balanced form. -Controllability and observiability gramians of the new system must be the same. 4. Now, truncation can be done. -Decompose the state variables of the balanced state space system. 5. Select the dimension of the state variable matrix. -This depends on the purpose of reduction. 6. Partition the balanced system using truncation of non-important states. -Set the non-important states to be equal to zero. -Set the non important derivatives of the states to zero. 7. Obtain the reduced system.	MATLAB	**3-** Machine, **11-** buses, Distribution network with Diesel Generator.
(Davodi et al., 2008)	Hierarchical Clustering	The equations of the network for the buses	1. Each generator is placed in one cluster (Davodi et al., 2008). 2. From the total of the clusters, find pairs of the clusters which have the maximum closeness of the coherence measure compared to the other clusters (Davodi et al., 2008) 3. Compute the distance between the new formed clusters and each of the old clusters (Davodi et al., 2008) 4. Repeat steps 2 and 3 till all samples are grouped into single cluster with the size of the certain cluster (Davodi et al., 2008)	Not specified	New England test system
(DeMarco and Wassner, 1995)	Slow Coherency Algorithm for hierarchical Network decomposition.	Differential Algebraic Equations	1. Read the system admittance data and form a matrix. 2. Seek natural boundaries along which the system may be separated. 3. Locate the smallest generalized eigenvelues and associated eigenvectors by using a generalized inverse power method. 4. Calculate the gradient quantity. - Ensure that for each component, the gradient vector must be non-negative.	MATLAB POWER SYSTEM TOOL BOX.	140- bus system

			5. Find the smallest positive real constant such that for some index approach to a value zero. 6. The algorithm will terminate so as to separate the system in a number of iterations that are in the worst-Case bounded by the number of transmission lines in the network. 7. Partition the system into slow and fast sets using singular perturbation technique. 8. Obtain the reduced network.		
(Wang et al., 2008)	Kernel- based clustering algorithm	Linear Swing equations for generators.	1. For a given contingence, a set of coherency measure indices are calculated from conventional time domain simulation. 2. Define affinity matrix K and construct the Matrix L . 3. Treating each row of Y as a point, cluster them into K cluster. 4. Finally, assign the original point to cluster if and only if the matrix Y was assigned to the cluster.	MATLAB	491- Generators 4268- Buses 3597 transmission lines.
(Nilsson and Rantzer, 2009)	Gramian method (discrete- time counterpart of the average gramian method)	Nonlinear discrete time system. - Difference Equations	**1. Linearization along trajectory.** -To Select training input signal. -Input must be selected to obey physical restrictions on the signal and to excite all relevant dynamics. **2. Compute the time varying Gramians.** - For time-varying systems the controllability Gramian can be computed according to the difference equation. -This can be done by applying balanced truncation method procedure. **3. Determine the average Gramians.** - The time-invariant matrices contain information of how strongly the states are connected to the input and output on average over the training trajectory. **4. Find balancing coordinate- change** - This step is done to extract the relevant state subspace using the information gathered in the average Gramians. - Select both Active and Reactive powers as if they belonged to a linear time-invariant system. Follow the balanced truncation method procedure. **5. Truncate states.** - Applying the truncated coordinate change to the original system formulation to give rise to the reduced order system. - Derive the reduced system through symbolical Substitution -This is highly dependent on the format the original model implementation.	MATLAB/ SIMULINK	An engine controller used in current production cars.
(Annakkage et al., 2012)	Coherency-based dynamic reduction	Linearised state-space model	**1. Identification of the groups of coherent generators;** - coherency identification is performed by using the eigenvectors of	DYNRED, PSCAD/EMT	Topology of the distribution test

			the system matrix (Annakkage et al., 2012) 2. Aggregation of the generator busses (Annakkage et al., 2012) 3. Aggregation of generator models and their associated control devices (Annakkage et al., 2012). 4. Reduction of load buses.	DC	system 2- Generators 6- buses
(Choi et al., 2008)	Frequency Domain Based Excitation Model Reduction	Non-linear Exciter model Equations	1. All auxiliary inputs other than terminal voltage are removed. 2. Nonlinearities present in the model such as the exciter saturation function, are linearised around an operating point. 3. All limiters are moved over to the output generator field voltage. 4. Then the linearised model is reduced to a simplified model using a proper reduction method.	Not specified	1. 23-bus, 6-generator system 2. 12,000 bus system.
(Almeida et al., 2010)	Coherency application	State-Space And Linearised Model	1. Start with a certain number of clusters, each containing an eigenvector (Almeida et al., 2010). 2. Compute the similarity between them (Almeida et al., 2010). 3. Find the pair of most similar groups/ clusters and merge them. 4. Recalculate the similarity of the group merged with other groups. 5. Repeat step.3 and step.4 until the similarity is less than the angle of tolerance (Almeida et al., 2010). 6. Now, the reduced model is obtained.	CEPEL, PACDYN, ANATEM, AND ANAREDE	Brazilian National Interconnected System **170**-Generators, **3771**- Buses, **3511**-Lines, and **1924-** Transformers.
(Chia-Chi Chu et al., 1976)	Second-Order Arnoldi (SOAR) algorithm for model reduction	Linear Second-order swing equations	1. Pole location capturing. 2. Obtain frequency response of the system. 3. Time domain simulations verification by means of comparing step responses of a system. 4. Limit the error to 0.0025 rad/s. 5. Compute the reduced system produced by block version of SOAR (BSOAR). 6. Compare the results with both time domain and frequency domain.	Not specified	50- generators 145- bus power system
(Marinescu et al., 2010)	SME	Differential and Algebraic Equation (DAE)	1. Choose the inputs and the outputs of the power system according to the reduction objectives (Marinescu et al., 2010). 2. Select a chord from the transfer matrix from the inputs to the outputs based on the balanced realization. 3. Choose the reference machines which correspond to the chord using the aggregation method based on the Gauss pivot. 4. Reduce the grid (Marinescu et al., 2010). 5. Compute the correction factors as parameters of power injectors for the non-reference machines (Marinescu et al., 2010). Notice that step 4 of the procedure is optional. When used, it is based on a Ward-type reduction. The correction factors of step 5 should in this case integrate supplementary terms for the suppressed lines.	SMAS3 software	The France-Spain Interconnected Systems:
(Ali Asghar Shojaei, 2009)	Truncated balance reduction (TBR)	Lyapunov equations	**1. Enumerate voltages with Internal nodes.** - Join the injection buses, the injection phasors the buses of interest and voltage phasors of the model. **2. Calculate the common bus and new lines to join buses.**	MATLAB	(a) A 2-Bus system with generators and reactance

			3. Create another bus and step generation aggregation. - Calculate the transient and inertia reactance of the corresponding generators. - Transform internal voltages to the general bus voltage. **4. Perform generator aggregation using a software program as follows:** (a) Start program. (b) Request for data file. (c) Check for required data. (d) Check number of generators. (e) Calculate injection current. (f) Calculate average internal voltage. (g) Calculate transfer ratio. (h) Calculate total inertia. (i) Calculate total transient reactance. (j) Calculate average internal voltage. (k) Calculate total bus injection. (l) Calculate line reactance. (m) Illustrate the answers. **5. Obtain the reduced model.**		(b) 3- Generators 4-Buses, 4-Line System.
(Yusaf et al., 1993)	Slow Coherency Decomposition Method	Augmented System State Equation (ASSE)	1. Choose the number of areas, (r) (Carte et al., 2007). 2. Compute the eigenvector matrix U of the (r) smallest eigenvalues. 3. Apply Gaussian elimination with complete pivoting on matrix U to obtain r reference machines. 4. Order the first (r) rows of U (called U,) according to the order found in Step 3 and solve for matrix L(Carte et al., 2007). 5. Use the L matrix to assign other machines to the coherent areas according to the largest entry in each row of L (Carte et al., 2007).	PEALS (Program for Eigen analysis of Large Systems)	39-bus **NPCC** system and the 118-bus IEEE system the TNB (Tenaga Nasional Berhad) of Malaysia and **348-bus,** **77-generators** TNB/PUB **System** the PUB (Public Utility Board) of Singapore
(Chang et al., 2000)	Slow Coherency	Active and reactive Power equations.(eigen value for the jacobian matrix)	1. Generators which generate under 50 MW are substituted for negative load (www.eeserver.korea.ac.kr). 2. The generators are grouped to a coherent group by the specific (www.eeserver.korea.ac.kr) method (the analytic method which is two-time scale method and weak-link method) 3. The generators and their controllers in each coherent group are aggregated to an equivalent generator (www.eeserver.korea.ac.kr). 4. The network is reduced using sub-transmission reduction.	Not specified	The KEPCO system which consists of 237 generators.

(Chen and Bose, 1988)	Adaptive Reduction Method	The real and reactive power flows equations	1. Determine the window of interest. 2. From the window of Interest, define the path. The buses in the path are to be retained. 3. The others are external buses to be eliminated. Find the boundary buses. All buses are now classified as external, boundary **or** internal. 4. Using the fast forward method on the factorized original network matrix, obtain the equivalent reduced network.	Dynamic Reduction Program (DYNRED)	IEEE **118** bus system and a Southwester USA 904 bus system.
(Ma and Vittal, 2012)	Slow coherency based on ANN-Based Boundary Matching Technique	Linear DAEs	1. Initialize the power injections of the ANN-based Equivalent (Ma and Vittal, 2012). 2. Calculate the voltage response in the reduced system with the power injections of the ANN-based equivalent fixed. **3.** Calculate the power injection increments of the ANN-based equivalent (Ma, 2012). 4. Update the power injections of the ANN-based equivalent. **5.** Check for the time instant until which the responses are compared, if is positive, stop, otherwise go to step 1. **6**.Load the power flow and dynamic data into (Ma and Vittal, 2012) DYNRED (all the coherent generators are identified using the weak-link method) 7. The coherent generators are aggregated and replaced by an classic equivalent generator model (Ma and Vittal, 2012) 8. Compute the network reduction and load aggregation. 9. Obtain the reduced system.		

(McCalley, 1993)	EPRI Dynamic Equivalencing Reduction Software)	The nodal Admittance Equation	1. Determine the number of decoupled subsystems comprising a Group (g). 2. Determine the dominating bus *j k* for each decoupled subsystem of the group (g). 3. Compute the impedance of the equivalent connection between the boundary bus and the equivalent bus *e* as the parallel combination of the impedances computed in the last step. 4. Compute *Z,,,* the Thevenin impedances seen looking from boundary bus 2 through the external system to boundary bus, for each pair of boundary buses, with all other boundary bus to external bus connections open. 5. Replace all external buses in the group g with a single equivalent bus connected to each boundary bus through a branch with unknown impedance. 6. For each pair of boundary buses, equate the sum of the two boundary buses to an equivalent bus impedances to the corresponding Thevenin impedances computed in Step 1. 7. The number of equations formed in step 6 must be equal to the number of boundary bus pairs, which are the boundary buses taken 2 at a time.	GALRED, LODRED, Programs	**1696** bus model of the PG&E transmission system representing **1996** summer peak conditions **(HS96)**
(Ma and Vittal, 2011)	Slow coherency	Jacobin matrix	1. Linearize the power system model. 2. Subject the system to the disturbance. 3. Identify generator candidates with large (Ma, 2012) power transfer distribution factors (PTDFs) in the initial external area. 4. Obtain new system condition. 5. Calculate system state matrix perturbation for new operating condition (Ma and Vittal, 2012). 6. Estimate the eigen value solutions and coherency indices for the new operating condition. 7. Retain the critical generators and associated buses in the initial external area and revise the boundary via breadth first search (BFS). 8. Reduce the network and aggregate the coherent generators to form an equivalent system using DYNRED. 9. Obtain the reduced system.	DYNRED	5186-bus representation of a portion of the WECC system
(Chaniotis and Pai, 2002)	Krylov Subspaces Method	Time-Invariant System Equation	1. Construct a base for the Krylov subspace whose eigenvalue behaviors suit the preconditioning analyses. 2. Avoid the ill-conditioning caused by repeated multiplications. 3. Perform moment matching computation (www.pserc.wisc.edu). 4. Replace Krylov subspaces by block-Krylov subspaces to account for the multi-dimensional input and output matrices. 5. Apply Rational Krylov for multiple interpolation points. 6. Eliminate the network algebraic equations. 7. Obtain the reduced network.	Not specified	50-Generators System

(Chang and Adibi, 1970)	Slow coherency	Linear network equation.	1. Simplify the system for transient stability study by replacing all generators and synchronous Condensers less than 50-MVA by constant impedances. 2. Ensure that the initial network voltages, the impedances, and the generators supplied at the same currents to the network. Introduce a disturbance to the system. 3. Identify coherent generators. 4. Aggregate coherent generators in to a single equivalent generator. 5. Obtain the reduced system.	Not specified	118-bus IEEE test system
(Undrill et al., 1971)		Linear Differential Equation	1. The construction of a comprehensive linear differential equation describing the external system. 2. Separation of natural modes of response by transforming the equations into a simplified canonical form. 3. Reduction of the order of the canonical form equations by the deletion of selected natural modes. 4. The integration of the reduced linear differential equation, in conjunction with the nonlinear differential equations of the study system, to run a simulation of the study system as it is' affected by the external system.		New England system
(Undrill et al., 1971)		Linear Differential Equation	1. Obtain base case, faulted case, and post fault load flows for the complete system. 2. Execute a reference simulation of the complete system. 3. Partition the system and obtain base case load flows for each part to match the base case for the complete system. 4. Construct an equivalent of the external area. 5. Execute the combined solution for study area and the equivalent using input conditions identical to those used in step 2. 6. Plot and compare transient responses from step 2 and step 4.		New England system 10 -generators
(Price et al., 1978)	Stability Program Implementation	Linearised State Equations	1. The equivalencing program generates a set of matrices for each external system. 2. The equivalent branches between terminals which are included in the "**D**" matrix from the equivalents are added to the branch admittance tables of the study system. The self admittance elements for the terminal buses are augmented by the diagonal elements of the "**D**" matrix. 3. At every time step during the computation the matrices for each equivalent are rolled into storage and used to update the rate of change of the state variables and the terminal current injections. 4. The injected current at the terminal nodes due to the equivalents are then added into the nodal iterative voltage solution equation for the terminal buses. 5. Obtain the reduced admittance matrix.	A revised version of QUEEQ7 called MADEQ.	48 generators, 136- bus system representative of the major generation and transmission facilities of the NPCC

(Price et al., 1975)	Likelihood Technique	Linear DAEs	1. Read input system data 2. Construct state equation matrices. 3. Compute filter gain covariance matrix 4. Input measurement set 5. Compute like Lihood function 6. Determine new parameter values. 7. Check for like Lihood function 8. Test validity 9. Obtain equivalent.	Power System Simulator Program (POSSIM)	New England Electric System
(Cai et al., 2010)	Empirical Mode Decomposition (EMD)	Discrete Stochastic state space model	1. Find all the local maxima and the minima of the signal. 2. Connect the maxima forming a curve as the upper envelope; repeat the procedure to the minima forming the lower envelope. 3. Identify the mean. 4. Subtract the mean from the original signal, and regard original signal as the new signal to repeat the steps 1-4 until original signal meets the IMF's conditions. 5. Separation of IMF to get the quasi-residue function, Repeat the loop on the quasi-residue until original signal has only one extreme or it becomes monotonous function 1. Read power system data. 2. Obtain generator rotor speed by using Wide Area Measurement System (WAMS) 3. Apply (EMD) to the system. 4. Apply (SSI) to the system. 5. Obtain the phase diagram. 6. Obtain coherent generator.	EPRI	EPRI-36 system
(Tianqi et al., 2009)	Fuzzy Clustering Method based on ART and Kohonen (A-K) Networks		Step1: Give the threshold value, which can control the effectiveness of classification. Step2: Produce the first cluster Step3: Read a new input pattern vectors. Step4: Read the input pattern vectors of a similar pattern vector of the fuzzy similar matrix and calculate the Euclidean distance between the matrix and the centre of the clustering, also the value of weighted parameters. Step5: Find the minimum Euclidean distance to the existing clusters Step6: If Euclidean distance is smaller than the threshold value, the pattern belongs to the cluster, and update the coordinates of the centre of the clustering, also the value of weighted parameters.	Not Specified.	EPRI-36 bus model of PSASP
(Yang et al., 2010)	Slow Coherency	Node Admittance Equations	1. Dividing research area and external system by introducing a three phase short fault lasting for 0.1 seconds. 2. Identification of coherent generator groups by obtaining the rotor angle swing curves of generators in the external system with power	Power system simulator PSASP	EPRI 8-generator 36-bus ac/dc hybrid power system

			system simulator PSASP. 3. Form Bus combination of coherent generators 4. Network simplification 5. Parameter aggregation of coherent generators by using Frequency domain method and weighting method. 6. Obtain the reduced model.		
(Agrawal and Thukaram, 2011)	Slow Coherency based on Support vector clustering (SVC) algorithm	Coherency Matrix	1. Input Data Set 2. Formulate Coherency Matrix 3: Firstly, power angle of the individual generator is obtained through Phasor Measurement Units (PMUs). 4**:** Coherency matrix is formulated using the coherency measure. 5: Value of the kernel parameter is initialized to a minimum value and the soft margin constant is considered as 1. 6: Maximum number of iteration **(N)** is specified with desired kernel parameter step value. 7: SVC algorithm is performed to obtain the number of clusters. 8: Validity measure **(XB)** is computed. 9: If the number of iteration is less than (**N**), then increase the value of the kernel parameter and go to step 3. Otherwise, stop the Support vector clustering (SVC) algorithm. 10: The optimal number of clusters and suitable value of the kernel parameter can be identified, corresponding to minimal validity index. 11. Obtain Clustering Results.	Not Specified	**15**- generators **72**-bus system, an equivalent of Indian Southern grid
(Oirsouw, 1990)	Slow Coherency based on modal coherency and frequency response	Linear Differential Equations	1. Model creation 2. Coherency determination generators rotor angle 2.1 Linearization of the dynamic system 2.2 Diagonalisation of the linearised system 2.3 Frequency response of the diagonalized system 2.4 Evaluation of coherency indices 2.5 Grouping of coherent external units 2.6 Information about coherency is now available: go back to the original non-linear system 3. Aggregation of units within each coherent group into equivalent units 4. Network reduction using standard Ward technique.	Apollo DN330 computer (approx. 1 MIPS), using the IMSL library	The Dutch Power System, which is coupled with the West-European UCPTE Power System. **11**- generator units in the internal and **177** in the external network. The total UCPTE 170 generating units
(Ghafurian and Siving, 1982)	Slow Coherency based	Admittance matrix	1. Subject the system into the disturbance. 2. Identify coherent generators by using angular speed and terminal voltage. 3. Represent each group by a single appropriate equivalent generator. 4. Obtain the reduced model after step3.	Not Specified	**17-** generators, **162-** bus-bars and 284 lines; the second system includes

					12- Generators and **16-** bus-bars.
(Rudnick et al., 1981)	Slow Coherency based on Rate of change of kinetic energy	Kinetic energy equation for a synchronous generator	1. Pre-fault stage system and machine data-input load-flow check. 2. Fault-data input 3. Post-fault network reduction 4. Faulted network reduction 5. Determine RKE(rate of change of kinetic energy) = 0 6. Computation of rotor angles between fault occurrences and fault clearance as a consequence of the integration. 7. RKE calculation with post fault information. 8. Check if RKE magnitude is smaller than (rate of change of kinetic energy) RKEs, otherwise go to step 6. 9. Compare the output of the clearance condition of the RKEs during the fault and after fault clearance. 10. Coherency recognition of groups. 11. Group aggregation - equivalents produced.	Modified full transient stability (MFTS)	**34-** synchronous machines and **250**- bus bars
(Haque and Rahim, 1990)	Slow coherency based on energy function		1. Obtain the tentative coherent generator groups by using indexes. The approximate unstable equilibrium points (AUEPs) required for this computation are obtained. 2. Consider a three phase fault or disturbance at a particular location. Identify the set of generators which are in the vicinity of the disturbance (or in the study system). 3. Identify the final coherent generator groups by checking the relative rotor angle deviations of the pair of generators are equal or smaller than the predetermined quantity among the generators which were found to be coherent tentatively in step 1. Exclude the generators which are in the study system. 4. Obtain the reduced network.	Not Specified	(a)**10**-Generator New England system (b)**11** Generator Bangladesh system **(c)17** Generator Iowa system
(Yang et al., 2011)	Parameter Identification method based on Particle Swarm Optimization (PSO) algorithm	Non-Linear DAEs	1. Read input data 2. Initiate the parameter vector. 3. Calculate the fitness and determine the best fussy extreme and best group extreme. 4. Set k = 0 5. k = k + 1 6. Update the speed and the location of particles. 7. Calculate the fitness and update particular extreme set and group extreme set. 8. Check if k = $k_{\max}$. 9. Obtain the best output group extreme.	Power system analysis software, PSASP	CEPRI 8-machine 36-bus example system

1) The Table 2.1 includes the algorithms of the existing methods for order model reduction.

2) The algorithms are done in a point form, in order to understand better the method.

3) A short presentation of their procedures is done and comparison of their capabilities is done.

4) The methods that are reviewed are:

   - Problem formulation and idea for ROM techniques
   - Synchrony based method
   - Coherency based method
   - Intergral manifold based method
   - Non-linear decomposition methods
   - Software applications for building of the ROM

2.3 Problem Formulation: Idea for model order reduction

The problem for the model order reduction can be formulated in the following ways:

- The full nonlinear model of the interconnected high dimentional power system is given
- Find a reducedorder model of the power system in such a way that the dynamic behaviour of the full and the reduced order models is the same in the framework of some allowed small error.

In order to have an idea for the mathematical aprouch towards the model order reduction, a linerarised version of the non-linear full models is considered.

Linear models of large interconnected power systems can be considered in the following form:

$$\dot{x} = \mathrm{A}x + BW \tag{2.1}$$

where, ,

$A \in R^{nxn}$ is the numerical constant matrix about the operating point.

$B \in R^{nxm}$ is the numerical constant matrix about the operating point.

$W \in R^{m}$ is the vector representing the perturbations of inputs such as load power demand.

$x \in R^{n}$ is the perturbation of the system state.

The reference (Ramaswamy, 1995) used a three generator power system to describe model reduction approach. Suppose, for instance that in a known chord v it is

discovered that there are two unique constants k_{12} and k_{13} so that (Ramaswamy, 1995);

$$x_1(t) = k_{12}x_2(t) + k_{13}x_3(t) \quad (2.2)$$

For all initial conditions in such a way that only the modes within the chord v are excited (Marinescu et al., 2010).

where ;

x_1 is the state variable

x_2 and x_3 are the basis variables

Then, it is assured that, only the initial conditions which excite the variables only in the chord v are considered. It is not essential to keep x_1 in the reduced-order model as long as x_2 and x_3 are retained. This means in practice that the motion of the generator *G1* can be represented by the two generators *G2* and *G3*.

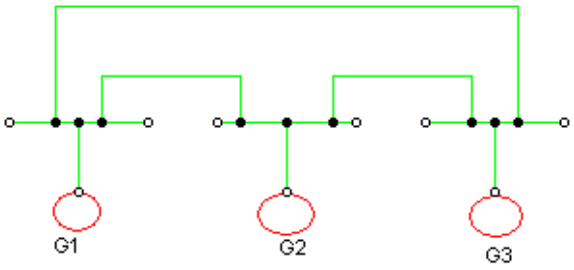

Figure 2. 2: **A 3- Generator power system (Ramaswamy, 1995)**

Figure (2.2) shows a typical three generator power system model. In this case, it can be assumed that x_1 is (x_b, v) - synchrony with respect to basis variables x_2 and x_3 in chord v (Ramaswamy, 1995), where $x_b = [x_2\ x_3]^T$ consists of basis variables x_2 and x_3.

Definition 1: For a system $\dot{x} = Ax$, the state variable x_i is synchronic with respect to the basis variables x_b in the chord v, or is (x_b, v)-synchronic, if there exists a column vector k_{ib} such that, for any initial condition and for all the trajectories $x_i(t)$ and $x_b(t)$ it is satisfied that (Ramaswamy, 1995);

$$\overline{x_i}(t) = x_i(t) - k_{ib}^T x_b(t) \quad (2.3)$$

where, $\overline{x_i}(t)$ consists of none of the modes in chord v. To establish some notation in the case of multi-dimensional synchrony, there are three types of variables:

(a) n_s -study group variable x_s ;

(b) n_b - basis variables x_b and,

(c) n_z - non relevant variable x_z (Ramaswamy, 1996; Ramaswamy, 1995).

Then the system (1) can be presented as follows:

$$\begin{bmatrix} \dot{x}_s \\ \dot{x}_b \\ \dot{x}_z \end{bmatrix} = \begin{bmatrix} \mathrm{A}_{ss} & \mathrm{A}_{sb} & \mathrm{A}_{sz} \\ \mathrm{A}_{bs} & \mathrm{A}_{bb} & \mathrm{A}_{bz} \\ \mathrm{A}_{zs} & \mathrm{A}_{zb} & \mathrm{A}_{zz} \end{bmatrix} \begin{bmatrix} x_s \\ x_b \\ x_z \end{bmatrix} + \begin{bmatrix} \mathrm{B}_s \\ 0 \\ 0 \end{bmatrix} W \tag{2.4}$$

where, $\mathrm{A}_{ss} \in R^{n_s x n_z}$, $\mathrm{A}_{sb} \in R^{n_s x n_b}$ $\mathrm{A}_{sz} \in R^{n_s x n_z}$, $\mathrm{A}_{bs} \in R^{n_b x n_s}$, $\mathrm{A}_{bb} \in R^{n_b x n_b}$, $\mathrm{A}_{bz} \in R^{n_b x n_z}$, $\mathrm{A}_{zs} \in R^{n_z x n_s}$, $\mathrm{A}_{zb} \in R^{n_z x n_b}$ $\mathrm{A}_{zz} \in R^{n_z x n_z}$, B_s is the constraint matrix, and W is the external vector input directly applied to the system .

The relevant variables x_r can consist of the study-group variables and the basis variables, and can be written as;

$$x_r = \begin{bmatrix} x_s \\ x_b \end{bmatrix} \tag{2.5}$$

$$\dot{x}_s = \hat{\mathrm{A}} x_S + \hat{\mathrm{B}} W \tag{2.6}$$

According to (Ramaswamy, 1995; Ramaswamy, 1996), $\hat{\mathrm{A}}$ was chosen to retain the relevant modes because of the modal-based approach applied. Thus leads to impose a constraint:

$$\hat{\mathrm{B}} = \mathrm{B}_s \tag{2.7}$$

Need to find a mathematical dependence between the non-relevant variables and the basis variables in order to represent the non relevant variables by the basis ones. It is proposed a special matrix K to be considered to express this connection. K can be assumed to be in the following structure (Ramaswamy, 1995),

$$\mathrm{K} = \begin{bmatrix} 0 & k_b \end{bmatrix} \tag{2.8}$$

,so that the matrix k_b satisfies;

$$x_z = k_b x_b \tag{2.9}$$

From Equation (2.4), the description for the reduced order system can be represented by substituting Equation (2.5) in Equation (2.4), then the reduced-order model can be found as (Ramaswamy, 1996; Candas, 1996; Bruce, 1981; Nath and Rao, 1985):

$$\begin{bmatrix} \dot{x}_s \\ \dot{x}_b \end{bmatrix} = \begin{bmatrix} \mathrm{A}_{ss} & \mathrm{A}_{sb} + \mathrm{A}_{sz} k_b \\ \mathrm{A}_{bs} & \mathrm{A}_{bb} + \mathrm{A}_{bz} k_b \end{bmatrix} \begin{bmatrix} x_s \\ x_b \end{bmatrix} + \begin{bmatrix} \mathrm{B}_s \\ 0 \end{bmatrix} W \tag{2.10}$$

The algorithm of this example can be considered further as a part of the coherency based method.

2.4 Synchronic Modal Equivalencing (SME) method

SME is described as a method for reducing the order of dynamic models that is based on synchrony of the generators. The following procedures were used to achieve the model order reduction:

- Generator partitioning,
- Selection of study area,
- Modelling of the less-relevant non-basis generators in the external areas as dependent current sources.
- Equivalence of the load buses into current sources (Jesko, 1997).

(Ramaswamy et al., 1995) proposed SME method based on synchrony and modal equivalencing. Modal analysis is also another concept in model reduction as it is presented in references (Undrill et al., 1971; Price et al., 1978; Martinset al., 1996; Martins and Quintao, 2003; and Verghese et al., 1983). Algorithms for developing an operative dynamic equivalencing were also implemented in (Dukic and Saric, 2012).

Reference (Hockenbeny, 2000) explained that SME is a heuristic technique for dynamic equivalancing of power grids. This is a modal-based structure of the linearised power systems for grouping the system nodes. It is also stated that, even though SME has some drawbacks, it has features which make it appealing on uncertainty analyses (Hockenbeny, 2000). This technique is also easily extended and used on nonlinear models.

Nevertheless, most power system models do exhibit structure which can be guaranteed to approximately compensate the requirements for the supporting theory, in that way the algorithm is absolutely not without basis (Hockenbeny, 2000). Moreover, the original and the reduced models might be either linear or non-linear. The non-linear ones must be linearised first due to the fact that, the theorems of the methods are based on a linear system analysis (Hockenbeny, 2000; Jesko, 1997). SME is a method of reducing model order and is based on the motion of synchrony, a more general concept than a slow coherency. The difference between slow coherency and synchrony are: SME requires only the motion of each bus in an area to be linear combination of the motion of a set of basis generators in the area and its chord is more general than in the slow coherency (Jesko, 1997). It does not require identical motion of the buses when only the slowest modes are excited. The SME partitioning method is tied very closely to the eigenstructures of the system. Buses are grouped according to the degree of the synchrony they have with a chosen set of basis machines. Slow coherency is motivated by the weakly-coupled, multi-area swing model (Hockenbeny, 2000; Jesko, 1997; Ramaswamy, 1995)

According to reference (Hockenbeny, 2000) generators can be partitioned into study areas, and the less-relevant generators. The non-basis generators in external areas

are modeled as dependent current sources, driven by the motions of the basis generators (Ramaswamy et al., 1997; Undrill and Turner 1971; Lee, 2009; Ram et al., 1985).Load buses which are only connected to each other and to less-relevant generators are named less relevant load buses, and these can also be equivalent to the current injectors. The necessary extensions are required to group load buses as well as generator buses. The presentation here borrows heavily from all the related possible sources, more especially recommended in (Ramaswamy et al., 1997; Hockenbeny, 2000; Ramaswamy et al., 1996; Wang et al., 1997and Undrill and Turner 1971).

SME uses the method of modal structure or linearization of the system in order to group the system according to the selected groups to produce a study area; all other groups will be replaced by significantly smaller equivalents (Ramaswamy et al., 1997; Hockenbeny, 2000; Jesko, 1997; Ramaswamy et al., 1996; Ramaswamy, 1995).

2.4.1 Standard steps for Synchronic Modal Equivalencing (SME) method

Reference (Ramaswamy et al., 1996) recommended the following steps for the SME procedures.

Step 1: Structure a detailed nonlinear model and discover its nominal equilibrium. The full detailed model of a large power system typically is constructed in the form of a system of differential-algebraic equations whose structure reflects the system;

$$\begin{cases} R(t) = f(R(t), S(t) \\ 0 = g(R(t), S(t)) \end{cases} \quad (2.11)$$

where; $R(t)$ is the vector of differential variable at time t, and $S(t)$ is the vector of algebraic variables (www.archives.ece.iastate.edu). The application of a standard steady-state analysis leads to the constant solutions; $R(t) = \overline{R} \quad S(t) = \overline{S}$

The accepted model for the application of the SME method is the linearised undamped swing-equation model known as classical model. It can be used to partition the system into groups (Hockenbeny, 2000; Jesko, 1997). The detected model of the power system is given by the swing equation

$$M\ddot{\delta}_i = P_{mi} - P_{ei} \quad (2.12)$$

where the load equations are cut (suppressing load buses)

M is the diagonal matrix of generator inertias.

P_{mi} is the vector of the mechanical input power to each of the generators.

P_{ei} is the vector of electrical output power of each of the generators.

δ_i -is the vector comprising the generator's internal angle deviations from a synchronously rotating reference frame.

The following assumptions are done

P_{mi} is a constant.

The Loads are represented by impedances after the load buses are eliminated

Then reference (Hockenberry, 2000) has given the admittance matrix of the system as

$$Y = G + jB \tag{2.13}$$

where

Y – Shunt admittance matrix.

G – Shunt conductance matrix.

jB – Shunt reactance matrix.

Equation for the reactive and real power for node in a n generator unit is:

$$P_i + jQ_i = V_i I_i \tag{2.14}$$

where

jQ_i is the reactive power of the generator.

V_i is the complex voltage of node i.

I_i is the complex current flowing out of the generator node i. Then it can be written

$$I_i = \sum_{j=1}^{n} Y_{ij} V_j \tag{2.15}$$

Using equations (2.13) and (2.14) it can be obtained;

$$P_i = |V_i|^2 G_{ij} + \sum_{j=1,\, j\neq i}^{n} |V_i||V_j|\left(B_{ij} Sin(\theta_i - \theta_j) + Q_{ij} Cos(\theta_i - \theta_j)\right) \tag{2.16}$$

Where;

$$Q_i = -|V_i|^2 B_{ij} + \sum_{j=1,\, j\neq i}^{n} |V_i||V_j|\left(G_{ij} Sin(\theta_i - \theta_j) - B_{ij} Cos(\theta_i - \theta_j)\right) \tag{2.17}$$

where,

θ - angles of the voltages at the buses to which the generators are connected.

Step 2: Linearisation about the operating point. Since the models for most power system components are analytically specified, this step deals with the elimination of the perturbations in all variables except the bus voltages.

Normally the linearised system is in the form of a set of linear differential algebraic equations (DAE), (Smith, 1976; Schlueter and Ahn, 1979), where the differential variables correspond to generators as well as loads which are modeled dynamically.

The algebraic variables are typically voltages and currents which describe the interconnections in the system. These equations will be used to extract a simplified model and its eigenvalues, as well as eigenvectors are calculated (Hockenbeny, 2000).

After linearization with respect to the internal angles and the voltage magnitudes and elimination of the reactive power equations, the linearised model is:

$$M\ddot{\Delta}\delta = C_1\Delta\delta + C_2\Delta\delta|V| \tag{2.18}$$

$$0 = C_3\Delta\delta + C_4\Delta\delta|V| \tag{2.19}$$

where

$$(C_1)_{ij} = \left\{ \overline{|V_i|}\,\overline{|V_j|}(B_{ij}\cos(\overline{\delta_i} - \overline{\delta_j}) - G_{ij}\sin(\overline{\delta_i} - \overline{\delta_j}) - \sum_{k=1,k\neq i}^{n}(C_1)_{ik} \right\} \tag{2.20}$$

$$(C_2)_{ij} = \begin{Bmatrix} -\overline{|V_i|}(B_{ij}\sin(\overline{\delta_i} - \overline{\delta_j}) + G_{ii}\cos(\overline{\delta_i} - \overline{\delta_j})) - 2\overline{|V_i|}G_{ij} \\ -\sum_{k=1,k\neq i}\overline{|V_k|}\left(B_{ik}\sin(\overline{\delta_i} - \overline{\delta_k}) + G_{ik}\cos(\overline{\delta_i} - \overline{\delta_k})\right) \end{Bmatrix} \tag{2.21}$$

$$(C_3)_{ij} = \left\{ -\overline{|V_i|}\,\overline{|V_j|}(G_{ij}\cos(\overline{\delta_i} - \overline{\delta_j}) + B_{ij}\sin(\overline{\delta_i} - \overline{\delta_j})) - \sum_{k=1,k\neq i}^{n}(C_3)_{ik} \right\} \tag{2.22}$$

$$(C_4)_{ij} = \begin{Bmatrix} \overline{|V_i|}(G_{ij}\sin(\overline{\delta_i} - \overline{\delta_j}) - B_{ij}\cos(\overline{\delta_i} - \overline{\delta_j})) - 2\overline{|V_i|}B_{ii} \\ +\sum_{k=1,k\neq i}^{n}\overline{|V_k|}(G_{ik}\sin(\overline{\delta_i} - \overline{\delta_k})) - B_{ik}\cos(\overline{\delta_i} - \overline{\delta_k}) \end{Bmatrix} \tag{2.23}$$

where, $\overline{\delta}$ is the steady state value of the angle.

The resulting C_i matrices are as follows;

C_1 is now symmetric and C_4 can be assumed as being symmetric which makes

$$C_2 = cC_3^T \tag{2.24}$$

where, c is any scalar.

Under the further conjecture that all of the voltage magnitudes are equal, C_4 can be denoted as being symmetric and both C_2 and C_4 can be obtained in the following form:

$$(C_4)_{ij} = \overline{|V_1|}^2 (C_2)_{ji} = \left\{ -\overline{|V|}^2 B_{ij}\sin(\overline{\delta_i} - \overline{\delta_j}) - \sum_{k=1,k\neq i}^{n}(C_3)_{ik} \right\} \tag{2.25}$$

It has been stated that it is always assumed for approximate decoupling between (P,δ) and ($Q|V|$).

Step 3: Obtain a straightforward linearised model of the undamped swing dynamics. This step concerns the formation of the core models of the system and to know the order of the models which is said to be equivalent to the number of generators of the network.

The creation of a model with one variable per generator can be done by defining a matrix F as follows (Hockenbeny, 2000):

$$F = C_1 - C_2 C_4^{-1} C_3 \tag{2.26}$$

$$M\Delta\ddot{\delta} = F\Delta\delta \tag{2.27}$$

$$\Delta\delta = M^{-1}F\Delta\delta \text{ , or } (M^{-1}F\Delta \mathrm{I})\Delta\delta = 0 \tag{2.28}$$

$M^{-1}F$ is called core matrix which was used to select the chord, the basic generators and to do partition of the remaining generators (Hockenbeny, 2000).

The following assumptions were done in the derivation of (2.26 -2.28) according to the reference (Hockenbeny, 2000):

- With an assumption of G being equivalent to zero even though this is certainly reasonable for the transmission lines, where inductance is larger than the conductance, this is not easy to proof for the loads (Hockenbeny, 2000).
- F is symmetric and has zero eigenvalues with a corresponding right eigenvector of all ones, which is not difficult to be verified by noting that C_1 and C_3 have the property that every row in the matrix sums to zero; consequently, $M^{-1}F$ also has these properties (Hockenbeny, 2000; Chow et al., 1983).
- The load conductance terms appear not only on the diagonal of G but also in the off-diagonal terms because the nodes without generators have been algebraically eliminated using a standard Ward-type reduction (Yang et al., 2006).

Step 4: For the straightforward model, choose a good chord, locate basis generators for one-dimensional synchrony, and develop synchronic groups. Reference (Ramaswamy et al., 1997) noted the following procedures to implement this step:

- Selecting a good chord
- Recognizing synchrony,
- Finding basis generators,
- Choosing the number of groups, and
- Forming synchronic groups,

The selection of chord can have a major overall impact on the process of reducing the model order. SME is the latter form of a model reduction technique and key part of defining what system behaviour to be retained. In the reference (Hockenbeny, 2000), it is assumed that, the system modes can be divided into extensive and local modes. The chord can be selected in such a way that it has the most essential of the extensive modes of the system. Any generator in the system considerably contributes in the extensive mode (Yang et al., 2005).

Firstly, the zero-mode is widespread by referring to the form of the connected right eigenvector. Although, applying the right eigenvector is absolutely relevant, some crises with this approach are real. Most essentially, the right eigenvector was discovered as a generating unit dependent (Hockenbeny, 2000).As a result, right eigenvector has the characteristics as follows:

- Generating units of the corresponding variable in the system
- The non scale-invariant shape

Another possibility is the participation factors (Verghese et al., 1982).

Participation factors are realistic, scale-invariant substitute to right eigenvector entries. Participation factors can be defined and their relations to eigenvector can be brought out (Verghese et al., 1982). The following state-space model can be examined for this purpose:

$$\dot{x} = \mathrm{A}x \tag{2.29}$$

Where, A is the state space matrix.

x denotes the state variable

The right and left eigenvector matrices are:

$$U = \begin{bmatrix} 1 & & 1 \\ U_1 & \cdots & U_n \\ 1 & & 1 \end{bmatrix} \tag{2.30}$$

$$\lambda^T = \begin{bmatrix} & \lambda_1^T & \\ \cdots & \vdots & \cdots \\ & \lambda_n^T & \end{bmatrix} \tag{2.31}$$

where , U is the right eigenvector matrix.

λ^T is the left eigenvector matrix.

And $w^T V = I$ (2.32)

Where:

V is the column for the right eigenvectors of the model matrix

w is the column for the left eigenvectors of the model matrix

The system response to the initial condition $x(0)$ is easily written in terms of eigenvectors and eigenvalues (Date and Chow 1991; DeMarco and Wasser, 2005).

$$x(t) = \sum_{i=1}^{n} w_i^T x(0) V_i e^{\lambda(it)} \tag{2.33}$$

λ is the element of the left eigenvector

$x(0)$ can be restricted to be the k_t standard unit vector which means it has all elements equal to zeroes except the entry k. Therefore, a description of the system response to the initial disturbance of variable k;

$$x(t) = \sum_{i=1}^{n} ((\lambda)_i^T) k(V_i) k_i e^{\lambda(it)} \tag{2.34}$$

Participation of the i^{th} mode on the k_t variable can be described as P_{ki}:

$$P_{ki} = (\omega_i^T) k(V_i) k = \lambda_{ki} U_{ki} \tag{2.35}$$

For the normalization of the eigenvectors, the participation factors are corresponding to a particular variable sum to (Date and Chow 1991; DeMarco and Wasser, 2005).

$$\sum_{i=1}^{n} P_{ki} = \sum_{k=1}^{n} P_{ki} = 1 \tag{2.36}$$

Moreover, for a symmetric matrix A, the participation factors are presently the squares of the entries in the right eigenvector matrix. Generally, the participation factors can be positive, negative or even complex. The mode can only be extensive on the condition that, the participation factors are evenly distributed over all the variables. Therefore, this approach can be called variance of participation factors approach. The magnitudes of the participation factors for every mode are then renormalized and calculation of the sample variance of the results can also be done. As a result, if the sample variance is low, the conclusion is made that the mode is extensive since that selects a mode with approximately equal participation from all the variables. The above examination was conducted in the reference (Hockenbeny, 2000) in order to describe the participation factors and to give their relations to eigenvectors in a simple state-space model form in the Equation (2.35).

After the selection of the chord, the next procedure is to choose a set of basis generators by applying only the dynamics described by the modes. For that reason, the modes of the system can be split into approximately two groups which are extensive and local groups. When creating the equivalent, the aim is to retain the local modes which are local to the study area; the reduction is perfectly a consequence of disregarding all of the other local modes. Basis generator selection

can be done such that the response of any other generator within the system can be described as a linear mixture of the responses of the basis generators. In accordance to the reference (Hockenbeny, 2000), all the non-basis generators exhibit synchrony in relation to the basis generators. Reordering the right eigenvector matrix in such a way that the modes in the chord appear first, then the modes can be easily alienated as the following (Hockenbeny, 2000):

$$U = U_u \left| U_{u^c} \right. \tag{2.37}$$

where,

u - denotes eigenvectors associated with eigenvalues

u^c - denotes the complement of the eigenvector set.

The thesis, (Hockenbeny, 2000) described very well the algorithm for selecting basis generators. First, the algorithm seeks basis generators whose corresponding rows in U_u are as mutually orthogonal as possible. Secondly, the basis generators selected by the algorithm have large participation in the chord (Hockenbeny, 2000)

Step 5: Choose a study group. Selection of a study group consideration includes any generators which are able to be disturbed. The good choice of study group may not be evident.

It was already mentioned earlier that, the generators are partitioned into areas in order to perform the equivalence in SME (Ramaswamy et al., 1997; Lawler and Schlueter, 1982; Ramaswamy et al., 1996; Mallem and Rouco, 2010). (Ramaswamy et al., 1997; Jesko, 1997; Chow, 1982; Ramaswamy et al., 1995; Ramaswamy, 1995; Whang, 1982; Candas, 1996).

1. The chord v is selected by using the sequential procedures. To start, two modes of the model are selected. These initial modes normally consist of the zero modes and another extensive mode. While different measures of extensiveness exist, the one used in previous works is the spread index which can be defined as the reciprocal of the variances of the absolute values of the participation factors in the mode, (Jesko, 1997; Chow, 1982; Candas, 1996).

   The modes corresponding to the inter-area modes of the three synchronic groups from section 2.3 namely: partitioned basis generators, study area, and less relevant generators will include the initial modes plus one more. The additional mode becomes the third mode in the chord. The procedure is then repeated looking for four modes in the chord and the constructed chordal eigenvector U_v matrix is as shown below (Jesko, 1997);

$$U_v = \left[U_{1v} \vdots U_{2v} \vdots \cdots \right] \quad (2.38)$$

Where; U_{1v} - the eigenvector corresponding to the i^{th} mode of the chord. Each of the rows of U_v corresponds to one generator. The chord corresponding to the specialized case of slow coherency would only contain the slowest mode, which is named slow chordal matrix, (Chow, 1982; Ramaswamy et al., 1995; Whang, 1982).

2. The basis generators are selected sequentially from the rows of U_v (Lee and Schweppe, 1973; Lawler and Schlueter, 1982).The first basis generator chosen is the one with the highest participation in the chord. The second basis generator chosen is the one with the highest synchronic distance from the first. The synchronic distance of row i from row j is given by;

$$d_{ij} = \|a_i\| \sin \varphi_{ij} \quad (2.39)$$

Where:

a_i is the i^{th} row of U_v,

$\|.\|$ is the vector norm (Candas, 1996),

φ_{ij} is the angle between rows i and j of U_v (Jesko, 1997).

The third basis generator is that with the highest minimum synchronic distance from the first two. Basis generators are picked until the number of the basis generators is equal to the number of the modes in the chord. Once the basis generators are picked, the remaining generators are grouped with one or another of the basis generators, based on the degree of synchrony between two generators expressed as the cosine of the angle between the rows of U_v corresponding to the generators (Jesko, 1997; Candas, 1996).

$$\bar{d}_{ij} = \cos \varphi_{ij}, \quad (2.40)$$

3. Each non-basis generator is grouped with the basis generator with which it has the highest degree of synchrony.

Step 6: Establish synchrony-derived form on the full, unreduced model. This step involves the two different options of basis generators:

- Full basis, both the external basis generators and the study-group basis generators are used.
- External basis, only the external basis generators are used.

Step 7: Obtain the structure of the SME equivalent. The use of the SME structure is conducted with the application of the Selective Modal Analysis.

Step 8: Load Partitioning

With the understanding of the model applied to do the generator partitioning, the generalization allowing for to also partitioning load nodes is comparatively easy. All the voltages are measured in per unit and all have approximately unit magnitude. The details of the simplified model extraction and load partitioning are presented in a set of the following equations.

$$\begin{bmatrix} \mathrm{M} & 0 \\ 0 & 0 \end{bmatrix} \begin{bmatrix} \Delta\delta \\ \Delta\beta \end{bmatrix} = \begin{bmatrix} F_1 & F_2 \\ F_3 & F_4 \end{bmatrix} \begin{bmatrix} \Delta\delta \\ \Delta\beta \end{bmatrix} \tag{2.41}$$

where;

β - the voltage angles only at the load nodes.

$$\mathrm{M}_{ext} = \begin{bmatrix} \mathrm{M} & 0 \\ 0 & 0 \end{bmatrix}$$

$$F_{ext} = \begin{bmatrix} F_1 & F_2 \\ F_3 & F_4 \end{bmatrix}$$

The common factor between the above equations and those of the core matrix can be more readily recognized when noting the following relationship between F and sub matrices of F_{ext} :

$$F = F_1 - F_2 F_4^{-1} F_3 \tag{2.42}$$

Practically, this is how F can be assigned: firstly, F_{ext} is computed and then further reduction of the system is done to obtain F . They generalized eigen analysis on the equations, while the resulting eigenvalues and right generalized eigenvectors cannot be affected by their left multiplication, then left generalized eigenvector can be affected. It is clear that both left and right generalized eigenvectors take a role in partitioning the load nodes, therefore a distinctive set of equations must be determined (Hockenbeny, 2000).

Step 9: Compute the modal correction (Ramaswamy et al., 1997).

This step is conducted in order to make sure that, the inter-group electromechanical modes of the system are significantly excited outside the study area. Another reason was, for a given synchrony in the inter-group modes, the aim is to verify that the angle and speed part of the variable will be nearly combinations of the basis variables when only the inter-group modes are excited.

The above steps will produce a reasonable reduced order model if the following assumptions are done.The proposed equivalents will be reasonable, based on the assumptions:

- 1- A given event in the system is not highly sensitive to the details of every component in the system, while the effect of distant generators, load and transmission lines must certainly be taken into account for accurate simulation results.

- 2- The grouping algorithm was formulated under the assumption that each node in the system is represented by exactly one variable in the system matrix (Hockenbeny, 2000).

2.4.2 Discussion

The concurrence among full and reduced order model outputs in the reduction order methodology that preserves the true meaning of the variables. The technique contains the process to methodically advance the solutions of the easy model. Synchronic modal equivalencing is basically intended at structure preserving equivalencing of large power system models. SME supplies a motive to the slow-Coherency method for system partitioning and aggregation, however its formulation and associated computational algorithms are more prevalent in some essential respects. Perfect synchrony of a group of generators needs the motion of each generator in the synchronic group to be a linear mixture of the motions of fixed set of basis generators in the group, when some subset of the system modes is exited. SME keeps entire dynamic models of all the generators external to the group. The model of each remaining generator is replaced by an absolute non-dynamic linear circuit that consists of a dependent current source driven by the motions of the basis generators. The remaining part of the network can be left unmodified. Furthermore, (Mallem and Marinescu, 2010) depicts the new technique called border synchrony and show combination of the synchrony and balance realization to develop equivalent model of the power system. More details about synchrony-based border equivalent are well presented in (Mallem and Marinescu, 2010).

As a result of the literature review, some findings about SME method can be presented as follows:

- Based on the motion of the synchrony;
- Requires only the motion of each bus;
- Synchrony accommodates for predictability of the motion, not just egalitarianism of the motion;
- Synchrony permits for both multi-dimensional and one-dimensional correlations.
- Chord is more general (Ramaswamy et al., 1997; Hockenbeny, 2000; Jesko, 1997; Ramaswamy, 1995).

2.5 Coherency based Method

Coherency technique is normally applied to generator buses to reduce their number in the power system models (Podmore and Germond 1977; Lawler and. Schlueter, 1982; Chow et al., 1995).This implies that all the non-generator buses in the coherent area are not needed in the algorithms. Normally coherency can be done based on the

time responses of the generators to choose faults (Kasztel and Erlich, 2001). The techniques such as coherency are conducted in (Chaniotis and Pai, 2005; Avramovic et al., 1980 and (Pai and Adgaonkar, 1979). The Krylov subspace bases (Chaniotis and Pai, 2005) are obtained by projecting linear power systems onto recognizeing coherent generator in the external area. Moreover, this is considered as the primary step in the procedure for model reduction of non-linear system and coherent generators can be substituted in a simpler means of an equivalent generator which can give out their characteristics in simulation studies (Wang et al., 1997; Chaniotis, and Pai, 2005; Kokotovic et al., 1982).

Generally, dynamic equivalencing methods can be categorized into the following groups: coherency-based technique (Podmore, 1978; Joo et al., 2004; Nababhushana and Veeramanju, 1998; Gacic et al., 1998; Haque and Rahim, 1988; Hussain and Rau, 1993) and modal equivalencing techniques (Nishida and Takeda, 1984; Nishida and Takeda, 1988; Chow, 1993). And the references (Undrill et al., 1971; Price et al., 1978; Martins et al., 1996; Martins and Quintao, 2003 and Verghese and Péres-Arriaga, 1983) also presented the modal based equivalencing.

There is also a common technique utilized in model reduction in the literature called: Singular perturbation analysis presented in (Kokotovic et al., 1980 and Chow et al., 1990). Different coherency measures (Joo et al., 2004) such as the Root Mean Square (RMS) coherency measure (Lawler, and. Schlueter, 1982; Troullinos and Dorsey 1989) and the electromechanical distance measure (Verghese et al., 1982) have been applied for coherent identification of generators. The Coherency-based method was initially proposed in (Smith et al., 1976; Winkelman et al., 1981; and Joo et al., 2004) in the year 1980s (Chow, 1993).And more improvements were developed. It is normally adopted method for coherency identification (Joo et al., 2004).

The process of equivalencing for coherency methods is made-up of three main steps (Joo et al., 2004; Mittlestadt, 1973; McCauley, 1975; Chow et al., 1986; Machowski et al., 1988; Singhavilai et al., 2009):

- Coherency identification,
- Aggregation of coherency.(Inertial aggregation and slow coherency), and
- Building of the reduced model, (Lei et al., 2002; Pyo et al., 2010; Joo et al., 2004; Abd-Aal et al., 2006; Dukic and Saric, 2012; Mittlestadt, 1973; McCauley, 1975; Chow et al., 1986; Machowski et al., 1988; Singhavilai et al., 2009).

2.5.1 Step1: Applying of disturbance for the Identification of coherency groups of generators

There are a number of techniques utilized for model order reduction (Price et al., 1975; Ibrahim et al., 1976; Trudnowski, 1994; Yu and El-Sharkawi, 1981; Djukanovic et al., 1992; Ganapati et al., 1996; Wehenkel, 1995 as well as Arredondo, 1999). There are assumptions usually used for the coherency identification procedure. These are as follows (Verghese et al., 1982; Joo et al., 2004; Gacic et al., 1998; Haque and Rahim, 1988; Wang et al., 1997; Brucoli et al., 1983; Caprio, 1981; Caprio, 1982; Dorsey and Schlueter, 1984; and Wu and Narasimhamurthi, 1983).

- Non-generator dynamics may be neglected,
- Classical generator models can be applied,
- The linearised model retains well the developments of coherency (Perez-Arriaga and Schweppe, 1982; Wang et al., 1997; Ishchenko et al., 2006).
- Coherency of the generator is independed of the magnitude of the disturbance, (www.innovexpo.itee.uq.edu.au; Winkelman et al., 1981).
- Excitation and governor systems only have an effect on the damping of the transients but do not considerably fluctuates natural frequencies and mode shapes of the system response (Joo et al., 2004; Gacic et al., 1998; www.innovexpo.itee.uq.edu.au: Haque and. Rahim, 1988).

In the occurrence of an interruption, specific quantity of swinging will be acquired by the generating units. Some groups of the generators in the power system model can experience indistinguishable wave shape of the swing curves of the rotor angles due to the arbnormal conditions in the network. These sets of generators are then said to be coherent and they can be abridged into a single generator or into a simplified equivalent system. Both the acceleration and rotor speed of the generator are applied to determine the coherency among generators (Chow et al., 1984; Podmore, 1978; Germond and Podmore, 1978; Winkelman et al., 1981; Wang et al., 1997; Lim, 2003; Joo et al., 2001; Tianqi et al., 2009; Rimjhim and Thukaram, 2011; Oirsouw, 1990; Ghafurian and Siving, 1982; Haque and Rahim, 1990; Alsafih and Dunn, 2010; www.innovexpo.itee.uq.edu.ac).

According to (Lim, 2003) swinging equation can be used to identify coherency.

Mathematical model for the calculation of the swing equation

For the reason that the full generating unit model has a considerable impect on the swing curves, the effect of the damping, is unconsidered as it is uneffective to the natural frequencies and the mode curves. Thus, an easy model, such as a standard model, also called the constant voltage behind transient reactance (www.innovexpo.itee.uq.edu.ac) $(X_d^{'})$ model, can be applied to symbolize the

generating unit (Badeeb and Hazza, 2004). The second-order system can be written as (www.innovexpo.itee.uq.edu.ac):

$$\frac{d\delta_i}{dt} = \omega_i - \omega_s \tag{2.43}$$

$$\frac{2H_i}{\omega_s}\frac{d\omega_i}{dt} = Tm_i - Te_i - D_i(\omega_i - \omega_s) \tag{2.44}$$

$$T_{ei} = \sum_{j=1}^{n} E_i E_j \left[B_{ij}\sin(\delta_i - \delta j) + G_{ij}\cos(\delta_i - \delta_j)\right] \tag{2.45}$$

For $i = 1,2,.....,n$, where

δ_i is the stroboscopic rotor electrical angle (rad)

ω_i i is the rotor electrical speed (rad/s)

E_i is the (constant) voltage behind transient reactance (PU)

T_{mi} is the (constant) input mechanical torque (PU)

T_{ei} is the electromagnetic torque (PU)

B_{ij} = is the (i,j)th entry of the susceptance matrix B

G_{ij} = is the (i,j)th entry of the conductance matrix G

H_i = is the inertia constant (MW - s/MVA)

D_i = is the damping constant (s/rad) (Badeeb and Hazza, 2004; www.manchesteruniversitypress.co.uk).

With the assumption that any form of disturbance is situated away from the external area such that the coherent groups of generators do not dependent on the size of the disturbance, the linearised power system model becomes (Badeeb and Hazza, 2004; www.innovexpo.itee.uq.edu.ac):

$$\begin{bmatrix} \Delta\frac{d\delta}{dt} \\ M\Delta\frac{d\omega}{dt} \end{bmatrix} = \begin{bmatrix} 0 & I_n \\ -K & -D \end{bmatrix}\begin{bmatrix} \Delta\delta \\ \Delta\omega \end{bmatrix} \tag{2.46}$$

where:

$$K_{ij} = E_i E_j \left[B_{ij}\sin(\delta_i - \delta_j) + G_{ij}\cos(\delta_i - \delta_j)\right]$$

$$K_{ij} = -\sum_{j=1}^{n} k_{ij} \quad \text{for} \quad j \neq i$$

$$M_i = 2H_i$$

Neglecting damping constant D_i and transfer conductance G_{ij} terms, which are small compared with the B_{ij} terms, the linearised model is (Badeeb and Hazza, 2004)

$$\Delta \frac{d\delta^2}{dt^2} = -M^{-1} K \Delta\delta \tag{2.47}$$

$$\Delta \frac{d\delta^2}{dt^2} = A \Delta\delta \tag{2.48}$$

Solution of the above Equations gives the swing curves for every generator. These curves are used to identify the coherent generator groups.The grouping algorithm is recapitulated as follows:

Step 1: select the number of the groups and the modes.

Step 2: Calculate a basis matrix V of the eigenspace for a matrix A

Step 3: Use Gaussian elimination with full pivoting to (www.innovexpo.itee.uq.edu.ac) V and select the pivots of Gaussian elimination as the reference states and situate them in a matrix V_1.

Step 4: Put together matrix V as:

$$V = \begin{bmatrix} V_1 \\ V_2 \end{bmatrix} \tag{2.49}$$

where V_2 are the remaining generators.

Step 5: Calculate a Dichotomic (www.innovexpo.itee.uq.edu.ac) matrix L for the set of reference states selected in step 3 utilizing

$$V_1^T L^T = V_2^T \tag{2.50}$$

Step 7: Assign largest numbers on the rows of matrix L_g corresponding to the reference machines and define slow coherent areas.

Step 8: Print the slow coherent areas (Nath et al., 1985; Chow et al., 1990; Ahmed-Zaid and Awed-Badeeb, 1991; Badeeb and Hazza, 2004).

2.5.1.1 Weak links

This method resolves coherency by examining the grouping of generators in the state matrix. If the coupling coefficients between the generators are high, they are identified as coherent generators (Ishchenko et al., 2008; Nath et al., 1985; Winkelman et al., 1981; Wang et al., 1997).

2.5.1.2 Two time scale

This technique is focused on the abstract idea that a slow swinging of generators is produced by two groups of robustly coherent generators interconnected via weak ties. Two swing curves for the generator groups can be simply recognized applying the eigenvector aligned with the mode of oscillation. Moreover, with this method the power system can be partitioned into a random number of coherent generator groups by means of examining the same number of the slowest modes of oscillations (Ishchenko et al., 2008; Winkelman et al., 1981; Wang et al., 1997; www.manchesteruniversitypress.co.uk).

2.5.1.3 Linear time simulation

This is a conventional technique to recognize coherent machines. Response of time domain of the power system is effective dealing with a certain disturbance in the power system, and also the generator rotor angles are compared. Those generators with rotor angles swinging together are identified as coherent; therefore the procedure to follow is the generator aggregation. In most cases, the generator aggregation is conducted in two forms (www.manchesteruniversitypress.co.uk; Podmore, 1978; Galarza et al., 1998; Joo et al., 2004; Wang et al., 1997).

2.5.2 Step 2: Algorithms for aggregation

There are many methods for the generators in the power system network. Some of them are described as:

2.5.2.1 Classical aggregation (www.manchesteruniversitypress.co.uk)

Generators in a coherent group are symbolized by an equivalent classical generator model. In its straightforward form, the equivalent inertia is the total number of the inertia of all generators in the group, as well as equivalent transient reactance is acquired by paralleling the transient reactance of all generators in the group (Podmore, 1978; Galarza et al., 1998; Joo et al., 2004; Wang et al., 1997).

2.5.2.2 Detailed aggregation

On the condition that same or all generators in a coherent group have the same control systems, they are aggregated to a complete generator model with an equivalent exciter, stabilizer, as well as governor (Joo et al., 2004; Nababhushana and Veeramanju, 1998). The obtained equivalent generator parameters can be

introduced by comparing its frequency responses behaviours to the ones of the aggregated generators only if more detailed models are utilized (Cai and Wu, 1986).

The equivalent model parameters are obtained applying combination of the two techniques:

- A smallest square fit of the frequency response of showing the linear behaviours and;
- An assessment of the time domain restraints to set non-linear behaviours (Smith, et al., 1976; Podmore, 1978; Joo et al., 2004;Wang et al., 1997).

2.5.2.3 Slow coherency aggregation algorithm steps using relation error

The role of the slow coherency approach is to discover coherent generators based on the disturbance introduced to the system. The generators that swing together can be grouped to develop a single equivalent generator. Every group is represented by an equivalent generator which has the same power as this of the sum of the individual generator in the group.

The steps of the algorithm are (Kim et al., 2004):

Step-1- Initialize the generators to constitute group respectively.

Step-2- Determine relation errors using the following equation;

$$L_{ij} = \sqrt{\sum_{k=1, k\neq i, j}^{m} \mu_1 \left(R_{ik} - R_{jk}\right)^2} + \sqrt{\mu_2 \left(R_{ij} - R_{ji}\right)^2} + \sqrt{\mu_3 \left(R_{ii} - R_{jj}\right)^2} \quad (2.51)$$

Where, L_{ij} is the relation factor.

R_{ij} is the relation factor of machine j towards machine i.

R_{ii} is the self-relation factor.

R_{ik} is the relation factor for the machine k towards machine i

μ_1, μ_2, and μ_3 are the weighting coefficients for relation factor error.

Step-3- Select the smallest relation error.

Step-4- Assert two machines having the selected relation error into the same coherent group. If it is selected, the coherent group is updated as

$$G_p = G_p \cup G_q \quad (2.52)$$

where,

G_p and G_q are the sets having generators coherent with the generators j and i respectively.

Step-5- Increase each participation number of machines i and j by the value 1.

Step-6- Stop if the number of coherent groups equals the specified number.

Step-7- Select the next smallest relation error.

Step-8- Stop if the relation error is greater than the allowable relation error; otherwise, go back to step 4.

2.5.2.4 Steps of slow coherency aggregation algorithm

An experience-based algorithm which works very well is applied to discover the coherent groups of generators in a multi-machine system, such that each coherent group satisfies the coherency criteria. The criteria may be developed in the computer program for coherency aggregation if it is larger and fewer algorithms which can be summarized as follows (Schlueter and Ahn, 1997; Chow et al., 1995). The various steps of the aggregation in the coherent groups are: (Figure 2.3).

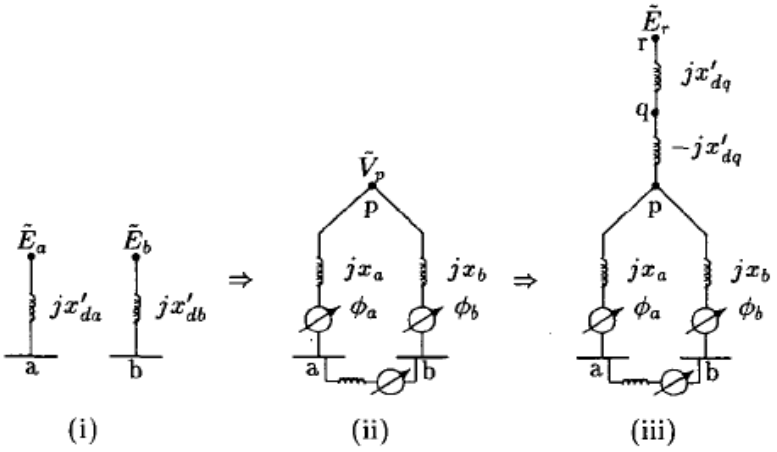

Figure 2. 3: **Slow Coherency Aggregation (Chow et al., 1995)**

- Computing the voltages at the internal buses **'a'** and **'b'**
- Implimenting the common bus **'p'**
- Linearizing about the generator buses and internal nodes
- Transforming to slow and fast variables
- Obtaining the slow subsystem
- Generator aggregation
- Implimantation of bus **'q'**
- Adjusting generation on buses **'a', 'b'** and **'q'** (www.innovexpo.itee.uq.au)

2.5.3 Step 3: Building of the reduced model

The main principle in developing power system network equivalents is to embody a portion of a network which has many buses but having only a few "*boundary buses*" by a reduced network containing only the boundary buses and a few selected buses from within the full sub-network.

The total of load, generation, and losses in the equivalent generator, must be equivalent to the sum of the coherent generators in the group from the complete external area. Nonetheless, the load, generation, and loss totals in the equivalent may not individually match those of the complete external system. Kron's elimination algorithm can be utilized to build the reduced model.

Steps for the Kron's algorithm

Kron elimination is done on each diagonal element $y'_{m,m}$, starting with $y_{1,1}$, and continuing through $y_{N-1,N-1}$. Starting with Row $m = 1$, and continuing through Row $m = N - 1$, the algorithm of Kron reducing $I = YV$ is

1. Divide the elements in Row m, that are to the right of the diagonal, by the diagonal element $y'_{m,m}$.

2. Replace element I'_m with $\frac{I'_m}{y'_{m,m}}$.

3. Replace diagonal element $y'_{m,m}$ with unity.

4. Modify the Y' elements in rows greater than m and columns greater than m using

   $y'_{j,k} = y'_{j,k} - y'_{j,m}y'_{m,k}$, for $j > m$, $k > m$.

5. Modify the I' elements below the *mth* row according to

   $I'_j = I'_j - y'_{j,m}I'_m$, for $j > m$

6. Zero the elements in Column m of Y' that are below the diagonal element.

2.5.4 Discussion

According to work conducted by (Ramaswamy, 1995) the synchrony based grouping can manage to produce all the oscillatory electromechanical modes of the system, with each group also picking up exactly one of the inter-area modes as well. The experience with the coherency-based grouping was not very satisfactory (Ramaswamy, 1995). Slow coherency technique has a tough mathematical foundation; it still needs long computation of the eigen subspaces (www.manchesteruniversitypress.ac.uk) and a strong technique for the best choise of the number of coherent areas. To defeat these computational drawbacks, special proposed developments are suggested (Nath et al., 1985; Chow et al., 1990; Badeeb and Hazza, 2004; Ahmed-Zaid and Awed-Badeeb, 1991). The advantage slow coherency based grouping has is that it does not generally depend on initial condition (You et al., 2004; www.manchesteruniversitypress.ac.uk).

The advantages of synchrony-based method over slow-coherency base method are as follows:

- *Improved decomposability*; Both the chord selection process and the adaptability to apply specific grouping features which are not limited to be equal to 1 obviously allow one to advance decomposability properties of the model. Synchrony decomposability can be enhanced even further in multi-dimensional relationships. Such decomposability is essential in the inter-group analysis, and also in time-domain studies (Ramaswamy et al., 1995; Ramaswamy, 1995).
- *Improved Localizability;* In the synchrony-based system partitioning is mainly for the reason that the adaptability in the chord selection and the accessibility of proficient procedure for the selection are improving localizability. Localizability is very essential in time-domain studies and also in intra-group analysis (Ramaswamy et al., 1995; Ramaswamy, 1995).
- *Dropping zero Mode from the Chord*; the inventive slow-coherency procedure (Avramotive, 1980) and the advanced tight-coherency procedure (Chow, 1993) are created on the assumption that the chord has the zero modes, and are doubtful to work absolutely if the mode is dropped from the chord. It is therefore highly recommended that the zero modes must be left out of the chord during partitioning. Synchrony-based partitioning enables zero modes to be dropped without any complexity at all (Ramaswamy, 1995).
- *Insensitivity to Coordinate Scalings;* Coherency-based grouping is perceptive to coordinate scaling, while synchrony-based partitioning is not perceptive to such scaling.
- *Relative Weighting of Modes;* the capability to initiate relative weighting of modes in synchrony-based partitioning through the matrix application is extremely remarkable. Nonetheless slow-coherency based method does not give such a luxury (Ramaswamy, 1995).
- *Improved Selection of Reference Generators*; Fuzzy clustering algorithm is competent of extremely useful clustering and excellent selection of reference generators. Slow-coherency is a Gaussian elimination based algorithm, which is not a clustering algorithm and it is therefore unable to work well in practice, and
- *Robustness in Grouping;* The degree of synchrony between generators i and j is determined rigorously by the modal data for the two generators. Hence, the grouping based on synchrony is rather robust, since changes of the selecting the reference generator for some other remote group will not affect the degree of synchrony between the generator i and j .

The sturdiness in the synchrony-based grouping is that the assignments are decoupled from one another, whereas in the slow-coherency case they are not (Ramaswamy et al., 1995; Ramaswamy, 1995).

The drawbacks of coherency technique can be pointed to be as follows (Ibrahim et al., 1976; Ma and Vittal, 2005; Brucoli et al., 1988; Tsai et al., 1982; and Troullinos et al., 1985):

- It is purely empirical;
- Accuracy of the equivalent developed is dependent on the perturbation selected to determine coherency, and
- Generator coherency is also dependent on the system conditions.
- It is only verifiable by experience or experiment;
- Accuracy of the equivalent developed is relying on the perturbation selected to identify coherency (Geeves, 1988);

- Generator coherency is also relying on system condition (Ma and Vittal, 2005)and
- According to (Rudnick et al., 1981) coherency is being the lengthy calculation time needed to recognize the coherent groups with full-time simulation.

Therefore, in (Troullinos et al., 1985) a balanced realization technique is combined with modal-coherency to make precise approximation for dynamic equivalents based on coherency aggregation.Few papers have used Real-Time Digital Simulator RTDS software such as RSCAD as it is a new technology.

In coherency technique there are approaches that can reserve a study area of the network (Ibrahimet al., 1976; Brucoli at el., 1988; Tsai et al., 1982). In (Troullinos et, al., 1985), they combined balanced realization technique with Modal-Coherency to make the precise approximates for dynamic equivalents based on coherency aggregation. Moreover, in (Pyo et al., 2010) is stated that three techniques; modal, coherency-based and slow coherency are combined in order to develop equivalents over the past decades. And coherency seemed to be simpler than the rest methods.

2.6 Integral Manifolds

Smooth s-dimensional surface S in the n-dimensional space R^n is described (www.waset.org) by $m=n-s$ independent algebraic or transcendental scalar equations. In their straightforward form, those equations convey certain m coordinates z as m explicit purposes of the remaining s coordinates x that is they define S by its graph (Sedighizadeh and Rezazadeh, 2008; www.waset.org):

$$S: z = h(x), z \in R^m; x \in R^s; m + s = n \tag{2.53}$$

It is imagined that, for all x in a domain of (www.waset.org) realistic interest, $\frac{\partial h}{\partial x}$ exists and has complete rank m. Estimated constructions of $h(x)$ are given in (Sedighizadeh and Rezazadeh, 2008; Kalantar and Sedighizadeh, 2005; and Rau and Hussian, 1998), It will also be presumed that higher order derivatives of $h(x)$ exist and are permanent. In a more wide-ranging situation the surface S can change with time t, then

$$S_t: z = h(x,t), z \in R^m; x \in R^s; m + s = n \tag{2.54}$$

It is assumed (www.waset.org; Sedighizadeh and Rezazadeh, 2008; Kalantar and Sedighizadeh, 2005) that $\frac{\partial h}{\partial x}$ exists and is constant over a time of interest $t \in (t_0, t_1)$, where it is possible that $t_1 \to \infty$

Using the identical coordinate's z and x, a dynamic system D_t can be expressed in R^n:

$$\frac{dz}{dt} = g(x, z, t).....z \in R^m \quad (2.55)$$

$$\frac{dx}{dt} = f(x, z, t).....z \in R^s, m + s = n \quad (2.56)$$

Where suitable, differentiability assumptions are done about g and f. The surface S_t and the system D_t have therefore been set up as two entities not related to each other. This investigation explores mainly a valuable relationship of S_t and D_t: when S_t is an integral manifold of D_t.

The term invariant manifold can be used when such an integral manifold is time invariant, which is when (www.waset.org)

$\frac{\partial h}{\partial t} = 0$ and $S_t = S$ as in Equation (2.53).

2.6.1 Manifold definition (www.waset.org)

Surface S_t is an integral manifold of D_t if every answer $z(t), x(t),$ of (2.55) – (2.56) is in S_t and at $t = t_0$ $Z(t_0) = h(x(t_0), t_0)$ (2.57)

Remains in S_t for all $t = \in (t_0, t_1)$, that is $Z(t) = h(x(t), t), t \in (t_0, t_1)$ (2.58)

This definition provides a situation which can be used to confirm whether $h(x,t)$ in (2.54) describes an integral manifold of (2.55) – (2.56) (Sedighizadeh and Rezazadeh, 2008; Kalantar and Sedighizadeh, 2005).

2.6.2 Manifold condition

In the case where $h(x, t)$ suits the partial differential equation:

$$\frac{\partial h}{\partial t} + \frac{\partial h}{\partial x} f(x, h(x,t), t) = g(x, h(x,t)t)) \quad (2.59)$$

the surface S_t given by (2.54) is an integral manifold of the dynamic system (2.55)-(2.56).

This condition is basically obtained by differentiating (2.58) with respect to t,

$$\varepsilon \frac{dz}{dt} = \frac{\partial h}{\partial t} + (\frac{\partial h}{\partial x} \times \frac{dx}{dt}) \quad (2.60)$$

Once the presence of an integral manifold S_t of D_t has been set up and its describing function $h(x,t)$ has been established, then the constraint of D_t to the manifold S_t is given by the s th-order equation (Sedighizadeh and Rezazadeh, 2008; Kokotovic and Sauer, 1989; Kalantar and Sedighizadeh, 2005; www.waset.org).

$$\frac{dx}{dt} = f\left(x, h(x't).t\right), x \in R^s \tag{2.61}$$

which is achieved by the replacement of $z = h\left(x,t\right)$ into Equation (2.56).Additionally to being a technique for reduced order modelling, the idea of an integral manifold is also a decomposition technique. A reduced order model (2.62) is a proper picture of the dynamic D_t only when the initial state is in S_t, as in (2.57). When the initial state of D_t is not in S_t, the understanding of the manifold function $h\left(x,t\right)$ carries on to be constructive by allowing to substitute of the z-coordinates by the "off-manifold" coordinates η.

$$\eta = z - h(x,t)$$

$$\eta \in R^m \tag{2.62}$$

In terms of the new coordinates η and x the full systemEquations (2.55) – (2.56) becomes (www.waset.org):

$$\frac{d\eta}{dt} = g\left(x, \eta + h(x,t), t\right) - \frac{\partial h}{\partial x} f\left(x, \eta, h(x,t), t\right) - \frac{\partial h}{\partial x} \tag{2.63}$$

$$\frac{dx}{dt} = f\left(x, h(x,t), t\right) \tag{2.64}$$

The benefit of this full order explanation of D_t over (2.55) – (2.56) is that now the manifold situation is merely $\eta = 0$. The decomposition is obtained in the sense that on the surface S_t the subsystem (2.63) is balanced: $\eta\left(t_0\right) = 0$ means that, $\eta\left(t\right) = 0$ for all $t \in \left(t_o, t_1\right)$ as well as all x. The "off –manifold and in –manifold" explanation (2.63) – (2.64) is mostly cooperative when the manifold performance of D_t is of crucial interest and the off manifold variable is calculated separately as a modification expression.

The analysis obtained in (www.waset.org; Kalantar and Sedighizadeh, 2005) demonstrated both conceptual and computational benefits of the nonlinear decomposition approach.

2.6.3 Linearised model for the intergral manifold calculation

Most of the nonlinear full and the reduced order models can be linearised in the region of an operating point if it is imagined that the variables have adequately small deviations from the operating point. For instance the supposition is done in dynamic stability studies of power systems where it is expected to utilize a linearised model so that linear system analysis techniques can be suitably used.

The linearization procedure can be straight used for the n th order generator model. Nonetheless, the coefficients of the resultant equations, especially for the n th-order model, can have quite complex algebraic expressions (Sedighizadeh and Razazadeh, 2008). An equivalent approach is through linearization of the full n th order model deriving the linearised n th model by following the procedure. The linearised n th-order equation can be partitioned as

$$\frac{dz}{dt} = Dz + Cx \tag{2.65}$$

$$\frac{dx}{dt} = Bz + Ax + r \tag{2.66}$$

Where z denotes the variable whose transients are to be disregarded and x denotes the remaining variables.

For a linear time–invariant system with invariable input, u the integral manifold is required in the form (Kalantar and Sedighizadeh, 2005; Rau and Hussian, 1998):

$$z = px + q(r) \tag{2.67}$$

where p is a constant matrix

The substitution of (2.65) and (2.66) into derivative of equations (2.67) gives:

$$p\left(Ax + B(px + q(r) + r\right) = D\left(px + q(r)\right) + Cx \tag{2.68}$$

Collecting the x-reliant terms it is required that the constant matrix p to be an answer of the equation

$$pA - Dp + pBp - C = 0 \tag{2.69}$$

With such a matrix p , the u-reliant terms require that

$$\left(D - pB\right)q(r) - pr = 0 \tag{2.70}$$

$$q(r) = (D - pB)^{-1} pr \tag{2.71}$$

The explanation of the system (2.64) and (2.65) limited to the manifold (2.66) is known by the reduced order model (Sedighizadeh and Razazadeh, 2008; Kalantar and Sedighizadeh, 2005):

$$\frac{dx}{dt} = \left(A + pB\right)x + \left(B(D - pB\right)^{-1} p + I)r \tag{2.72}$$

$$\dot{z} = p\dot{x} \tag{2.73}$$

$$Dz + C\dot{x} = p\dot{x} \tag{2.74}$$

$$D(px + q(r)) + Cx = p\left[B\left(px + q(r)\right) + Ax + r\right] \quad (2.75)$$

$$x\left[Dp + C - pB - pA\right] + q(r)[D - pB] - pr = 0 \quad (2.76)$$

As x and r are not equal to zero, in order Equation (2.80) to be fulfilled:

$$Dp + C - pBp - pA = 0 \quad (2.77)$$

$$q(r)[D - pB] - pr = 0 \quad (2.78)$$

And, $q(r) = (D - pB)^{-1} pr$ (2.79)

If the initial conditions for x and z satisfied Equation (2.66), consequently, reduced order model is (2.78), however if initial conditions don't meet manifold conditions, the expressions are assumed to be analogous to the non-linear model.

2.6.4 Application to the Wind Park Model (Sedighizadeh and Rezazadeh 2008; Kokotovic and Sauer, 1989; Kalantar and Sedighizadeh, 2005)

This method was mainly applied on the wind park detailed model. Firstly, (www.waset.org) separation of the time variables in both slow and fast variables to enable the process of solving them in the suitable time scales is done. Slow variables can be considered as (Sedighizadeh and Rezazadeh 2008; Kokotovic and Sauer, 1989; Kalantar and Sedighizadeh, 2005):

- The stator flux linkage (α_1);
- First rotor circuit flux linkage (α_2), and
- The rotor speed**.**

The remaining ones were assumed as fast variables.

$$x = [\alpha_{1d} ... \alpha_{1q} ... \alpha_{2d} ... \alpha_{2q} ... s] \quad (2.80)$$

$$z = [\alpha_{3d} ... \alpha_{3q}] \quad (2.81)$$

α_3 = denotes the remaining rotor flux linkage.

$$\alpha_{3d} = h\left(\alpha_{1d}, \alpha_{1q}, \alpha_{2d}, \alpha_{2q}, s, \varepsilon\right) \quad (2.82)$$

$$\alpha_{3q} = p\left(\alpha_{1d}, \alpha_{1q}, \alpha_{2d}, \alpha_{2q}, s, \varepsilon\right) \quad (2.83)$$

Moreover, the identification of the small parameters is of paramount need. Under the above conditions, to obtain the slow sub-system, the wind park model has been rewritten to comply with the formulation given by Equations (2.54) and (2.55). The states z and x denote the real variables, but they are associated with a different system in which $\varepsilon \neq 0$.

Consequently, the assumptions for x and z were derived from equations (2.63) and (2.64) respectively (Kalantar and Sedighizadeh, 2005).

2.6.5 Discussion

The technique known in the literature is the integral manifolds; a principle of the motion of invariant subspace in a linear network (www.waset.org; Sedighizadeh and Rezazadeh, 2008; Tseng and Kokotovic, 1988).

With the aim of gaining some understanding with regards to the performance of every technique, a steady-state initiation interpretation is conducted using linear models in order to take gratification of their distinctive ease in (Sedighizadeh, and Rezazadeh, 2008; Rui et al., 1993; www.waset.org). Balanced reduction procedures for the methods of Integral manifold seize a somewhat strange of their inherent approach, since they are based on the input/output performance of the network (Sedighizadeh and Rezazadeh, 2008; Moore, 1981). In fact, the original state-space system is transformed into a new one that has the functions that each state-space variable is both observable and controllable. With the purpose of accomplishing a reduced order model, declares that are sturdily affected by the inputs and greatly connected to the outputs are preserved; on the contrary states which are weakly controllable and observable are truncated (www.waset.org; Sedighizadeh and Rezazadeh, 2008; Peter, 1994).This method appears to be more common, specifically in what is important to the foretelling of steady-state and transient character of the networks. Additionally, the agreement between full and reduced order models results, the advantages as follows must be mentioned:

- The reduction order methodology retains the physical meaning of the variables, and
- The method self has the procedures to systematically improve the answers of the non-complex modes (www.waset.org; Sedighizadeh and Rezazadeh, 2008).

Furthermore, the accuracy for this thechnique is excellent. According to literature, integral manifolds are to be the most promising reduction order technique, it is chosen as the source for the development of the dynamic equivalent (Sedighizadeh and Rezazadeh, 2008; www.waset.org) more especially in application to wind farm models.

2.7 Nonlinear decomposition approach (www.iptt.org)

This approach can produce a significant contribution to the efficiency of the computation of electrical power system. Normally it is tricky to apply model reduction techniques to nonlinear dynamical systems, since it leads normally to heavy

calculations (Prochaska et al., 2005; Maas and Pope, 1992; www.iptt.org). The diagonalisation of the linear part of the nonlinear systems can be used to discover the fast and slow state variables for a local state space reduction. In view of the fact that the linear part is prearranged by a linearization at a fixed point, the reduced model is only suitable in a limited region of the state space. Practically this approach is rendered not practical due to the changing of the modal coordinate's that lead to near singular and inadequately scaled transformation matrices. (www.iptt.org; Maas and Pope, 1992 ;Prochaska et al., 2005;) proposed another technique for the identification of slow and fast state variables which depends on a real Schur decomposition of the right hand side of the ordinary differential equations (ODE). This technique is declared to be rather effective for the reduced order modelling of combustion problems in the background of partial differential equations, where the rigidity is based on big dissimilarity between the real parts of the eigenvalues. Regrettably, electrical power systems are weakly damped: power systems are inflexible due to the large imaginary parts of conjugate complicated eigenvalues, while real eigenvalues are insufficient. Consequently the models of power systems have the quality of a well oscillatory system, which cannot be cleft by the other techniques introduced in the literature (www.iptt.org; Prochaska et al., 2005).

2.8 Softwares applied for building of the reduced order models

1. Exisisting software packages
2. Possibilities to use the RTDS/ RSCAD in the algorithms for model order reduction.

2.8.1 Algorithms set in EPRI software program

Slow coherency method is used in some software programs such as EPRI. The following algorithms are applied in the process of model reduction.

- LINSIM→ this is the simulation algorithm which allows the maximum and minimum coherency measure to be computed.
- GROUP→ A clustering algorithm which determines coherent groups based on the computed coherency measure.
- DYNAGG→ This aggregation algorithm consists basically from three distinct algorithms which aggregate coherent generator groups and conduct the network reduction in order to build the actual equivalent (Verghese et al., 1982; Podmore, 1978; Germond and Podmore, 1978).

The equivalencing procedure of modal methods consists of a mode selection, decoupling and equivalent model construction (Joo et al., 2004). The previous work in the literature has also showed techniques which request characterizations of modal behaviour in a linearised power system model which takes a broad view of the coherency concept (DeMarco and Wasser, 2005; Ramaswamy et al., 1993; Ramaswamy et al., 1995; and DeMarco and Wassner, 1995). Coherency based

method was presented in 1970s with the corresponding dynamic reduction software programs such as DYRED (Wang et al., 1997; Yang et al., 2005) as well as investigation Dynamic Equivalency (DYNEQ) (Podmore, 1978; Germond and Podmore, 1978; Wang et al., 1997; Podmore, 1977; Kim et al., 2004; Yang et al., 2005; Price et al., 1998). Electrical Power Research Institute (EPRI) software allows a model-coherent equivalent to be obtained which is more advantageous (Chow, 1982; Wang et al., 1997; Podmore, 1977; Kundur et al., 1993; Yang et al., 2005; Price et al., 1998). The dynamic reduction program Dynamic Reduction (DYNRED) in the power system analysis package (PSAPAC) (Kundur et al., 1993; You et al., 2004) was selected to make groups of coherent generators based on an enhancement to the slow coherency (www.certs.lbl.gov) technique produced in the literature (You et al., 2004; Price et al., 1995) to deal with large systems and accomplish more accurate results (Chow, 1982; Kundur et al., 1993; Yang et al., 2006; Price et al., 1995; Wang and Vttal, 2004; Zhao et al., 2003; Vittal et al., 1998; Jung et al., 2002; You et al., 2003). Reference (Ma et al., 2011) presents the new features of DYNRED being;

- Advanced graphical user interface;
- New presentation matrices for model validation;
- Preservations of models supported, and
- Elimination of many procedures for coherency identification such as singular perturbation and two-time scales (Ma et al., 2011).

The advantages of the EPRI method and software:

The advantages of the EPRI method and softwares are:

- The Root Mean Square (RMS) coherency measure has been arithmetically associated to the system model and the information of the modal disturbance, such that there is no need for simulation to establish coherent group.
- Coherent groups obtained applying the RMS measure and the modal disturbances are based only on system components which are not affected by the kind or location of any specific system disturbance. As a result, a single modal coherent equivalent can be applied in the transient stability study of the large interconnected system under disturbances.
- The modal-coherent equivalent retains both the coherent groups as well as modes of the full system model and is more reliable equivalent which does not usually retain modes (Lawler and Schlueter, 1982; Schlueter et al., 1978; Schlueter and Ahn 1979; Lawler, 1980).

2.8.2 Application of the Real-Time Digital Simulator (RTDS) in model order reduction

Wide-Band system technique was described as the new modelling approach that enables a real time modelling of large power systems with cheaper hardware cost (Lin, 2010; Liang, 2011). The developed equivalent model by this technique reduces a large interconnected power system model into a simple convenient equivalent model that retains full network performance. In references (Lin, 2010) and (Liang,

2011) both coherency based technique and this technique are used to implement a reduced order of a full electromechanical Transient Stability Analysis (TSA) network in real-time digital simulations. Furthermore, the behaviour of their equivalent model is replicated by a terminating Frequency Dependent Network Equivalent (FDNE). In order to prevent unstable simulations, the FDNE must be a passive network (Lin, 2010; Liang, 2011). Reducing the full system to an equivalent one is essential for real time power system simulation studies. The size of the equivalent system must be compatible with the modelling capability of the simulator (Pires and Souza, 2008).

Moreover, Table 2.2 shows the software used in the publications and compares the number of real-time simulations that have been conducted. Only five paper utilized a real-time environment simulation, and they are indicated with the * symbol.

Table 2. 2: **Comparison of real-time simulation type in the existing literature**

Software used	Papers	Real time simulation
CEL PEL	(Almeida et al., 2010)	Non
CPAT	(Yamagishi and Komami, 2008)	Non
DigSILENT	(Chen, 2009)	Non
DISCORE	(Lee and Schweppe, 1973)	Non
DYNRED	(Joo et al., 2004; Chow et al., 1995; Wang and Vttal 2004; Wang and Vttal 2001; Stankovic´, Saric´and Milo˘sevic 2003; Annakkage, 2012; Chen, and Bose, 1988; Ma and Vittal, 2005)	Non
EISPACK	(Chow, 1984; Winkelman, 1981)	Non
EPRI	(Lawler and Schlueter 1982; Joo, 2004; Chow, 1995; Lim, 2003; El-Arini and Fathy, 2011)	Non
ETMSP	(Joo, 2004; Vittal et al., 1998)	Non
EUROSTAG	(Ramaswamy et al., 1997; Hockenbeny, 2000;Jesko, 1997; Ramaswamy, 1996; Ramaswamy, 1993; Ramaswamy et al., 1994; Ramaswamy, 1995; Mallem and Marinescu 2010)	Non
GAL RED	(James, 1993)	Non
IMSL	(van Oirsouw,1990)	Non
MADEQ	(Price, 1978)	Non
MATLAB	(Ramaswamy et al., 1997; Hockenbeny, 2000; Jesko, 1997; Joo, 2004; Ramaswamy, 1996; Ramaswamy, 1993; Ramaswamy et al., 1994; Ramaswamy, 1995; Lim, 2003; Jooet al., 2001; Artenstein and Giusto, 2008; Ishchenko et al., 2006; DeMarco and Wassner, 1995; Wang et al., 2008; Choi, 2008;* Shojaei, 2009; Nilsson and Rantzer,2009)	(Nilsson and Rantzer,2009)
MFTS	(Rudnick, Patino, and Brameller 1981)	Non
NETOMAC	(Yang et al., 2005; * Lei et al., 2002)	(Yang et al., 2005)
PACDYN	(Almeida et al.,Silva, 2010)	Non
PEALS	(Yusaf et al., 1993)	Non
PSAPAC	(Wang and Vttal, 2004; Senroy, 2008)	Non
PSASP	(Yang et al., 2010; Wang Kui, and Buhan 2011) *	(Wang Kui, and Buhan 2011)
PSAT	(Artenstein and Giusto, 2008)	Non
PSCAD	(Annakkage et al., 2012)	Non
PSS/E	(Yang et al., 2005) *, Podmore, 1979; Pyo et al., 2010; Lee, 2009)	(Yang et al.,2005)
POSSIM	(Ibrahim et al., 1976)	Non
RSCAD	(Lin, 2010; Liang, 2011) *	(Lin, 2010; Liang, 2011)
UNIVAD	(Nath, Lamba, and Prakasa Rao 1985)	Non

2.10 Conclusion

From the research conducted, SME (Synchronic Modal Equivalencing) as well as Coherency based methods are the most used techniques from the year 1968 till present. Moreover, the years 2008, 2010 and 2011 seem to have highest number of publications on the study of reduced order models. The most used model to perform the studies is New England power system consisting of 10 generators, and 39 buses. The most used software environments are MATLAB, DYNRED, EUROSTAG, and EPRI respectfully. Simulation in real-time conditions is the drawback within the study of model order reducing techniques in power systems at the present. Therefore, the real-time digital simulation is highly recommended in this field for example with the application of RSCAD software.

Chapter 3 considers on the stability of power system due to the fact that power system stability is applied in this research to verify the results between the original and the reduced model.

CHAPTER THREE
POWER SYSTEM STABILITY

Introduction

The accuracy of reduced power systems can be verified by conducting stability analysis. Stability problems are caused by heavy demand, complex interconnected transmission lines of the network, and anything that perturbs the power system. To verify the transient behaviour of the network, power system stability is needed before and after the network reduction. However, the reduced system can be simply executed into a conservative stability plan. It is very important that both the reduced and full models have almost the same transient behaviour. Therefore, the study of power system stability goes hand in hand with model order reduction field. Stable model can allow safe operation of the network near to its limitations. The possibility of a power system to build up restoring forces equal to or greater than the disturbing forces to preserve the state of equilibrium is known as "***STABILITY***" (www.ethesis.nitrkl.ac.in). Since the industrial insurrection men necessitate for the consumption of energy has increased steadily. The main portion of energy requirements of a modern society is supplied by means of electrical energy. This huge enterprise of supplying electrical energy leads to several engineering problems which grant the engineer with a variety of challenges (Anderson and Fouad, 2003; Basu and Aiswaarya, 2009).

The crisis of concern (www.ethesis.nitrkl.ac.in) is one where a power system operating in a steady load condition is perturbed, making the re-adjustment of the voltage angles of the synchronous generators. If such an incidence generates disturbance between the system supply and load, it consequences in the creation of a new steady-state operating condition, with the successive change of the voltage angles. The perturbation might be a main disturbance such as the loss of a generator, loss of a line, or a fault or the mixture of such occurrences. It can also be a few loads or arbitrary load varies happening under normal operating conditions. The time for amendment to the new operating condition is named the transient period. The network performance through this time is called dynamic system performance, which is of major concern in defining system stability. The major principle for stability is that the synchronous generators retain synchronism at the end of the transient period. Hence one can say that if the oscillatory reaction of a power system for the duration of the transient period following a disturbance is damped and the system resolves in a finite time to a new steady operating condition, the system is stable. If the system is not in steady state, it is regarded as being unstable. This fundamental description of stability requires the system fluctuations to be damped. This situation is sometimes

termed asymptotic stability, which means that the system has inborn forces that have a propensity to decrease oscillations. This is an advantageous characteristic in various systems and it is regarded as essential for the power systems.

The description also eliminates constant swinging from the relations of stable networks, even though oscillators are stable in a mathematical sense. The rationale is practical in view of the fact that a frequently oscillating network would not be advantageous for both the supplier and the consumer of electric power. Therefore the description explains a practical requirement for an adequate operating condition. The stability predicament is concerned with the performance of the synchronous generators after a disturbance. For expediency of analysis, stability obstructions are commonly separated into two main categories - steady state stability and transient state stability (Anderson and Fouad, 2003; Basu and Aiswaarya, 2009; www.ethesis.nitrkl.ac.in).

The chapter is important for some of the steps of the methods for model order reduction. The motion for “transient stability” (www.waset.org) is used in order to compare the dynamic behaviour of the full and reduced order models in Chapters 4-7. This chapter describes the following points in the field of power system stability:

- Transient stability studies
- Small and large disturbance stability
- Synchronous machine stability basics
- Swing equations
- Stability enhancement
- Rotor angle stability
- Voltage stability
- Stability and model order reduction
- Power system security assessment
- Power system operating states
- Digital time simulation in power system studies, and
- Dynamic behaviour of power systems

Section 3.1 presents transient stability analysis studies in power systems. In section 3.2, the following parts have been explained in details:

- Small disturbance stability
- Large disturbance stability
- Swing equations
- Rotor angle stability, and
- Voltage stability.

Section 3.3, constitutes the relationship between the stability analysis and the model order reduction while section 3.4 constitutes digital time simulation in power systems. Consequently, section 3, 5 offers the conclusion of the chapter.

3.1 Transient stability studies

The transient stability studies engage the purpose of whether or not synchronism is retained after the generator has experienced harsh faults. This can be unexpected application of load, loss of large load, loss of generation, or a fault on the system. In the majority of disturbances, oscillations are of an extent that linearization is not acceptable and the nonlinear swing equation (www.ethesis.nitrkl.ac.in) must be worked out. The manner in which a system responds to a large disturbance such as short circuit or line tripping is a basic assessment technique to calculate the reduced order model of this power system. It is the problem of large disturbance stability analysis, and the consequence that such a disturbance has on the system performance. This analysis is called transient stability analysis (Kundur, 1994; Anderson and Fouad, 2003; Aiswaarya, 2009**;** Prajapati, 2011).

An assumption is considered that before the abnormal condition occurs, the power system was working at some initial stable steady state operating condition. The power system transient stability problem is defined as that of assessing whether or not the system will reach an acceptable steady operating state. Evidently, in order to confirm the system transient stability, according to the various initial conditions and diverse disturbances, profuse calculations must be done. During these processes, the power system behaves as a nonlinear system which requires application of nonlinear differential equations for its representation. There are two methods to approximate the transient stability problem - the time simulation technique and the transient energy function technique (Chen, 2009; Prajapati, 2011)

3.2 Small disturbance stability

If the amount of the disturbance is sufficiently small such that the system response in the initial stage is basically linear, the stability may be classified as small-disturbance stability (or small signal stability, or stability in the small) (Kundur, 1994).Small-disturbance stability is guaranteed if the eigenvalues of the suitable dynamic model, linearised about the equilibrium point, have negative real parts. If there is an eigenvalue with positive real part, the system is not stable. Complex eigenvalues arise in conjugate pairs. They indicate oscillations, with the negative real parts dampened out. Note that when a linearised model predicts instability (one or more eigenvalues with positive real part) it does not inevitably follow that the oscillation

amplitude following a disturbance will boost indefinitely. As the oscillation amplitude increases beyond a certain point, system nonlinearities and equipment restrictions may play a prevailing role and a limit cycle may be reached. Hence, the true system response can only be achieved via a solution of the complete nonlinear model. It should be noted that, in certain small disturbance situations, equipment limit may be encountered so that linearisation may not be permissible and the stability should not be classified as such (Kundur , 1994).

Even though negative real parts of eigenvalues of the linearised system provide sufficient conditions for small-disturbance stability, in some situations, other simpler criteria may be applicable. Information on small-disturbance stability can also be obtained from the solution of the original non-linear equations, utilising a small but finite disturbance.

3.2.1 Large disturbance stability

Large-disturbance stability is guaranteed if the system state at the end of the disturbance lies within the region of desirability of the stable equilibrium state of the post-disturbance system. The consideration of large-disturbance stability would normally necessitate mathematical simulation. The meaning of the idea of the region of desirability is that, in some situations, it can be determined with a priori that the disturbed state is within the region of desirability of the stable post disturbance equilibrium, thus preventing the need for numerical simulation (Pal, 1972; Anderson and Fouad, 2003).

At the point where the receiving system requires a small additional load ΔP, the generator becomes just unable to deliver without a change in the field excitation. This point corresponds to the steady state stability limit. Therefore, the limit $\frac{dP}{d\delta} = 0$.

Where, P is the active power

δ is the rotor angel

This is the condition at which $P = 0.85$, and $\delta = 90^0$, where $\frac{dP}{d\delta}$ is measured on curve *c* of **Figure 3.1** (Pal, 1972; Anderson and Fouad, 2003). If a higher load is taken, the initial angle is greater than 90^0 , and $\frac{dP}{d\delta}$ becomes negative, when measured along the corresponding power angle curve for constant field excitation, (Pal, 1972; Anderson and Fouad, 2003).

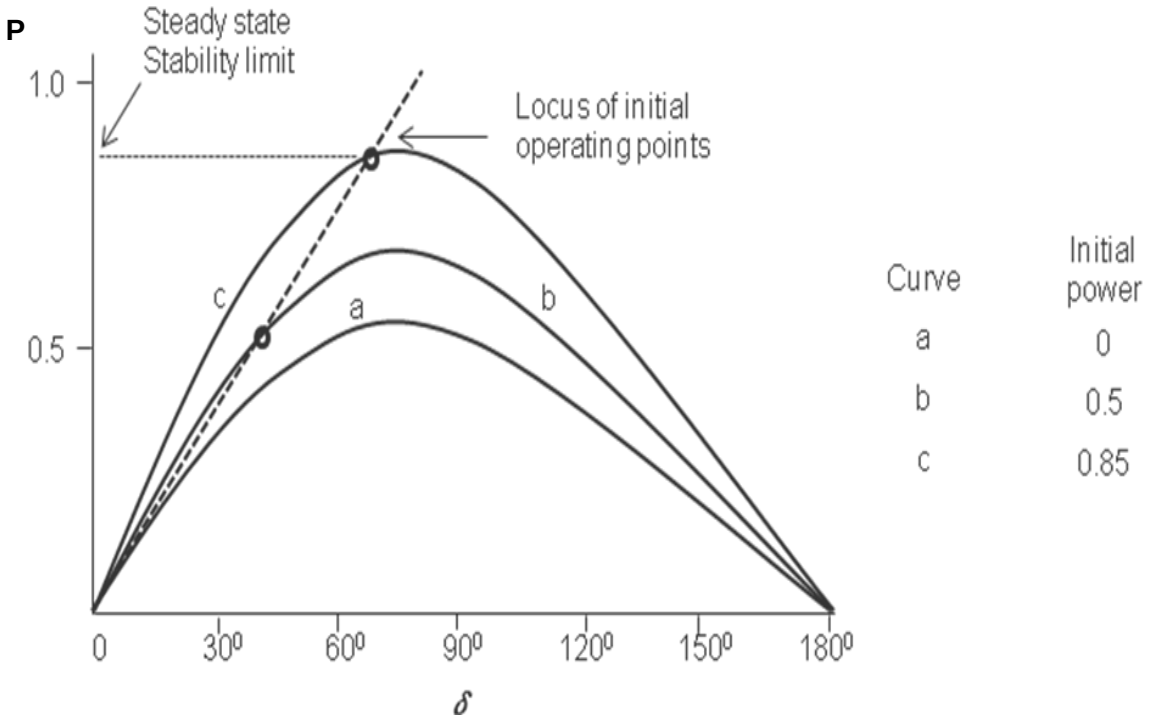

Figure 3.1: Power behaviours as a function of angle at invariable field excitation, showing determination of steady state stability limit (Pal, 1972; Anderson and Fouad, 2003)

3.2.2 Synchronous machine stability basics

The check of the transient stability of the operation of the synchronous machine requires an analysis of the solution of a system of coupled non-linear differential equations. Generally, no analytical solution of these equations is present. Nonetheless, techniques are available to achieve approximate solution of such differential equations by numerical methods and one must then resort to numerical computation techniques, usually known as digital simulation (www.ethesis.nitrkl.ac.in; Pal, 1972; Anderson and Fouad, 2003).

3.2.3 The swing equation

When the system is under normal operating conditions, the position of the rotor axis and the resultant magnetic field axis are fixed. The angle between the two is known as the power angle or torque angle. Under fault conditions, rotor will either decelerate or accelerate with respect to the synchronously rotating air gap (www.ethesis.nitrkl.ac.in) Magneto-Motive Force (M.M.F), and a relative motion of the synchronous machines begins. Figure 3.2 (Pal, 1972) shows the above information.

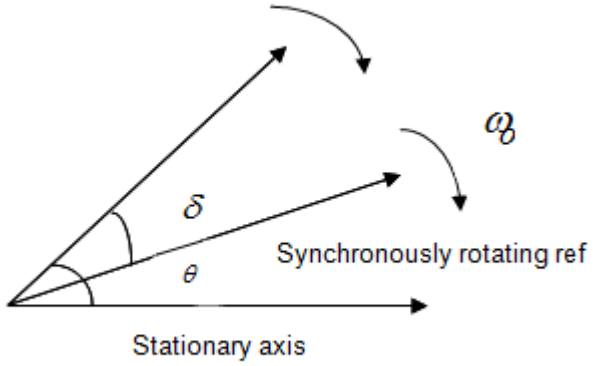

Figure 3. 2: Swing Equation Phenomena (Pal, 1972).

where,

w_o is the synchronous speed.

δ is the rotor angle in radians

θ is the rotor's mechanical angle in radians with respect to a fixed reference

The equation explaining this relative motion is known as the swing equation. If after the period of oscillation, the rotor locks back into synchronous speed, the generator will sustain its stability. If the disturbance is formed by a change in load, generation, or network conditions, the rotor approaches a new operating power angle relative to the synchronously rotating field.

Applying the laws of mechanics to the rotational motion of a synchronous generator, it can be written (Pal, 1972; Anderson and Fouad, 2003)

$$J\frac{d^2\theta}{dt^2} = T_a. \tag{3.1}$$

Where,

J is the rotor system's moment of inertia

T_a is the net torque acting on the machine.

The net torque T_a is the accelerating (or retarding) torque given by (Pal, 1972; Anderson and Fouad, 2003):

$$T_a = T_m + T_e \tag{3.2}$$

Where,

T_m is the shaft mechanical torque, corrected for rotational losses

T_e is the electromagnetic torque

In the steady state T_a = 0. If the angular position and velocity were measured with respect to a synchronously rotating reference axis, instead of a stationary axis (Figure 3.2), then

$$\delta = \theta - \omega_0 t \tag{3.3}$$

$$\frac{d\delta}{dt} = \frac{d\theta}{dt} - \omega_0 \tag{3.4}$$

$$\frac{d^2\delta}{dt^2} = \frac{d^2\theta}{dt^2} \tag{3.5}$$

Therefore, Equation (3.1) becomes

$$J\frac{d^2\delta}{dt^2} = T_a \tag{3.6}$$

Equation (3.6) can be written as

$$J\omega_0\frac{d^2\delta}{dt^2} = T_a\omega_0 \text{ or } M\frac{d^2\delta}{dt^2} = T_a\omega_0 \tag{3.7}$$

where,

$M = J\omega_0$ is the angular momentum.

At normal speed ω_0, the value of M is called the inertia constant of the machine. Equation 3.6 (Pal, 1972; Anderson and Fouad, 2003) can also be written in terms of the stored kinetic energy at rated speed, as follows:

$$\frac{2}{\omega_0}\frac{1}{2}J\omega_0^2\frac{d^2\delta}{dt^2} = T_a\omega_0 \text{ , or } \frac{2H}{\omega_0}\frac{d^2\delta}{dt^2} = T_a\omega_0 \tag{3.8}$$

Where,

$$H = \frac{1}{2} J \omega_0^2 \text{ or } H = \frac{1}{2} M \omega_0 \quad (3.9)$$

H is the inertia constant

The mechanical angle and speed are related to the electrical quantities by the relations

$$\delta = \frac{p}{2} \delta_m \ , \ \omega = \frac{p}{2} \omega_m .$$

Where,

p is the generator's number of poles

δ_m is the mechanical power angle

ω_m is the mechanical speed

While mechanical input and electrical output are usually expressed in terms of power, it is convenient to convert torque into power using the relation

$$T_m = p \, . \quad (3.10)$$

Therefore, equation (3.8) reduces to

$$\frac{2H}{\omega_0 \, p/2} \frac{d^2\left(\delta \frac{p}{2}\right)}{dt^2} = \frac{p_a}{\omega_m} \omega_0 \ . \quad (3.11)$$

Where P_a is the number of poles for generator a

The above derivation of the swing equation is done for the reasons as follows:

- To understand the notion of the synchronously rotating reference of the generator
- To know the relationship between the rotor speed, synchronous speed, and the rotor angular position with respect to the synchronously rotating axis
- The relationship between the acceleration and the mechanical torque of the generator.

The role of the swing equation in the power system stability studies is to determine rotor dynamics of the synchronous generators. Figure 3.2 gives relevant description of the phenomena of the swing equation.

In the north shell, the definition of the stability of power system is as follows:

A power system at a given operating state is stable, if following a given disturbance, or a set of disturbances, the system state stays within specified bounds and the system reaches a new stable equilibrium state within a specified period of time (Pal, 1972; Anderson and Fouad, 2003).

3.2.4 Stability enhancement

The enhancement of power system stability can be done, and its dynamic response enhanced by correct system planning, operation and design. Therefore, the following features assist to make better stability (Machowski et al., 1997):

- Ensuring a suitable reserve in transmission capability
- Use of single-pole circuit breakers so that during the faults such as single-phase fault only the faulted phase is cleared and the phases not affected remain intact
- Avoiding the operation of the system at low frequency and/ or voltage
- Application of protection schemes which ensure the fastest possible fault clearing
- The use of a system configuration that is appropriate for the special operating conditions
- Preventing weakening the network by the simultaneous outage of a large number of lines and transformers

3.2.5 Rotor angle stability

A synchronous generator is generating power by a direct current excitation of the field winding in the rotor. A rotating magnetic field in the field windings will induce an alternating voltage in the three phases of the stator. The frequency of the current and voltage in the stator windings depend on the speed of the rotor. The frequencies of the voltages and currents are in synchronism with the mechanical rotor velocity, hence the name, synchronous machine. The correlation between the power transfer to the loads and the rotor angle is very non-linear. The angle difference, or angle separation, is the sum of the angle that the generator rotor leads the field in the stator windings, the angle between the generator and the consumer, and the internal angle of the consumer. If the consumer is represented by a motor, the internal angle is the angle, which the rotor field lags the revolving field of the stator. When connecting a number of synchronous machines, the rotor frequency in all machines must be equal, otherwise the frequency of the power output will not be in synchronism. When one synchronous machine is faster than the others, the rotor angle of the faster machine will develop into larger one, relative to the rest of the machines (John, 2009; Kundur, 1994). This will result in an increased angle partition and increased power transmission until a certain limit. Above this limit, usually 90^0, the increased angle

partition will reduce the power transmitted, which will increase the angle partition further and the system can become unsteady.

The rotor angle stability depends on the generator rotor positions in the system, after a disturbance, which results in an adequate torque to re-establish the steady state operation. The rotor angle stability is affected if one or a group of synchronous machines are getting out of step. If the torque in each machine is not sufficient for regaining synchronism, it can lead to non periodical changes in the rotor angle separation. Rotor angle stability is split into two categories; small signal and transient signal (John, 2009; Kundur, 1994).

Small signal rotor angle instability happens constantly in the power system, attributable to fluctuations in the load as well as in the power production. A creation of small signal fluctuation is the balanced state form, where the rotor angle is increased for the reason of deficient synchronising torque. Rotor oscillation, which has rising amplitude, takes place in generators where the damping torque is inadequate to absorb the small signal fluctuations. Oscillations are the major small signal rotor angle stability crisis in the power system and have numerous modes (John, 2009; Kundur, 1994). It can happen as a confined phenomenon where single generating unit is oscillating in relation to the rest of the system. It can as well happen as one group of generators oscillate in opposition to another group. Groups of generators oscillating in opposition are frequently seen where two strong interconnected areas are weakly interconnected. The small signal instability is capable of also being associated to the system control, underprivileged tuning of exciters and turbine governors or in view of the fact of HVDC-converters and static Var compensators.

The shaft connecting the turbine and the generator can also generate small signal instabilities (John, 2009; Kundur, 1994).Transient rotor instability causes unsteadiness as a result of large transitory disturbances and it involves extensive excursions of the generator rotor angle (John, 2009; Kundur, 1994). The transient rotor angle stability is influenced by the correlation among rotor angle partition and the power flow transfer. The response is reliant on the preliminary conditions and how harsh the disturbance is. Transient stability is frequently sustained, due to the safeguards taken in the phase creation. For instance, various forms of faults' impact on the stability are inspected and corrected. Transient faults have three particular characteristics, as listed below, and their responses are illustrated in Figure 3.3 (John, 2009; Kundur, 1994), where:

.

Case 1: The rotor angle is increasing to its maximum value, and subsequently it reduces its amplitude oscillation in anticipation for a steady state.

Case 2: Generally, this is called the first swing instability. The rotor angle is increasing in anticipation for a loss of synchronism. The rotor angle does not go back to the steady state due to lack of synchronising torque (John, 2009; Kundur, 1994).

Case 3: The third type of instability will sustain stability in the first swing and subsequently turns out to be unstable. This response frequently happens and it is attributable to an initial condition, including small signal instability.

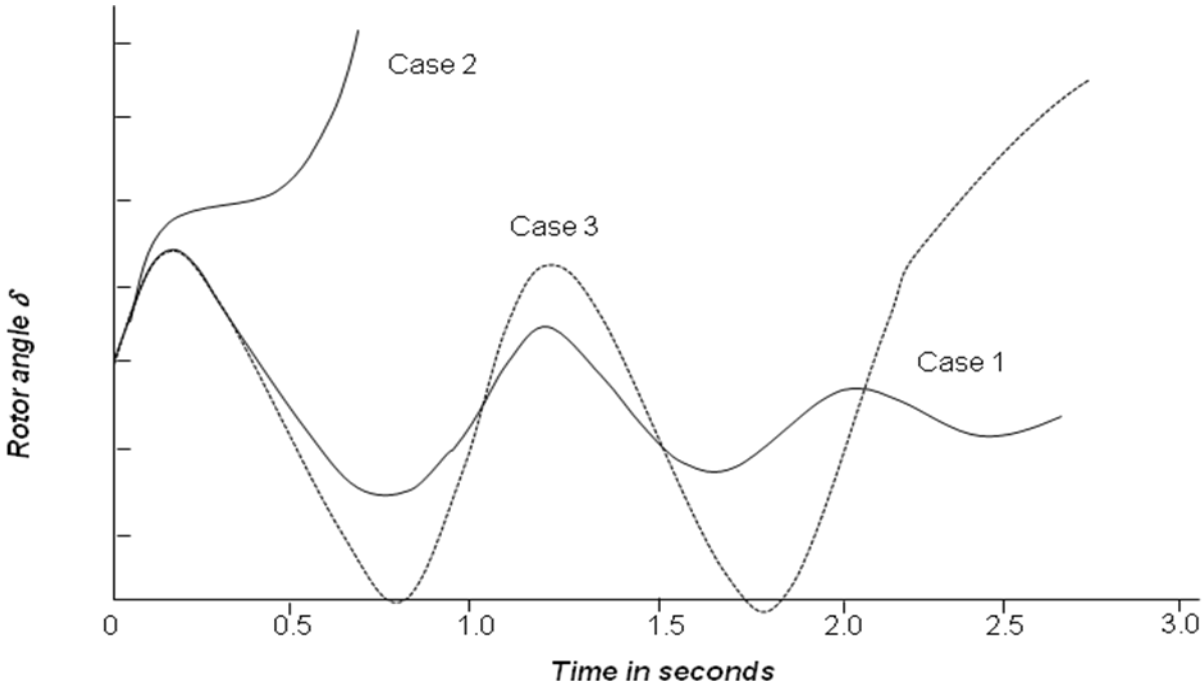

Figure 3. 3: **Rotor angle response to a transient disturbance (John, 2009; Kundur, 1994).**

3.2.6 Voltage stability

Voltage stability is defined by the capability of a power system to sustain balanced acceptable voltages at all the buses in the entire system under normal operating conditions as well as after experiencing a severe disturbance. Voltage instability distresses the capability of sustaining a satisfactory stable voltage on each bus-bar in the power system, both throughout steady state operation and subsequent to a fault. The major justification for voltage instability is insufficient reactive power in the system: It can be formed by the transmission of active and reactive power through inductive transmission lines. Voltage instability is frequently associated to rotor angle instability. If the rotor angle partition is out of step, for instance, a constant decrease of synchronism, the voltage will drop. Voltage stability is sustained if the voltage on all bus-bars in the power system rises as the reactive load on the same bus bar

increases. If this principle is not satisfied on one bus-bar, the power system is not in voltage equilibrium per definition (John, 2009; Kundur, 1994; Barbier and Barret, 1980).

The voltage stability depends on the voltage, the active power as well as the reactive power in the system. In Figure 3.4 (Kundur, 1994) the correlation linking the above three quantities is shown (Kundur, 1994).

Where,

V_R is the receiving end voltage

V_S is the sending end voltage

P_R is the receiving end power

The dotted line signifies the limit for suitable operation point. An impulsive alteration in the power factor will cause an increase in the reactive power output and thus the operating point is situated below the dotted line. Consequently the operation conditions will be tedious and perhaps unsteady. Voltage stability issues can arise from small disturbances and extensive disturbances that create voltage instability. Extensive disturbances may possibly be system faults such as loss of a generator. Small disturbances may possibly be attributed to fluctuations in demand (John, 2009; Kundur, 1994; Barbier, and Barret, 1980).

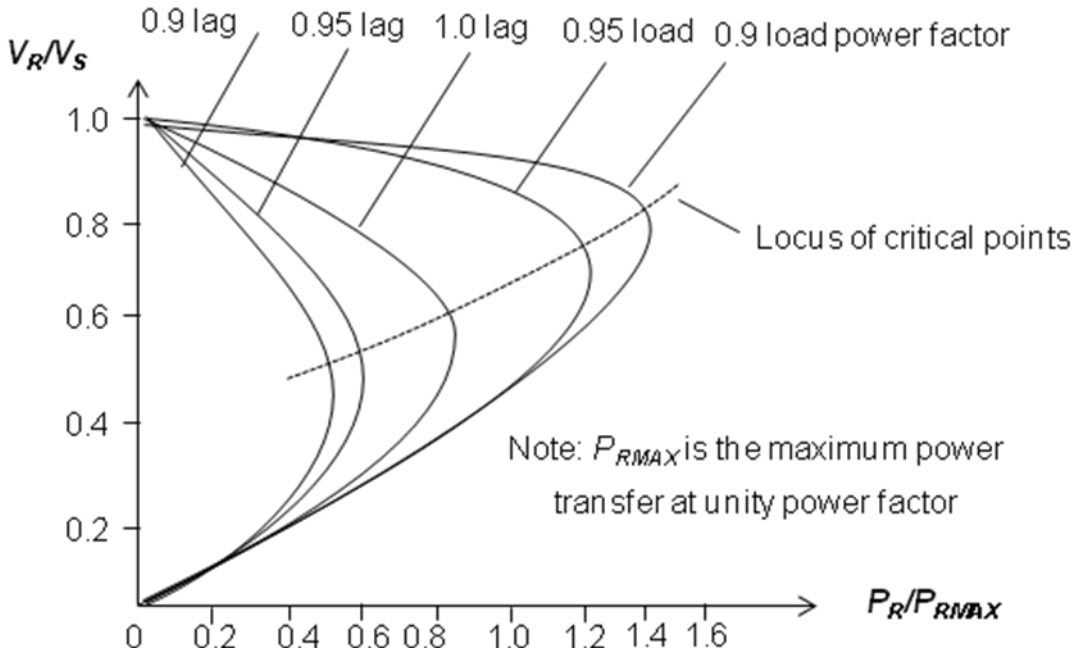

Figure 3. 4: **Voltage-power characteristics with different load-power factors (Kundur , 1994)**

3.3 Stability and model order reduction

In accordance with what has been explained before in this chapter, power system stability is a broad issue in the field of power engineering. It can be classified as shown in Figure 3.5 (Kundur, 1994).

Angle stability, voltage, and transient stability analysis are utilized in the algorithms of the model order reduction according to Chapter two knowledge and these are used for coherent identification of generator after being subjected to the disturbance and comparison between the full and the reduced models

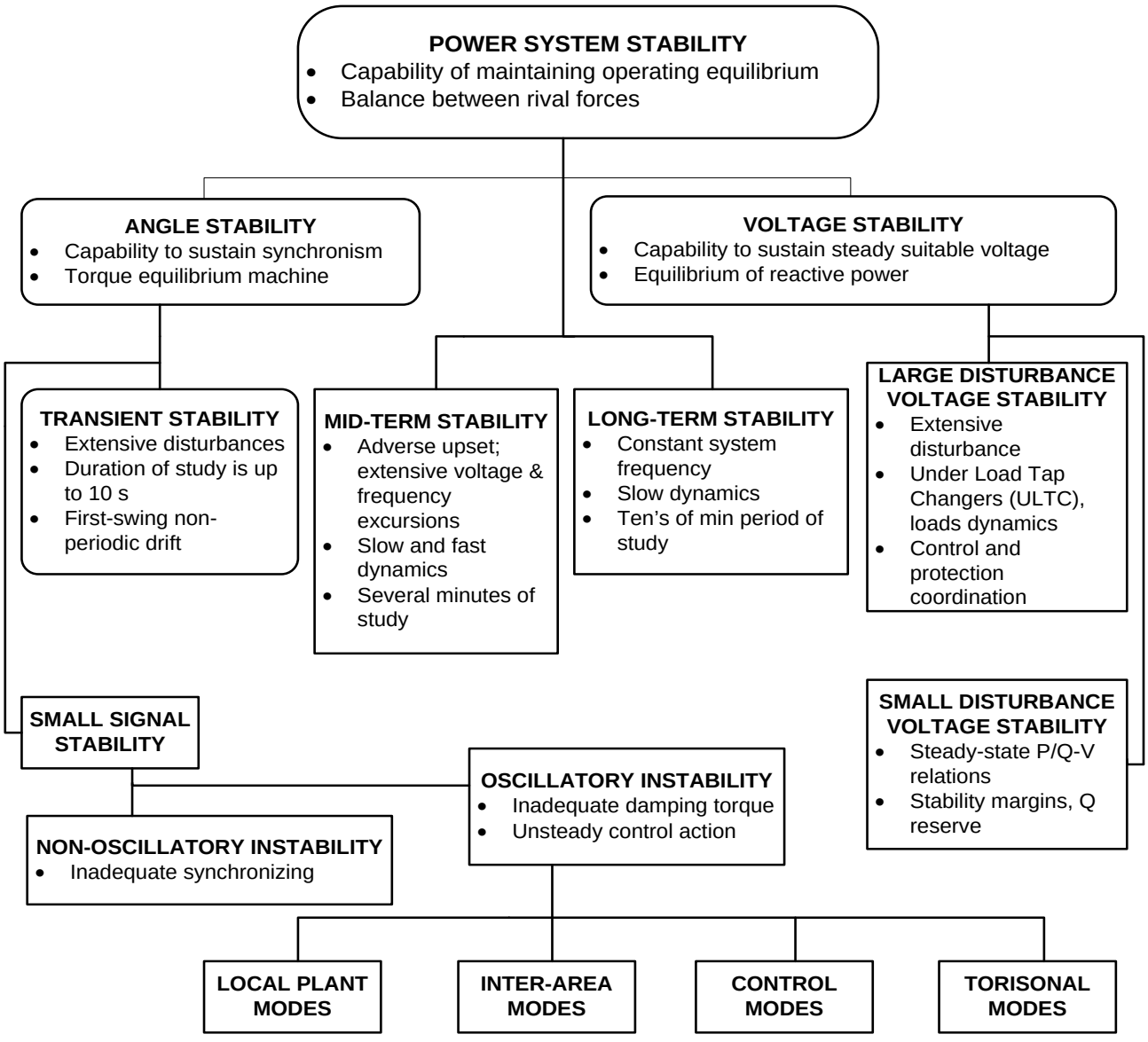

Figure 3. 5: Classification of Power System Stability (Kundur, 1994)

3.4 Digital time simulation in power system studies

For the reason that, the scale of power networks is very large and their structures and components are complicated, it is not easy to build and maintain a scaled down physical model of a power system with suitable accuracy. This makes power system models to require sophisticated simulation tools for the system study. Digital time domain simulation is very essential because most of the algorithms for simulations are based on numeral methods. This type of simulation can be understood as a set of algorithms run on computers, on which the nonlinear differential equations are evaluated by applying step-by-step numerical integration techniques.

Power system models characteristics can be well simulated by nearly selecting models, algorithms, and time step size.

Since the 1960's, digital time-domain simulator tools have been extensively used in power system studies. In many areas, such as transient stability analysis, switching over-voltage analysis, power electronic studies etc, and digital time-domain software for simulation has become the industry standard tool. There are many factors that lead to the popularity of digital time-domain simulations, some of which are:

- A single component of the power system such as a synchronous generator can be very complex and often requires very detailed time domain modelling to represent the full range of phenomena.
- The time frames of the important behaviours of the power system range from microseconds to hours. For example, a voltage collapse may involve induction machine stalling, which happens in a couple of seconds, transformer tap change, whose time frame is tens of seconds, Automatic Generation Control (AGC) actions, whose time frame is minutes, and many other actions with time frames ranging from second to tens of minutes. There are very complex interactions between these behaviours. The time domain simulation is the only accurate way to study these behaviours.
- Modern power systems are very large dynamic systems. Dynamic interactions between equipments are critical to the power system. Steady state analysis methods like power-flow are not sufficient for studying the power system. (Xi , 2010; Yuefeng, 2011),
- Many components of the power system have nonlinear characteristics, as well as non-continuous characteristics.

Power system dynamic characteristics consists of several transient phenomena. A simple classification of these phenomena is given in Figure 3.8 (Watson and Arrillaga , 2003; Xi , 2010; Yuefeng , 2011).

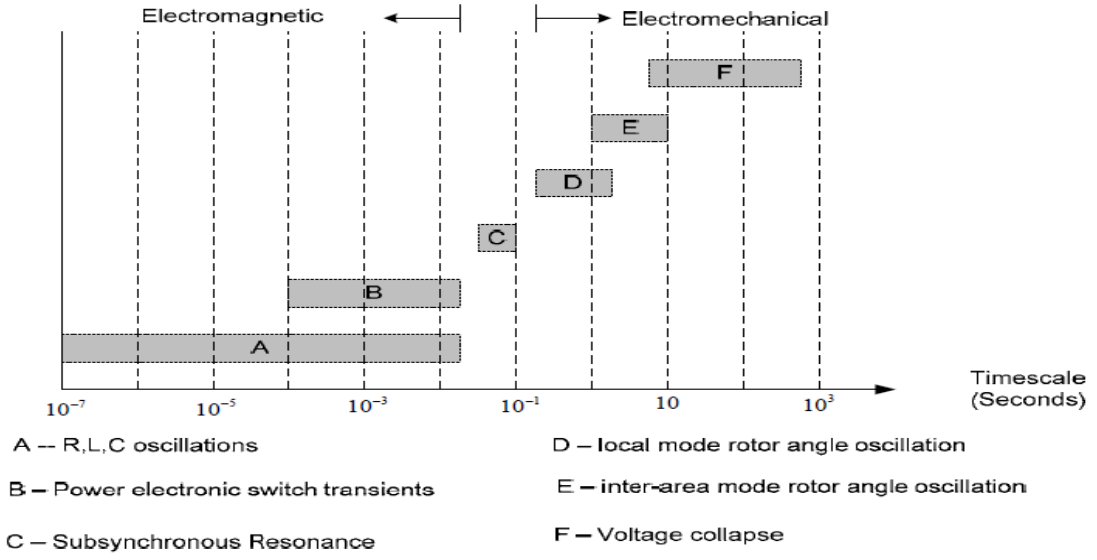

Figure 3. 6: **Time Frames of Power System Dynamics (Watson and Arrillaga, 2003; Xi, 2010; Yuefeng, 2011).**

By appropriately choosing the models, algorithms and time-step sizes, power system behaviours can be well emulated, predicted and studied. Normally there are two major types of digital time domain tools used in power system studies, namely Electromechanical Transient Simulation and Transient Stability Analysis (TSA), commonly used for predicting whether a large power system can regain an acceptable equilibrium point after experiencing large disturbance. The main concerns on such studies are both dynamic characteristics components and dynamic interactions between them which can cause large energy flow variations. Electromagnetic Transient (EMT) simulation focuses on simulating the detailed behaviour of the components of the power system. The major applications of EMT simulation tool are to simulate very detailed switching transients (Yuefeng, 2011; Xi, 2010). This simulation is normally called instantaneous value simulation of electromagnetic transient phenomena. Shorter times constant parameters are involved in this method of simulation, as a consequence, components of power system model are complex. The equations of the power system model require the time step in μs to be used in computations (Ejigu, 2009).It focuses on emulating the detailed behaviours of the components of the power system, such as voltage spikes, current surges, voltage and current waveform distortions, harmonics etc. As power electronic devices are widely applied in modern power systems, simulating the very detailed semiconductor switching transients has become one of the major applications of EMT simulation tools (Xi, 2010; Yuefeng, 2011).

EMT and TSA simulation tools have been developed separately since the 1960s. The TSA simulation tool is mainly used for predicting whether a large power system can regain an acceptable equilibrium point (stable and secure) after being subjected to

big disturbances, which may include short circuit fault; disconnection of lines, transformers, and generators; controls misbehaviour; or the so called *contingencies* . In such studies, the dynamic behaviours of large inertia power system components and the dynamic interactions between them which cause large energy flow variations are of main concern. In such methods, the major part of the electrical network can be represented as a quasi-steady state Phasor model, with the large inertia components being represented with time domain differential equations (Xi, 2010; Yuefeng, 2011).

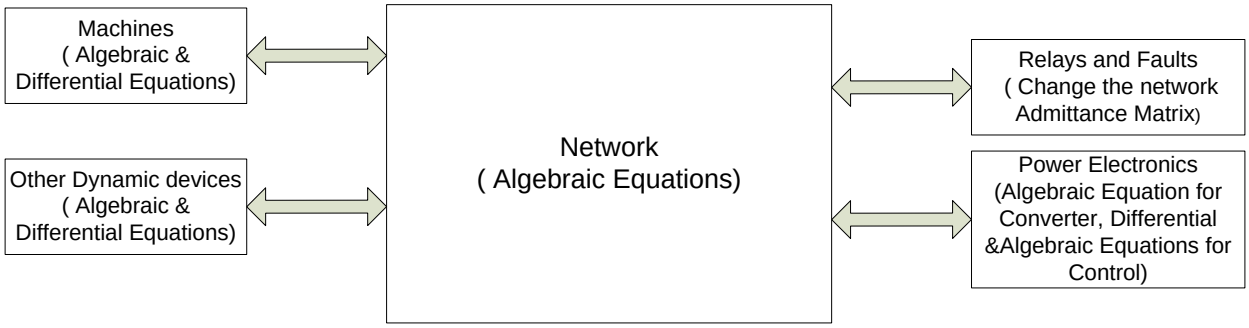

Figure 3. 7: Structure of the power system model for TSA simulations (Xi, 2010; Yuefeng, 2011)

TSA simulation does not consider instantaneous AC voltage and current waveforms. This type of simulation is mostly using algebraic equations of phasor quantities more than the differential equations. With the assumption that, the frequency of the power system model is close to the fundamental frequency, the system is represented by a complex admittance matrix. Also the disturbances such as faults are modelled by effective impedance in the system. Figure 3.7 shows the structure of the power system model for TSA simulations.

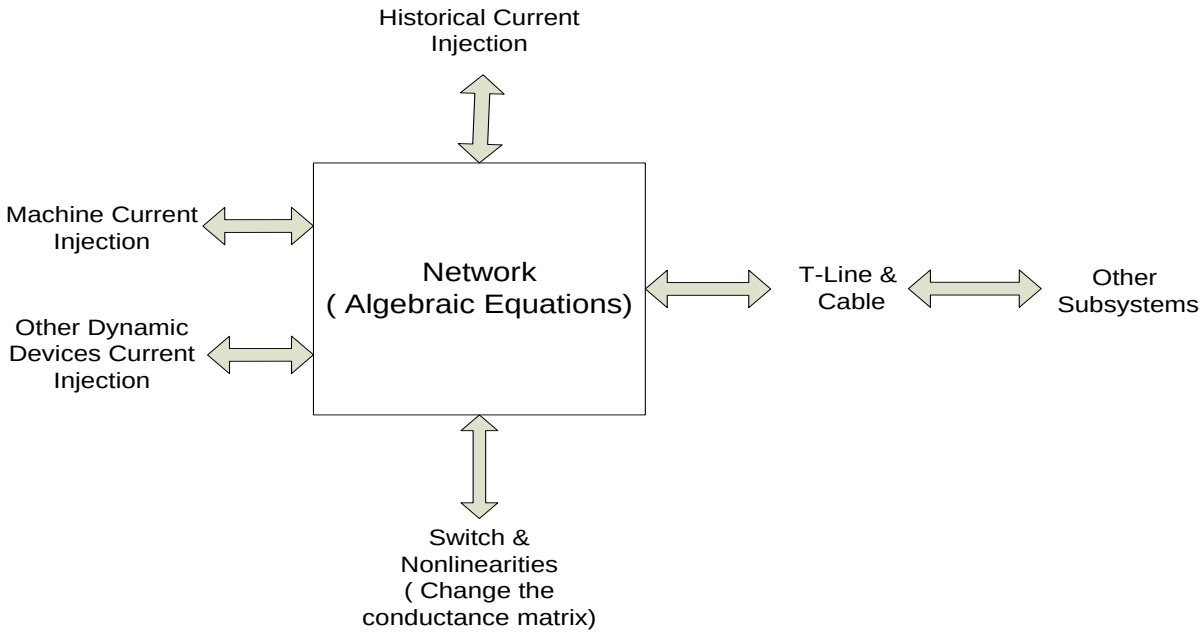

Figure 3. 8: Structure of the power system model for EMT simulations (Xi, 2010; Yuefeng, 2011)

EMT model structure deals with all transmission and electromechanical elements modelled using detailed differential equations. Transformation of differential equations into an equivalent constant conductance which is in parallel with history current components is conducted. Figure 3.8 depicts the structure for EMT model simulations. Therefore, all the power system components can be reduced to the Norton equivalent form, to evaluate the whole system. This is done by using trapezoidal integration rule (Xi, 2010; Yuefeng, 2011).Table 3.1 gives the differences between the EMT and TSA tools for simulation. The EMT model type of simulation will be used for the simulation case studies in this research.

Table 3. 1: Comparisons between the EMT and TSA

EMT	TSA
Real physical values such as instantaneous voltage and current are directly computed.	Built in the fundamental frequency, positive sequence, Phasor domain
Covers all the phenomena from A to F in Figure 3.8	TSA simulation cannot simulate the phenomena from A to C in Figure 3.8
Needs long time for culculation	

In this thesis, both RSCAD and DigSILENT software packages are utilised to fulfil the objectives of the project. Table 3.2 depicts the summary comparison between the two software packages. Real Time Digital Simulator (RTDS) performs real time execution of EMT simulations. To accomplish real-time simulation speeds, the power system to be simulated is alienated into parts by using the travelling wave attribute of transmission lines. The relativistic speed limit permits full partition of the systems if simulation time step is less than the travelling time of light over the transmission line distance. DigSILENT is the simulation platform for power systems analysis applications at generation level, transmission level, distribution level, and in industrial systems (www.rtds.com; www.DigSILENT.de).

Table 3. 2: Comparisons between the DigSILENT and RSCAD

Component Model		DigSILENT	RSCAD
	Transmission Line Model	PI- Model Distributed Line Model	PI- Model Distributed Line Model
	Static Load Model	Exponential and ZIP Load ((Z) Impedanc, (I) constant current, and (P) constant power)	Exponential and ZIP Load ((Z) Impedanc, (I) constant current, and (P) constant power)
Solution Method	Load Flow (Iteration method)	Newton-Raphson	Newton-Raphson
	Dynamic Solution (numerical integration)	Variable Step Trapezoidal	Variable Step Trapezoidal
	Simulation Time Step	User defined in µs or ms	User defined in µs
User Interaction	Event Definition and Modelling	GUI and using DigSILENT Programming Language (DPL) or Data Definition Language (DDL)	GUI using the Library Components
	Data Input	GUI Input Window	GUI Input Window
	Data Output/ Display	Graph	Graph
Simulation Type	Electromagnetic Transient	Yes	Yes
	Dynamic Simulation	Yes	Yes

Subsequently the complicatedness of power system simulation analysis and element modelling is based on the required phenomena under research (Ejigu, 2009). Figure 3.9 depicts the dynamic system characteristics. Both transient and electromagnetic characteristics are being used in this thesis.

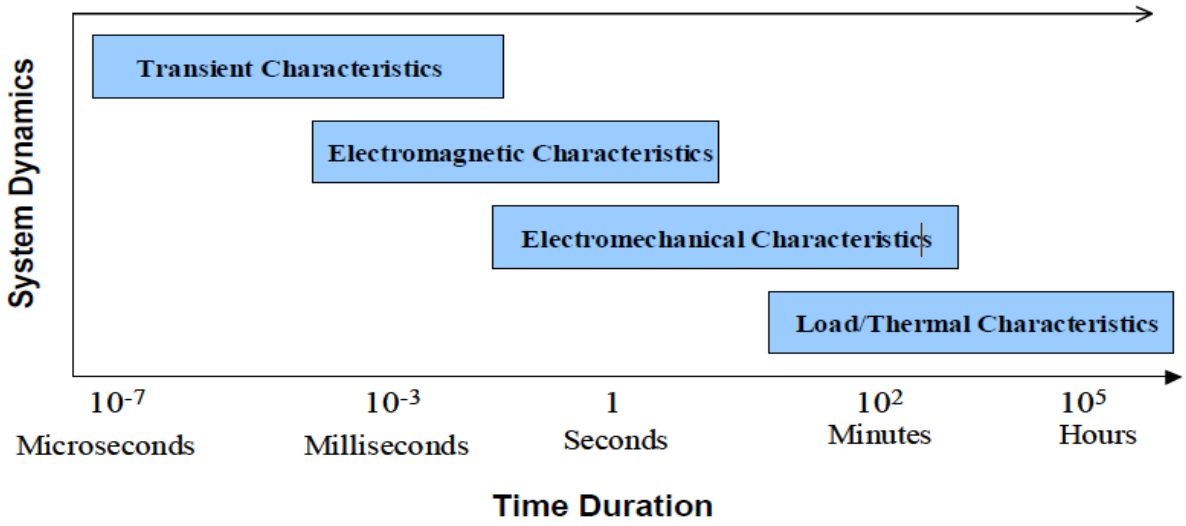

Figure 3. 9: Spectrum of power system dynamics (Xi, 2010; Yuefeng, 2011)

3.5 Conclusion

As previously mentioned in Chapter 2, the complexity of power system networks is increasing. This chapter studied the power system stability which involved voltage stability, transient stability, small and large stability, synchronous machine stability as well as rotor angle stability. A brief description on how to enhance stability was also dealt with. The main issue is to learn how to ensure that, the power from the point of generation to the end consumer is reliable. In reality, power system networks are continuasly changing. The change in demand for electricity necessitates instantaneous changes in electricity production. As a result of this, voltages, currents, and power flows are dynamically changing at all times, across the power grid. The main challenge is to make sure that the changing power system operating conditions remain within the safe limits in the present and during the potential future contingencies. Unstable oscillations of power system models can lead to a total blackout, therefore it is essential to maintain the stability of power systems.

With a view to reduce the power system networks models order in the real sense, simulations need to be put in place. This allows the power system network engineers to study the behaviour of the network before and after reducing their models. Network model order reduction is necessary in order to make troubleshooting easy for the network engineers. A simulation mostly is needed for the planning, operation and designing of power system networks. Accurate model reduction does not affect the characteristics of the networks both at their complex and the reduced states.

The simulation of 9- bus IEEE network in Chapter 4 considered the characteristics of both the full and the reduced networks as one of the important point of the model order reduction algorithm.

CHAPTER FOUR
DEVELOPMENT OF COHERENCY-BASED ALGORITHMS FOR MODEL ORDER REDUCTION

Introduction

This chapter describes the application of Coherency based technique to develop reduced models of a power system. Procedures and algorithms are developed to implement the main steps of the coherencybased method. Generally, dynamic equivalencing techniques can be categorized into two groups: coherency-based technique (Joo, et al, 2004; Podmore, 1978; Smith et al., 1976; Hussain and Rau, 1993), and modal equivalencing techniques (Nishida and Takeda, 1984; Olivera and Massaud, 1988; Chow, 1993). The process of equivalencing for coherency methods is made-up of three main steps:

- Coherency identification,
- Aggregation of coherency generators, (Inertial aggregation and slow coherency) and
- Network reduction

The coherency based method is the most used one in literature. This method allows an observable relationship with the initial model and is computationally attractive in comparison to the modal based methods (Chen, 2009). It is necessary to investigate how the full application of Coherency method expressed by the selected three steps in the reduction algorithm will reduce the error between the initial full and the obtained reduced model. Comparison of the two models is done in the thesis using RTDS (Real-Time Digital Simulator).

Section 4.1 describes the theoretical background of the study, explains the algorithm of coherency based method, constant admittance representation of load buses and Kron's node elimination algorithm. IEEE 9-bus system reduction studies are covered in the whole of section 4.2 .While section 4.3 deals with coherency procedures for the reduction of IEEE 9-bus system and the application of coherency- based method to IEEE 9-bus system. All the results obtained during the process of reduction, verification and the comparison of the results are deployed in section 4.4. Load flow results of the reduced model are also presented in this section. Section 4.5 presents the discussion and recommendation of the study. Consequently, section 4.6 concludes what has been achieved during this study.

4.1 Theoretical background of the coherency based method

The literature review has shown that different calculation procedures/methods can be selected to perform the process of the power network reduction. Different criteria can

be used to select between these procedures. The criteria considered in the thesis are:

- The capability of the procedure to keep physical connection between the full and the reduced model,
- The capability to implement the process of reduction with simple and low number of calculations and transformations.

On the basis of above the following procedures are selected to implement the three steps of the Coherency-based method:

- Division of the power system model of a study and external areas.
- Determine the slack generator.
- Apply the fault in the study area.
- Solve swing equations.
- Analyse the swing curves to determine the groups of generators.
- Aggregation of the coherent generators (Inertial aggregation).
- Application of reduction using the Kron's method.

If the angular speed oscillations, and phase voltages of the coherent generators in a constant complex ratio are the same, they can be grouped together. A coherency of generators can be depicted as the similarity of the behaviour of the generators after being subjected to a disturbance. A coherency method has three steps but implementation of these steps can be done by application of different calculation procedures as implemented in the previously selected "study" and "external areas" of the power system model.

Linear Time simulation of the full and reduced models is used. This type of simulation is used to identify coherent generators. Decomposition based Gaussian elimination is used to aggregate coherent generators and finally Kron's elimination method is used to do network reduction. The reduced admittance matrix is used to draw the reduced power system model. Validation of the results is based on the requirement for <5% difference between the full and the reduced models.

4.1.1 Step 1: Coherency identification

Step 1 starts with divition of the one-line diagram of the power system in two areas: study and external. A three phase fault is applied to the study area. Linear time simulation of the transient behaviour of the full model as a result from the three phase short circuit is performed in order to identify coherency of the generators.

Assessment of the behaviour of rotor angle during the model transient behaviour has become a serious matter in power system engineering field. There are two major methods to evaluate rotor angle which are (Olulope et al., 2012);

- Centre of Inertia (COI), and;
- Considering one generator as a reference generator (Olulope *et al.*, 2012).

The second method of a reference generator is used in the thesis.
The aim of this step is to determine groups of coherent generators in the external area. It is based on application of a fault in the study area of the model and simulation of the power system in order to obtain transient behaviour of the generator rotor angles.
This research utilized the method of linear time simulations to receive the transition behaviour of the generators in the external area.

Linear time simulations technique uses an assumption that coherent generators are grouped independently from the magnitude of the disturbance and the complete generator model. The selection of the coherent generators can be done using different criteria for comparison of the behaviour of the rotor angle curves as Coherent Index, Weak Links Method, Hilbert-Hang transform, Relation Factor, Modal analysis, Hierarchical clustering, Non-linear time simulations, Linear time simulations, Unstable equilibrium point, Principal Component Analysis, Equal acceleration and velocity, Moment matching method, Artificial neural networks, Generator speed measurements with Fourier analysis, and Two time scale method (Nath et al.,1985; Singh et al., 2011). In Chapter 3, the swing equations were explained. The Equations (4.2- 4.4) are used to model the power system dynamic behaviour for typical fault clearing times in a modern day power system. Swing equations model represents the dynamics of synchronous generators on departure from equilibrium. These equations can be described as the rotor dynamic equations for synchronous generators of the power system or, dynamic model of synchronous generators for the stability analysis which includes the non-linear machine model representation of the synchronous generator. Therefore, the following assumptions are considered to model synchronous generators dynamic responcea to electrical disturbances in power system network:

- Under normal conditions, the relative position of the rotor axis and the stator magnetic field axis are fixed (www.eng.fsu.edu).
- The angle between the two is the power angle or torque angle.
- During a disturbance, the rotor will accelerate or decelerate with respect to the rotating stator field.

- Acceleration or deceleration causes a change in the power angle (www.eng.fsu.edu).

The non-linear equations for the dynamical power system transient behaviour are represented as follows:

$$\frac{d\delta_i}{dt} = \omega_i \tag{4.2}$$

$$M_i \frac{d^2\delta i}{dt^2} = P_i - P_{ei} - \frac{M i}{M_T}(P_{mr} - P_{er}) \tag{4.3}$$

$$P_{ei} = D_{ii} + \sum_{\substack{j=1, j\neq i \\ i=1,n}}^{n} C_{ji}\left[\sin\left(\delta_{ir} - \delta_{jr}\right) + D_{ij}\cos\left(\delta_{ir} - \delta_{jr}\right)\right] \tag{4.4}$$

Where,

$$D_{ij} = E_i E_j E_{ij}, \quad C_{ij} = E_i E_j B_{ij}, \quad Y_{ij} = G_{ij} + jB_{ij}, \quad M_{ij} = \frac{M_i M_j}{M_i + M_j}$$

n is the number of the generators,

δ_i is the i th generator angle

ω_i is the angular speed deviation with respect to synchronous speed of reference machine,

M_i is the i^{th} generator inertial constant,

D_i is the damping coefficient for the i^{th} generator

P_{mi} is the i^{th} generator mechanical power

P_{ei} is the i^{th} generator electrical power

E_i is the i^{th} generator voltage behind transient reactance,

Y_{ij} is the element between generator internal buses i ,and j of the post fault system.

B_i is the i^{th} generator susceptance.

G_i is the i^{th} generator conductance.

The results from the simulation are used to determine which of the generators in the external area are coherent.

Coherency Index (CI) is introduced in order to verify if grouped generators swing together utilizing Equation (4.1) to get CI between a pair of generators (Podmore, 1978; Singh et al., 2011).

$$C_{ij} = \max\left|\Delta\omega_i(t) - \Delta\omega_j(t)\right| f_0 \quad (4.1)$$

Where, C_{ij} is the coherency Index between generators i and j

$\Delta\omega_i(t)$ is the rate of change of the angular speed for a generator i

$\Delta\omega_j(t)$ is the rate of change of the angular speed for a generator j

f_0 is the frequency in hertz.

This is a means of evaluating a degree of coherency between the i^{th} and the j^{th} generators. The nature of swing equations of the generator can be further compared using C_{ij} tolerance which is specified by the practitioner.

The algorithm for completion of the step 1 is:

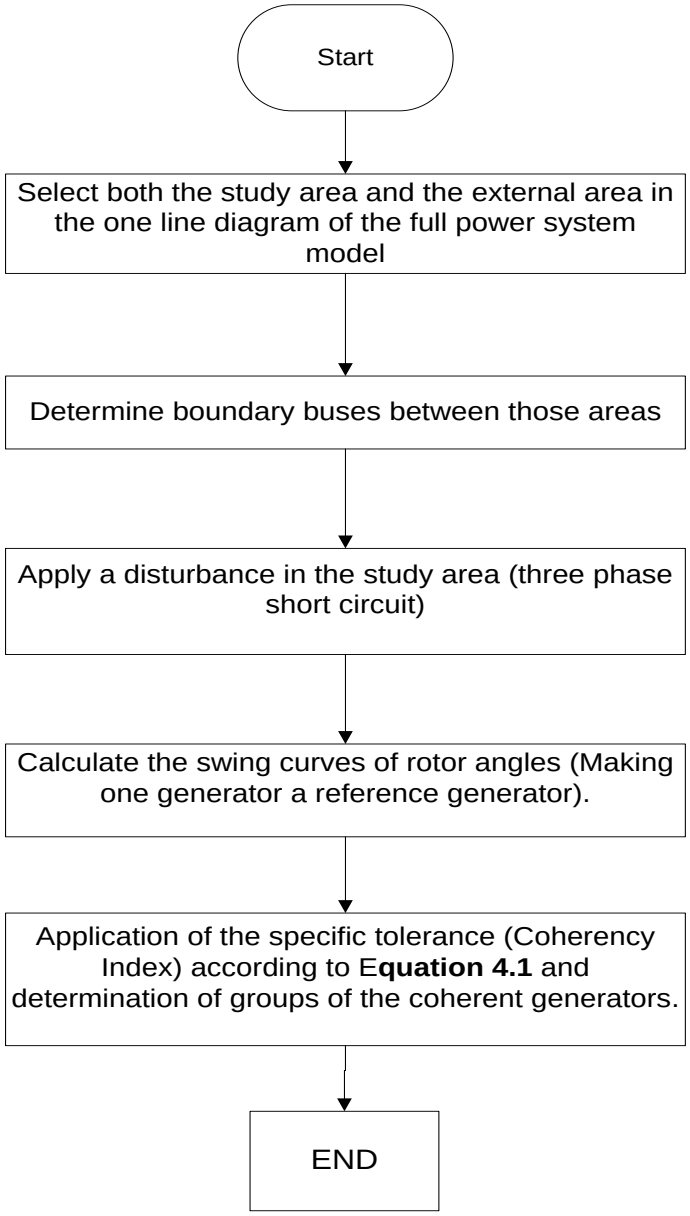

Figure 4.1: **The flow chart of the step 1 of the coherency based method**

Simulation procedures in DigSILENT software are given in Appendix A.

4.1.2 Step 2: Aggregation of the coherent generators

The aim is to obtain only one equivalent generator for each group of coherent generators. This equivalent generator is connected to the boundary bus. Methods that are used for determination of the equivalent generators are (Singh et al., 2011): Inertial aggregation, Terminal bus, Decomposition based aggregation; Synchrony based aggregation, Frequency weighting, Frequency weighted time domain, and Structure preservation method. Decomposition based aggregation (Singh et al., 2011and Chow et al., 1995) is considered as the best aggregation method for this research.

Decomposition based Gaussian elimination procedure is based on two- level aggregation concept to aggregate identified coherent generators into a single equivalent one using the swing equation and the admittance value at the boundary bus. This technique does not need a measurement data from the original generator. It is easily applicable for on-line application (Singh et al., 2011; Chakrabortty, 2011). The algorithm is (Singh et al., 2011; Chakrabortty, 2011):

- Establish the augmented matrix for the system linear equations in MATLAB.
- Use elementary row operations on the augmented matrix to transform it into an upper triangular form. If a zero is located on the diagonal, switch the rows until a non-zero is in that place. If it is not possible to do so, stop; the system has either infinite or no solutions.
- Use back substitution to transform the matrix.
- Pivoiting can only be done if the matrix solution needs to be iliminated further.

The flow chart in Figure 4.2 depicts the algorithm procedures explained above. This is applied to aggregate the coherent generators. The coherent generators are reduced to a single equivalent generator based on the swing and nodal equations. Procedures for applying fault are presented in Appendix A1 and A2. Steps for getting simulation graphs are given in Appendix A3, A4, and A5.

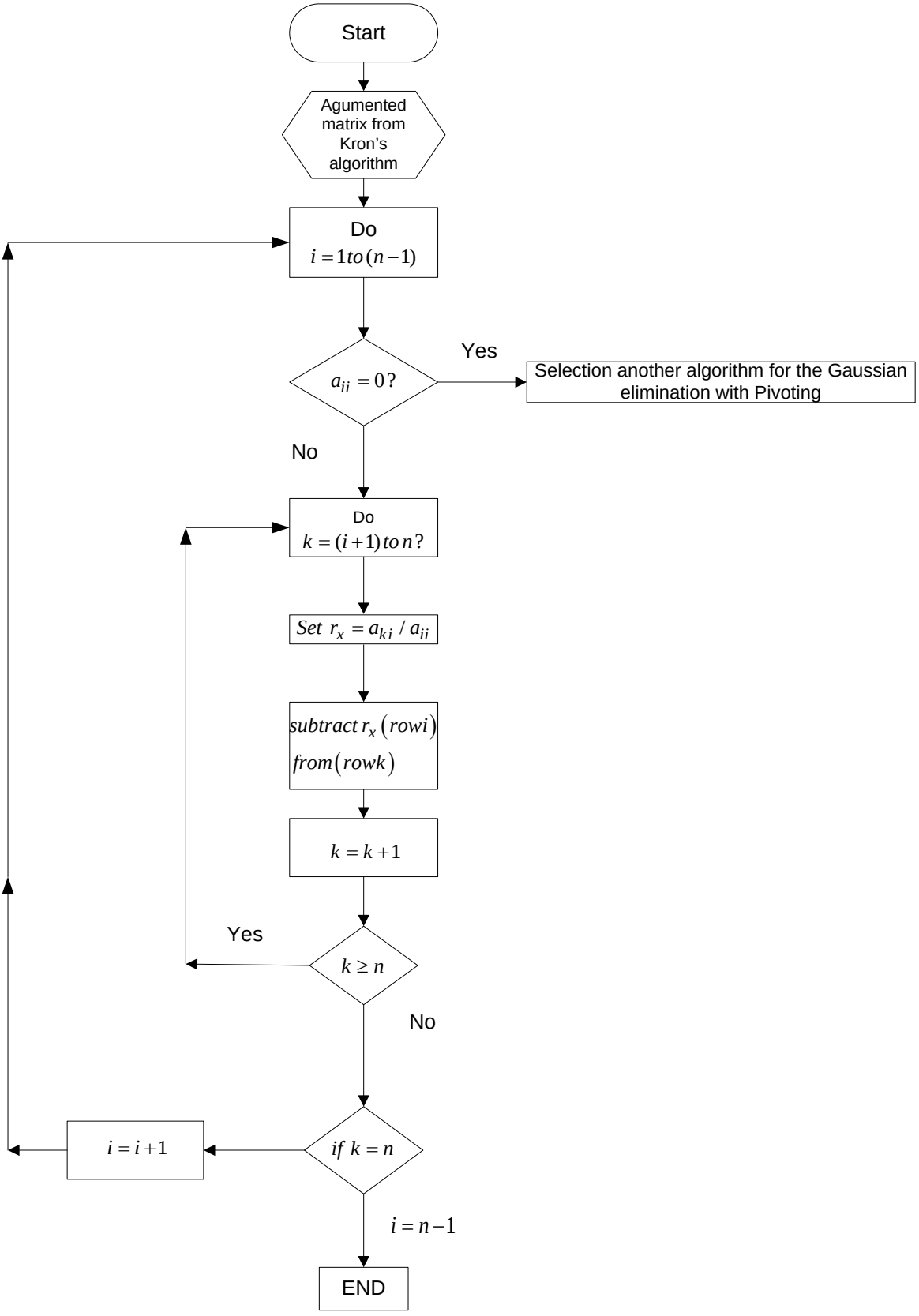

Figure 4.2: **Flow chart for gaussian elimination (www.cs.uiuc.edu)**

Where, a is the augmented matrix

a_{ij} is the mutual element of matrix a

r_x is a row used for computation

The aggregation is based on the Gaussian elimination method and Intertia aggregation method. The obtained matrix is used to calculate the equivalent generator.

4.1.3 Step 3: Network reduction, computation of a bus admittance matrix of the full and reduced models

IEEE 9-bus data is given in Appendix B 1. Additional generator data and preliminary calculations for the model are given in Appendix B 2 and B 3 respectifuly.

Computation of the bus admittance matrix follows the given below procedure:

- Transformation of load buses of the full model to equivalent admittances
- Building of admittance matrix of the full model software in MATLAB
- Reducing the admittance matrix
- Drawing of the one-line diagram of the reduced model.

These procedures are described below.

1) Constant admittance representation of the load

Admittance matrix is needed to be calculated for the application of these methods: Gaussian elimination, and the matrix Elementary and Kron's elimination (Radhakrishna, 2010; Kayira, 2009 and Osorno, 2003).
In stability studies of interconnected power system, the loads are usually converted to constant admittances. Loads are converted to admittance by using the Equations (4.5) - (4.7), while P_{mi} and E_i are kept constant at their pre-fault stages.

$$P_L + jQ_L = V_L I_L^* \tag{4.5}$$

$$V_L I_L^* = V_L\left(I_L^*(G_L - jB_L)\right) = V_L^2(G_L - jB_L) \tag{4.6}$$

$$Y_L = \frac{P_L}{V_L} - j\left(\frac{Q_L}{V_L^2}\right) \tag{4.7}$$

Where; for a load bus having voltage V_L, active and reactive power are P_L and Q_L, and the current is I_L. Y_L is the admittance of the load bus. Connected loads are converted to equivalent admittances. Data for this conversion is obtained from the output of the load flow study. The admittance matrix is established for the application of Kron's elimination based on the admittance matrix in MATLAB environment. This information is provided in the Appendix B. Finally, the reduced network admittance is used to draw one- line diagram of the equivalent network.

Conversion of load buses to equivalent admittance representation is done by different methods. They are: Constant Admittance, Constant Power, and Constant Current representation (Chen, 2009), (Lee and Schweppe, 1973).Result is that the behaviour of the load buses is the same as the behaviour of the buses without generators and both types can be grouped together. Normally elimination of the buses without generators and of the transformed load buses is done by building and reducing of the Admittance matrix of the system.

2) Building of the admittance matrix in MATLAB

An m-file is developed in MATLAB to build the admittance matrix of the full model. The script file is given in Appendix C 2.

3) Reduction of the the admittance matrix: Kron's node elimination algorithm

Computations are required to reduce the order of the system by bus elimination. The buses to be eliminated have to be selected. Normally, this elimination is done, based on the fact that there is no current being injected and or the bus is of no relevance to the analysis (Anderson and Fouad, 2003), (Radhakrishna, 2010), (Kayira, 2009), and (Osorno, 2003). MATLAB script file is given in Appendix C 3.

The standard node equations in matrix notation of power system network are expressed as;

$$[I_{Bus}] = [Y_{Bus}][V_{Bus}] \tag{4.8}$$

where, $[I_{Bus}]$ is the column matrix of current

$[V_{Bus}]$ is the column matrix of voltage.

$[Y_{Bus}]$ is the symmetrical square matrix of admittances.

Assuming that $[I_{Bus}]$ and $[V_{Bus}]$ can be expressed in the following way due to the fact that, column must be arranged in such a way that buses to be eliminated are in the lower rows of the matrices. Therefore, they can be expressed as follows;

$$[I_{Bus}] = \begin{bmatrix} I_{Bus-E} \\ I_{Bus-R} \end{bmatrix} ; [V_{Bus}] = \begin{bmatrix} V_{Bus-E} \\ V_{Bus-R} \end{bmatrix} \tag{4.9}$$

$$[Y_{Bus}] = \begin{bmatrix} Y_{mm} & Y_{mn} \\ Y_{nm} & Y_{nn} \end{bmatrix} \tag{4.10}$$

where, $Bus-E$ denotes the buses to be eliminated

$Bus-_R$ denotes the buses to be retained

m denotes load buses

n denotes generator buses

Using Equations (4.8), (4.9) and (4.10), the node equation in matrix notation of the power system network is expressed as;

$$\begin{bmatrix} I_m \\ I_n \end{bmatrix} = \begin{bmatrix} Y_{mm} & Y_{mn} \\ Y_{nm} & Y_{nn} \end{bmatrix} \begin{bmatrix} V_m \\ E_n \end{bmatrix} \tag{4.11}$$

Where, E_n is the generator bus voltage.

If there are no sources of generators at load buses;

$$\left[I_m \right] = \left[I_{Bus-_E} \right] = 0 \tag{4.12}$$

Then from Equation 4.12

$$0 = Y_{mm} V_m + Y_{mn} E_n \tag{4.13}$$

and

$$I_n = Y_{nm} V_m + Y_{nn} E_n \tag{4.14}$$

From Equation (4.8), it can be written

$$V_m = -Y_{mm}^{-1} Y_{mn} E_n \tag{4.15}$$

Substituting V_m into Equation (4.9) (Radhakrishna, 2010), (Kayira, 2009) it is obtained

$$\left[I_n \right] = \left[I_{Bus-_R} \right] = \left(Y_{nn} - Y_{mn}^T Y_{mm}^{-1} Y_{mn} \right) E_n = Y_{Bus(reduced)} E_n$$

where,

$$Y_{Bus(reduced)} = \left(Y_{nn} - Y_{mn}^T Y_{mm}^{-1} Y_{mn} \right) \tag{4.16}$$

This $Y_{Bus(reduced)}$ is the solution of performing the Kron's elimination algorithm

An engineer can perform node elimination bus by bus instead of taking inverse of Y_{mm} therefore the bus admittance matrix can be written as follows:

$$\left[Y_{Bus} \right] = \begin{bmatrix} Y_{11} \cdots Y_{1r} \cdots Y_{1n} \\ Y_{21} \cdots Y_{2r} \cdots Y_{2n} \\ \vdots \\ Y_{r1} \quad Y_{rr} \quad Y_{rn} \\ \vdots \\ Y_{n1} \quad Y_{nr} \quad Y_{nn} \end{bmatrix} \tag{4.17}$$

With reference to the above equation, the aim is to eliminate bus r. More so, $[Y_{Bus}]$ will be reoriented in such a way that bus r elements take position in the last raw as well as column.

$$[Y_{Bus}] = \begin{bmatrix} Y_{11} \cdots Y_{1n} & Y_{1r} \\ Y_{21} \cdots Y_{2n} & Y_{2r} \\ \vdots \quad \vdots & \vdots \\ Y_{n1} \cdots Y_{nn} & Y_{r} \\ Y_{r1} \cdots Y_{rn} & Y_{rr} \end{bmatrix} \tag{4.18}$$

Consequently, the new elements are obtained by application of Equation (4.19).

$$Y_{ij(new)} = Y_{ij(old)} - \frac{\left(Y_{ir(old)} * Y_{rj(old)}\right)}{Y_{rr}} \tag{4.19}$$

Where, $Y_{ij(new)}$ is the new value of each element of the reduced network and its dimensions are less than the old value in the full network.

The Equations (4.17 – 4.19) were applied to obtain the reduced system in Figure 4.19.The flow chart of the Kron's procedures of elimination implemented bus by bus is given in Figure 4.3 where NB denotes the number of buses.

4) Drawing of the one-line diagram of the reduced model.

This is done based on the values of elements of the $Y_{Bus(reduced)}$. The interconnection of transmission lines is determined by the admittance matrix obtained.

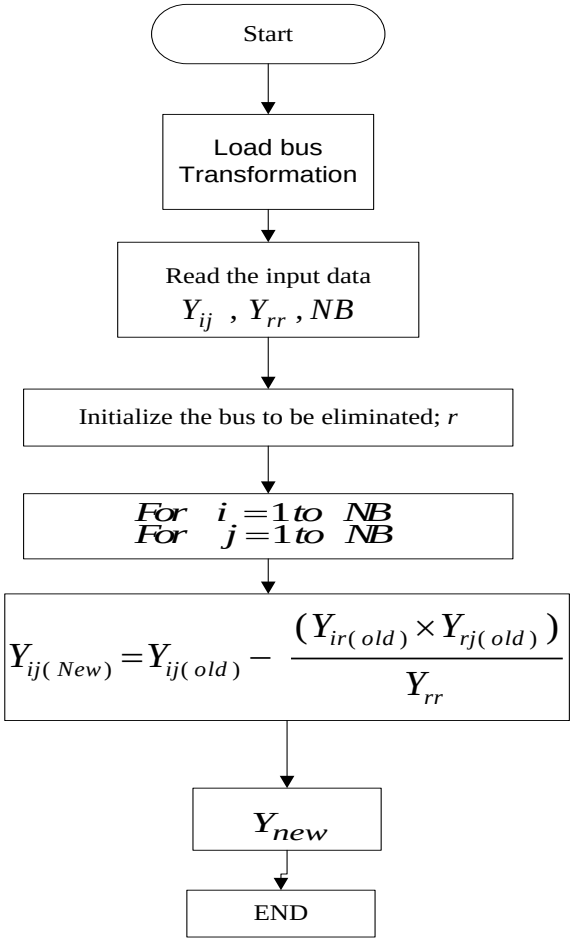

Figure 4.3: **Kron's elimination procedure flow chart**

4.1.4 Coherency procedures for model reduction

The research investigates well the joint application of these three procedures to fulfil the requirements for errors between the full and reduced models for the voltage and active power (or rotor angle and reactive power) are less than 5%. The investigations in the thesis are done using IEEE standard model and data. Comparison of the two models is done in the thesis using RTDS (Real-Time Digital Simulator) and DigSILENT. The results obtained from the initial full model simulations are used for verification of the process of reduction of the initial model network.

Procedures for the coherency based method model reduction are applied in this investigation as follows:

- Full network is simulated in DigSILENT for both load flow and stability analysis
- Coherent generator groups can be identified by using step2
- Apply Kron's algorithm for bus admittance as explained in step3
- After obtaining the reduced network, perform both load flow and stability analysis for the verification of the results, and

- Calculate error percentage using Equation (4.22) which is described later in this chapter.

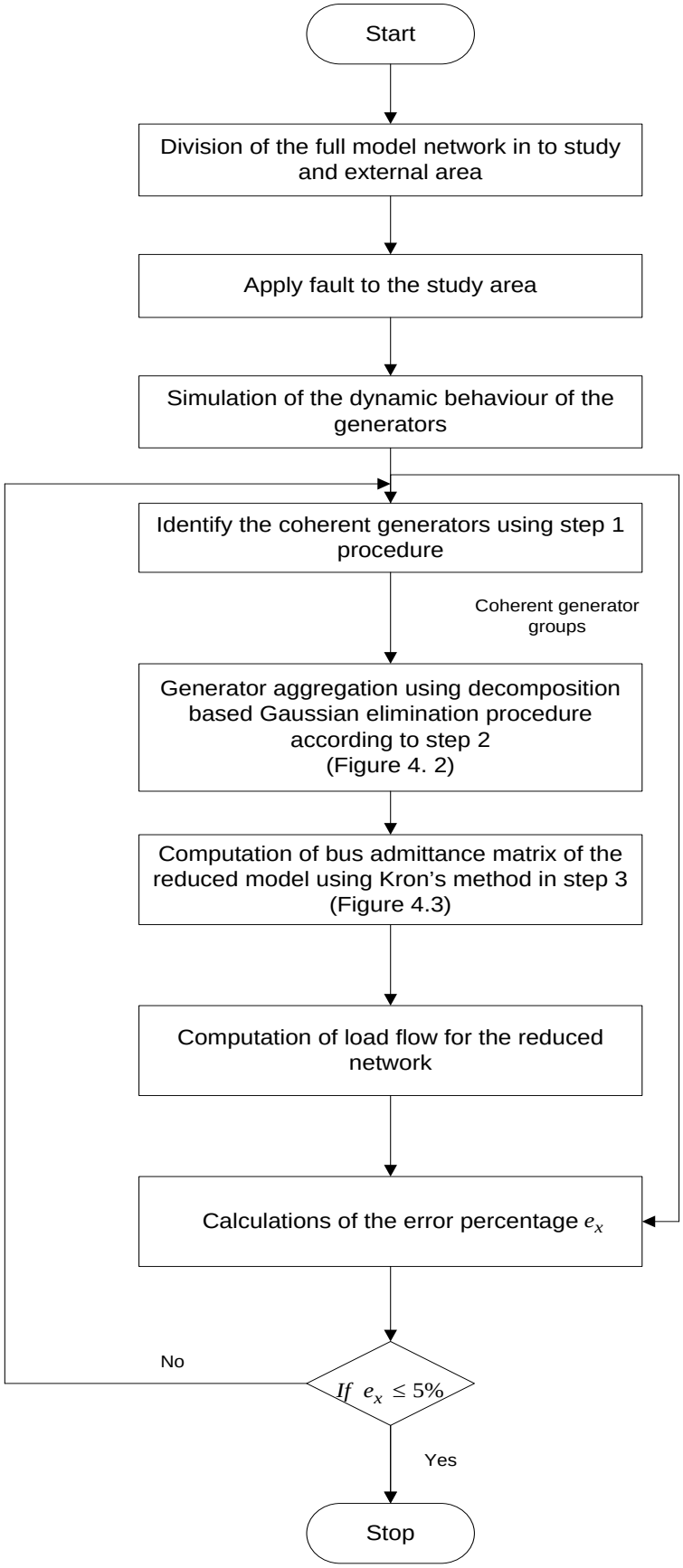

Figure 4.4: **Flow chart of the coherency based method**

The flow chart of the coherency based method is presented in Figure 4.4. This has been applied to the model of IEEE 9-bus system.

4.2 Case study: IEEE 9-bus system

IEEE 9-bus system was used for the assessment and development of a reduced order power system model. This system consists of three generators, three transformers, three loads, and six transmission lines. Data is given in Appendix B and the system base is 100MVA (Anderson and Fouad, 2003). Figure 4.5 depicts the original 9-bus system one line diagram. The process of reduction of the full model is done using DigSILENT software for finding solutions of the following investigations:

- Simulation of the full model;
- Fault analysis;
- Stability analysis, and
- Simulation of the reduced model.

The DigSILENT Power Factory is known as a graphical environment based software for building single line diagrams of power system models. DigSILENT is an appropriate software package for transient simulation and analysis. The research scope is to use DigSILENT for simulation, but the DigSILENT is not the scope of the thesis. The models of all power system components enclosed in this study were introduced into the DigSILENT Power Factory: Synchronous generator, Transformer, load, bus-bar and transmission lines were all programmed within the Power Factory: so as to represent a real-life power system performance (“DigSILENT Power Factory User’s Manual,” tech. rep, Gomaringen, 2011.) After the completion building of the power system model within the software, simulations were done in order to achieve the objectives of the study.

MATLAB software is used for calculations, Kron’s elimination, and error percentage calculation (Appendix C 3). The rest of the algorithm is based on relations of the coherency based method for network reduction.

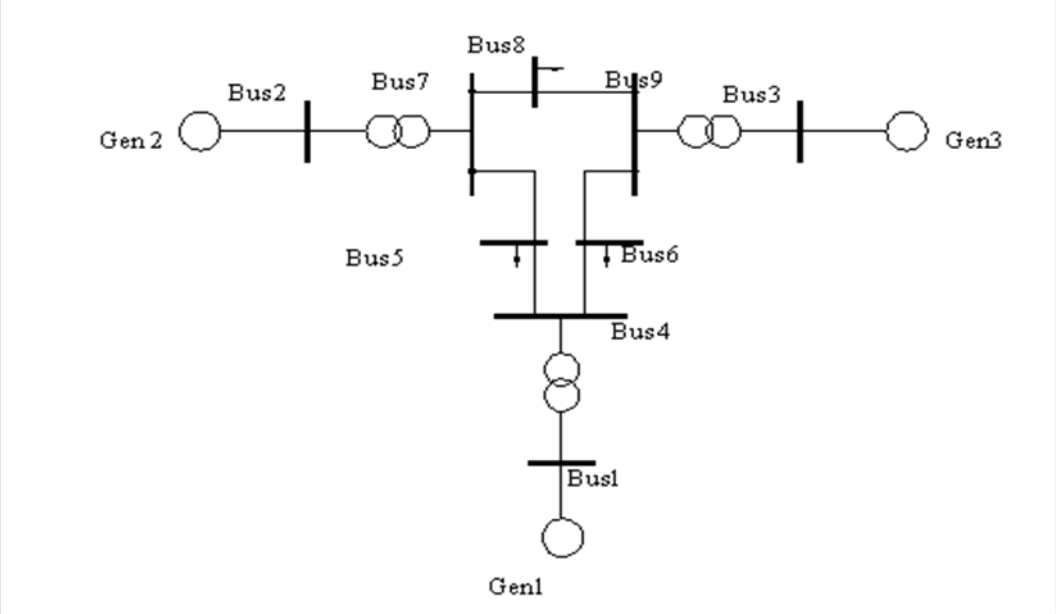

Figure 4.5: **Full system network of IEEE 9- bus system**

Before the process of network reduction, the model of the system was built and tested by means of load flow studies (Appendix C4) to ensure that the results are in line with the IEEE ones. The following input was used to calculate the load flow of the considered network- Figure 4.5, Table 4.1. The model was simulated in DigSILENT Power Factory software to obtain the correct load flow results. The one in DigSILENT environment is given in Appenix C1.

Table 4. 1: **Input data for load flow calculations**

Bus Number	1	2	3	4	5	6	7	8	9
Voltage	16.5kV	18kV	13.8kV	230kV	230kV	230kV	230kV	230kV	230kV

The results are shown in Table 4.2. Simulation procedures in DigSILENT software are in Appendix A.

Table 4. 2: **DigSILENT Load flow results**

Bus number	**Voltage [kV]**	**Active power [MW]**	**Reactive power [MVars]**
1	17.16	74.9	27.21
2	18.45	163	7.16
3	14.14	85	-10.12
4	235.93	33.23	1.42
5	229.98	-14.14	-38.18
6	229.75	-58.69	-13.87
7	229.89	85	-8.67
8	231.13	-77.51	-11.29
9	229.98	60.01	-17.77

These results are compared with the set of the IEEE ones as shown in the Figure 4.6. Blue and green colours represent IEEE and DigSILENT power factory results respectively. The deviations of the values for the voltages of the buses are calculated and shown in Table 4.3 where IEEE results for the load flow voltages are assumed to be 100%.

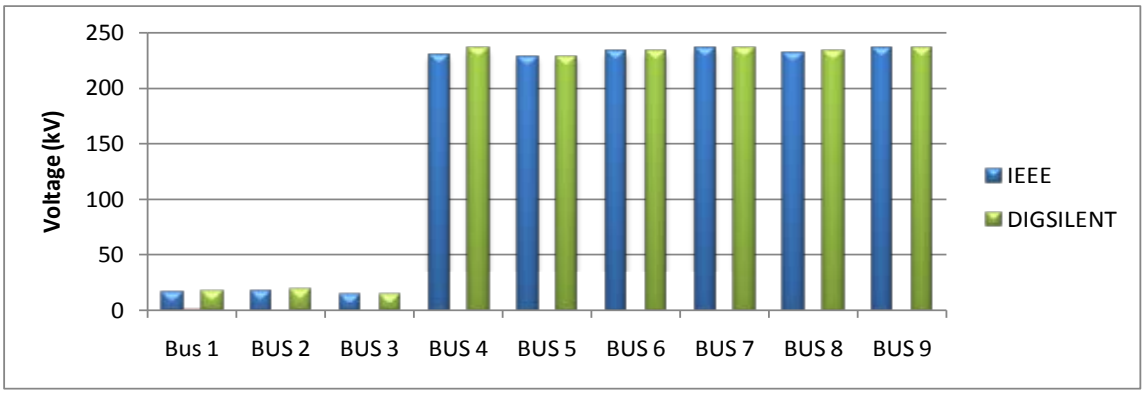

Figure 4.6: **Comparison of IEEE and DigSILENT power factory load flow results for the bus voltages**

Table 4.3 presents the comparison between the IEEE load flow bus voltages and the percentage deviation. Percentage deviation obtained is within $\pm 5\%$ which shows that the built in DigSILENT model can be used for reduction purposes.

Table 4. 3: **Comparison of IEEE and DigSILENT load flow results for the bus voltages**

BUS	IEEE%	DigSILENT	Percentage Deviation
1	100%	104%	4%
2	100%	102.5%	2.5%
3	100%	102.46%	2.46%
4	100%	102.58%	2.58%
5	100%	99.99%	-0.01%
6	100%	99.89%	-0.11%
7	100%	99.95%	-0.05%
8	100%	100.49%	0.49%
9	100%	99.99%	-0.01%

The results for the active and reactive power from Table 4.2 are shown in Figure 4.7 and Figure 4.8 respectively. Table C1in Appendix C gives load flow report for the full IEEE 9-bus system in DigSILENT software.

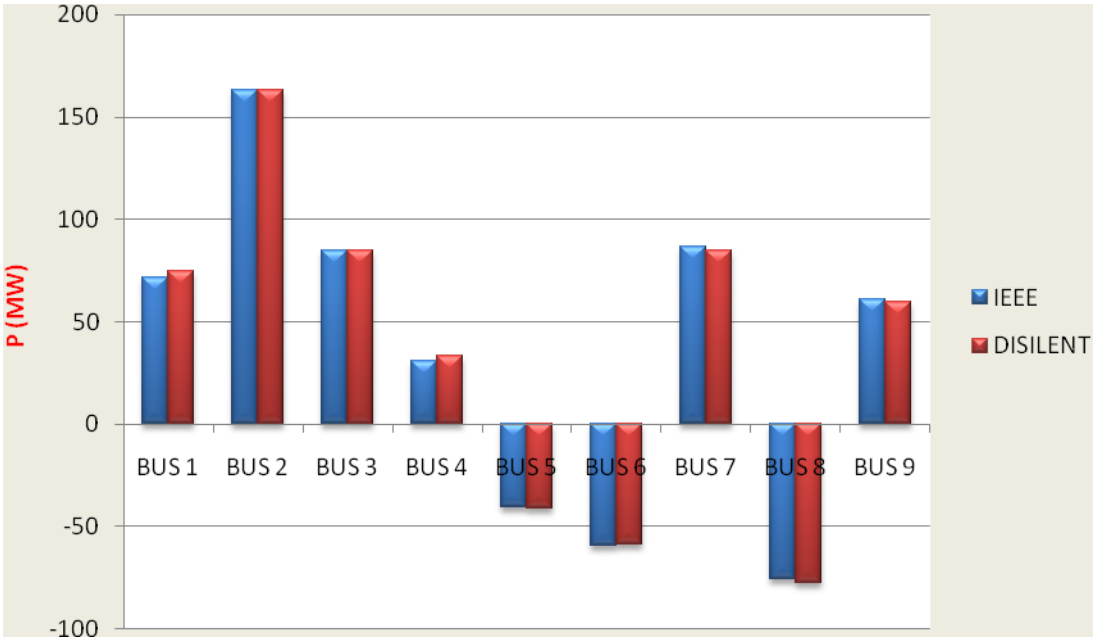

Figure 4.7: **Comparison of IEEE and DigSILENT power factory load flow results for the active power**

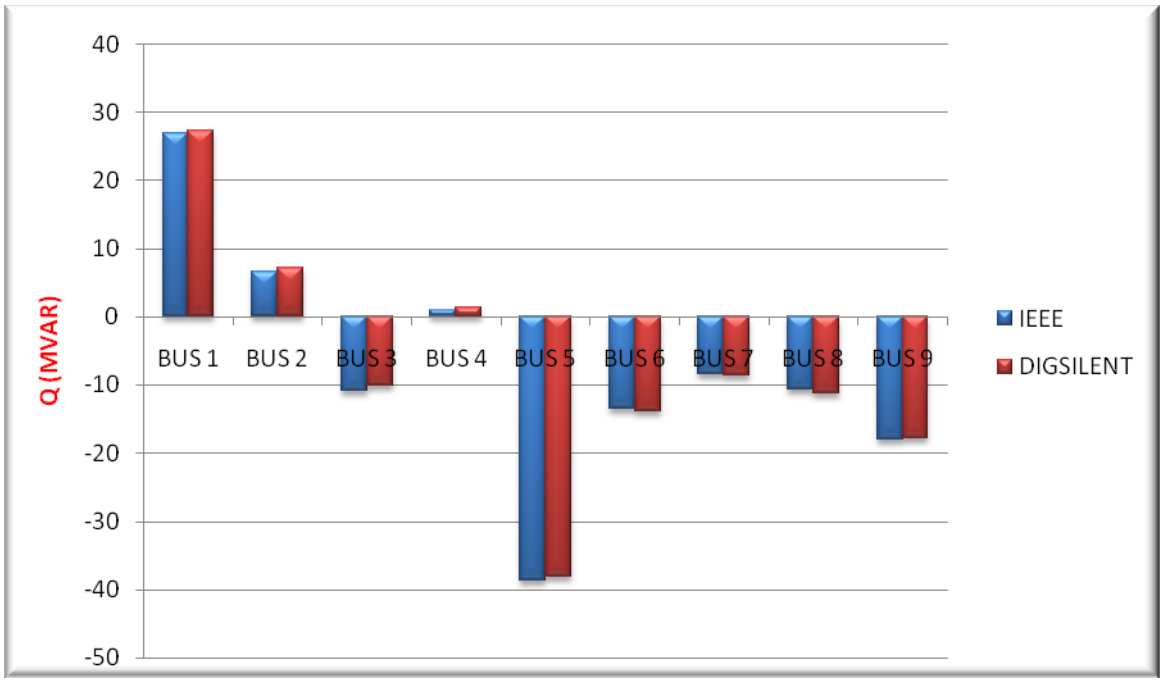

Figure 4.8: **Comparison of IEEE and DigSILENT power factory load flow results for the reactive power**

The deviations of the values for the reactive and active powers for the DigSILENT results are shown in Table 4.4

Table 4. 4: Comparison of IEEE and DigSILENT load flow results for the active and reactive power

BUS	IEEE%	P	Percentage Deviation	Q	Percentage Deviation
1	100%	104.19%	4.19%	101%	1%
2	100%	100%	0%	100.78%	0.78%
3	100%	100%	0%	104.71%	-4.71%
4	100%	102.58%	2.58%	104.2%	4.2%
5	100%	102.5%	2.5%	99.986%	-0.013%
6	100%	99.987%	-0.0127%	97.994%	-2.005%
7	100%	98.15%	-1.85%	96.786%	3.214%
8	100%	97.88%	2.12%	105.514%	5.514%
9	100%	101.299%	1.299%	98.722%	-1.278%

Analysis of the results for the load flow from Table 4.3 and Table 4.4 show that simulation with DigSILENT results in less than (+/- 5%) voltage deviation from the IEEE results which was a go ahead for the study of the network reduction.

4.3 Application of coherency based method

The steps explained in section 4.1 were computed, and the swinging curves were obtained for the two study cases.

4.3.1 Power network division and fault application

The network can be divided into three areas, namely; study area, external area and boundary area. ***The study area*** is the portion of the network to be retained after the process of model reduction; detailed model needs to be preserved. The selected in the considered case study area consists of a generator 2 and the buses 2 and 7.
External area is the portion of the network to be reduced. ***Boundary area*** consists of buses which connect the study area with the reduced external area. Boundary buses are the buses at the far end of the interconnecting line, and are recognizable because the near end bus voltage and the tie-line flow are taken into consideration. For this interconnected network, boundary buses are ***bus-5-, bus-6-, and bus-7.*** Figure 4.9 shows the two areas of the system. The area inside the circle is the study area and the rest of the system is the external area.

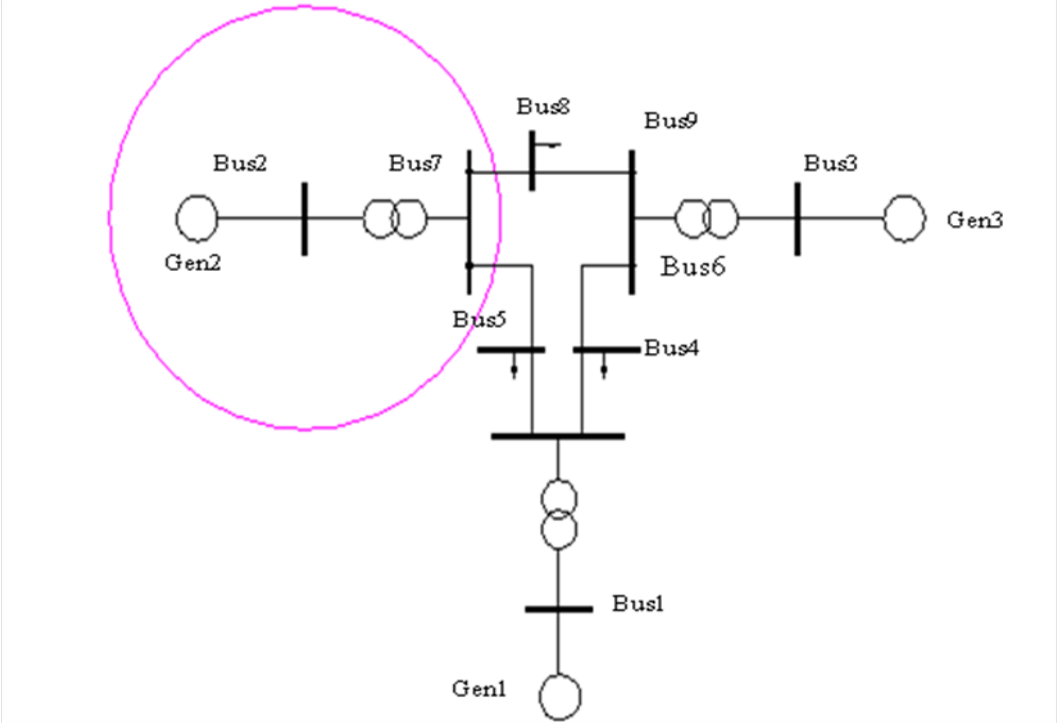

Figure 4.9: Study area and external area

The study and external areas of the network are preliminary selected on the bases of the analysis of the structure of the network. The boundary buses are determined and they are retained. Study area will be retained and the external one will be reduced by aggregation of the coherent generators and elimination of the load buses.

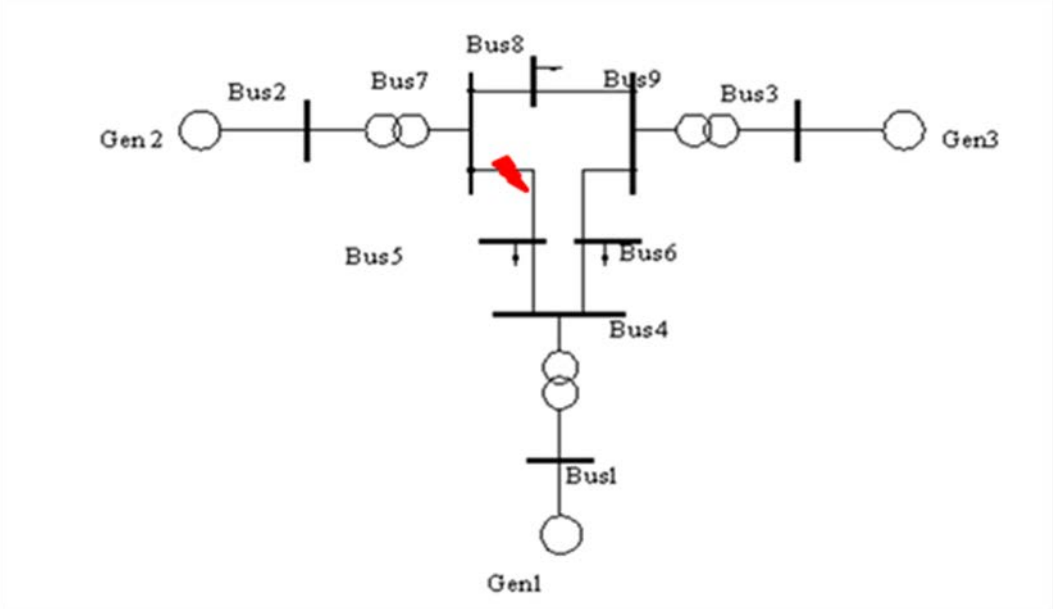

Figure 4.10: Fault location in the study area

4.3.2 Results from the system reaction to the applied faults

Three phase short circuit was applied on line-2 (between bus 7 and bus 5) to introduce the disturbance to the network as shown in Figure 4.10.

Once the system is subjected to the disturbance, simulation program evaluates the non-linear equations representing the dynamics of the generators, as well as algebraic power flow equations representing the algebraic equations. In this study, the generator-1- was selected as the reference generator for the fact that it is a slack generator.

Simulations were conducted utilizing DigSILENT Power Factory; Figures 4.11 to Figure 4.13 depict the swing curves for the three generators after subjected to the disturbance. They show rotor angles with reference to the reference machine angle in degrees.

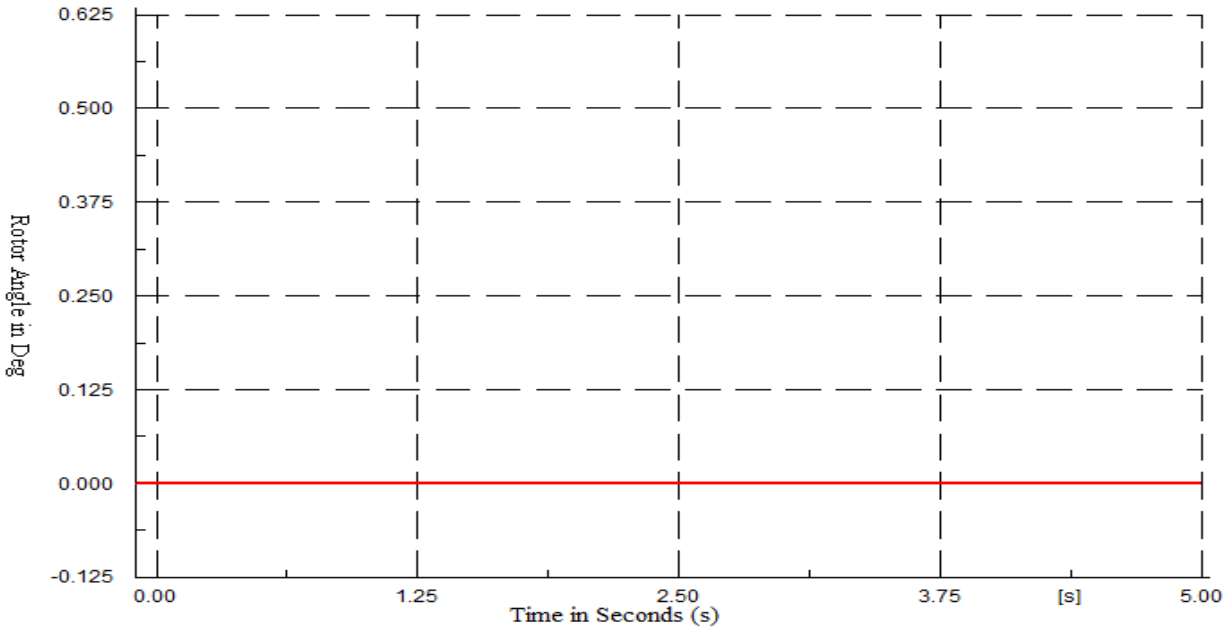

Figure 4.11: **Full system swing curve for the generator-1- using DigSILENT**

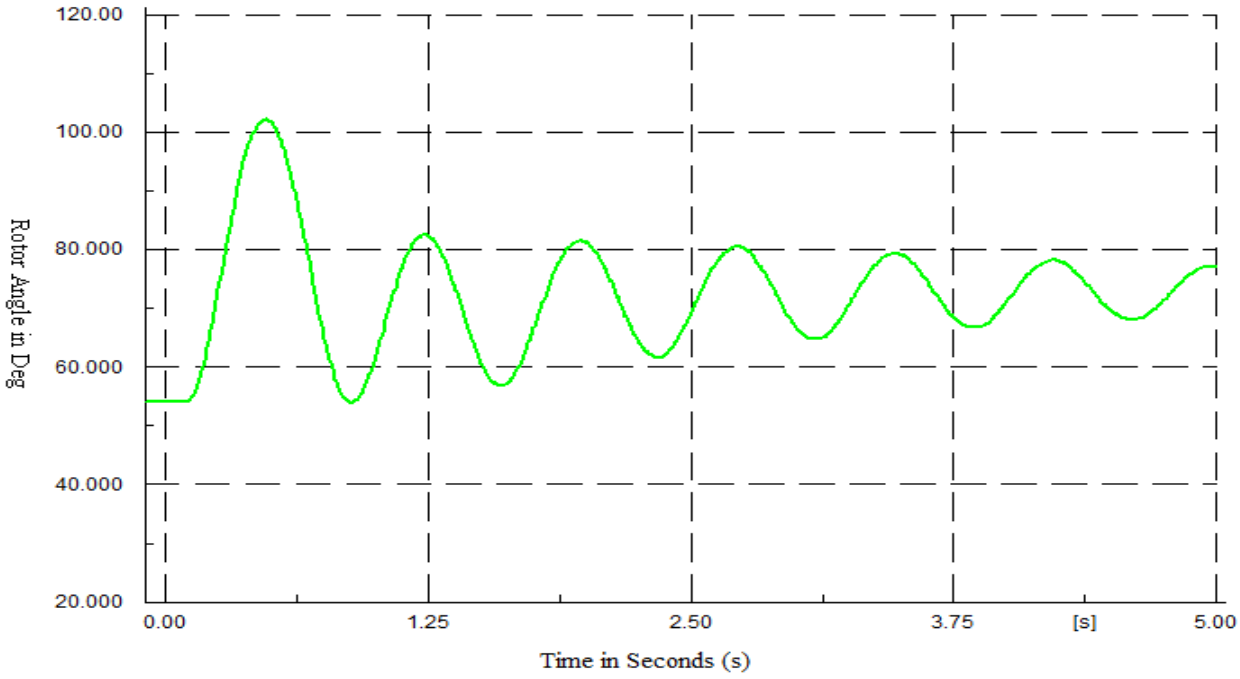

Figure 4.12: Full system swing curve for the generator-2- using DigSILENT

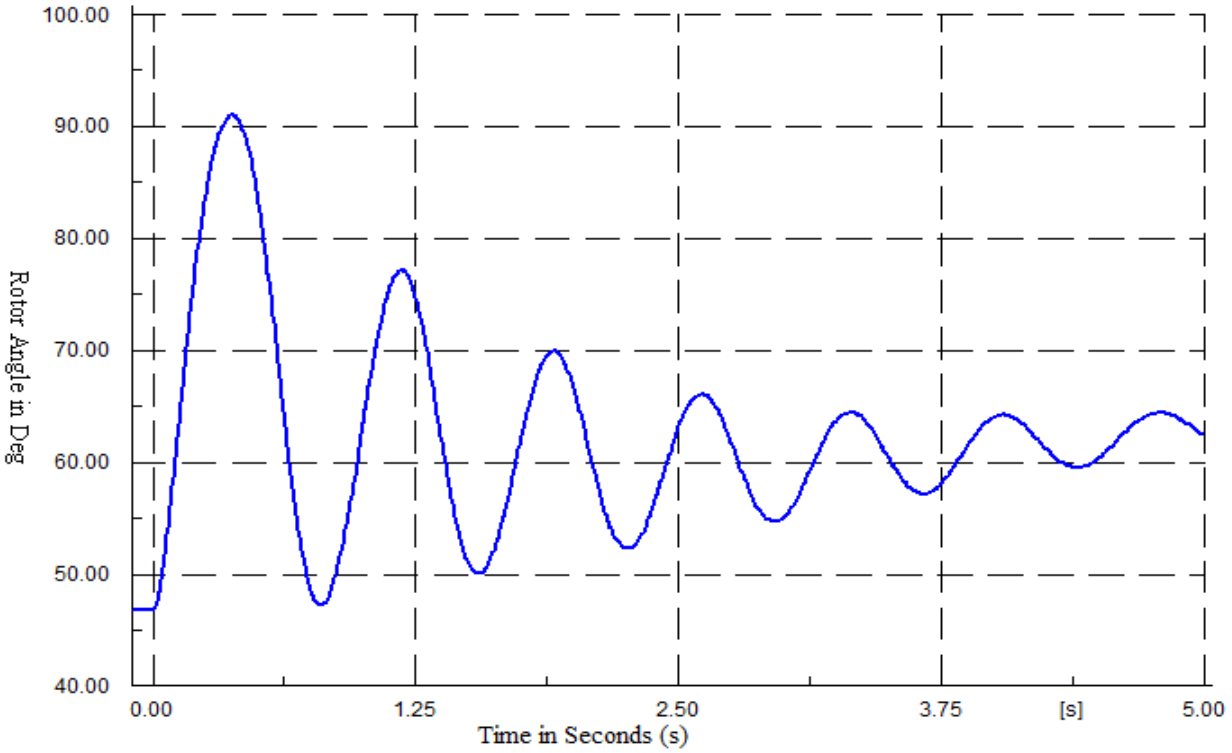

Figure 4.13: Full system swing curve for the generator-3- using DigSILENT

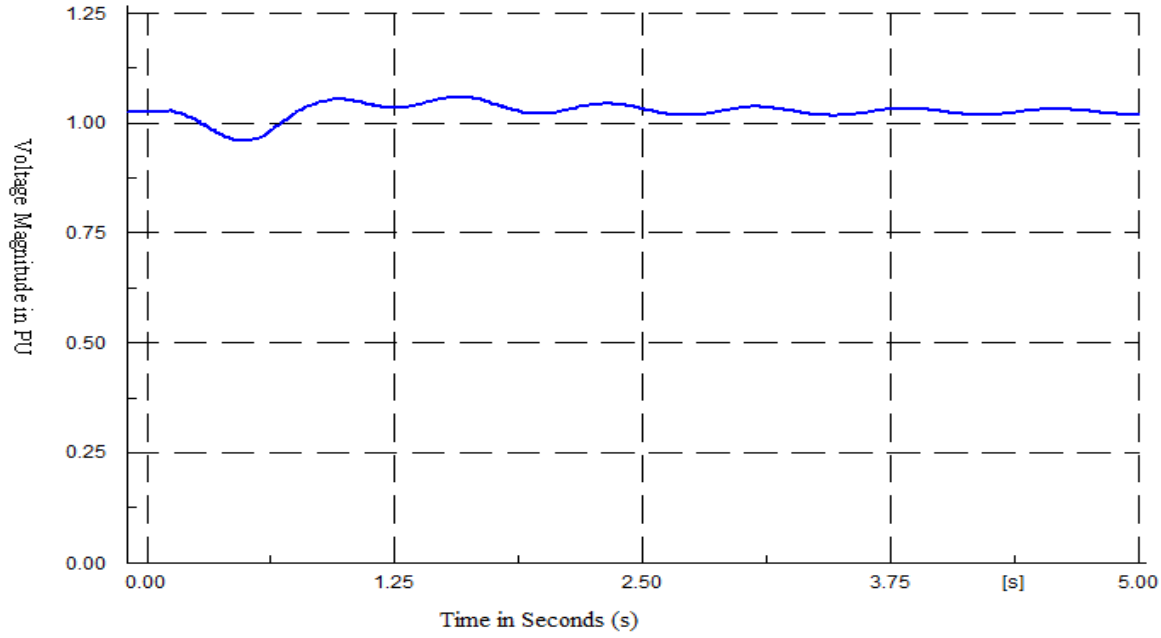

Figure 4.14: Full network voltage magnitude in PU for the generator-2- using DigSILENT

Figures (4.14 – 4.16) attempt to present the dynamic behaviour of generator 2 due to the fact that the generator 2 is in the study area as indicated by the fault location as shown in Figure 4.10.

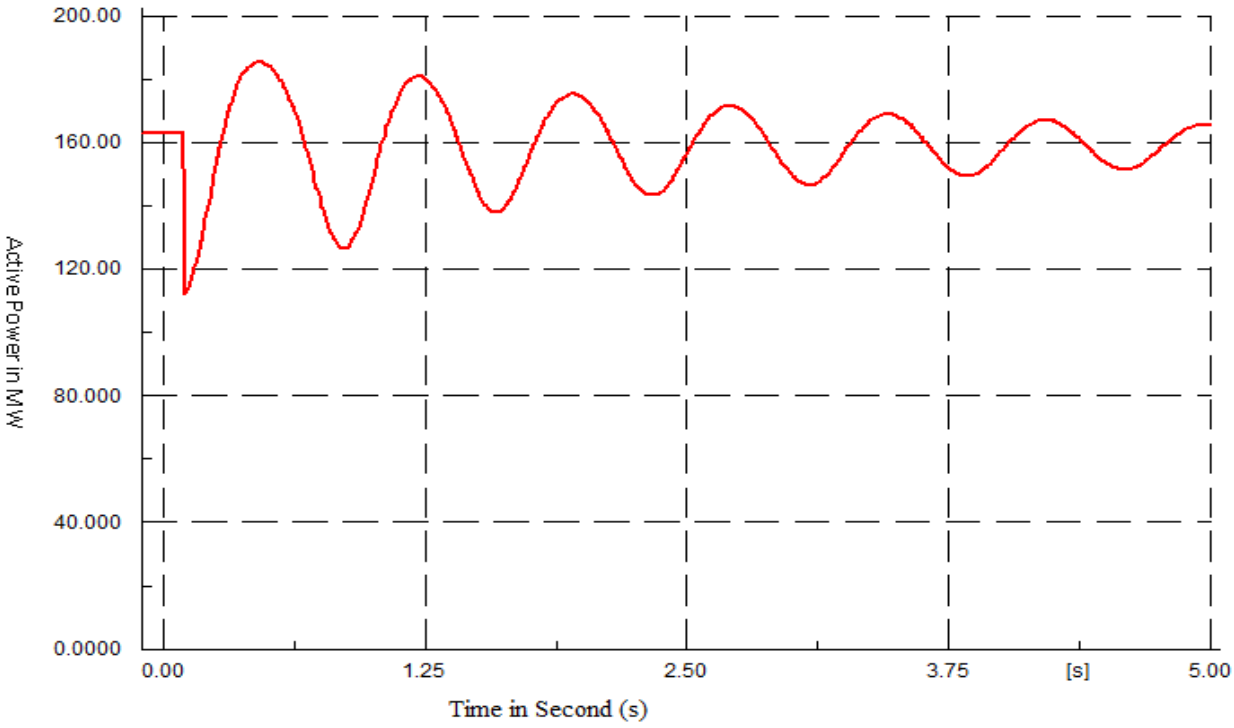

Figure 4.15: Full network active power in MW for the generator-2- using DigSILENT

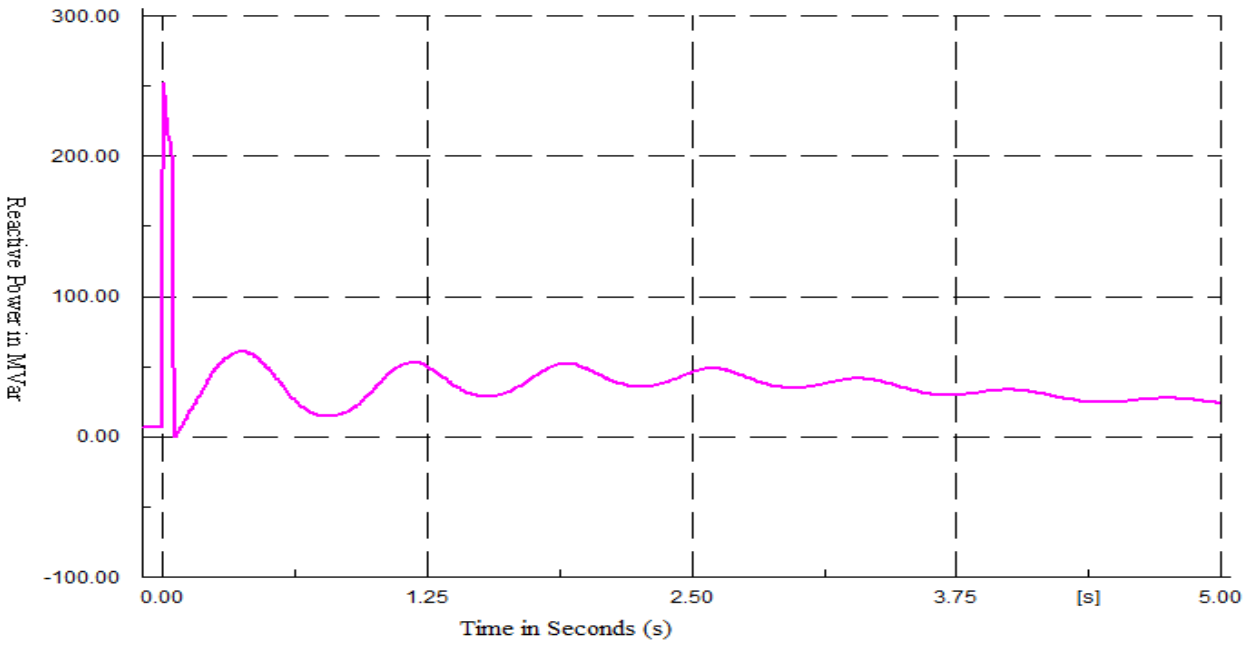

Figure 4.16: **Full network reactive power in MVars for the generator-2- using DigSILENT**

The system responded to the disturbance by large changes in generator rotor angles (Figure 4.12), bus voltages, power flows, as well as the other system variables. The results obtained showed that generators 3 and 1 are not coherent because they do not have similar swing curves. Therefore, they can not be grouped together.

If the generators in the external area swing together, they can be grouped together. Nonetheless, if they do not swing together, they cannot be grouped together. Consequently, the external part was divided into two sub-areas (**B** and **C**) due to the fact that ***generator-1- and generator-3-*** do not swing together. Figure 4.17 shows three areas of the network after the disturbance application.

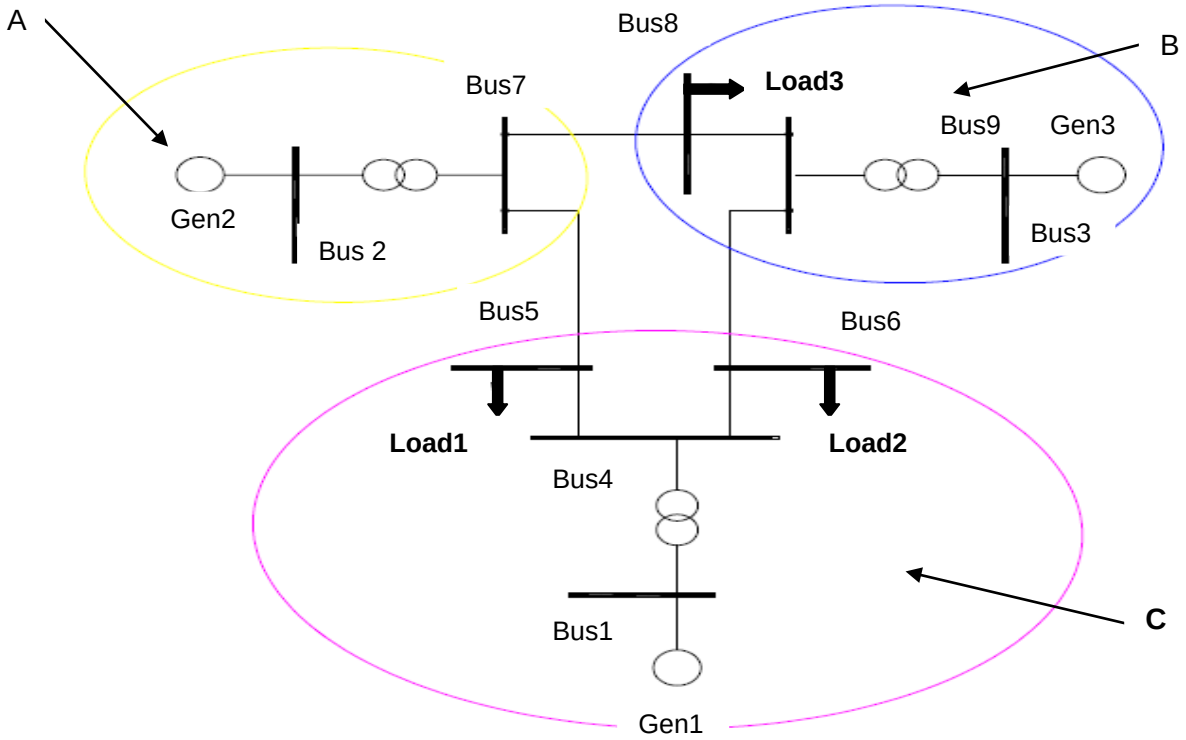

Figure 4. 17: External area identification

4.3.3 Results for load buses representation

Load buses are bus 5, 6 and 8 in the model. Applying Equation 4.7, the following calculations were carried out to receive the load buses admittances.

In order to calculate the reactances of the transmission lines, all the base values must be known. Base impedance can be calculated as follows:

$$S_{Base} = 100\text{MVA}, V_{Base} = 230kV, Z_{Base} = \frac{V_{Base}^2}{S_{Base}} = \frac{(230\times10^3)^2}{(100\times10^6)} = 529\ \Omega \quad (4.20)$$

The base value of the impedence is used to calculate the actual value of the impedence so that admittance can be obtained. The calculations in MATLAB software environment are given in Appendix C 2.

The results obtained for the load buses are given in Table 4.3. These are used to build the admittance matrix of the full network.

Table 4. 5: Results for load buses representation

Load	Active Power [MW]	Reactive Power [Mvars]	Voltage [kV]	Admittance(Y) [S]
1	125	50	230	1.25-j0.476
2	90	30	230	0.8993-j0.317
3	100	35	230	0.9998-j0.3703

4.3.4 Results from application of the Kron's method

The reduced Y_{Bus} matrix was obtained after the Kron's node elimination, and further elementary matrix operations carried out in order to make the connections of the reduced system. Figure (4.18) depicts the reduced system consisting of three generators, six buses, two loads and 4 transmission lines. The admittance matrix of the reduced network is expressed in Equation (4.21).

$$Y_{BusR} = \begin{bmatrix} Y_{11} & Y_{21} & Y_{31} & Y_{51} & Y_{61} & Y_{71} \\ Y_{12} & Y_{22} & Y_{32} & Y_{52} & Y_{62} & Y_{72} \\ Y_{13} & Y_{23} & Y_{33} & Y_{53} & Y_{63} & Y_{73} \\ Y_{15} & Y_{25} & Y_{35} & Y_{55} & Y_{65} & Y_{75} \\ Y_{16} & Y_{26} & Y_{36} & Y_{56} & Y_{66} & Y_{76} \\ Y_{17} & Y_{27} & Y_{37} & Y_{57} & Y_{67} & Y_{77} \end{bmatrix} \tag{4.21}$$

The values of each element of the matrix in Equation (4.21) are as follows;

$$Y_{BusR} = \begin{bmatrix} (0.2524 - j6.12) & 0 & 0 & (98.01 + j11.53) & 0 & 0 \\ 0 & -j5.485 & 0 & 0 & 0 & (2.488 - j23.742) \\ 0 & 0 & (-1.23 + j0.348) & 0 & 0 & (222.15 - j4.546) \\ (j8.4459) & 0 & 0 & (799.83 - j720.35) & (0.368 - j0.143) & (1.358 + j0.286) \\ 0 & 0 & 0 & (119.32 + j36.89) & (2.212 - j2.516) & (-1.843 + j14.8) \\ 0 & j5.4855 & (0.156 + j1.12) & (-1.19 + j5.98) & (0.658 + j2.036) & (1.561 - j18.55) \end{bmatrix}$$

where, Y_{BusR} is the representation of the admittances matrix of the reduced model which was used to build one line diagram of the reduced network shown in Figure 4.18. one-line diagram of the reduced model for IEEE 9-bus system in DigSILENT software environment is given in Appendix C4.

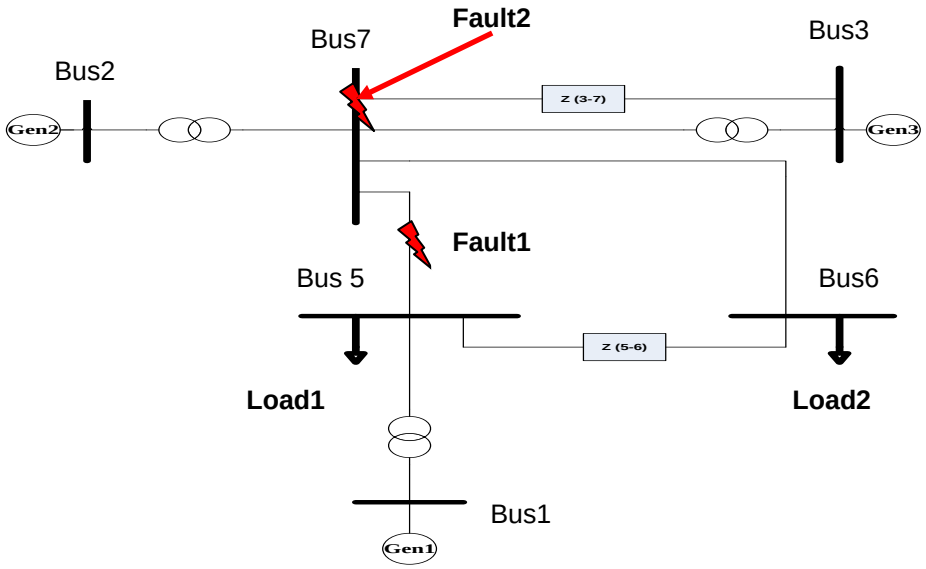

Figure 4.18: One line diagram of the reduced system

The impedances in a box on the diagram between (bus 7 and bus 3) and (bus 6 and equivalent bus (4-5) represent the total equivalent impedance obtained after the reduction process.

4.3.5 Verification of the reduced model

DigSILENT software is used to validate the reduced model behaviour results. Bus 7 was selected as one of the buses of the study area and as a boundary bus. The most essential part of the system is the study area, which is composed of the generator 2, the bus 2, and the bus 7. Due to this, their load flow results must be approximately equal to the ones in the full system. This determines the accuracy of the reduction process.

Equation (4. 22) was utilised to compute the percentage of retaintion.

$$\%Rate\,R_{ret} = \frac{\mathrm{R}_a}{Fa} \times 100 \qquad (4.22)$$

The rate of reduction is the $R_{red} = 100\% - \%Rate\,R_{ret}$.

Where, a denotes either the number of buses or transmission lines.

R denotes the reduced network

F denotes the full network

The results obtained applying the above Equation (4.22) is presented in Table 4.6.

Table 4. 6: Comparison of the reduced and full system

System	Full model	Reduced model	% Rate of retaining	% Rate of reduction
Number of Buses	9	6	66.67	33.33
Number of Lines	6	4	66.67	33.33

Table 4.6 shows what part of the full model is kept in the reduced model. The reduced order model represents 66.67% of the full one.

4.3.6 Simulations results comparison

The Equation (4.23) was used to compare the results between the reduced and the initial model as follows:

$$e_x = \frac{(x_{Full} - x_{Red})}{x_{Full}} \tag{4.23}$$

Where $x = V, P, Q, \delta$

The nodes voltage magnitude results from load flow calculations of both the original and the reduced models are shown in Table 4.7. The values for the bus 2 and bus 7 are are given in bold. The steady state results from the swing model simulation for the generator in the study area (generator 2) in order to evaluate its stability are shown in Table 4.8. Load flow simulation report is shown in Table C2 (Appendix C).

Table 4. 7: DigSILENT load flow results for the bus voltages

Full network		Reduced network		e_v [%]
Bus number	Voltage [kV]	Bus number	Voltage [kV]	
1	17.16	1	17.16	0
2	**18.45**	**2**	**18.53**	**-0.4336**
3	14.14	3	14.14	0
5	229.98	5	235.83	-2.546
6	229.75	6	235.83	-2.646
7	**229.98**	**7**	**236.5**	**-2.835**

Table 4. 8: DigSILENT stability analysis results for the study area generator

x	Full model	Reduced model	e_x%
V [PU]	1.025	1.029	-0.39
δ [Deg]	53.025	48.037	8.022
P [MW]	163.013	164.32	-0.802
Q [MVAR]	7.163	7.423	-3.63

4.3.7 Comparison of dynamic results for the two fault locations in the study area

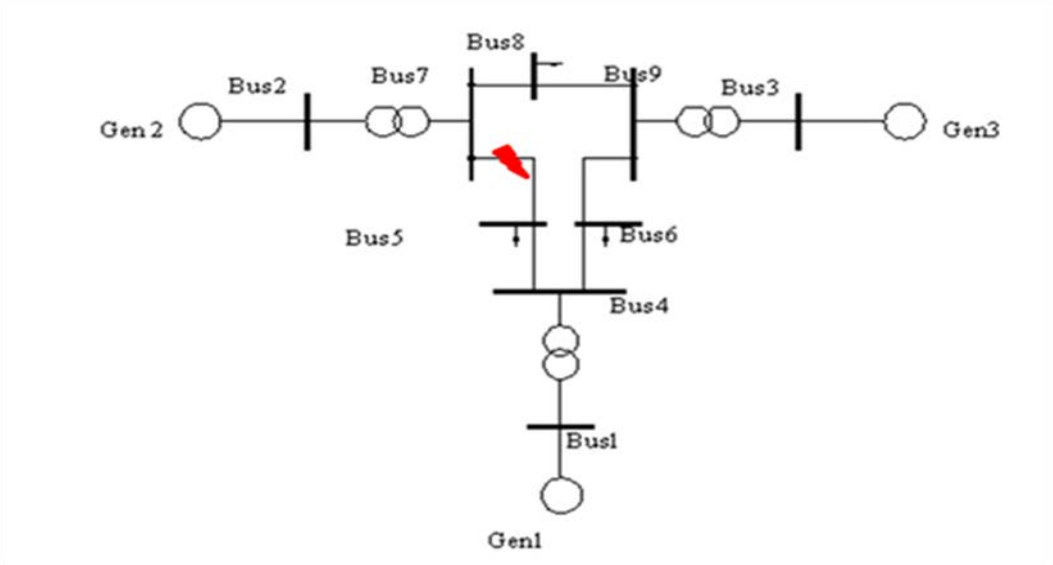

Figure 4. 19: First fault location diagram.

- **First fault location**

Dynamic bdhaviour of the full and reduced model is simulated for two faults in the study area, applied to different places of the study area.

Figures (4.20-4.23) depict the compared results of both the reduced and full system for voltage magnitude, active power, reactive power, and rotor angle of generator-2- after subjected to the disturbance for the reduced model Figure 4.18. The solutions are obtained after simulation of the swing equations for the generator 2. The dotted line symbolizes the reduced network, while the solid line is for the full network.

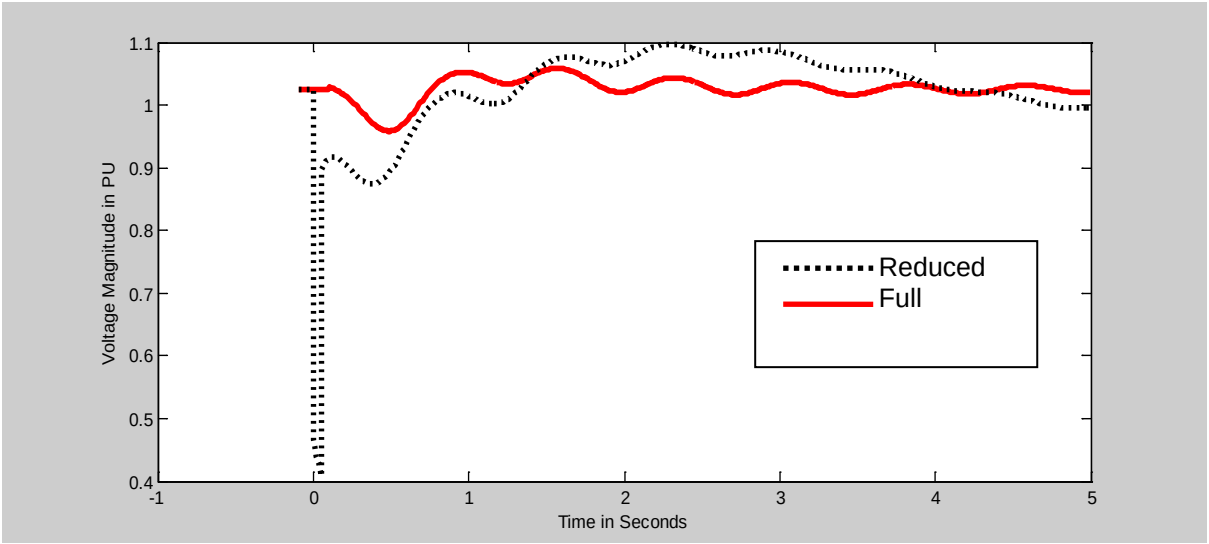

Figure 4.20: Comparison of the dynamic behaviour of the voltage magnitude in PU of the full and the reduced models for the generator-2- first fault location

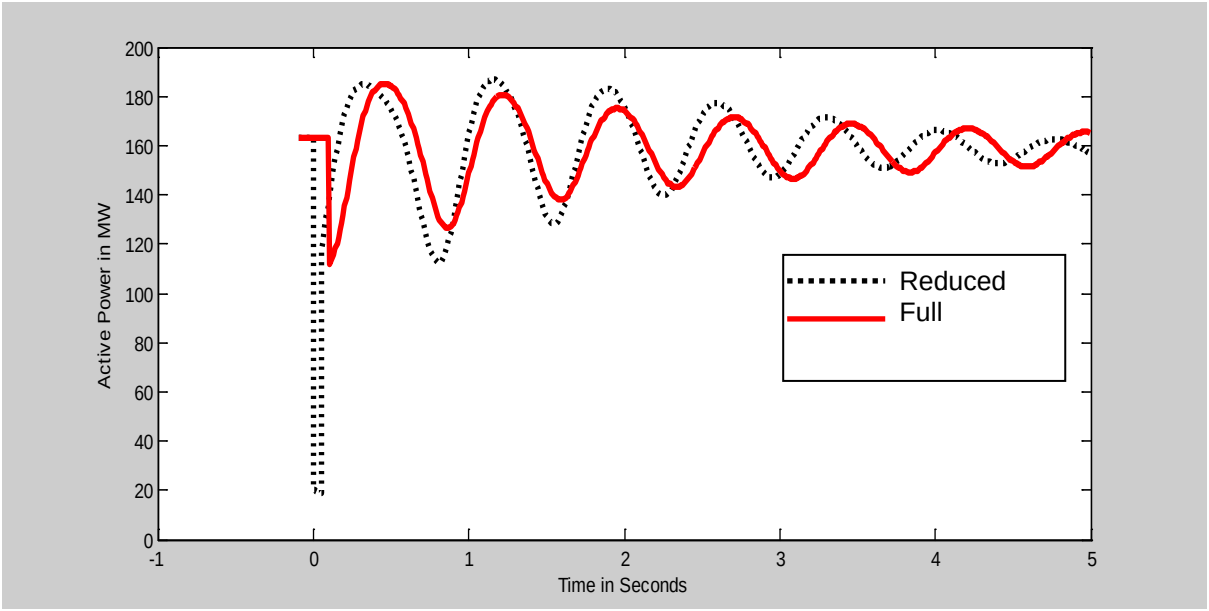

Figure 4.21: Comparison of the dynamic behaviour of the active power in MW of the full and the reduced models for the generator-2- first fault location

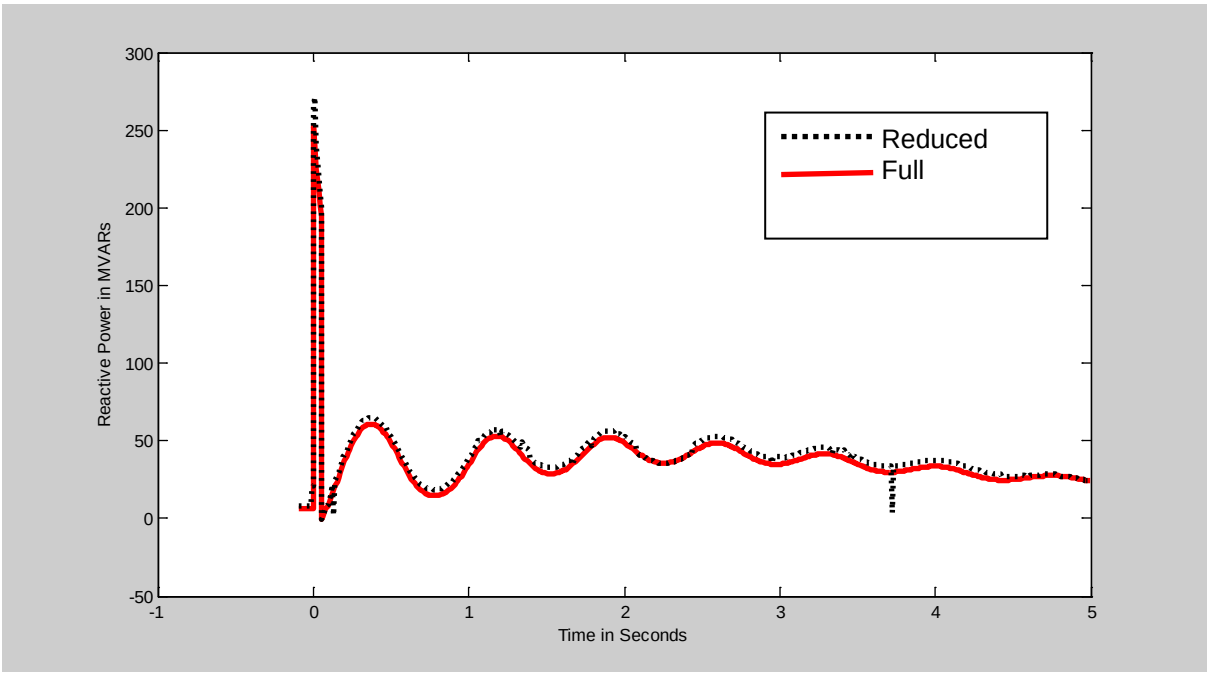

Figure 4.22: Comparison of the dynamic behaviour of the reactive power in MVar's of the full and the reduced models for the generator-2- first fault location

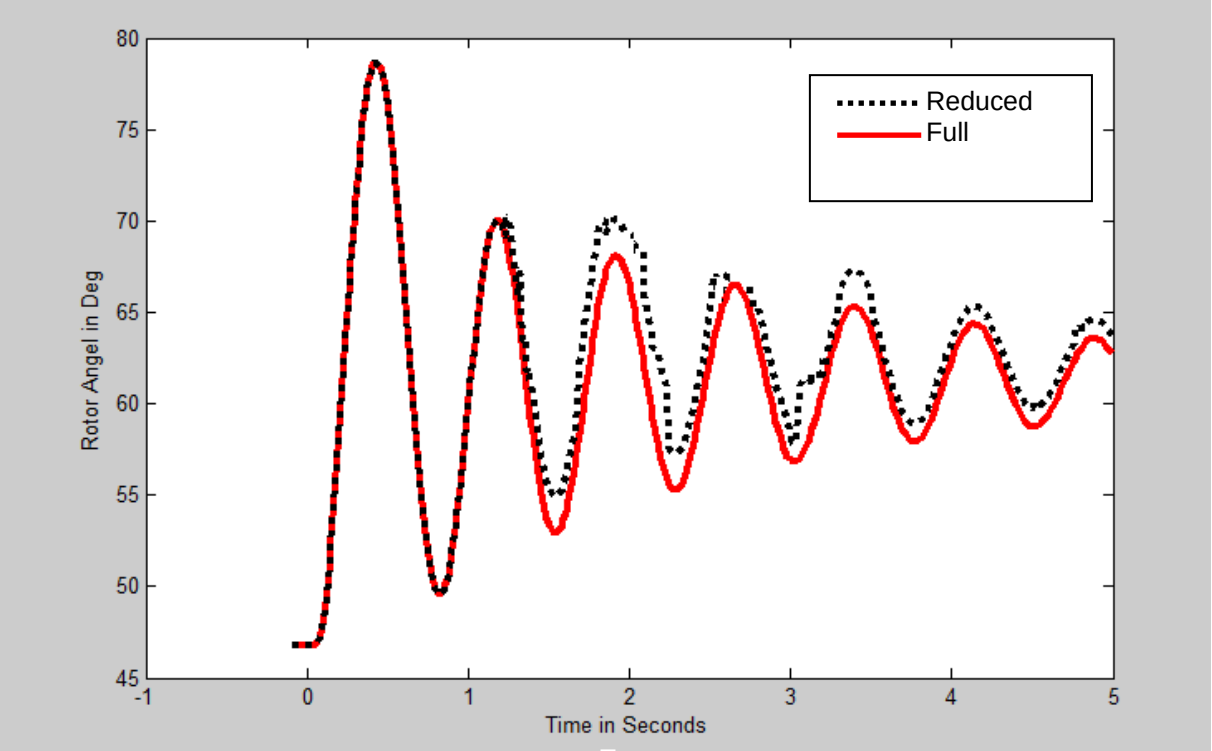

Figure 4.23: **comparison of the dynamic behaviour of the rotor angle in degrees of the full and the reduced models for the generator-2- first fault location**

- **Second fault location**

Again three phase short circuit is introduced on bus 7 as shown in Figure 4.24 and the transient behaviour of generator 2 for the second fault location is depicted from Figure 4.25 to Figure 4.28.

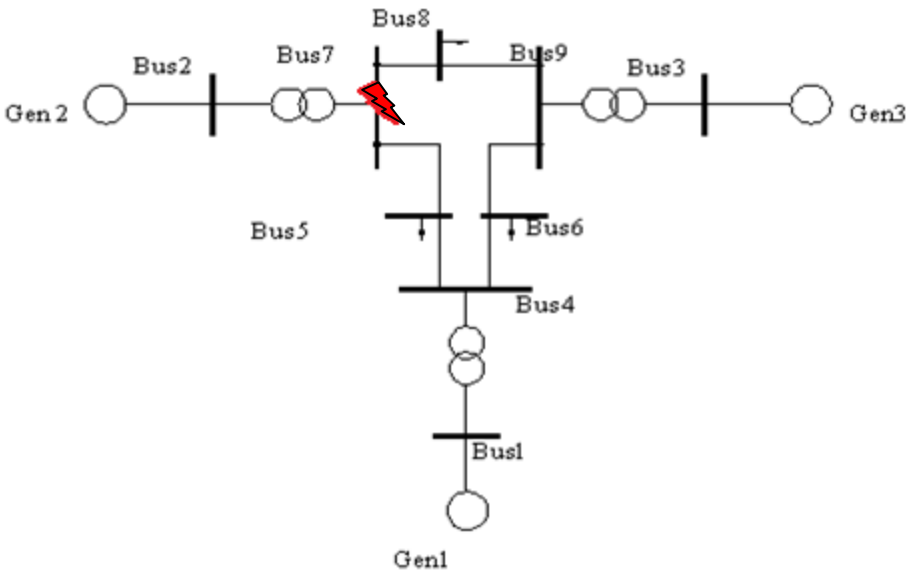

Figure 4. 24 : **Full network with the second fault location**

The dotted line curve is for the reduced network while the solid line is for the full network.

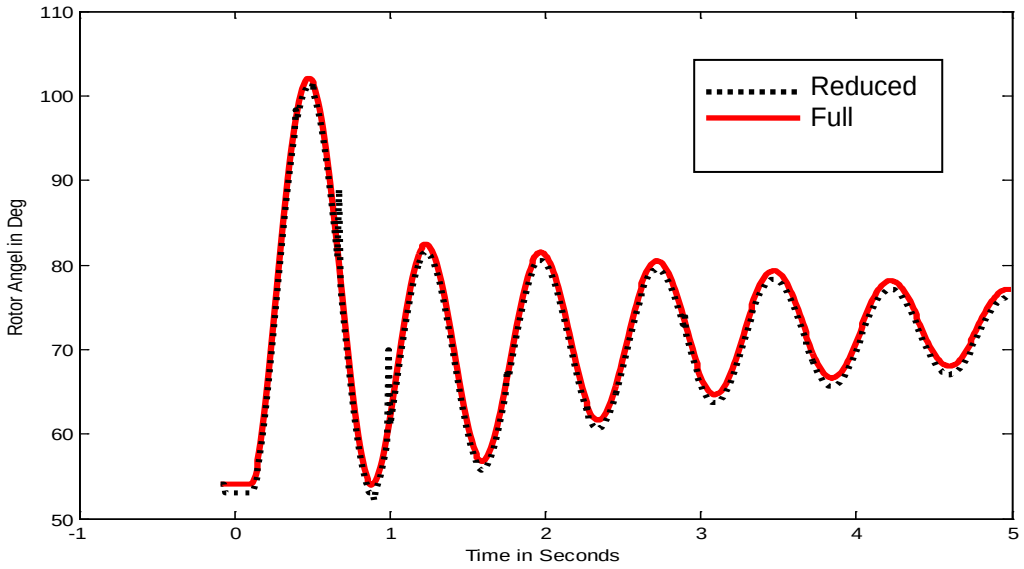

Figure 4. 25: **Comparison of the Rotor angle dynamic behaviour for the reduced and the full model for the generator-2- second fault location**

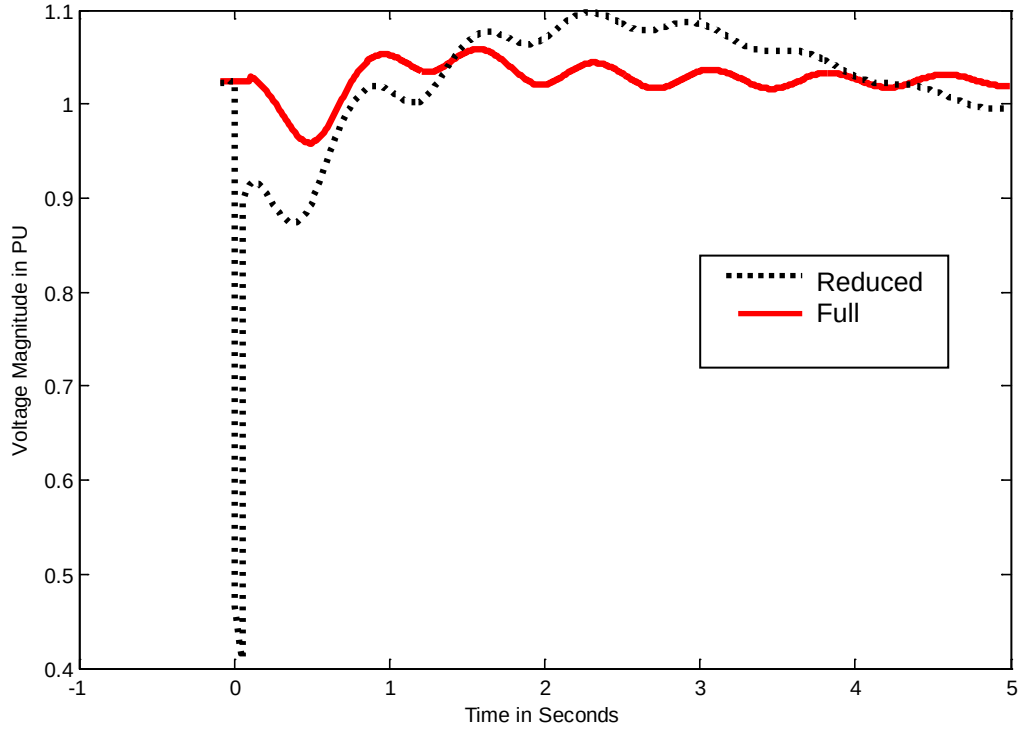

Figure 4. 26: **Comparison of the voltage magnitude dynamic behaviour for the full and the reduced models for the generator-2- second fault location**

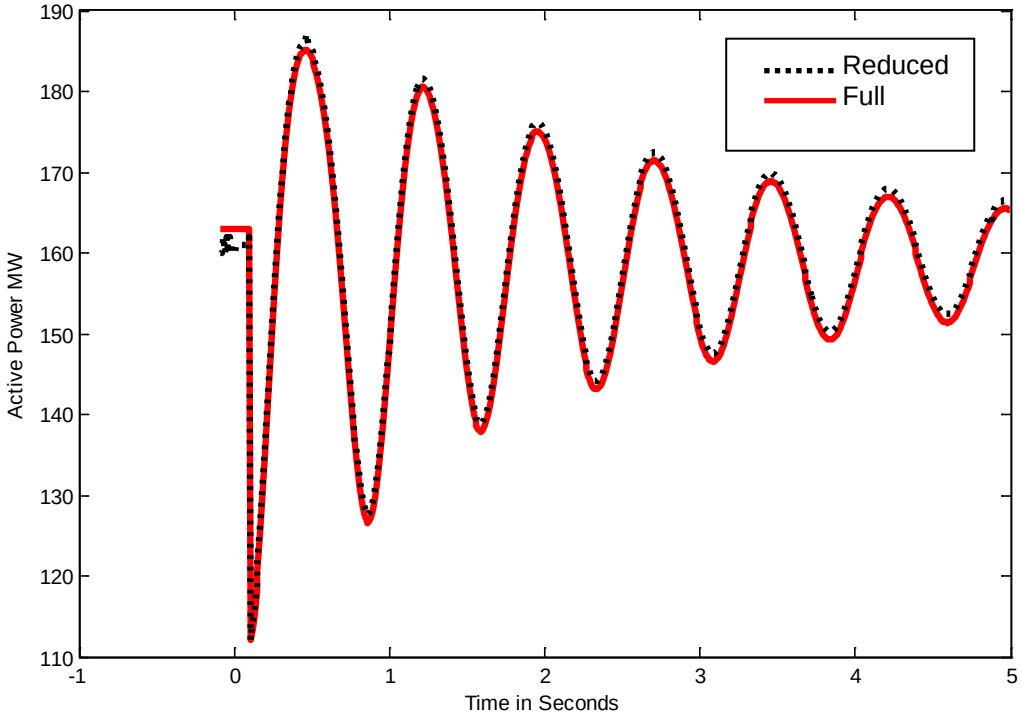

Figure 4. 27: Comparison of the active power dynamic behaviour for the full and reduced models for the generator-2- second fault location

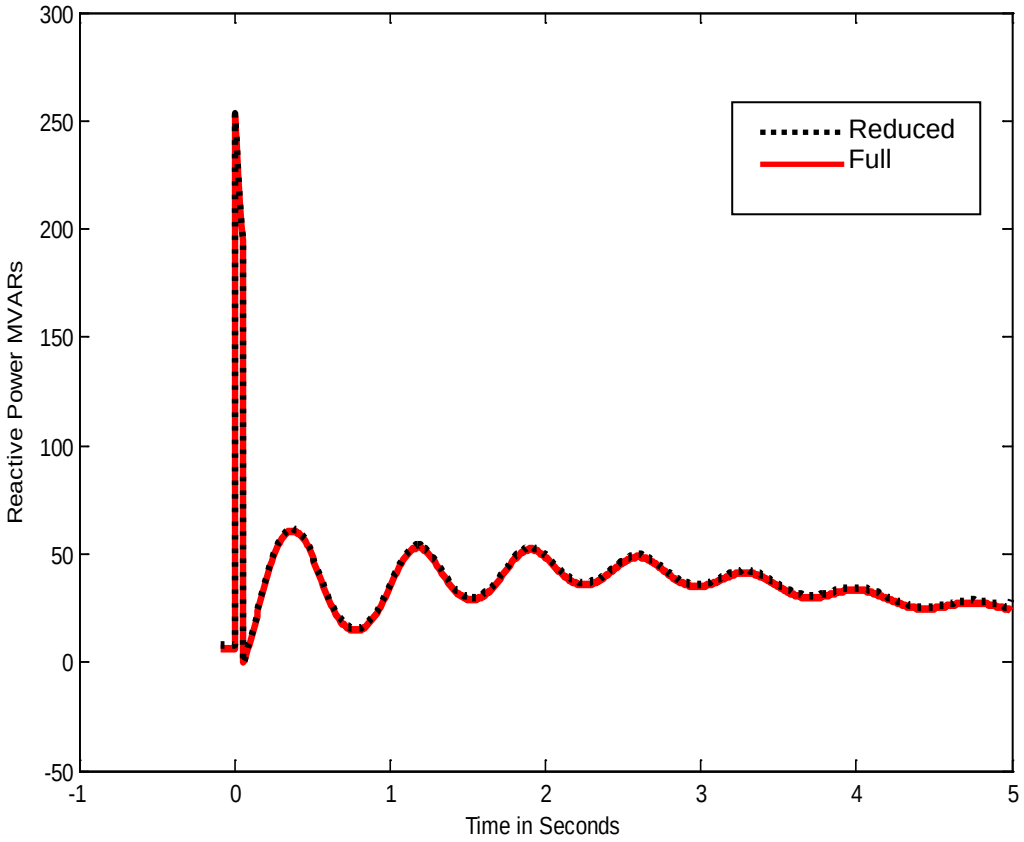

Figure 4. 28: Comparison of the reactive power dynamic behaviour for the full and the reduced models for the generator-2- second fault location

The error between the full and the reduced models for the two fault location seem to be more or less equal.

4.4 Load flow results of voltage magnitude for the reduced model

After the reduction process, the reduced model was simulated again on DigSILENT software package. Figure 4.29 depicts the results obtained, red, and blue colour represent IEEE, and DigSILENT respectively. Voltage deviations seem to be within the limits for both of the results as compared to the ones for IEEE load flow results. The most essential part of the system is the study area which is composed of bus2 and bus7; as a result, their load flow results must be approximately equal to the ones in the full system. This determines the accuracy of the reduction process

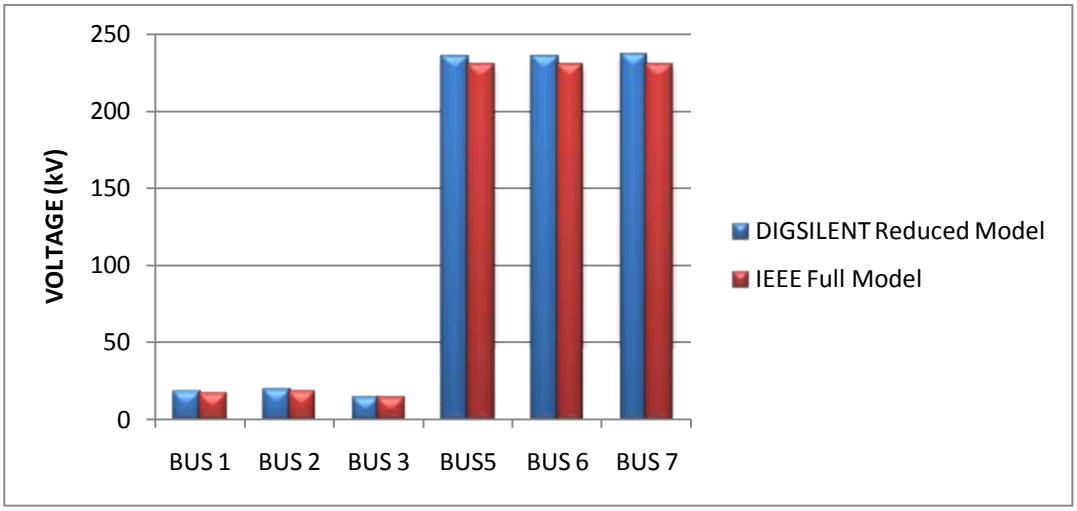

Figure 4.29: Load flow results for the reduced model

Table 4. 9: Comparison of voltage magnitude between the IEEE full model and the reduced model

Bus	IEEE / Voltage	Reduced model	% e_v
1	16.5	17.16	-4
2	18	18.522	-1.917
3	13.8	14.145	-2.5
5	230	235.75	-2.5
6	230	235.74	-2.49
7	230	236.51	-2.83

Table 4.9 present the load flows values for the reduced model and the IEEE to show the error in percentage. The accuracy of the reduced model seemed to be good for the fact that the error percentage is within the range of $\pm 5\%$

4.5 Discussions and Recommendations

The time domain simulation of the reduced model (www.eeserver.korea.ac.kr) at the contingency that is the resilient case as compared to the original full system is used to verify the reducing process. It can be seen that the bus voltage and the power flow of the reduced system are very similar to those of the full system. Reduced system is verified by the evaluation of the similarity for the static aspect of both full and reduced model behaviour (www.eeserver.korea.ac.kr). For this case study, the size of the network has been reduced but the number of generating units is unchanged.

The analysis of the results shows the following capabilities of the developed procedures and algorithms to provide exact reduction process as follows:

- Even though the analysis and results depicted in this thesis are provoked by the importance of conducting voltage instability analysis, it is proved for the reduced system to be correct for both transient and oscillatory analysis as well.
- The obtained model results are compatible with the present power flow and stability software, and they symbolize practical fundamentals so as not to make misunderstanding among analysts which are not proverbial with the reduction methods.
- The consequences of the reduced system on the study area must be signified accurately for the full case conditions and abnormal conditions.

4.6 Conclusions

This chapter developed a coherency-based model order reduction algorithm. IEEE 9-bus system with 6 transmission lines was successfully reduced to 6-buses, system with 4- Transmission lines. Percentage rate of the reduction seemed to be good. The error percentage is within the limits.

According to the literature, reduced system must retain high accuracy for voltage deviations of up to 10% caused by increased power flow. To preserve this accuracy, the reduced system must precisely model the voltage control characteristics of the generation connected to the transmission system and those parts of the transmission system that are in parallel with the high voltage system.The review conducted in Chapter 2, shows that there are very few real-time environment simulations put in place to provide simulation in support of the process of model order reduction. Hence, this kind of simulation needs to be investicated.

Chapter 5 will present the simulations of both the full and the reduced network utilizing the real-time environment software (RSCAD).

CHAPTER FIVE
IEEE 9 BUS NETWORK REDUCTION BASED SIMULATIONS IN RSCAD

Introduction

Modern power system networks need sophisticated analysis tools, such as RTDS, which are based on digital time domain simulation. In order to achieve real-time simulation speeds, RDTS is highly recommended. This chapter describes the implementation of the model of model reduction developed in Chapter 4, using RTDS software RSCAD. In this chapter, both the reduced and the full models are simulated and assessed using RSCAD. The assessment is conducted by load flow and transient behaviour of the reduced and full models. Faults in two locations are conducted within the same study area.

Section 5.1 describes RTDS, its importance, applications in power systems, and the overview of the possibilities for simulations in RTDS. In section 5.2, software and the physical structure of RTDS is presented, while section 5.3 deals with the implementation of the model reduction in RSCAD, synchronous generator modelling, fault logic, output logic and elements of the model used for building of the IEEE 9 bus system. Section 5.4 presents load flow calculation of the full model and section 5.5 presents the building of the reduced model, load flow results for the reduced model, and transient behaviour of the full and the reduced models for the considered two fault locations. Verification of the results from (Chapter 4), of the implementation of the model order reduction method is done in section 5.6. Finally, section 5.7 and 5.8 presents the discussion of the results and conclusions respectfully.

5.1 Real-Time Digital Simulator (RTDS)

The RTDS simulator provides a modular, fully digital power system simulation which can be used for many studies. It performs electromagnetic transient simulations in real-time. This is used for high-speed simulations, closed-loop testing of protection and control equipment as well as Hardware In the Loop (HIL) applications. The final size and configuration of this simulator's hardware is based on the topology and size of the network to be studied (www.GEindustrial.com).

There are over 180 RTDS simulator installations around the world and more than 600 racks in operation. Most worlds' key manufactures of protective relays and power electronic systems use the RTDS simulator on a daily basis. Moreover, RTDS is used by several major utilities as well as their associated research centres. The simulator covers all parts of development and operation of a power system, such as planning,

design and also on-line operation. Research on the fundamental RTDS simulator technology began in mid 1980's with the first commercial simulator installation in 1993 (Singh, 2003). Because of these developments, high demands have arisen in terms of analysis of the power network conditions.

5.1.1 Importance of RTDS in power systems

The RTDS consists of typically designed hardware and software to study power engineering in real-time. Hardware is composed of Digital Signal Processors (DSP), which are used to perform complex computations. In addition, advanced parallel processing techniques are used to achieve the desired computational speed. RTDS software RSCAD is equipped with a library of accurate power system component models which can be used to build models of the power system network. Also the Graphical User Interface (GUI) is provided and can be used to design as well as analyze power system network models (Monali, 2002).

Analogue simulators are used to compute voltage and current values continuously; which limits their speed and capability. Digital simulators do computations when the state changes at discrete instants of time. This allows the simulator to work faster. It is easy to make changes in digital simulation schemas. With RTDS, system problems are discovered faster and the solutions can be designed as well as tested instantly. Evaluation and test of network designs or upgrades can be accurately performed using RTDS (Monali, 2002; Povh et al., 2004).

5. 1.2 Power system and control system component library

Digital Signal processor code is produced only if the compiler accesses library of pre-defined as well as pre-assembled power system components and control function block models. The longer the executable code, the longer the time-step Voltage Source Converter (VSC) sub networks will be. The following are the power system components libraries; real-time network solution, Transmission lines and cables, Machines, HVDC (High Voltage Direct Current), Switched Filter, FACTs (Flexible. AC Transmission Systems), Series Compensators, Transformers, Instrument Transformers, and Distributed Generation

The control system component library allows customized control systems to be created such that they can interact with models of the power systems as well as with the outside world. In addition to particular control blocks, some complex controllers have been assembled and included in the library.

The Control System Library has specialized components for Power System Protection and Automation (www.rtds.com). The protective relay models are helpful when real

devices are unavailable or for training and educational purposes (www.rtds.com). The IEC 61850 models are used to connect a physical device to the RTDS in a closed loop test environment. The SCADA component provides a DNP3 slave interface to the RTDS for an external master. The extended file playback model is important when a lot of data needs to be interfaced into the simulation in real time (www.rtds.com).

5. 1.3 Applications of RTDS in power system

There are many ways that RTDS is used in the field of Electrical Engineering. Figure 5.1 depicts the application of RTDS such as closed-loop testing of controllers, power system studies, closed-loop testing of protective and also education and training.

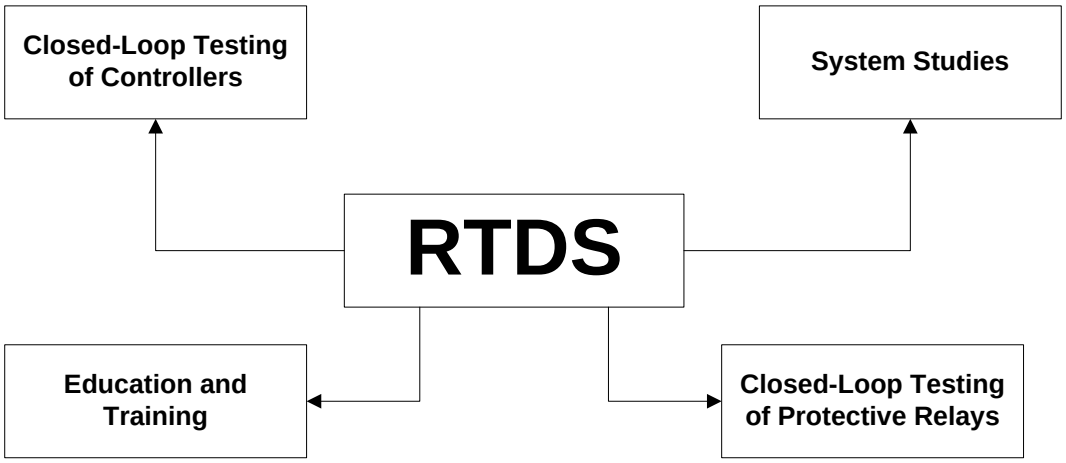

Figure5. 1: Descriptions of the RTDS applications (www.rtds.com)

The RTDS Simulator is currently applied to many areas of development, testing, and studying of the following (www.rtds.com):

- protective relaying schemes ;
- integrated protection and control systems;
- control system for High Voltage Direct Current (HVDC), Static Var Compensator (SVC), synchronous machines, and Flexible AC Transmission Systems (FACTS) devices ;
- general AC and DC system operations and behaviour;
- interaction of AC and DC systems;
- interaction of various electrical installations, and
- Demonstration and training (www.rtds.com), (www.GEindustrial.com).

5.1.4 Overview of the possibilities for simulations in RTDS

Real Time Digital Simulator (RTDS) performs electromagnetic transient (EMT) simulation. To accomplish real-time simulation speeds, the power system to be simulated is alienated into parts by using the travelling wave attribute of transmission lines. The relativistic speed limit permits full partition of the systems if simulation time

step is less than the travelling time of light over the transmission line distance. Thus the two systems can be simulated in parallel on various processors. A custom parallel working out platform is utilized to compute the nonlinear differential equations. Thus, the size of the system to be simulated is not restricted by one processor or one computer, and systems of hundreds of buses have been simulated in real time (Forsyth et al., 2001).The relativistic speed limit also without human intervention ensured convenient scalability. The size of the system is directly proportional to the number of interconnected subsystems, each connected to the others by dividing transmission lines. Yet, the size of each subsystem does not grow, and consequently, nor does the processing power needed to solve it. Therefore, the bigger problem can be solved merely by adding a larger number of processors (Yuefeng, 2011; Xi, 2010).

Simulations of the power system in real-time is not only for saving the computation time; more significant, actual protection relays and control equipments can be connected to the RTDS in a closed loop and be tested as if they are in a real power system (Mcharen et al., 1992). It must be noted that despite the fact that RTDS is an EMT type simulation tool, the technique constraints for it are considerably unlike from those for a non-real-time EMT program or those for a TSA type program (Yuefeng, 2011; Xi, 2010).

The main benefit of RTDS is that a real physical controller can be linked to it. Additionally, for the simulation running at real-world speed, it is also vital to run on a nonstop basis, such as minutes, hours, or even days. In this time frame, in a real power system, approximately all dynamic performances can happen. For a real controller, it is impossible to divide its “slow” and “fast” performances and characteristics, its reaction is a full range response, and thus the RTDS which is to be connected to the real controller is also estimated to symbolize a full range of performances and behaviours of a real power system. To accomplish this, in a RTDS simulation environment, not only does each of the power system components require to be modelled in full detail, but also a large number of components require to be modelled. Technically such a modelling approach can be used in RTDS, since its distributed calculation platform is possible to be scaled. On the other hand, to model a practical power system in full RTDS detail requires large amount of RTDS hardware and hence the hardware cost can be basically too expensive (Yuefeng, 2011; Xi, 2010).

5.2 RTDS RSCAD software

RSCAD, the digital time-domain simulation tool is being widely used in the power industry (Forsyth, et al, 2001; Mcharen, et al, 1992).

RSCAD consists of programs shown in Figure 5.2. The host operating system is connected to the RTDS rack via WIF (Workstation Interface) card which allows the simulation case preparation as well as compilation.

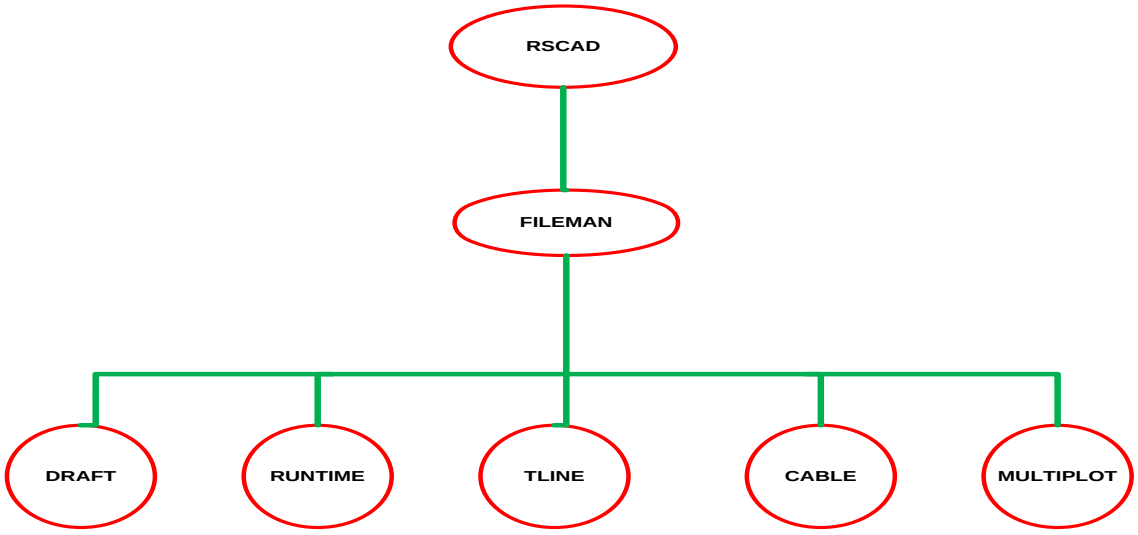

Figure5. 2: Real-Time Digital Simulator structure

Where, **File man** is the location where the model is being saved, **Draft** is the window where the one line diagram is implemented, **Runtime** is the window the simulation output graphs are done, **T-Line** is the window used to model transmission line towers parameters, **Cable** is the window used to model cable parameters, and **Multi-plot** is where the plots are generated.

5.2.1 RTDS hardware

Digital Signal Processors (DSP) of the RTDS hardware use improved parallel processing techniques for reducing the computation burden in real-time operation. There is an interaction of RSCAD software and RTDS hardware while the run-time is on. Thus carry out all computations in real time. A number of various racks are used to enhance the required real-time computation. A single rack (www.respository.tudelft.nl) has processing cards with digital and analogue I/O ports GIGA processor card (GPC), RISC processor card (RPC), triple processor card

(3PC), and communication cards. Common backplane is utilized to connect all the cards to facilitate data exchange between individual processors and between racks (Neville and Jos, 2003; RTDS User Manual, 2011; www.rtds.com; Rigby, 2012)

5.2.2 Processing cards

The characteristicts of the mentioned above 3 types of processing cards are compared in the Table 5.1.

Table 5. 1: Characteristics of the processing cards of RTDS

Processor Card	3PC	RPC	GPC
Processor type	Digital Signal 3ADSP-21062	Power PC 2IBMPPC750CX$_e$	Power PC 2IBMPPC750GX
Instruction Cycle	25ns	1.67ns	1ns
External Equipment Access	YES	NO	YES
Input/output Parts	Analogue output channels	Non	Analogue output channels

In conclusion, GPC card is considered to be the faster in calculation process.

5.2.3 Communication cards

RTDS has two communication cards, namely;

- Workstation Interface card (WIF), and
- Inter-Rack Communication Card (IRC)

Workstation Interface card (WIF): This card is responsible for the communication between the RTDS and the host PC in which the user can implement a model of the study system. In the process of the real time simulations, WIF cannot have impact on the model solution. Moreover (www.respository.tudelft.nl), data package exchange between racks and the workstation PC is also controlled and facilitated by WIF card. Figure 5.3 shows the structure of the RTDS which depicts clearly the RTDS rack, the process cards slots, the PC host, digital and analogue I /O cards, and the Ethernet communications connection of the structure. The user library, WIF card, GPC card, and the bi-directional Ethernet are used for the modelling of both full and reduced networks in the thesis.

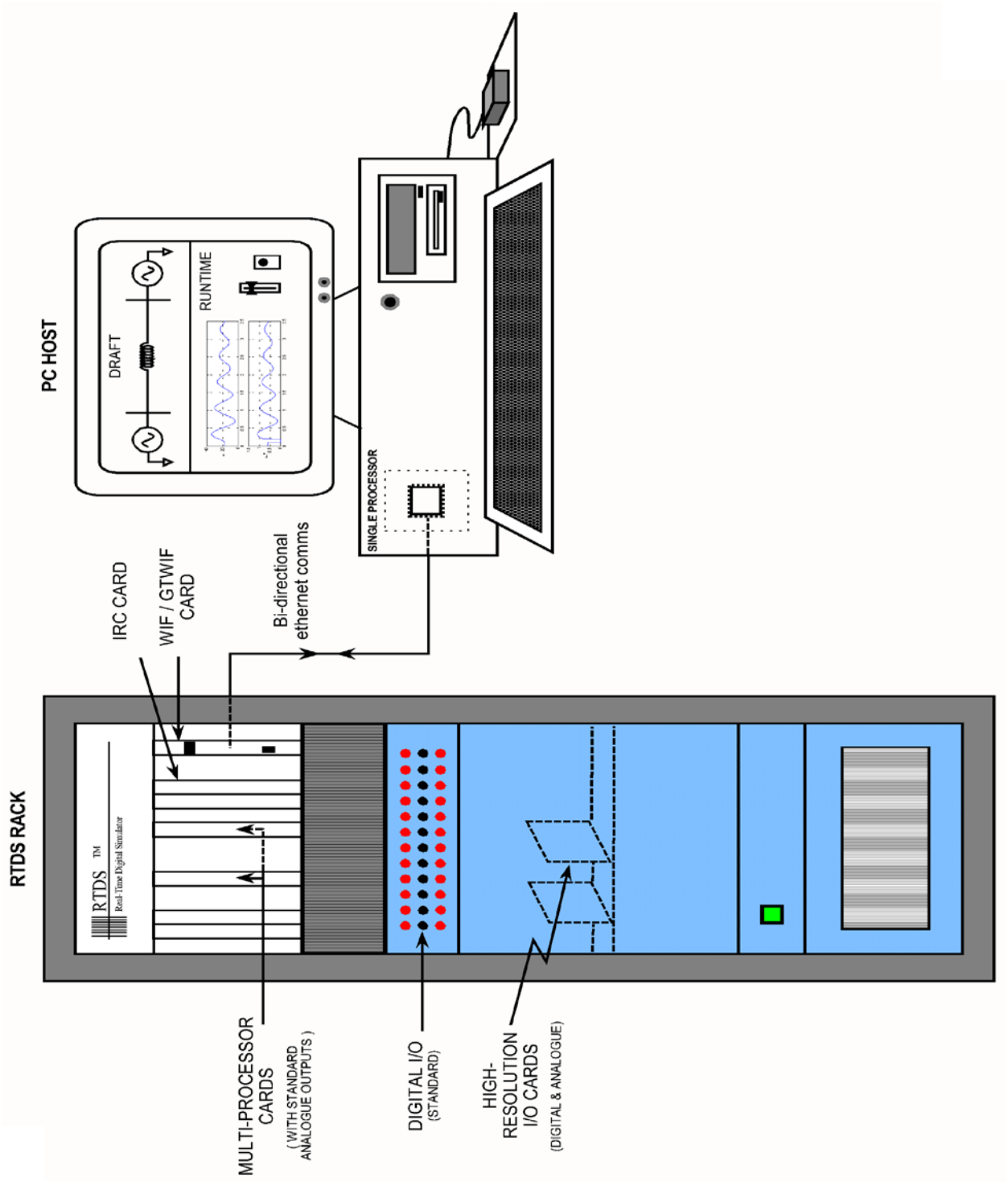

Figure5. 3: **Structure of the RTDS (Rigby, 2012)**

5.3 Building of the full order model of the IEEE 9-bus system in RSCAD

Both full and reduced power system networks are built in RSCAD software.The simulations are conducted in the real-time environment.

The same IEEE 9-bus system investigated in Chapter 4 is considered.

Figures 5.10 and 5.19 depict RSCAD models of the full network and reduced network respectfully. Developed reduced network in Chapter 4 is implemented but the

modelling of the elements in RSCAD is different from this in the DigSILENT software environment. Synchronous generators, transmission lines, bus-bars and the loads are quite slightly modelled differently. The models of the separate elements of the considered power network in RSCAD are described below and then the full model of the IEEE 9-bus system is built.

5.3.1 The synchronous generator transformer model

There are different types of synchronous generators in the user library. For this study, synchronous generator-transformer model is used because it has both an internal bus and a transformer. Figure 5.4 shows a typical model structure of the synchronous generator transformer in RSCAD environment.

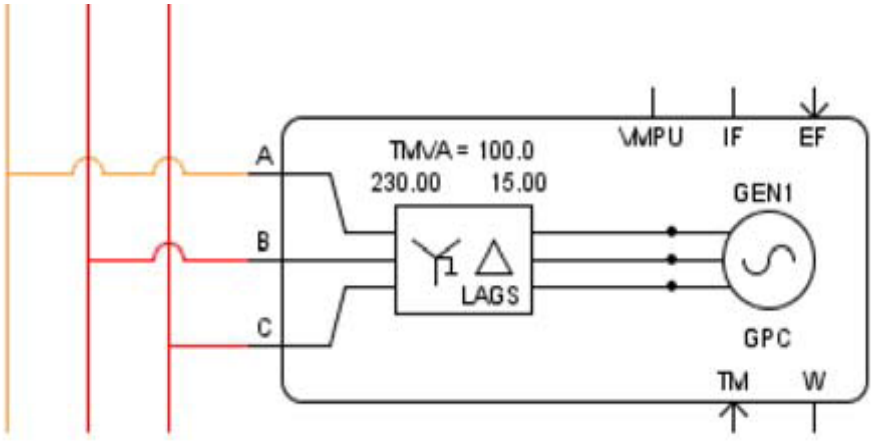

Figure5. 4: Synchronous generator transformer model (RTDS User Manual, 2011)

The generator part can be utilized as a generator, synchronous condenser, and synchronous motor depending on the settings selected by the user. This is possible due to the fact that the model has positive torque, negative torque and no torque options to be selected.

Where;

TM is a Mechanical Torque Input in PU

EF is a Field Voltage Input in PU

$VMPU$ is a Generator Terminal Voltage in PU

W is a Machine Speed Output in rad/sec

IF is a Field Current Output in PU

5.3.2 Excitation controller and governor

Due to the fact that, this study involves the stability analysis for the synchronous generators, the excitation controller and governor models must be connected to the synchronous generator model as show in Figure 5.5.

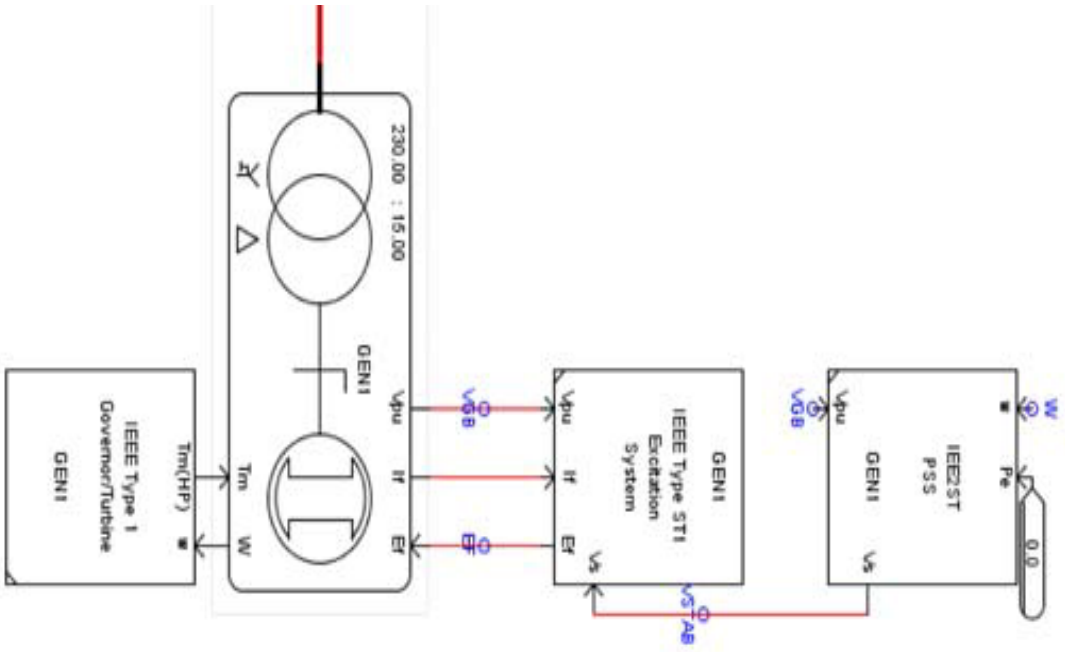

Figure5. 5: Synchronous generator model with excitation and governor (RTDS User Manual, 2011)

Voltage regulator inputs and outputs of the generator are provided through $VMPU$, IF and EF signals from the generator. These are available at the generator terminals as depicted in Figure 5.5. The power system stabilizer input is optional to the generator. Both excitation and governor controllers can be alternatively constructed using control function blocks (RTDS User Manual, 2011; www.rtds.com; Rigby, 2012).

5.3.3 Fault logic

Two three phase short circuit faults at the transmission line between bus 7 and bus 5 and on bus 7 as it was conducted in DigSILENT software are applied to the network. The draft schematic in Figure 5.6 has custom-designed logic to open the circuit breakers at either end of the faulted line in 0.07 seconds after the three phase short circuit fault incidence (RTDS User Manual, 2011; www.rtds.com; Rigby, 2012).

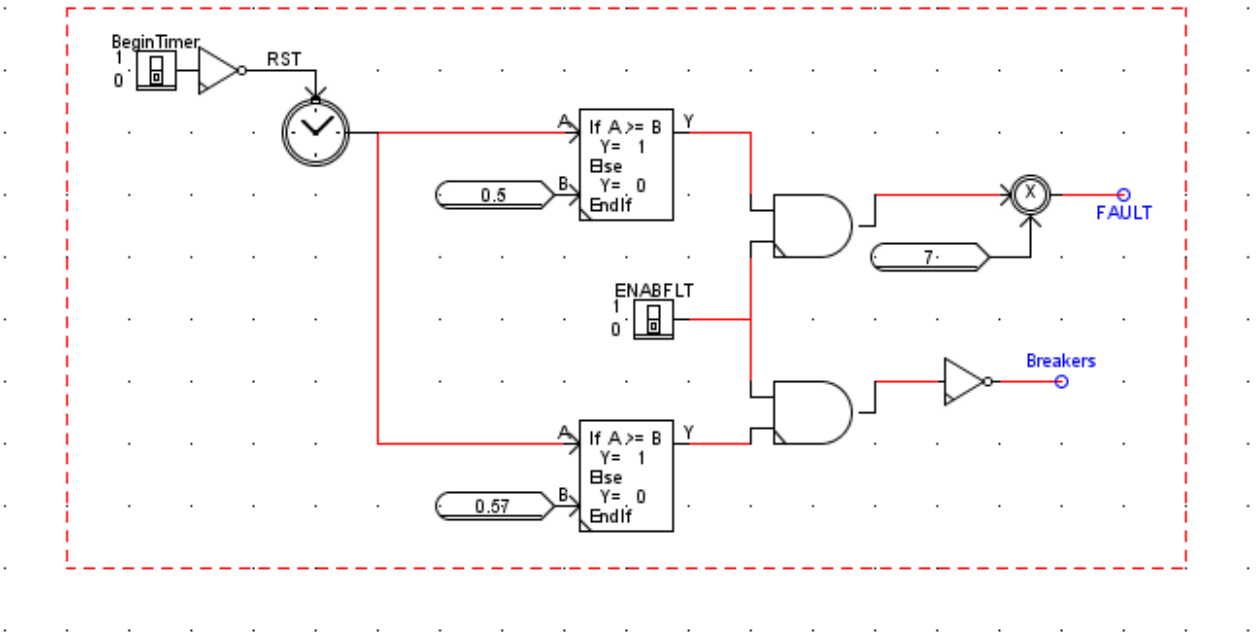

Figure5. 6: **Structure of the fault logic (RTDS User Manual, 2011)**

5.3.4 Output logic of the rotor angle

It is already mentioned in Chapter 4 about the methods to evaluate rotor angle of the synchronous generators. Figure 5.7 shows the output logic of determining the rotor angle. This is one of the differences between DigSILENT and RSCAD modelling of the parameters which makes the dynamic responses of the synchronous generators to be a bit different.

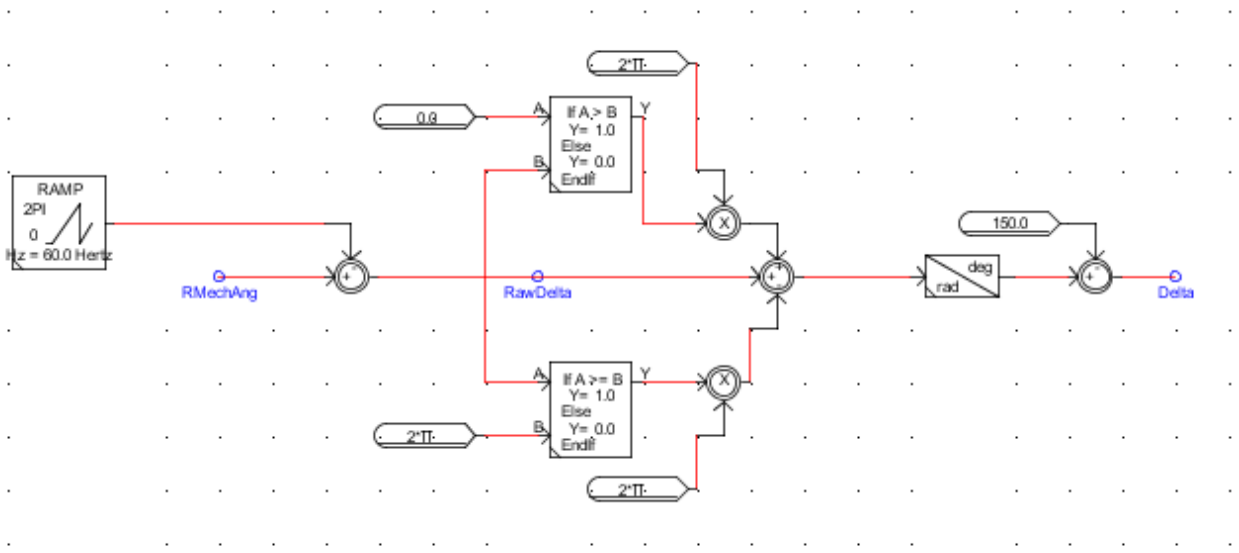

Figure5. 7: **Structure of the output logic for determination of the rotor angle** (RTDS User Manual, 2011)

The model of the full IEEE 9-Bus system was built in RSCAD software environment. The process of building the model is described below.

5.3.5 Other elements models used for building of the IEEE 9 bus system model

Bus-bar in RSCAD consists of three nodes N_1, N_2, N_3 and each bus in the library has unique nodes numbers. For an example, the nodes numbers for bus 2 are the next three numbers N_4, N_5, N_6. Figure 5.8 (a) depicts a typical bus 1 model. Nine of these models are used in Figure 5.8(a).

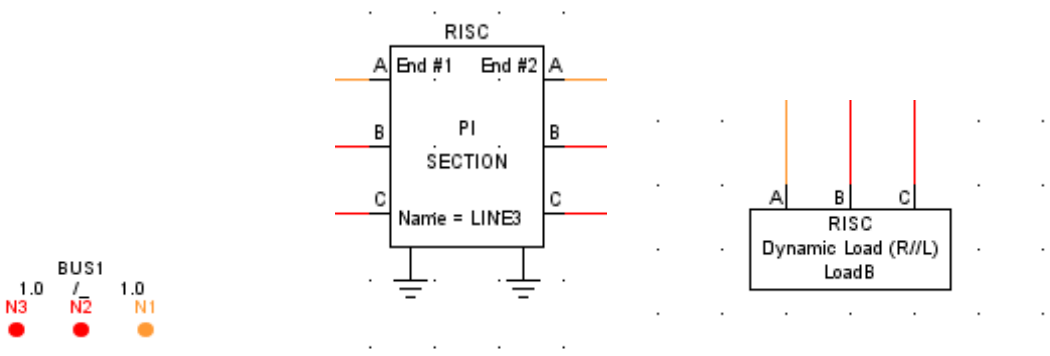

Figure5. 8: (a) Bus-bar model (b) RSCAD transmission line model (c) RSCAD Dynamic load model (RTDS User Manual, 2011)

Parameters of transmission lines such as resistance, reactance voltage magnitude and frequency are easily modelled in PI3 transmission line model shown in Figure 5.8 (b). Therefore six of these models are used for building of the full model.
Type of load used for modelling the system is dynamic load (R/L) as shown in Figure 5.8(c). Three of these models are used to build the full system model.

Single phase to ground fault model is used to introduce the disturbance to the system in order to perform the stability analysis. Figure 5.9 (a) shows a typical model of the fault logic. Both Figure 5.9 (a) and Figure 5.9(b) are used together and are from the same library.

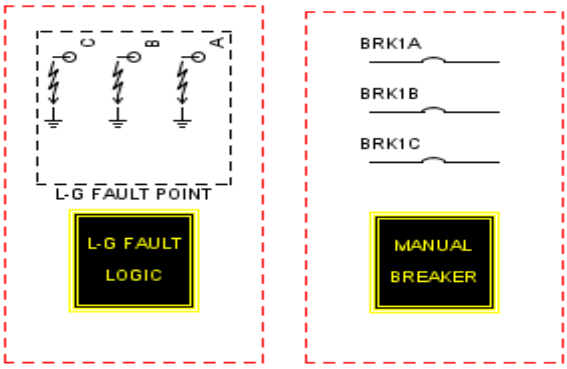

Figure5. 9:(a) RSCAD fault logic model and (b): RSCAD circuit breaker model (RTDS User Manual, 2011)

Figure 5.10 depicts the full order model of the IEEE 9-bus power system. The elements described in the previous section are utilized to build the system in RSCAD software environment. Next section presents parameter selection for the elements.

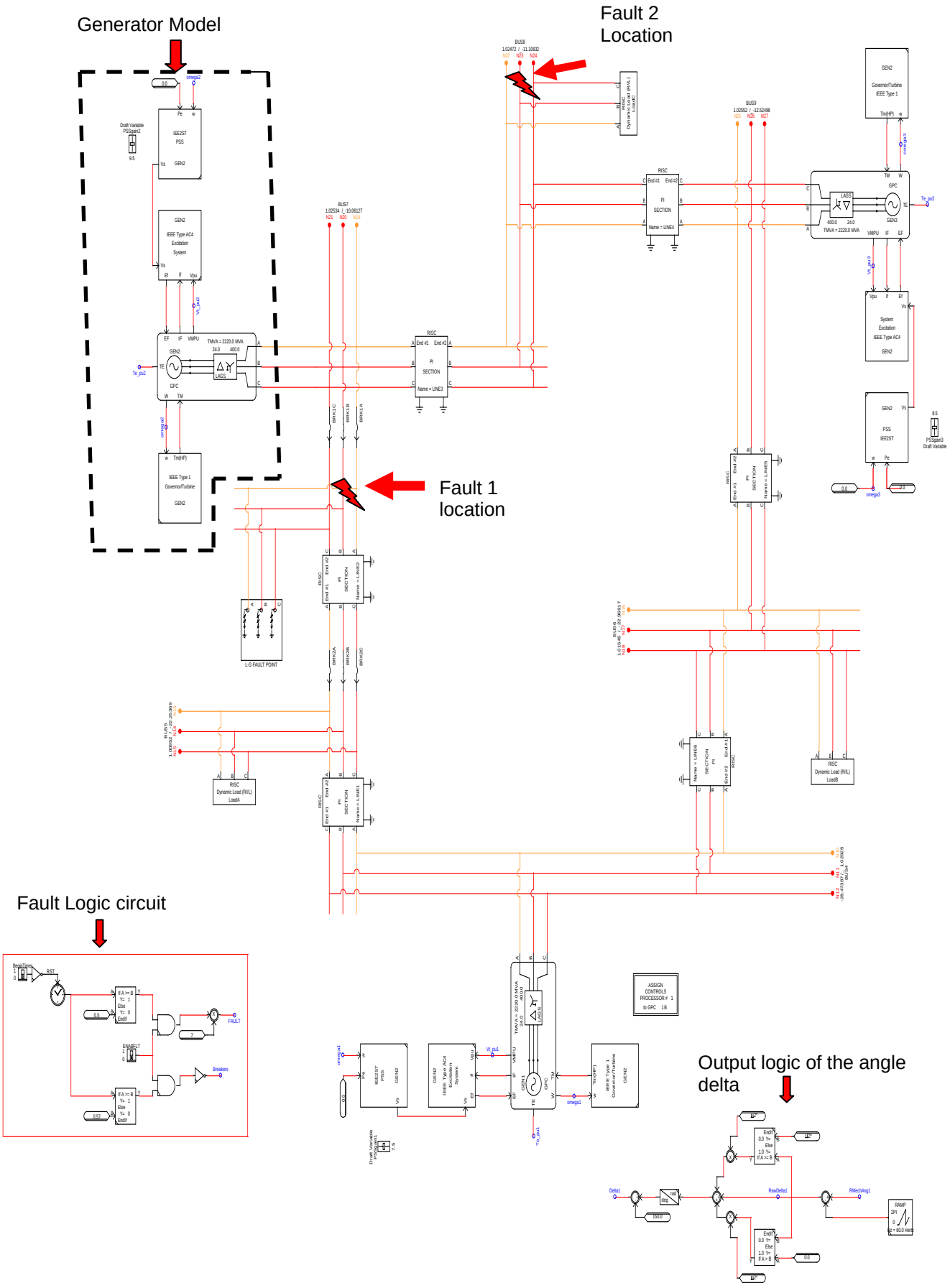

Figure5. 10: Full IEEE 9-bus system in RSCAD

5.3.6 Configuration of the synchronous generator in RSCAD software

Synchronous generator model in RSCAD is configured in a different way as compared to the DigSILENT software environments. This section explains shortly how the configuration of the synchronous generator is done in this research.

5.3.6.1 Parameter selection

Synchronous generator model in RSCAD software must be carefully parameterised and utilized otherwise, the load flow and fault simulations results will be not correct. Therefore, this part of the Chapter 5 describes the brief procedures of how the generators are modelled for this research. When initializing the generator according to a load flow, it is vital that the user select “Rated”. When the response of “zero” is given, then the ***MACHINE INITIAL LOAD FLOW DATA*** menu tab disappears. By double clicking on the generator model as shown in Figure 5.4; the following window pops up. Figure 5.11 shows the possible menu tabs for the machine. It is not necessary to model all the parameters; this depends on the interest of the user.

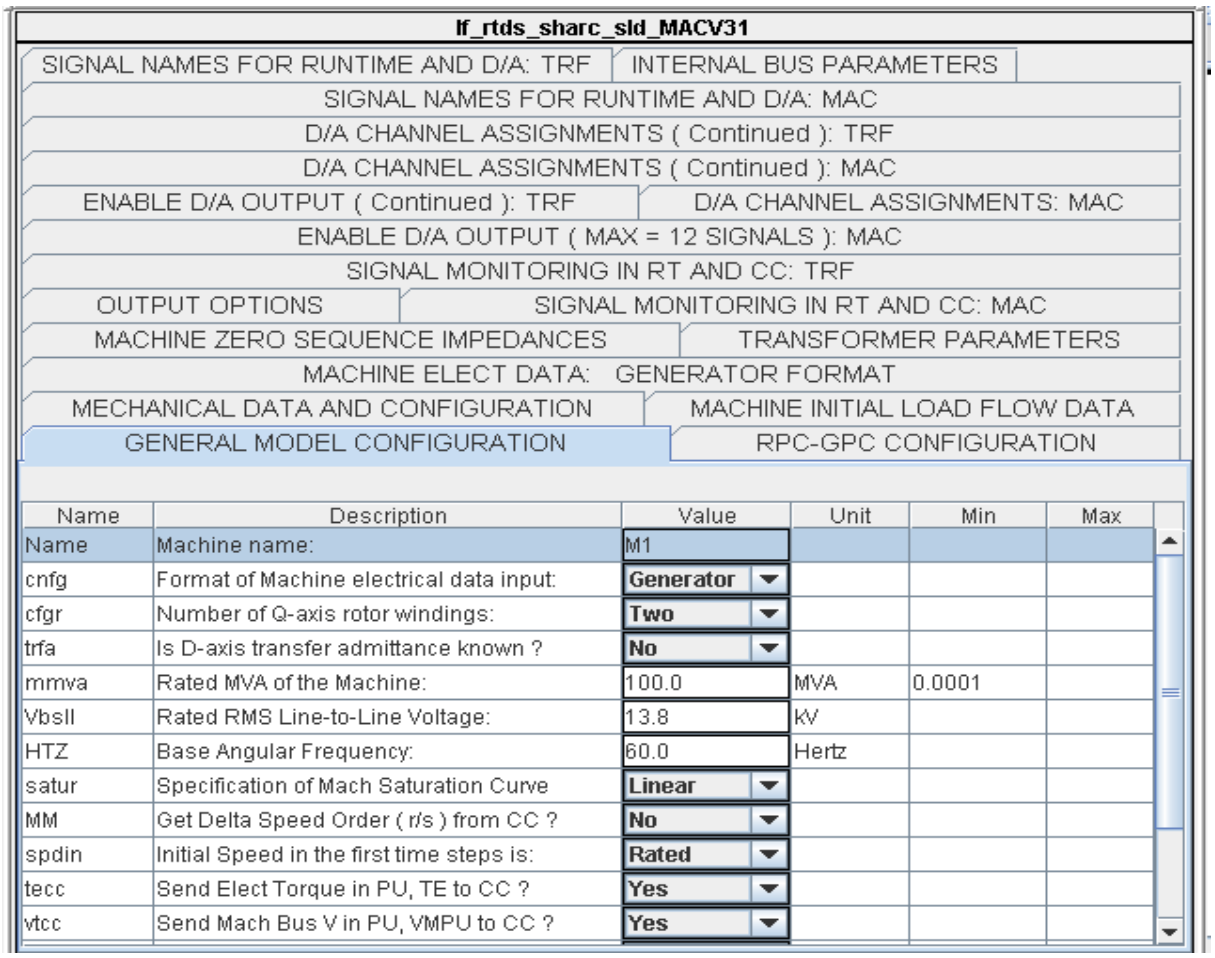

Figure5. 11: Synchronous machine parameters (RTDS User Manual, 2011)

The “MM” item in the column “Name” is specified as “No”, and then the MECHANICAL DATA AND CONFIGURATION menu Figure 5. 12, is made available for specifying the required mechanical data. The rotational energy saved in the machine rotor at rated speed per MVA of the machine is called inertia (H). In reference to the assumptions made for the modelling of synchronous generator for stability studies reported in Chapter 1, the synchronous damping torque factor is modelled with a value “0”. The generator runs in lock mode or free mode due to the settings of “MM” in the ***GENERAL MODEL CONFIGURATION*** menu set to “No” (RTDS manual, 2010).

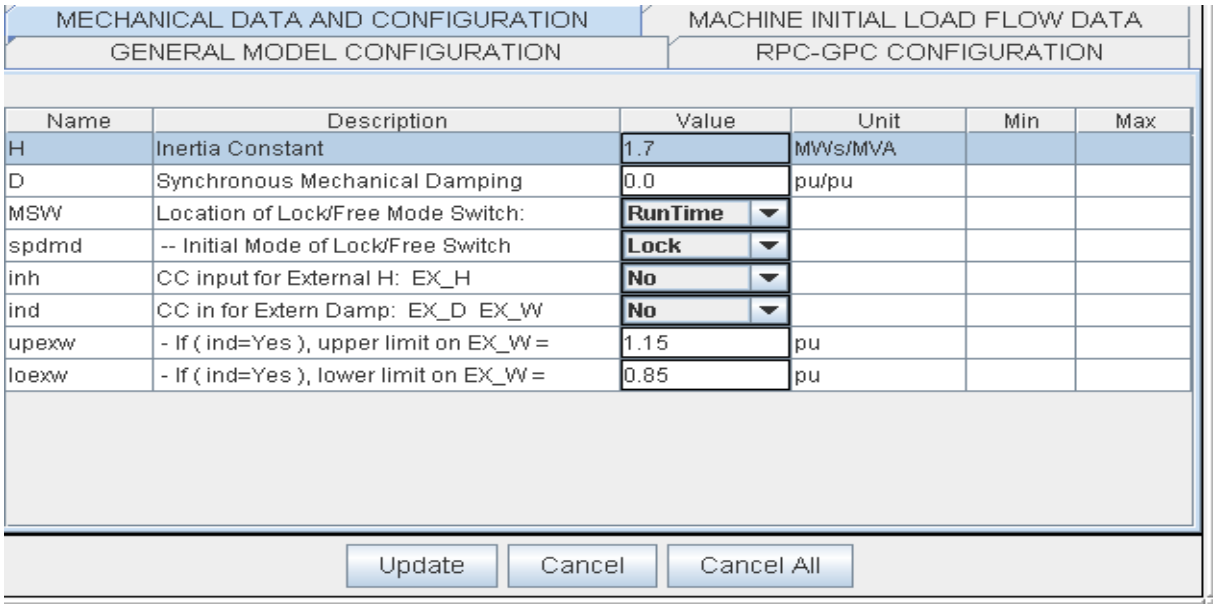

Figure5. 12: Mechanical data and configuration tab (RTDS User Manual, 2011)

The speed of the generator can be determined by the generator slider (CONSPD) in the run time window only when the generator is in lock mode. As for the free mode, the speed of the generator depends on the sum of the torques; mechanical, electrical, and damping torque that act on the total inertia of the generator. When starting simulation, the generator is set to run on locked mode until it reaches its synchronous speed. Then it can be changed to the free mode by using a Lock/free switch available in the run time window (RTDS manual, 2010).

5.3.6.2 The machine saturation curve menus of the synchronous generator in RSCAD

This is the option of selecting either linear, points, or factors method of specifying generator D-axis saturation to be selected. The common methods are points and factors. The impact of selecting points makes the saturation curve for the D-axis of the generator to be modelled utilizing the points on the curve.

The curve in the Figure 5.13 depicts the open−circuit stator voltage versus field current during synchronous speed operation (RTDS manual, 2010). The synchronous reactance and the induced Electro Magnetic Force (emf) can be determined by the open circuit test. When synchronous generator is running at synchronous speed, the stator windings can be open-circuited. Both stator winding voltage and the rotor field current are changing proportionally. The relationships between them are obtained by the open-circuit test as depicted in Figure 5.13.

where X_{mdo} is the internal reactance of the synchronous generator.

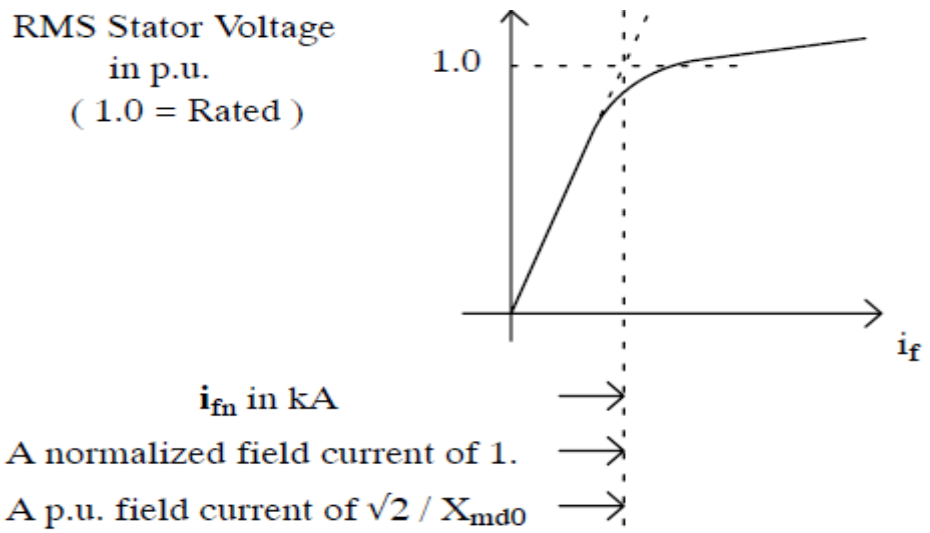

Figure 5. 13: **Machine saturation curve of the synchronous generator in RSCAD** (RTDS User Manual, 2011)

On the other hand, during selection of the saturation curve using factors method, the window on Figure 5.14 pops up to enable modelling of the open-circuit generator voltage values. This is relevant because the curve can be determined only during the operation of the open-circuit by changing the field current and monitoring the stator voltage as described by Figure 5.15 (RTDS manual, 2010).

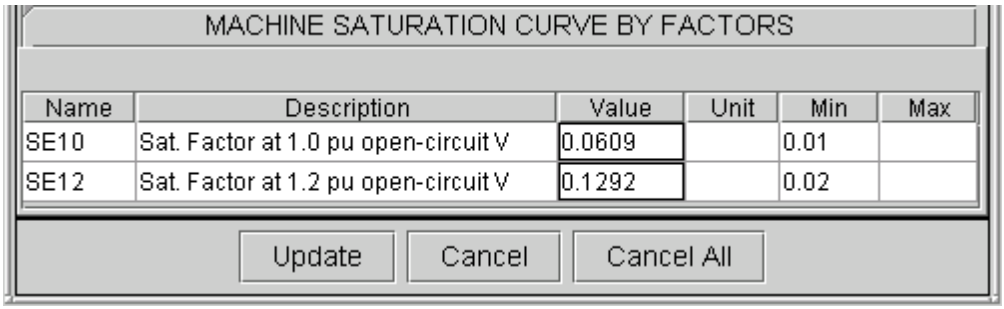

Figure5. 14: **Mechanical saturation curve by factors tab** (RTDS User Manual, 2011)

The saturation curve explained by the SE (1.0) and SE (1.2) factors is exchanged to the right side of the unsaturated curve by a quadratically incrementing number

explained by the two points. The two factors are also adequate to describe the point T where the saturation graph happens to be tangent to the unsaturated graph.

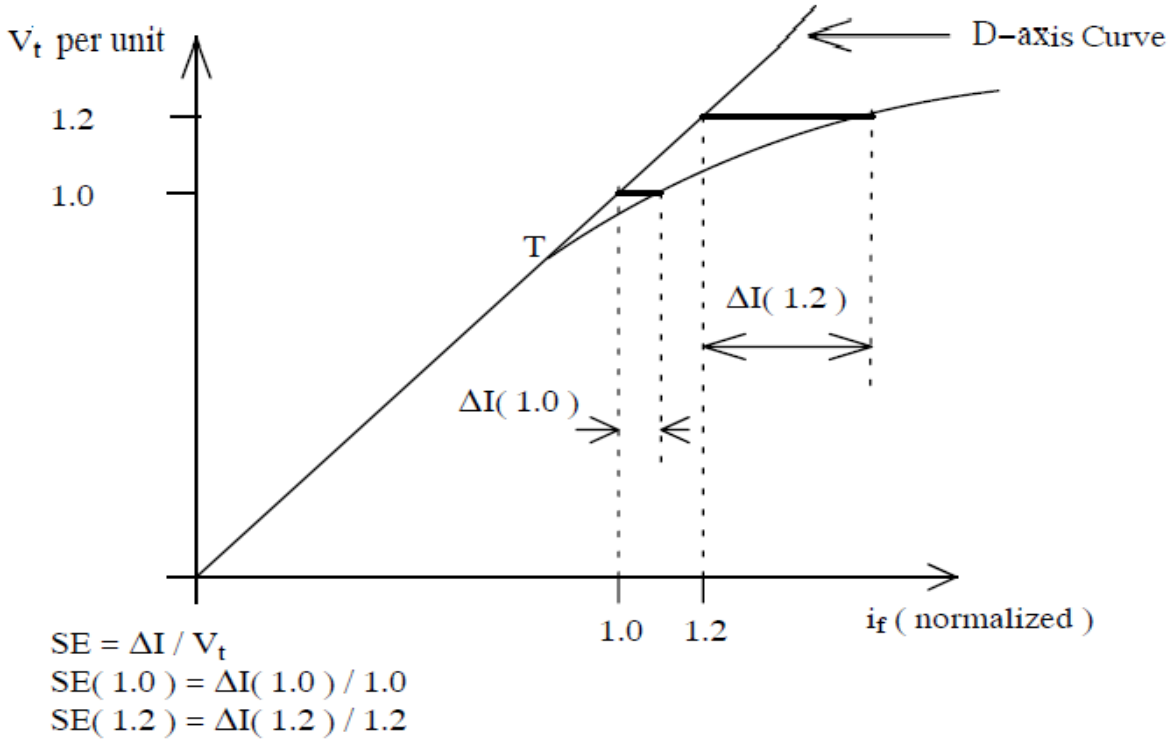

Figure5. 15: Mechanical saturation curve (RTDS User Manual, 2011)

5.3.6.3 Multi-machine operation procedure of the synchronous generators in RSCAD

In order to get correct and accurate results, it is very essential to follow the correct procedures of how the simulations are done. Therefore, the start-up procedures can be written as (RTDS manual, 2010):

- Begin the simulation with the generator in lock and (*single-mass*) modes Single mass mode simulates all masses as one equivalent lumped mass.
- Set the generator to free mode after the electrical system has reached stability.
- Change from single-mass mode to multi-mass mode immediately the generator is running at synchronous speed, and
- Subject the system to the disturbance.

5.4 Load flow calculation for the full model

The load flow simulation is performed in order to analyse how far the results obtained in RSACD are from the published one for the IEEE 9-bus system.

Table 5.3 depicts the initial voltage magnitudes of bus-bars in order to run the load flow calculations. The model was compiled before conducting the load flow calculations.

Table 5. 2: **Input data of IEEE 9 bus system for load flow calculation**

Bus Number	1	2	3	4	5	6	7	8	9
Voltage	16.5kV	18kV	13.8kV	230kV	230kV	230kV	230kV	230kV	230kV

The results from the load flow calculations for the voltage magnitudes and the magnitudes of the active and reactive power for every bus are shown in Table 5.3

Table 5. 3 **Active and reactive power load flow results**

Bus number	Voltage (kV)	Active power (MW)	Reactive power (MVars)
1	16.97	73.89	28.05
2	18.56	162.86	7.19
3	14.15	84	-9.92
4	233.89	32.83	1.45
5	231.82	-14.19	-37.22
6	228.44	-58.65	-13.84
7	230.81	84	-8.67
8	234.16	-77.51	-10.37
9	228.51	61.01	-18.05

Comparison between the bus voltage magnitudes between the IEEE 9-bus models published results and the results obtained from RSCAD is shown in Table 5.4. The IEEE values are accepted for 100%.

Table 5. 4: **Voltage bus magnitude load flow results**

BUS	IEEE	RSCAD	Percentage deviation
1	100%	102.85%	2.85%
2	100%	103.11%	3.11%
3	100%	102.54%	2.54%
4	100%	101.69%	1.69%
5	100%	100.79%	0.79%
6	100%	99.32%	-0.68%
7	100%	100.35%	0.35%
8	100%	101.81%	1.81%
9	100%	99.35%	-0.65%

Results for the percentage deviation are obtained by utilizing Equation 4.23 in Chapter 4. Percentage deviation of RSCAD from the IEEE results is within $\pm 5\%$. The fact that the differences in bus voltages magnitudes are small in the frame work of $\pm 5\%$ allows the full model of the IEEE 9-bus system to be used for application of the

Coherency based model order reduction method. Graphical outputs of load flow bus voltages from bus1 to bus 9 are depicted in Figure (5.14) – (5.16), where N is the node number and S represents the rack number of the simulator in RSCAD.

Figure 5.16 depicts the three phase waveforms of the voltage magnitudes of bus 1, bus 2 and bus 3 of the full model of the IEEE 9- bus system.

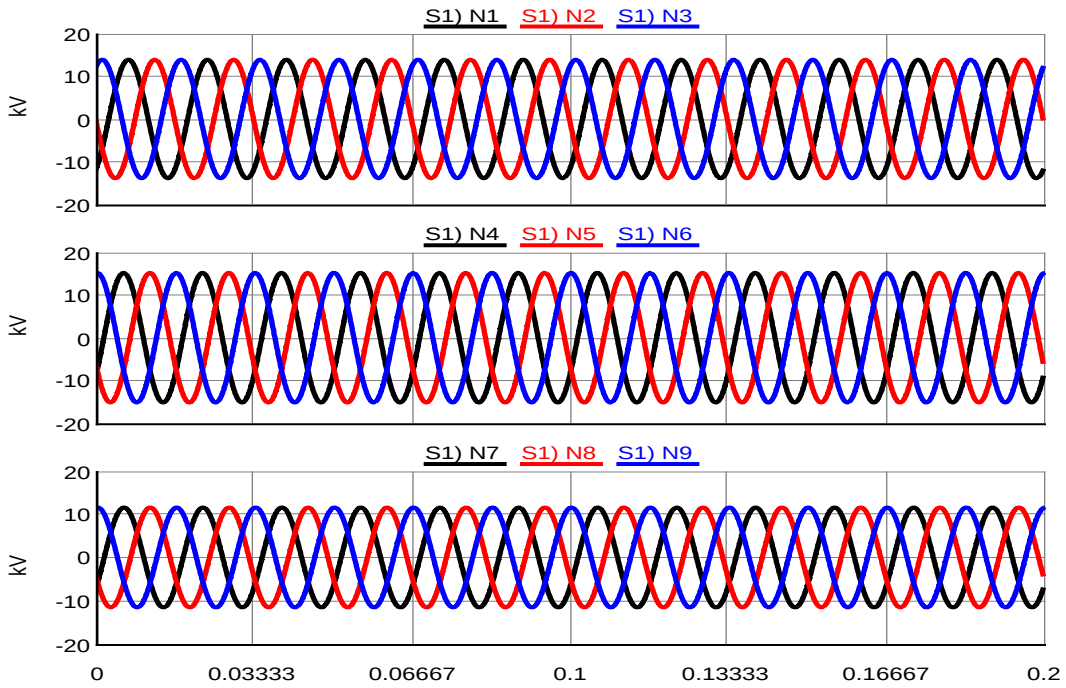

Figure5. 16: **Three voltage output of the buses -1-, -2-, and -3-**

Figure 5.17 depicts the three phase waveforms of the voltage magnitudes of bus 4, bus 5 and bus 6 of the full model of the IEEE9- bus system.

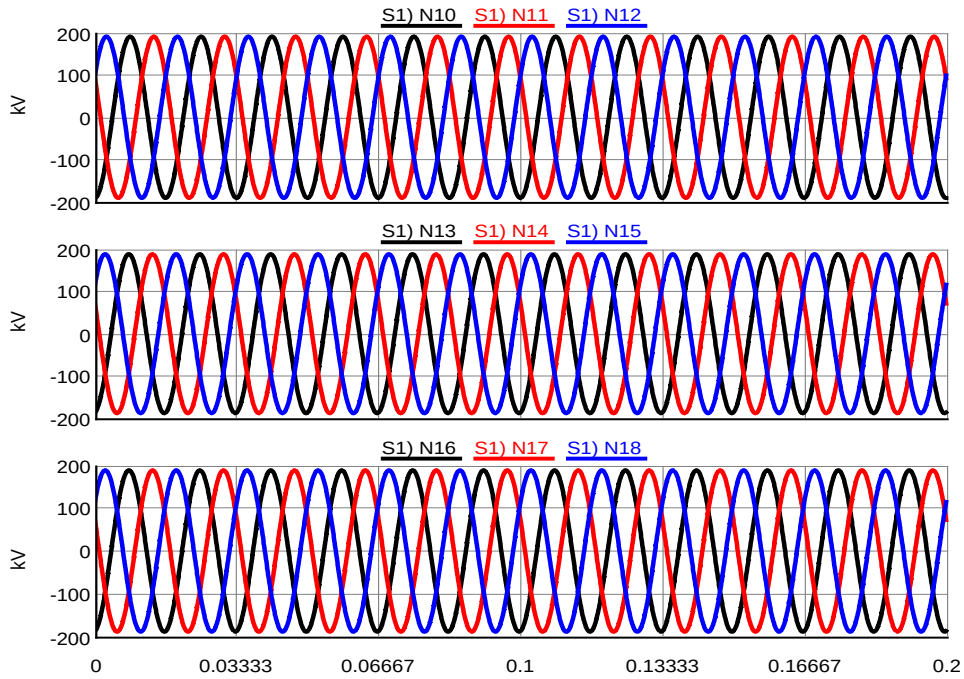

Figure5. 17: **Three voltage output of the buses -4-, -5-, and -6-**

Figure 5.18 depicts the three phase waveforms of the voltage magnitudes of bus 7, bus 8 and bus 9 of the full model of the IEEE 9- bus system.

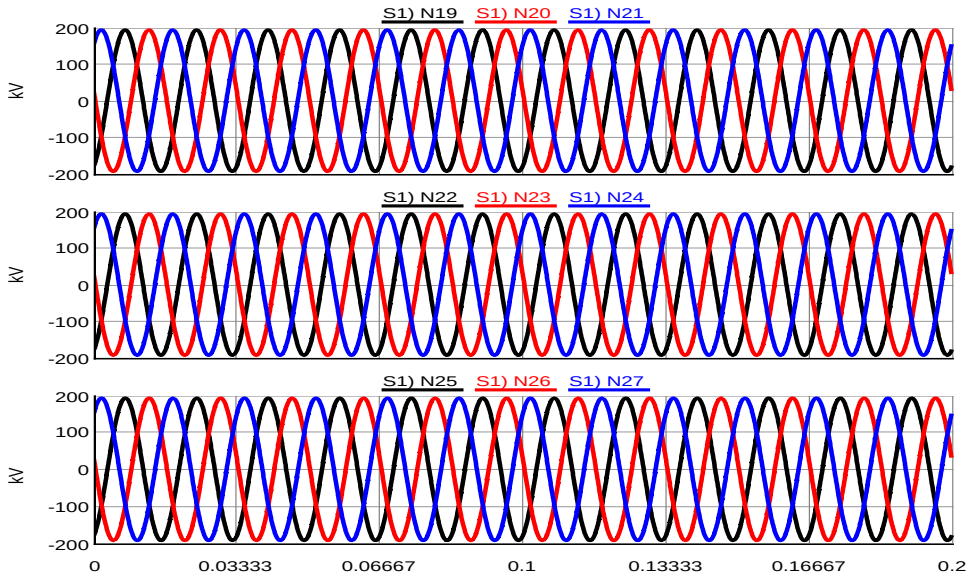

Figure5. 18: **Three voltage output of the buses -7-, -8-, and -9-**

5.5 Application of the coherency based method

The same procedures followed in Chapter 4 are used to develop the reduced order model. Three phase short-circuit fault is introduced on transmission line 2 to the system as shown in Figure 5.10 as the first fault location in the study area. The second fault is located on bus 7 of the system in the same study area.

Generators swing curves are simulated as results of the faults application. Based on them a conclusion is made that no Coherent generators exist. The computation of the constant admittance representation of the loads using Equation (4.2) has the same results as the ones presented in Table 4.5 in Chapter 4. Also the Kron's elimination and network reduction are the same as in Chapter 4.

5. 5.1 Building of the reduced model

Equation (4.21) is used to construct the reduced network. The same admittance matrix for the reduced model is obtained and Equation (4.14) is applied in order to implement one line diagram in RSCAD software environments. Figure 5.19 depicts the one line diagram of the reduced model built in RSCAD.

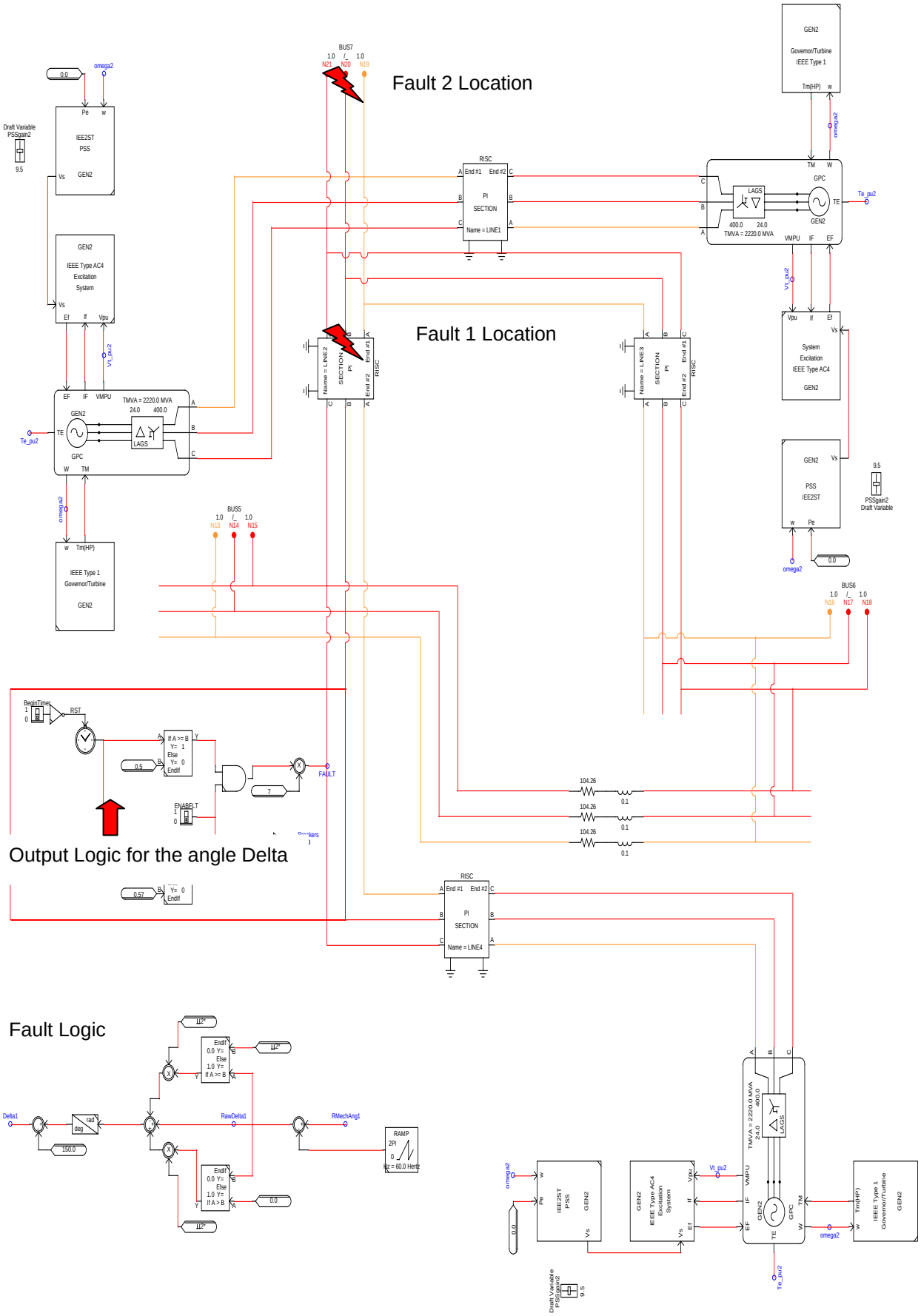

Figure 5. 19: Reduced network model in of the IEEE 9-bus system in RSCAD software

5.5.2 Load flow results of the reduced model.

The developed reduced network was also simulated following the same procedures as for the full one. Load flow responses of the reduced model are shown in Table 5.6 and Figure 5.23. Comparison between the results for the full and reduced models is done on the basis of error of calculation for every bus of the full model that is preseived in the reduced one. The biggest error is for bus 2 and 3, but the errors are in the framework of $\pm 5\%$. This means that the reduced model successfully can be used for load flow calculations.

Table 5. 5: RSCAD load flow results verification

Full network		Reduced network		e_v [%]
Bus number	**Voltage [kV]**	**Bus number**	**Voltage [kV]**	
1	16.97	1	16.51	2.71
2	**18.56**	**2**	**19.48**	**-4.96**
3	14.15	3	14.76	-4.31
5	230.5	5	230.9	-0.1735
6	231.4	6	232.1	-0.3025
7	**236.8**	**7**	**233.4**	**1.018**

5.5.3 Transient behaviour of the generator 2 in the full model for the first and second fault locations.

For the assessment of the developed reduced model, two locations of faults in the same study area are used to simulate the transient behaviour of the generator 2. The two fault locations are shown in Figure 5.19 Rotor angle, active power, reactive power and voltage responses of the Generator 2 in the study area as a response to the first location of fault of the full network are depicted in Figure 5.20.

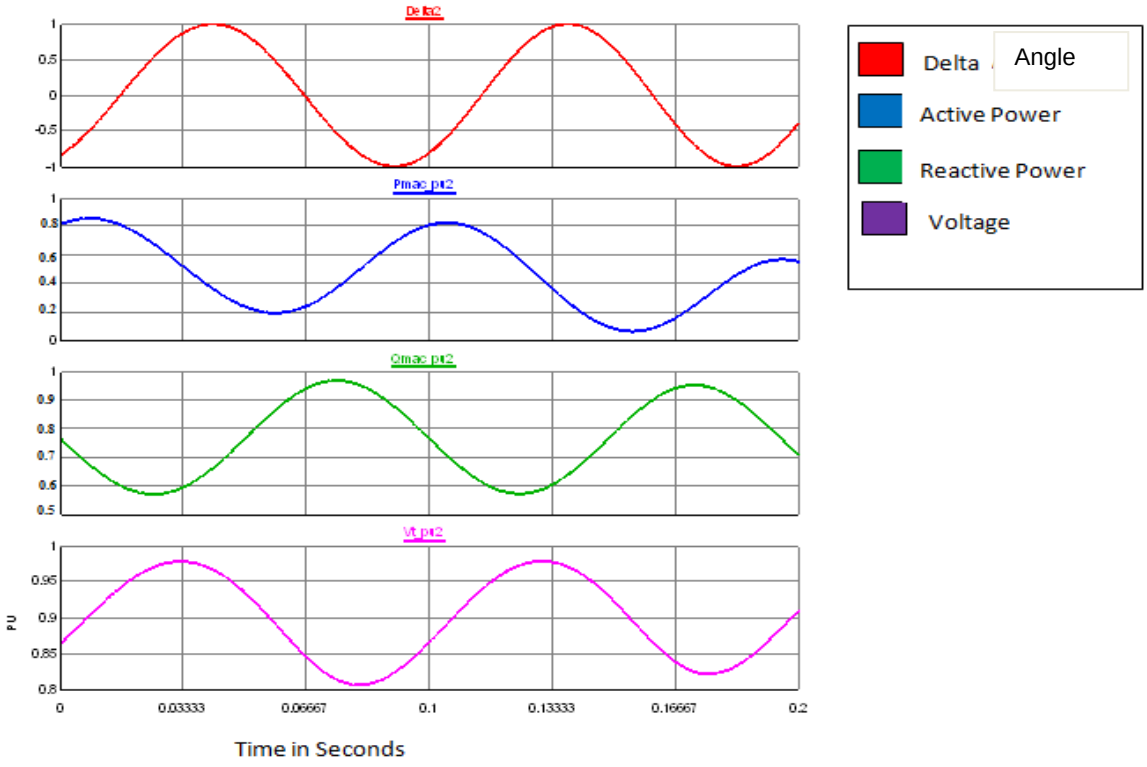

Figure 5. 20: **Transient results of the generator 2 from the study area of the full model for the first fault location in RSCAD**

Rotor angle, active power, reactive power and voltage responses of the generator 2 in the study area of the full model as a response to the second fault location are depicted in Figure 5. 21.

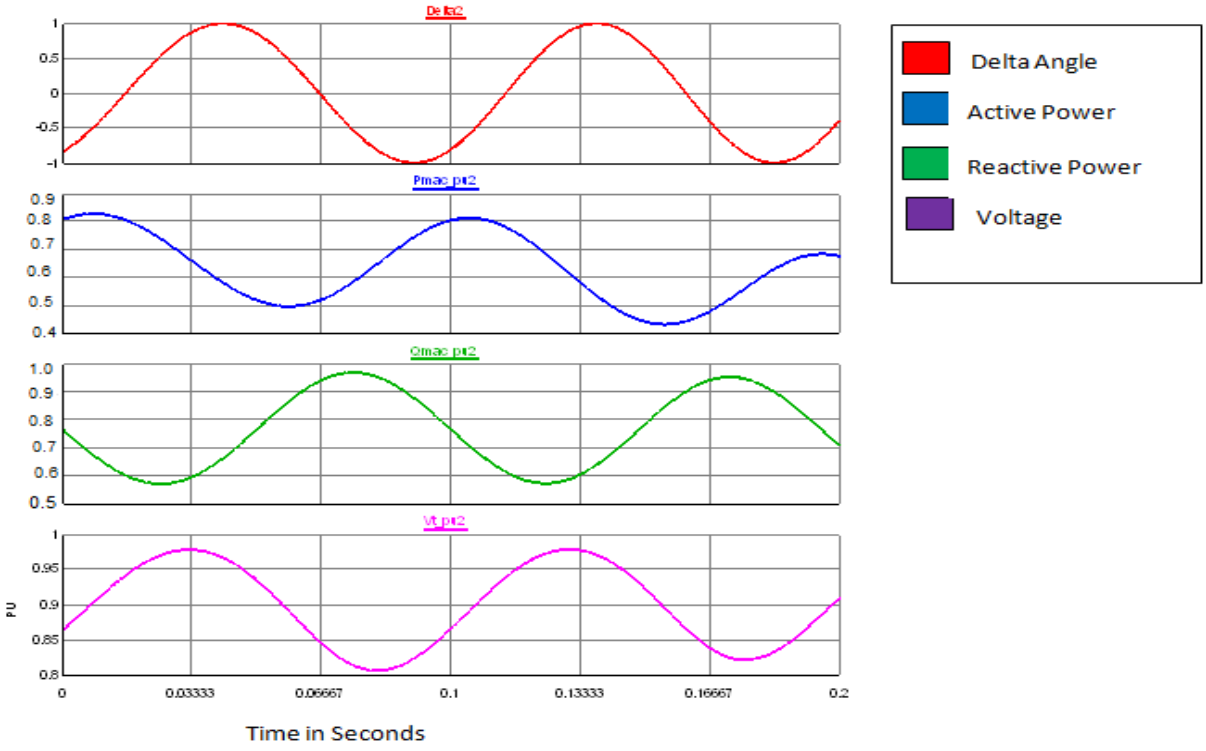

Figure 5. 21: **Transient results of the generator 2 from the study area of the full model for the second fault location in RSCAD**

5.5.4 Transient behaviour of the generator 2 for the first fault on the reduced model

In the same way as for the full model two faults are applied at different locations of the study area of the reduced model. The transition behaviour of the generator 2 is simulated for every one of these faults. The resulted swing curves are shown in Figure 5.21 and 5.23 respectively.

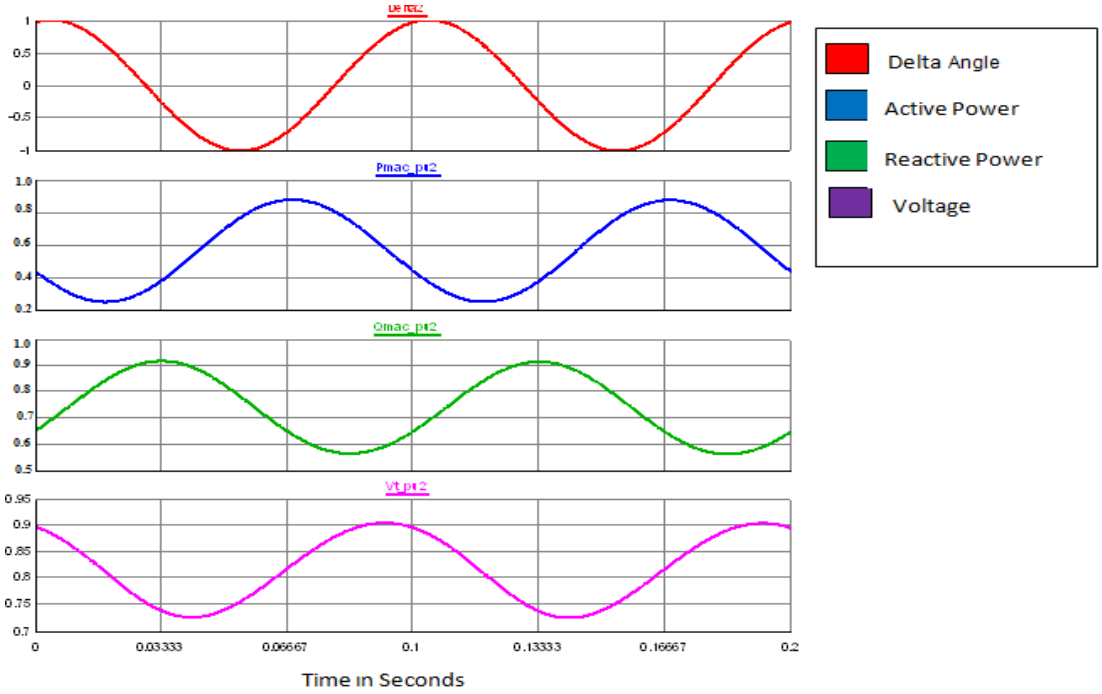

Figure 5. 22: Transient results for the generator 2 in the study area of the reduced model for the first fault location in RSCAD

5.5.5 Transient behaviour of the generator 2 for the second fault on the reduced model

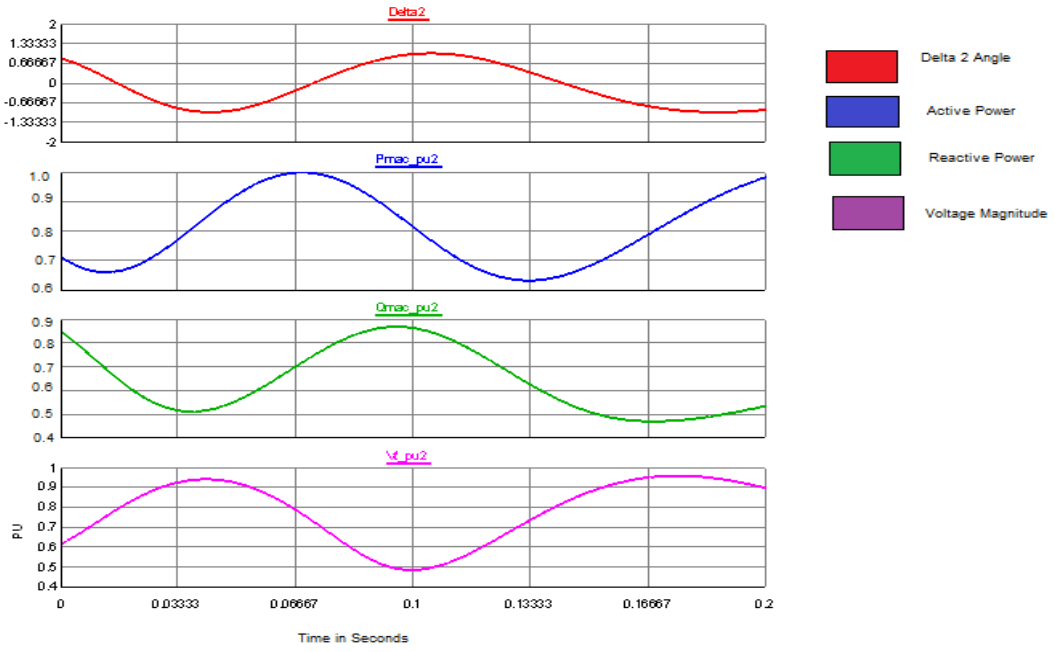

Figure 5. 23: Transient Results for the generator 2 from the study area of the reduced model for the second fault location in RSCAD.

Stability analysis results of generator 2 are shown in Table 5.6 and 5.7 for the first and the second fault location respectively. The tables show the steady state values achieved for the voltage, rotor angle, active power and reactive power after completion of their transient behaviour.

Table 5. 6: RSCAD Stability analysis results for the study area generator 2 for the first location of the fault

x	Full model	Reduced model	$e_x\%$
V [PU]	0.945	0.9	-0.39
δ [PU]	1	1	0
P [PU]	0.825	0.85	-3.03
Q [PU]	0.955	0.92	-3.66

On the basis of the obtained results can be concluded that

1) The reduced order model is stable.
2) The behaviour of the generator 2 for both full and reduced models is very close.

Table 5. 7: RSCAD stability analysis results of the study area generator for the second location of the fault

x	Full model	Reduced model	$e_x\%$
V [PU]	1.025	1.029	-0.39
δ [PU]	53.025	48.037	8.022
P [PU]	163.013	164.32	-0.802
Q [PU]	7.163	7.423	-3.63

5.5.6 Comparison of the computation time for the simulation of the full and the reduced models

Figures 5.24 -5.25 depict the time step information of both the full and reduced models to show that, the reduced models take less time for the computation of the system. Map files for the full and reduced models simulation are given in Appendix G.

```
RISC-based Network Solution for Subsystem #1 uses -->
          RPC-GPC Card #1 Processor A
 Network Solution Statistics for 1A:
   Number of nodes on this processor: 48
   Number of G values passed to this proc: 27
   Number of matrix pointers passed to this proc: 0
   Number of columns dynamically decomposed by this proc: 36
   Number of multiply-subtract operations
     for dynamic decomposition on this proc: 902
   Number of clocks pre-T0:      1610
      ( time = 1.610000e+000  uSec. )
   Number of clocks in main:     14032
        ( decomposition:     7287 )
        ( forward-backward:   5348 )
      ( time = 1.403200e+001  uSec. )
  The fill of the decomposed lower matrix is: 355 of 1176 locations.
 Hidden T2 Transfer List
```

Figure 5. 24: Computational time for simulation of the full IEEE 9-bus system

```
RISC-based Network Solution for Subsystem #1 uses -->
          RPC-GPC Card #1 Processor B
 Network Solution Statistics for 1B:
   Number of nodes on this processor: 33
   Number of G values passed to this proc: 18
   Number of matrix pointers passed to this proc: 0
   Number of columns dynamically decomposed by this proc: 27
   Number of multiply-subtract operations
     for dynamic decomposition on this proc: 667
   Number of clocks pre-T0:      1381
      ( time = 1.381000e+000  u Sec. )
   Number of clocks in main:     10040
         ( decomposition:     5429 )
         ( forward-backward:  3615 )
      ( time = 1.004000e+001  u Sec. )
   The fill of the decomposed lower matrix is: 239 of 561 locations.
  Hidden T2 Transfer List
```

Figure 5. 25: Computational time for simulation of the reduced IEEE 9-bus system

5.6 Comparison of the influence of the software environment over the load flow results

Figure 5.26 presents the bus voltage load flow results comparison for the full model. The results from DigSILENT and RSCAD software are compared with the IEEE 9-bus published results.

It can be observed that for bus1, bus2 and bu3 DigSILENT has better results as compared to the RSCAD, but RSCAD produces better results for the bus 5, bus 6 as well as bus 7.

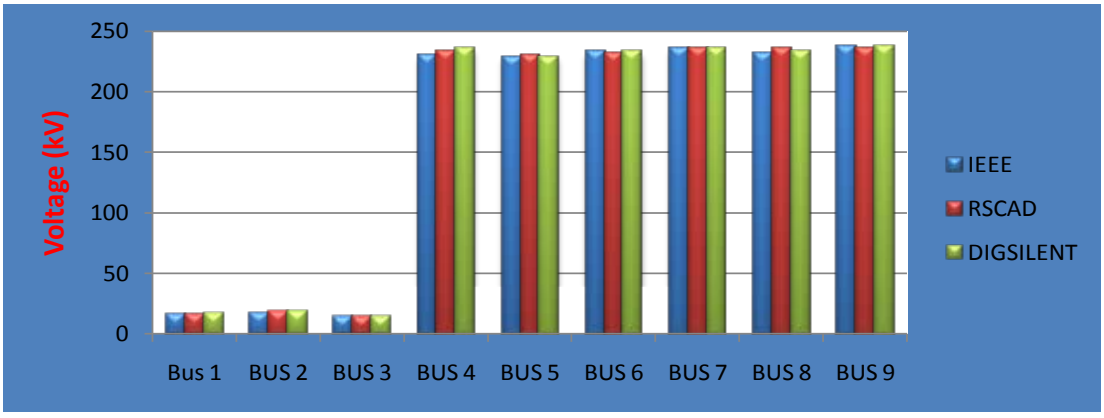

Figure 5. 26: IEEE, DigSILENT and RSCAD bus voltages of the full model

Figure 5.27 presents the bus voltage load flow results comparison for the reduced model in order to investigate the influence of the used software environment.

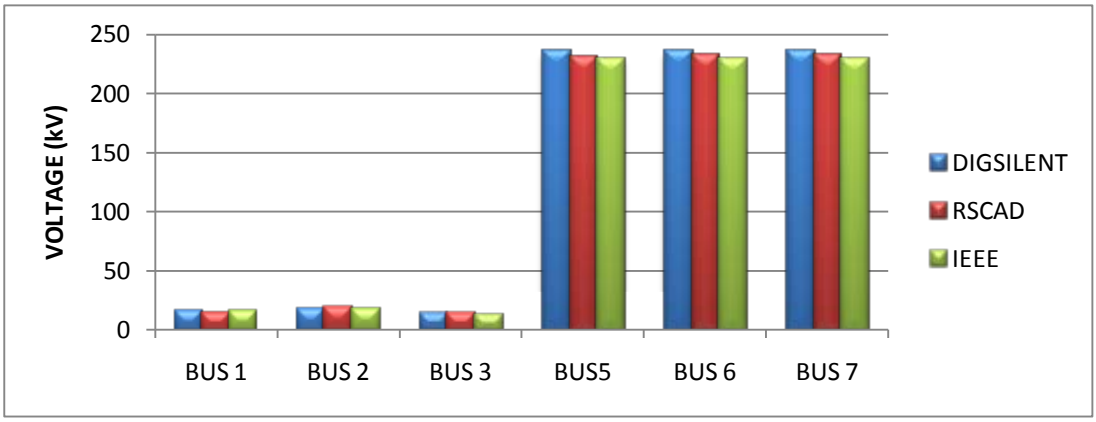

Figure 5. 27: **IEEE, DigSILENT, and RSCAD bus voltage results of the reduced model**

5.7 Discussion of the results

Comparison of the results is done according to:

- Load flow results
- Stability of the full and reduced models.

For every one of these points additional comparison is done to inverstigate which of the software environments DigSILENT or RSCAD can produce a reduced model with better characteristics (less error between the full and reduced models).

In reference to Table 4.7 in Chapter 4 and Table 5.5, the percentage error between the full and the reduced model in DigSILENT software environment is between **0** and **-2.835%.** While the one for RSCAD software environment is between -0.1735 and 2.71%. As for the stability analysis percentage error between the full and reduced model for the first fault location in DigSILENT is between **-0.39%** and **8.022%.** The percentage error of the RSCAD for the first fault location is between **0%** and **-4.76%.** From the load flow the comparison of the voltage for the reduced and full model in the study are more or less similar. The node voltage maximum error is within $\pm 3\%$ and the dynamic behaviour comparison is done based on the disturbance in the study area. The response between the reduced and the full model also show good results with average of $\pm 5\%$. It can be seen that the bus voltage and power flow of the reduced system are very similar to those of the full system. The simulations with the reduced systems are very close to the original initial system.

5.8 Conclusions

The time domain simulation of the reduced system at the contingency is the severe case as compared to the original full system to verify the capabilities of the reduction process. The reduced system is verified by the validation of the similarity of the static aspect, compared to the original system.

This chapter implemented the full and the reduced models of the IEEE 9-bus system. RTDs/RSCAD software is used instead of DigSILENT and the comparison is made between the two software environments for the full and the reduced models. The percentage error is presented in discussion section. The elements of the two softwares for building the models are different. For instance, synchronous generators load, and transmission lines are modelled in a different way.

One of the main objectives of the reduced order model is to reduce the computation time of the system. In this chapter, it has been achieved to proof the above mentioned objective. Figure (5.24) and Figure (5.25) depict that; the time the reduced model uses is less than the computation time the full model uses. Application of fault and determination of the rotor angle are different in the two software environments. In conclusion, Chapter 4 results are not exatly the same as these Chapter 5. The error percentagy is better for RSCAD than for DigSILENT application.
In this Chapters 4 and 5, the size of the network has been reduced, but the number of the generating units is unchanged.
Chapter 6 presents the development of the reduced order model of IEEE 14-bus system with the application of Coherency based method using DigSILENT software environment. In this case the number of the generating units in the reduced model is changed.

CHAPTER SIX
METHOD FOR MODEL ORDER REDUCTION BASED ON COHERENT GENERATORS AGGREGATION AND LOAD BUSES TRANSFORMATION

Introduction

This chapter deals with development of another application of Coherency based technique to reduce the IEEE 14-bus test bench model order. In this case a procedure for aggregation of the coherent generators and presented them by one equivalent is developed. This procedure is added to the procedures described in Chapters 4 and 5. It is based on the dynamic models of power systems developed under the following assumptions:

- There should be constant input of mechanical power
- Asynchronous power or damping is approximately zero
- Loads are converted to passive impedances
- Voltage behind transient reactance model for the (www.waset.org) synchronous generators is constant, and
- The angle of the voltage behind transient behaviour coincides with the mechanical rotor angle of the generator (Mahdi and Ahmed, 2010)

There are seven sections in this chapter. Section 6.1 introduces the coherency based method. Coherent generators aggregation using inertial aggregation algorithm and computation of load bus admittance is done in section 6.2. In section 6.3, the following parts are done;

- Application of coherency based method to IEEE 14-bus system
- Full model simulations.
- Definition of the study and external area.
- Results report of dynamic transient after the first fault application.
- Assessment of swing curves for grouping coherent generators.
- Dynamic response of the aggregated coherent generators, and
- Result Tables of the load bus representation and Kron's method scheme of the reduced network.

Moreover, section 6.4 presents the simulation results of the load flow and transition behaviour of the reduced model, while section 6.5 deals with all the results comparison between the full and the reduced model and the assessment of the reduced model. Finally, sections 6.6 and 6.7 present discussion of results and conclusions of this chapter respectfully.

The three general steps of the Coherency based method as elaborated in Chapter 4 are applied in this chapter. Due to more generators in this network, step 2 (Aggregation of coherent generators) is done in details. Step1 and 3 are done with the same procedures as conducted in Chapter 4.

6.1 Method of coherency

There are several techniques that can be applied to identify coherent generators as mentioned in Chapter 4. The same choice and procedures applied therein are as well utilized for this network model. The application of Linear Time Simulation is used for the first step of the coherency method. Coherency Identification and generator aggregation are achieved with respect to the following steps as mentioned in Chapter 4:

- Selection of both the study area and the external area.
- Determination of the boundary buses.
- Application of a disturbance in the study area (three phase short circuit)
- Calculation of the swing curves of rotor angles (Making one generator a reference generator).
- Application of a specific tolerance (Coherency Index) and determination of the groups of the coherent generators.
- Aggregation of the coherent generators, and
- Building of the admittance matrices of the full and reduced models.

The procedures included in the aggregation of the generators step are given below.

6.2 Coherent generators aggregation by calculation of an equivalent generator.

Chapter 4 and 5 do not include the process of aggregation of the coherent generators due to the nature of the model used. This step is presented now first by mathematical calculations and secondly by an example introduction. Generator data is given in Appendix D1.Some of the methods that are applicable for the coherent generators aggregation is already mentioned in Chapter 4. For this network, the Inertial Aggregation algorithm is applied to develop an equivalent coherent generator (Shojaei et al., 2011).

6.2.1 Conditions for replacing the coherent generator by an equivalent generator

The following conditions apply for replacing coherent generators by their equivalents (Mahdi and Ahmed, 2010; Shojaei at el., 2011):

- The generators must have the proportional to each other amplitude of the rotor swing curves, and
- They must have the same phase angle of the rotor swing curves.

Only generators, which show similar rotor mode shape in respect of both amplitude and phase angle for all considered modes, can be replaced by a single equivalent generator (Erlich et al., 2002).

Equations (6.1) – (6.9) are used to compute the equivalent values of the voltage, current, power, inertia, and damping coefficient of the equivalent generator (The internal voltage of the equivalent generator can be calculated using Equation (6.1).

$$E_e = \left(\frac{\sum_{i=1}^{m} E_i^* . I_i}{I_e} \right) \tag{6.1}$$

Where, E_e is the voltage value of the equivalent generator e

E_i is the voltage value of the generator i

I_i is the current value of the generator i

I_e is the current value of the equivalent generator

m is the number of generators.

To calculate the vector sum of the currents of the coherent group being replaced, Equation (6.2) can be used.

$$I_e = \sum_{i=1}^{m} I_i \tag{6.2}$$

The equivalent inertia H_e is given by:

$$H_e = \sum_{i=1}^{m} H_i \tag{6.3}$$

where H_i is the inertia coefficient of the generator i

The equivalent damping D_e coefficient (Mahdi and Ahmed, 2010) is as well given by:

$$D_e = \sum_{i=1}^{m} D_i \tag{6.4}$$

where D_i is the damping coefficient for the generator i

The equivalent P_{me} mechanical power can be computed from:

$$P_{me} = \sum_{i=1}^{m} P_{mi} \tag{6.5}$$

where P_{mi} is the mechanical power of the generator i

The sum of the powers of a coherent group S_T may be expressed as (Mahdi and Ahmed, 2010):

$$S_T = \sum_{i=1}^{m} E_i^* I_i \tag{6.6}$$

where

$$E_i = V_i + X'_{di} I_i \tag{6.7}$$

and

where V_i and I_i are the terminal voltage and current at the generator i, X'_{di} is the internal reactance of the generator i.

The internal reactance of the equivalent generator X'_{dei} can be computed using Equation (6.8).

$$X'_{dei} = \left[\frac{E_e - V_i}{E_i - V_i}\right] X'_{di} \tag{6.8}$$

The power delivered by the equivalent generator S_e is given as:

$$S_e = E_e I'_e \tag{6.9}$$

where $S_T = S_e$

Within coherency techniques, coherent groupings of generators are developed by analyzing the system response after being subjected to a fault placed in the study area. An equivalent of the external system is then developed by substituting the coherent group of generators by a single equivalent generator.

The coherent group of generating units for a given disturbance can be described as a group of generators that (Zhao, 2009) swing with the same angular speed and with terminal voltages in an invariable complex ratio. In consequence the generating units of a coherent group can be connected to a common bus and if required via an ideal complex ratio transformer (Chow et al., 1995; Izuegbunam et al., 2011; Shojaei et al., 2011).

Yuefeng, 2011, stated that, the dynamic equivalent of a coherent group (Zhao, 2009) of generating units is a large generating unit that shows the same speed, voltage and total mechanical and electrical power as the group in a process of disturbance where those units stay coherent.

6.2.2 Inertial aggregation algorithm for calculation of the equivalent generator based on generator's intertia

The basis and principle of this algorithm is that, generator internal voltages are calculated and these nodes are connected to a common bus with convenient means preserving power flow. Nonetheless, the connection of the internal nodes forms an equivalent generator. This can be demonstrated with a help of an example as follows (Chow et al., 1995; Izuegbunam et al., 2011; Shojaei et al., 2011):

Step1: Compute the voltages of the generator internal node using Equation (6.1).

These are computed from the bus power injections, done by computing the generator current injection phasors $\bar{I}_i\left(I_{A_1}, I_{A_2}\right)$ into buses A_1 and A_2 and the internal voltage phasors $\bar{E}_{A_1}$ $\bar{E}_{A_2}$ of the generators A_1 and A_2 as depicted in Figure 6.1(Erlich.et al., 2002; Joe and Pierre, 1995; Sung-Kwan at el., 2004).

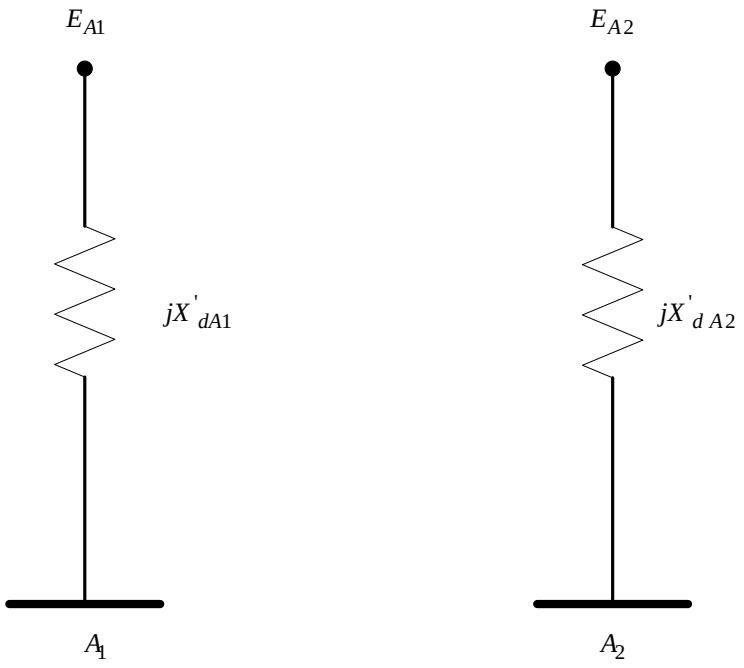

Figure 6. 1: Buses A_1 and A_2 from the full model

Step2: Create an artificial common bus "B".

This is the construction of the voltage V_B of the common bus B, making use of an inertial weighted average of the individual generator internal voltages $\overline{E}_i$, $I = I_{A_1}$, I_{A_2}.

Step3: Add new lines to connect buses A_1 and A_2 to bus "B"

Introduce new (innovexpo.itee.uq.edu.au) lines based on the generator transient reactance from the buses A_1 and A_2 to bus B as shown in Figure (6.2).

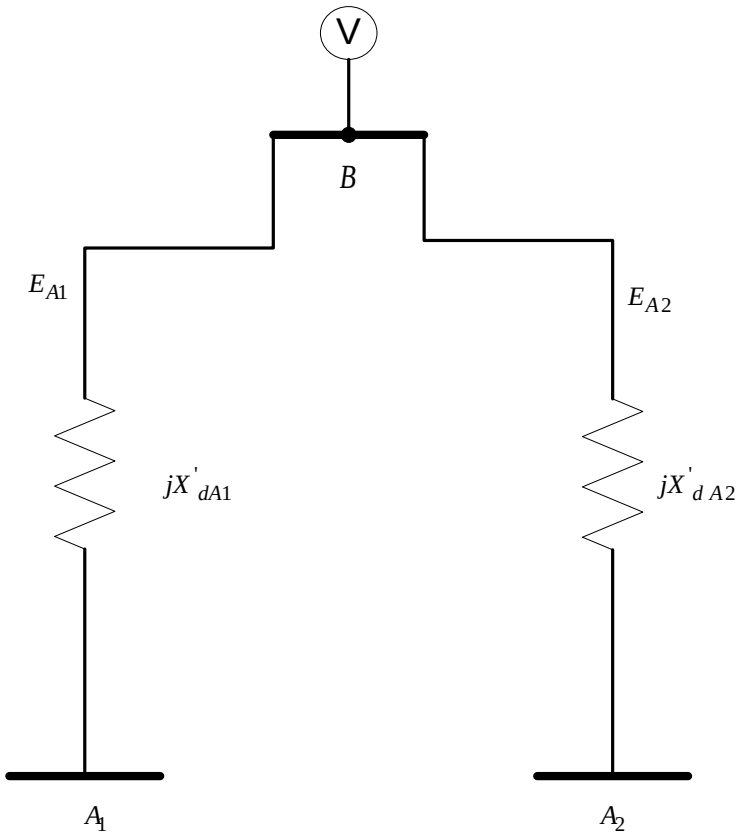

Figure 6. 2: Connection of the coherent generators to the artificial bus B

Step4: Aggregate the generator model.

Computation of the (innovexpo.itee.uq.edu.au) inertial and the transient reactance of the equivalent generator using Equations (6.3) and the damping coefficient calculation using Equation (6.4) respectively are done in this step.

Step5: Create a new terminal bus "G".

Extend bus B to bus G with the line of impedance $-jX'_{d\,g}$, then to the equivalent bus $"E"$ with the line of the impedance jX'_{dg}, so that the bus $"E"$ can have the same voltage as bus B. Figure (6.3) shows the connection of these buses. Therefore, bus G is used as the terminal bus, while bus $"E"$ as the internal bus of the equivalent generator (innovexpo.itee.uq.edu.au; Erlich et al., 2002; Joe and Pierre, 1995; Sung-Kwan at el., 2004).

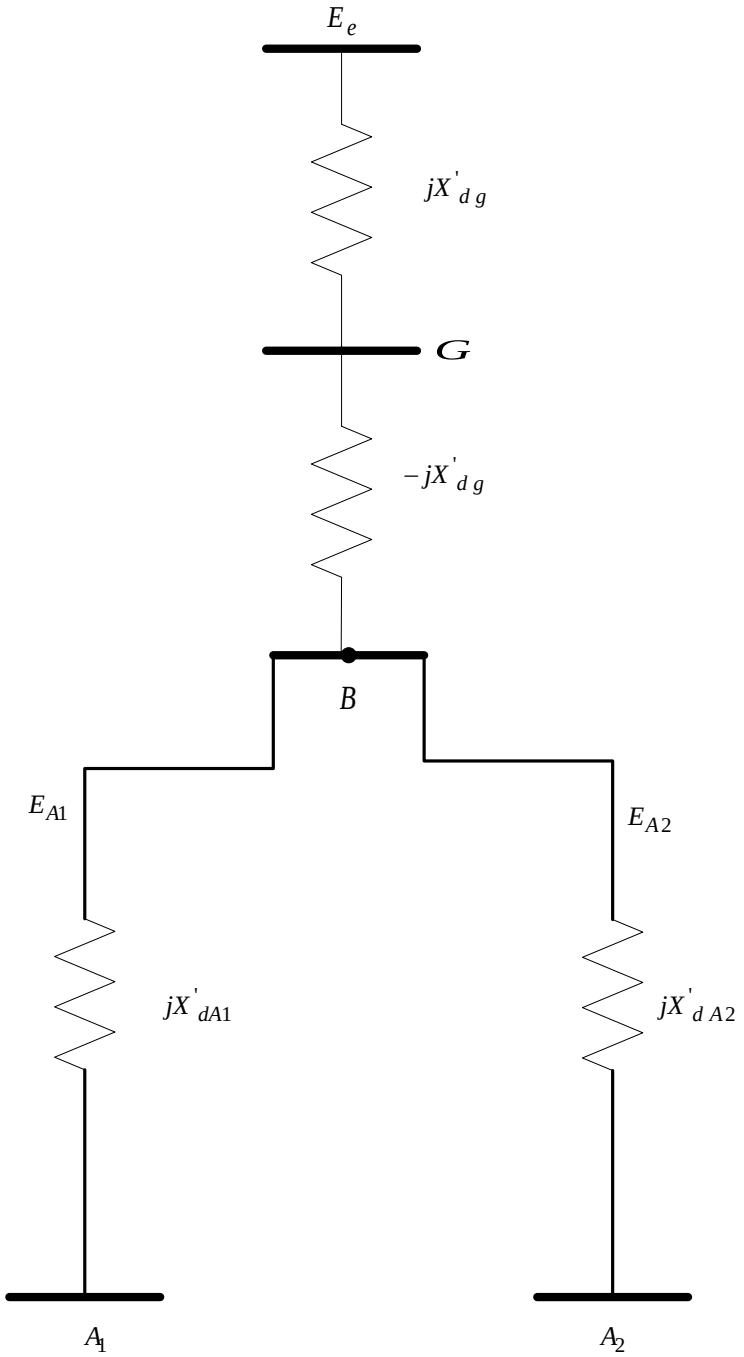

Figure 6. 3: **Building of an internal bus of the equivalent generator**

Step 6: Adjust the power generation on buses A_1 , A_2 and "B".

Bus A_1 and A_2 are no longer the generator terminal buses after the aggregation. Therefore, their generation powers are set to zero. Bus B can be eliminated because it is neither generator nor Load bus. Consequently, the new equivalent bus "E"is set equal to the power transferred to buses A_1 and A_2 (Syed and Jayapal, 2009; Erlich et al., 2002; Joe and Pierre, 1995; Sung-Kwan at el., 2004).

6.2.3 Computation of bus admittance

In reference to Chapter 4, the same Kron's node elimination algorithm for buses which are not relevant was used to reduce the number of buses. Before the elimination process, all the load buses are converted into a constant admittance, by applying Equation (4.19) (in Chapter 4).

6.3 Application of coherency based method to the IEEE fourteen bus system

The flow chart in Chapter 4, Figure (4.8) is utilized in order to develop the reduced network. A three phase short circuit was applied on bus-8- to introduce the disturbance in the network.

6.3.1 Full model simulation

The IEEE 14-bus network consists of five synchronous generators, three transformers, 14 bus-bars and 11 Loads. 100MVA was used as the base, and the system was modelled, Figure (6.4) and tested by means of load flow studies, to make sure that the results are in line with those of the IEEE data. The parameters of the system such as bus voltages, transmission line impedances (Table D4), the values of Load powers are given in Table D.1 in Appendix D, while the preliminary calculations are presented in Table D.2.Table-6.1 shows the voltage magnitude and percentage deviation between the IEEE results and the results obtained from the DigSILENT Power Factory simulation. The percentage deviation is calculated according to the Equation (4.23) in Chapter 4. The load flow results seem to give a good percentage deviation for the software. Consequently, the system is within $\pm 5\%$ voltage deviation which was considered as permission to apply the method of Coherency for the network model order reduction. Bus bar data is given in Table D3 in Appendix D. Simulation results report for the full model in DigSILENT software environment is given in Appendix F1. Both MATLAB scritps files for load buses convertion and Kron's elimination method for the IEEE 14-bus system are given in Appendix F2 and F3 respectifly.

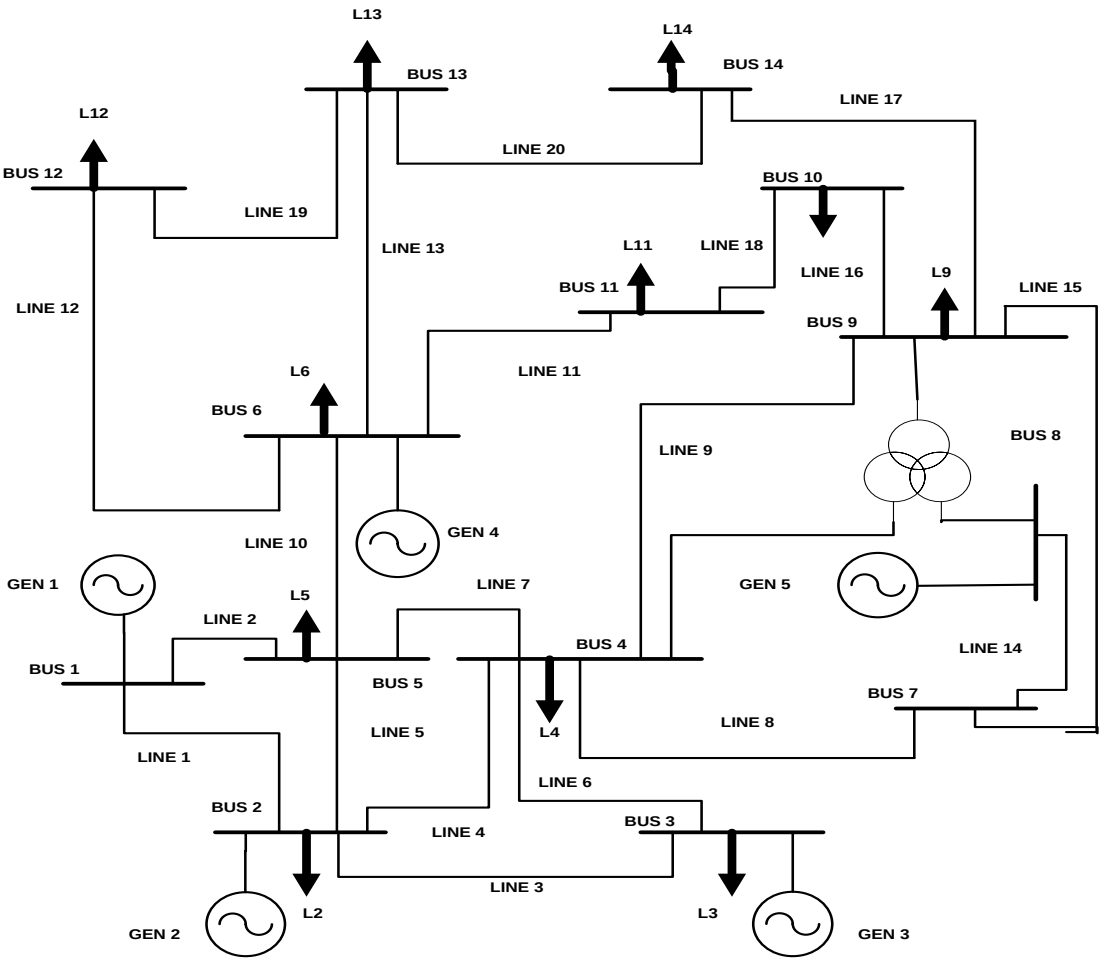

Figure 6. 4: Full network model of the IEEE 14- bus system built in DigSILENT software

Table 6. 1: Comparison of load flow results for the IEEE 14-bus system

Voltage / Bus	IEEE per Unit	DigSILENT Per unit	Percentage deviation
1	1.060	1.040	-1.886%
2	1.045	1.037	-0.7655%
3	1.010	1.010	0%
4	1.019	1.052	-0.3925%
5	1.020	1.025	0.4902%
6	1.070	1.070	0%
7	1.062	1.014	-4.5198%
8	1.090	1.044	-4.220%
9	1.056	1.013	-4.0719%
10	1.051	1.016	-3.330%
11	1.057	1.099	3.974%
12	1.055	1.052	-0.2844%
13	1.050	1.044	-0.5714%
14	1.036	1.008	-2.7027%

6.3.2 Definition of the study and external areas

The reduced order model is based on the impact of large disturbances in a specific area named study area. The remaining area is considered as the external area which is not of direct interest in the stability analysis. Izuegbunam et al., 2011 presented the available variant principles for determining the study area.It is already mentioned that, these study and external areas are preliminary selected based on the analysis of the network structure. The study area is the area of interest. Thus, it will be retained after the network reduction. Two faults are applied for comparison of fault locations in the study area.Figure (6.5) shows the fault location as well as the network division. The area in the circle is considered as study area, while the rest is the external area.

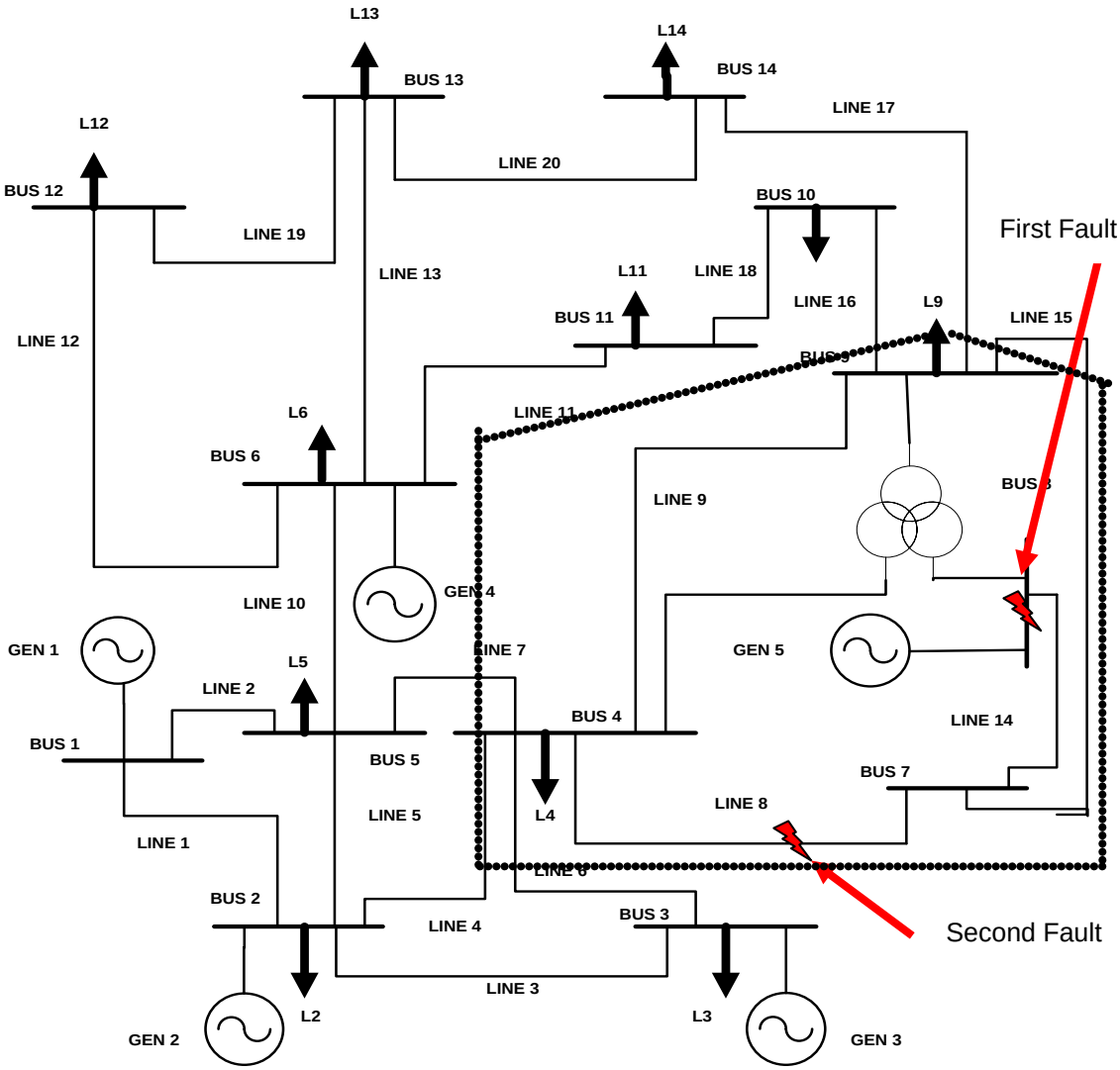

Figure 6. 5: Study and external area of the IEEE 14-bus system

Two fault locations are conducted in order to achieve the objectives of this chapter. The first fault is applied to determine the coherent generators while the second is used to assess the behaviour of the generator in the study area.

6.3.3 Results from the system reaction to the first applied fault

Figure (6.6) to Figure (6.10) show the swing curves for the five generators after being subjected to the disturbance. Generator 1 is selected as a reference generator because is the slack generator. The swing curves for generator 2 and generator 3 have similar shapes, so they form a coherent group. Generator 5, is the only one in the study area, so, it must be retained after the reduction process. Bus 4, bus 7 and bus 9 were observed as the boundary buses. The rest of the system refers to the external area.

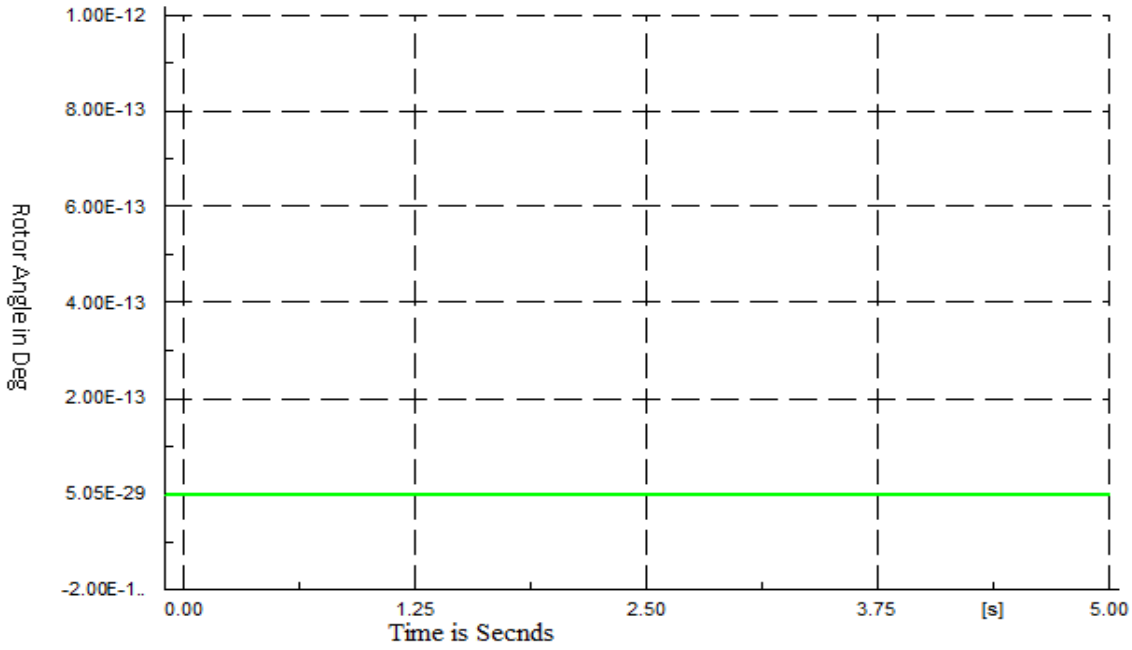

Figure 6. 6: **Generator 1 swing curve of the IEEE 14-bus system**

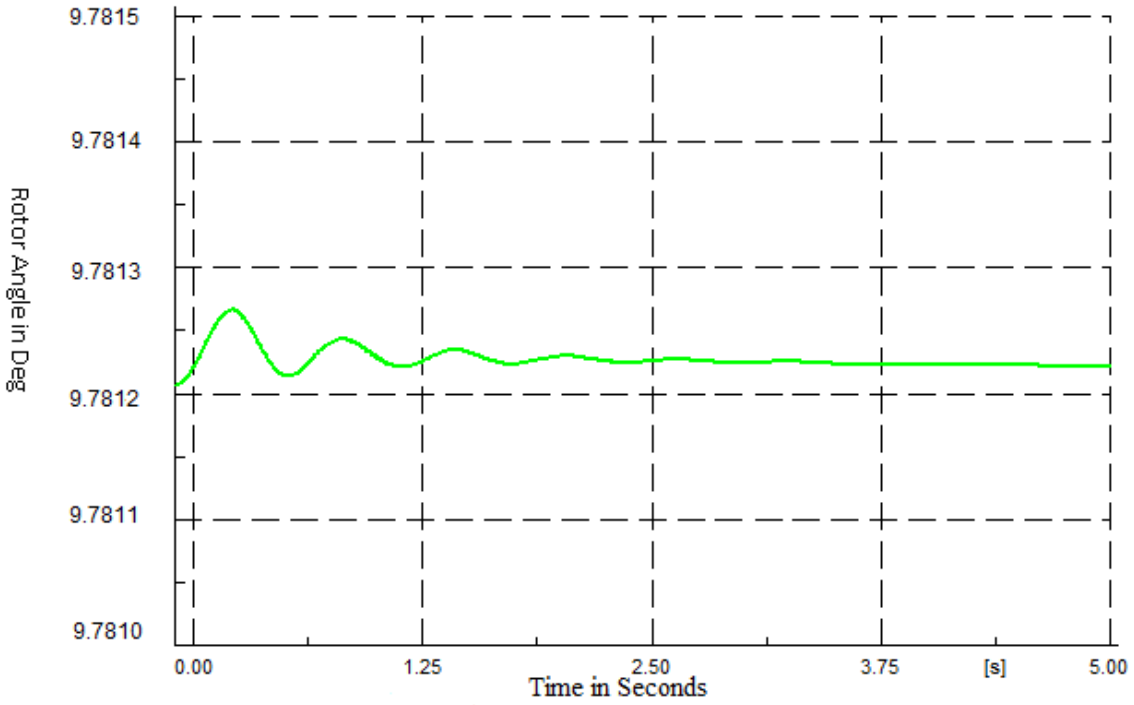

Figure 6. 7: Generator 2 swing curve of the IEEE 14-bus system

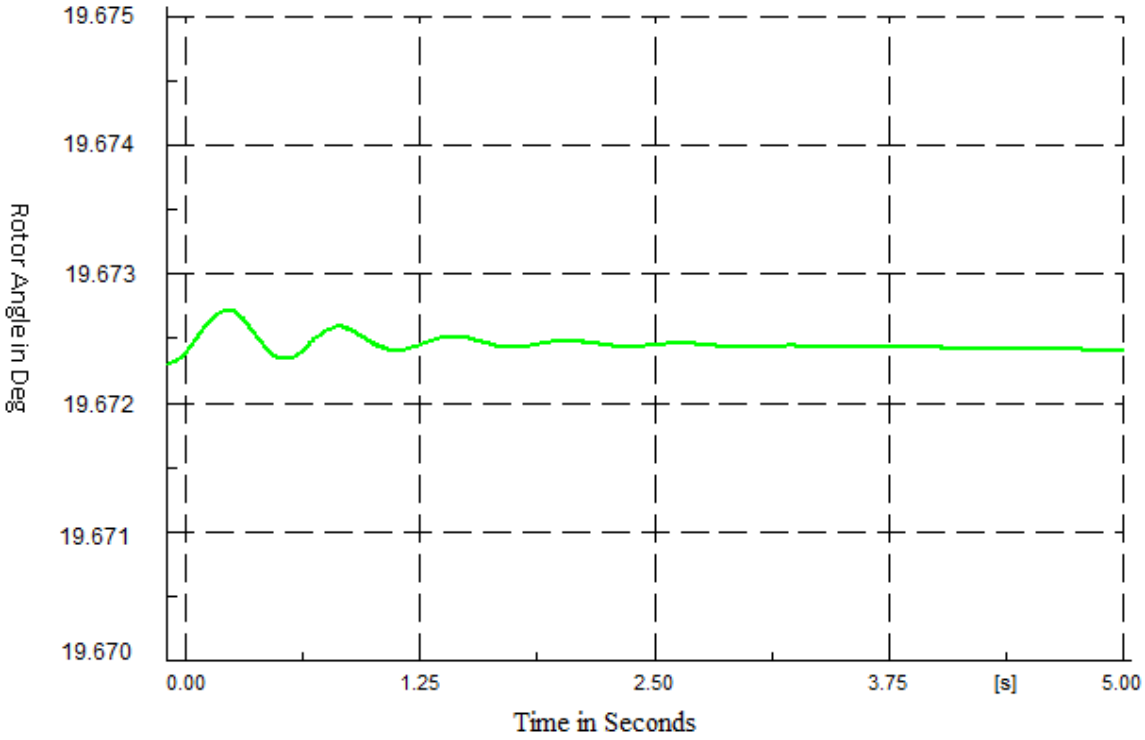

Figure 6. 8: Generator 3 swing curve of the IEEE 14-bus system

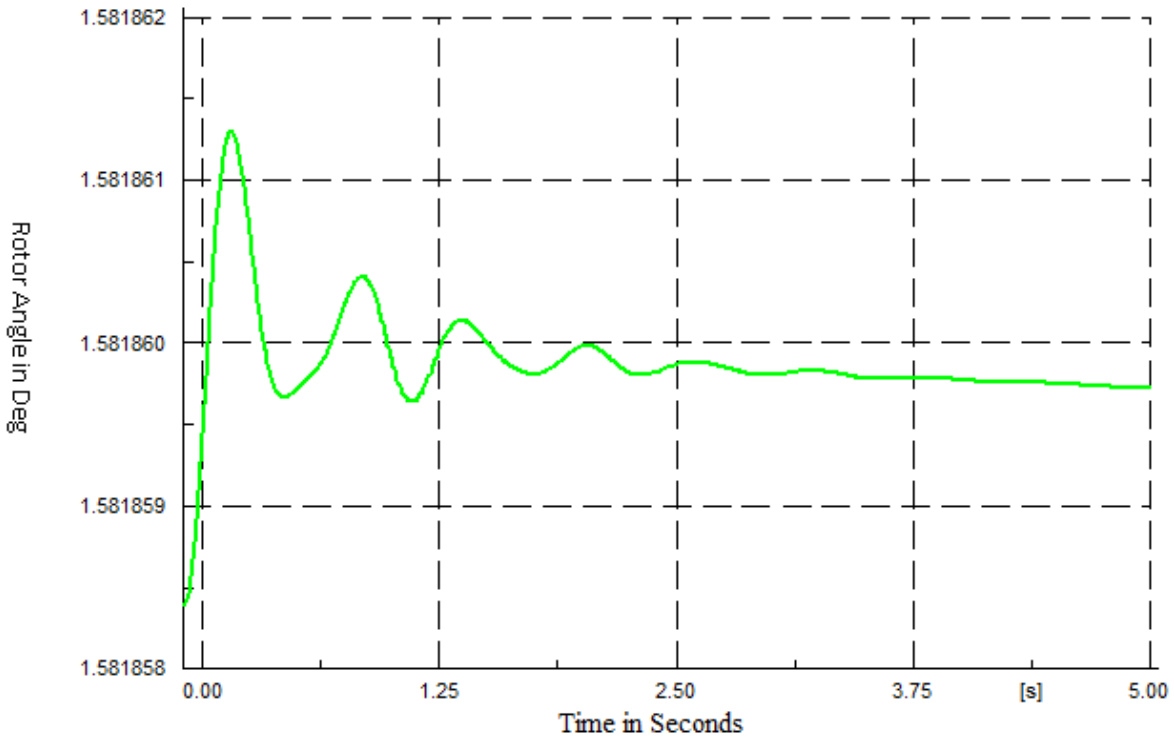

Figure 6. 9: Generator 4 swing curve of the IEEE 14-bus system

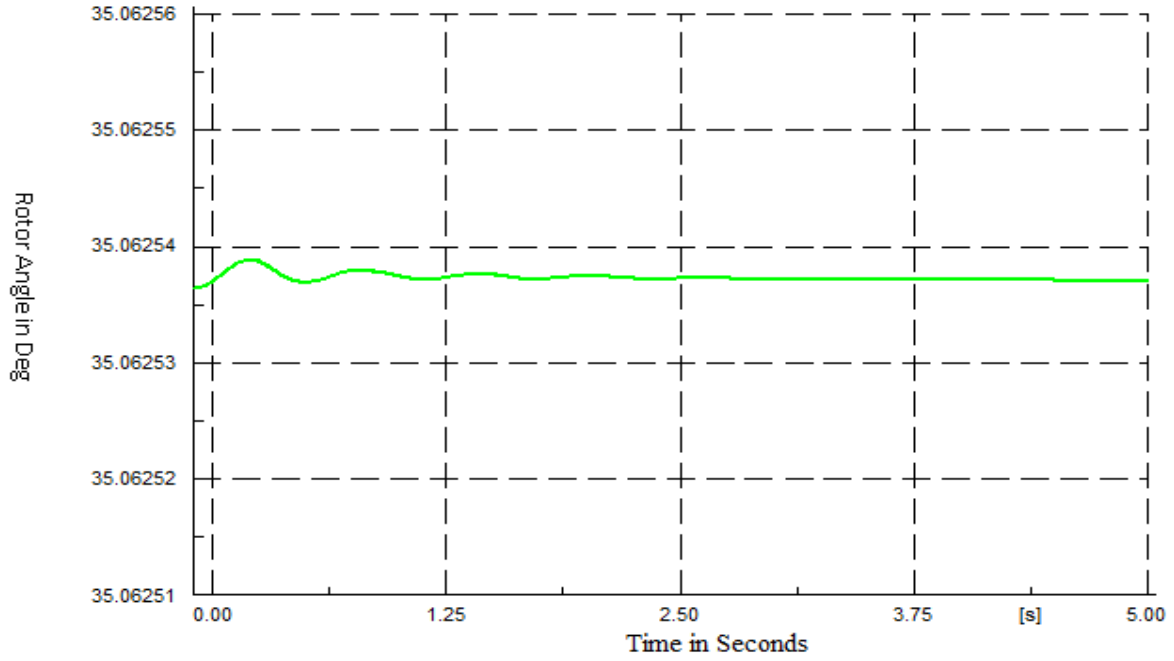

Figure 6. 10: Generator 5 swing curve of the IEEE 14-bus system

6.3.4 Assessment of swing curves for coherent group of generators 2 and 3

Generator 2 and generator 3 have the same shape of the swing curves, therefore they are considered to be coherent to each other. Figure (6.11) depicts the swing curve for the two generators.

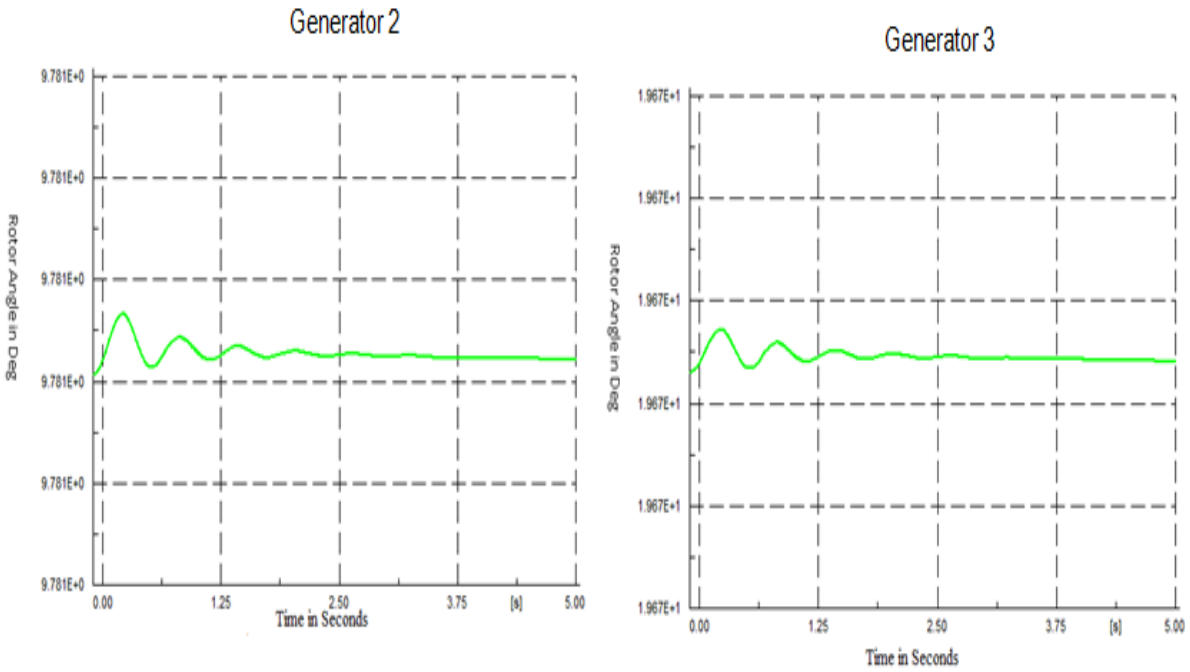

Figure 6. 11: **Generator 2 and generator 3 swing curves comparison**

On the basis of these conclusions generators 2 and 3 can form a coherent group. The swing curves for these two generators can now be checked for a coherency. The coherency of two generators in the external area of the model can be expressed as (Rau and Hussain, 1998) a difference between rotor angles of the two generators from coherent group.

$$C_{ij} \pm \varepsilon = \delta_i(t) - \delta_j(t) \; for \; 0 \le t \le t_{\max} \tag{6.10}$$

Where, δ_i is the rotor angle of the generator i

δ_j is the rotor angle of the generator j

ε is the specific tolerance

C_{ij} is the coherency of the generators i and j

$C_{ij} \le \varepsilon$ denotes that generators i and j are coherent.

Therefore, Equation (6.10) is utilized to group generator 2 and generator 3. The tolerance used for this computation is $\varepsilon \le \pm 10$. When $t = 0s$,

$\delta_2 = 9.781^{\circ}$

$\delta_3 = 19.67^{\circ}$

$\varepsilon \ge 10$

Applying Equation (6.10);

$C_{32} = 19.67 - 9.781$

$= 9.889$

Therefore the tolerance is within the specified value which confirms that the two generators can be grouped together.

6.3.5 Dynamic response of the aggregated coherent generators

Calculations of the equivalent values for the aggregated coherent generators are given in Appendix E.2.

Figure (6.12) to Figure (6.15) depict the dynamic results from the simulation of the equivalent rotor angle, voltage, active, and reactive power of the aggregated coherent generators 3 and 2 obtained by applying Equations (6.1-6.9). The calculated steady state valuesd of the rotor angle, voltage, active power and reactive power are shown in Table 6.2

Table 6. 2: **Steady state values for the equivalent generator**

Generator Variable	Generator 2	Generator 3	Equivalent Generator
Voltage [kV]	234.33	232.30	232.07
Rotor Angle [deg]	9.781	19.67	18.8
Active Power [MW]	40	51	91
Reactive Power [MVAR's]	45.41	14.39	46.8

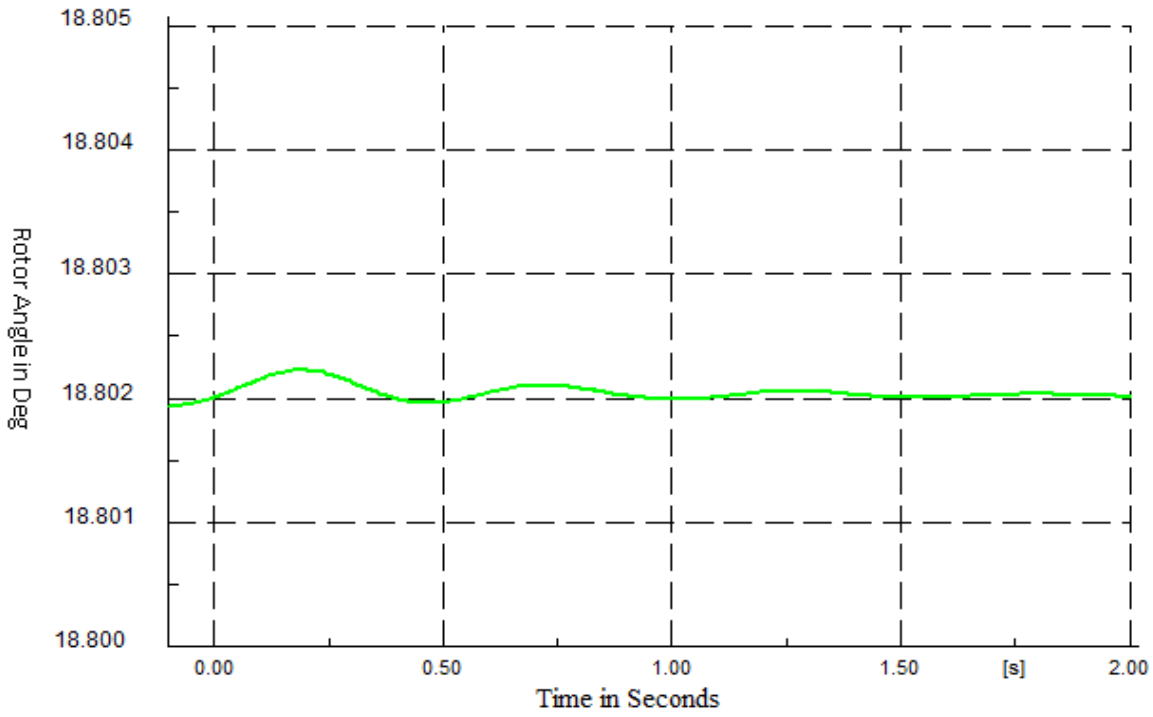

Figure 6. 12: **Equivalent Generator swing curve of the IEEE 14-bus system**

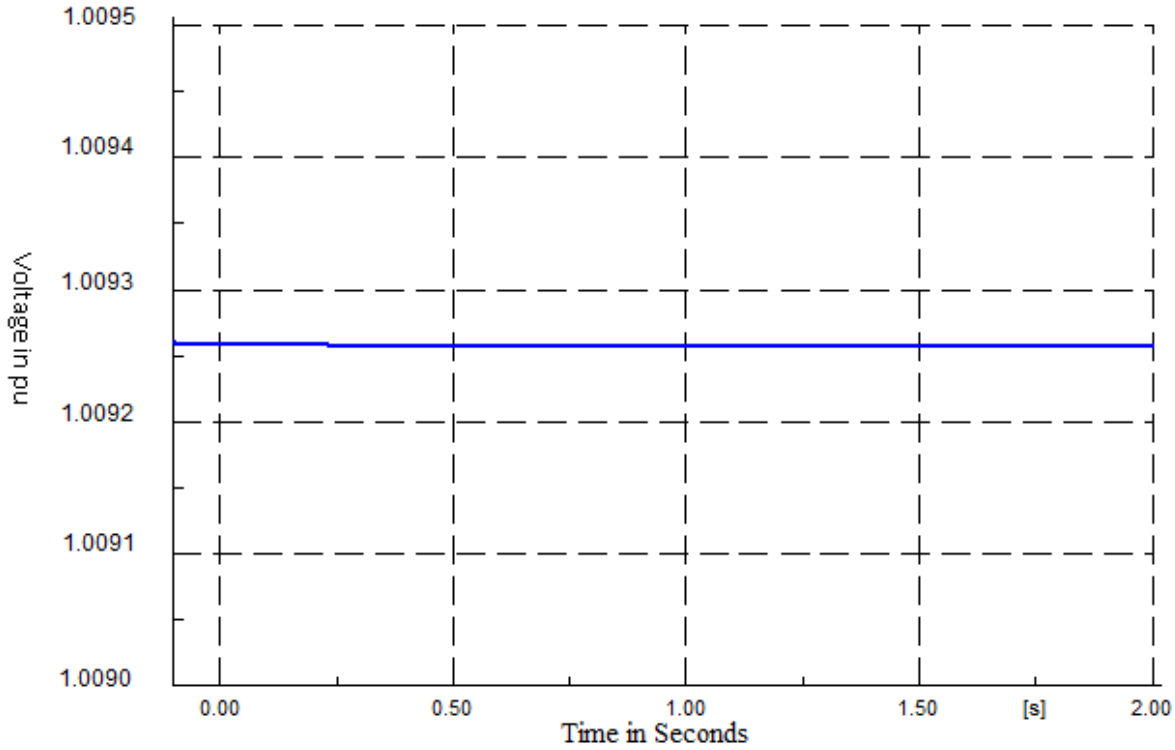

Figure 6. 13: Equivalent Generator Voltage magnitude in PU of the IEEE 14-bus system

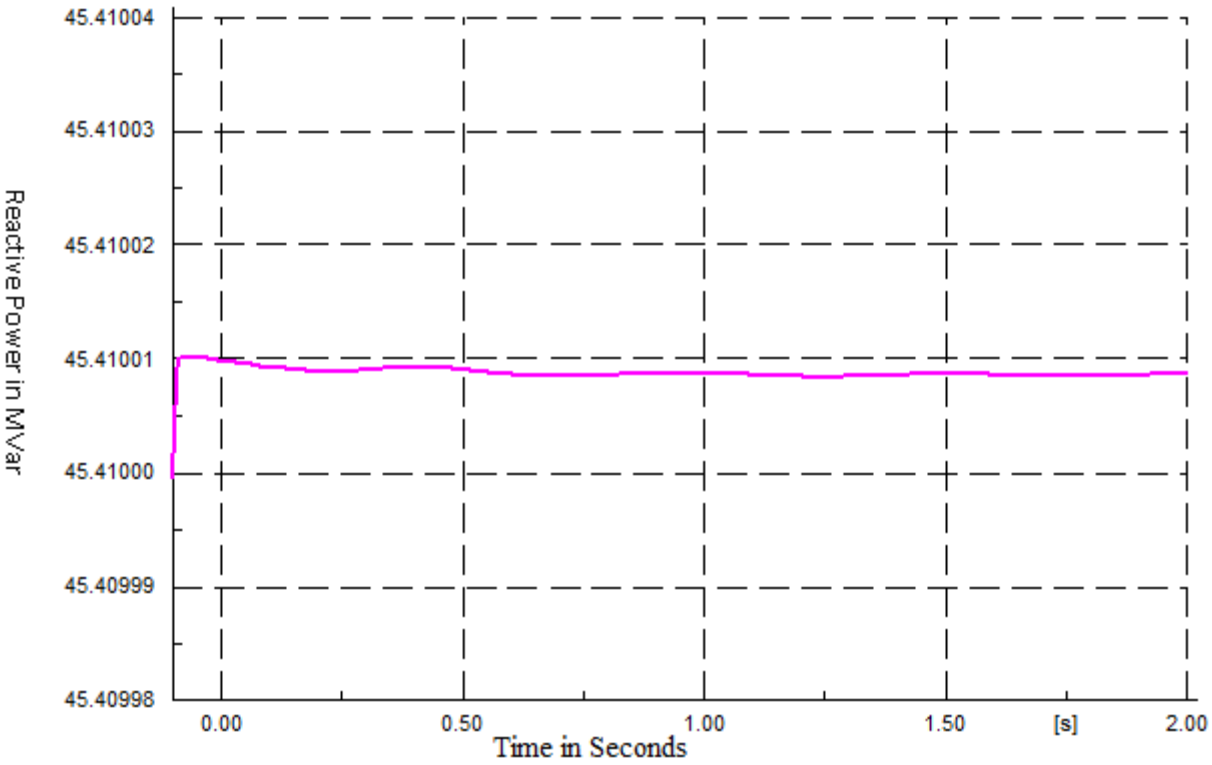

Figure 6. 14: Equivalent Generator Reactive Power in MVar of the IEEE 14-bus system

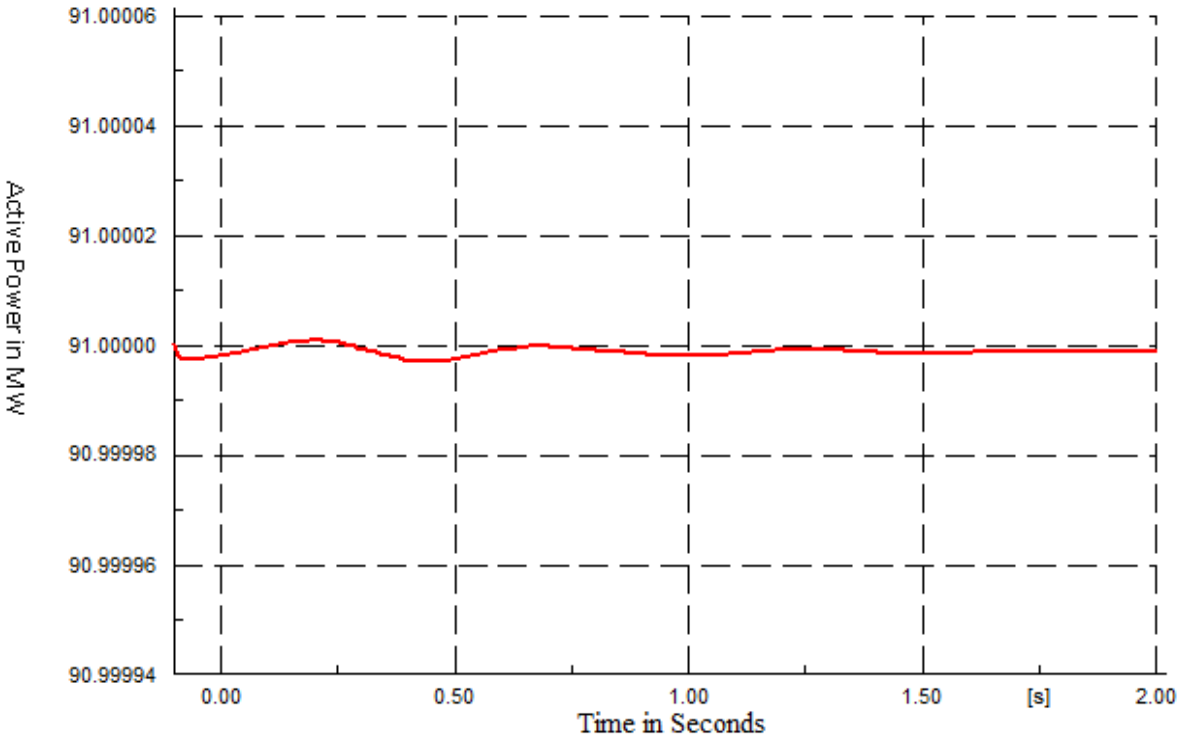

Figure 6. 15: **Equivalent Generator Active Power in MW of the IEEE 14-bus system**

The obtained steady state responses amplitudes from the simulations correspond with the calculated values of the equivalent generator in Table 6.2.

6.3.6 Dynamic simulations results for the generator 5 in the full IEEE 14-bus network.

The dynamic responses of the generator 5 in the full system, after being subjected to a three phase fault at bus 8 of the network, are depicted in Figure (6.16) to Figure (6.19).Generator 5 is used because it is in the study area and it has to be retained after the model reduction process. This simulation is done to be used for the comparison between the full and the reduced models later in this chapter. Second fault located on the bus 8 in the study area is applied for the verification of the dynamic response of the generator in the area of interest. The parameters to be assessed are voltage magnitude, rotor angle, active power, and reactive power of the generator 5.

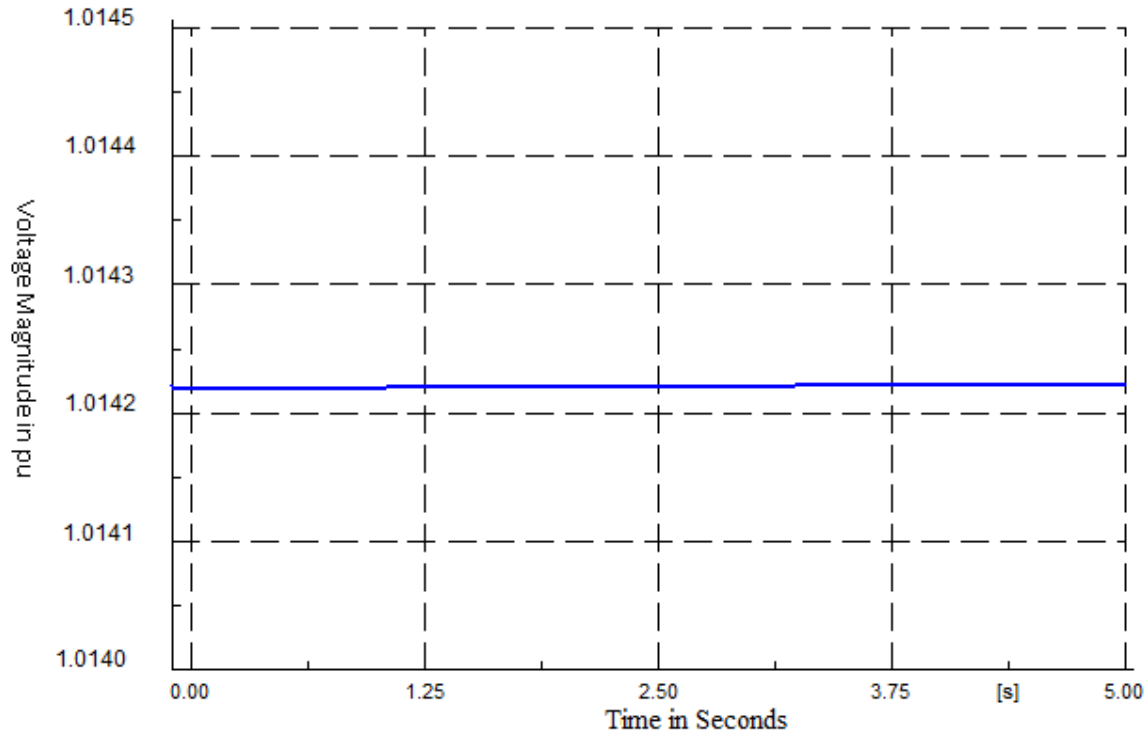

Figure 6. 16: Voltage Magnitude in **PU** for the generator 5 of the full IEEE 14-bus system

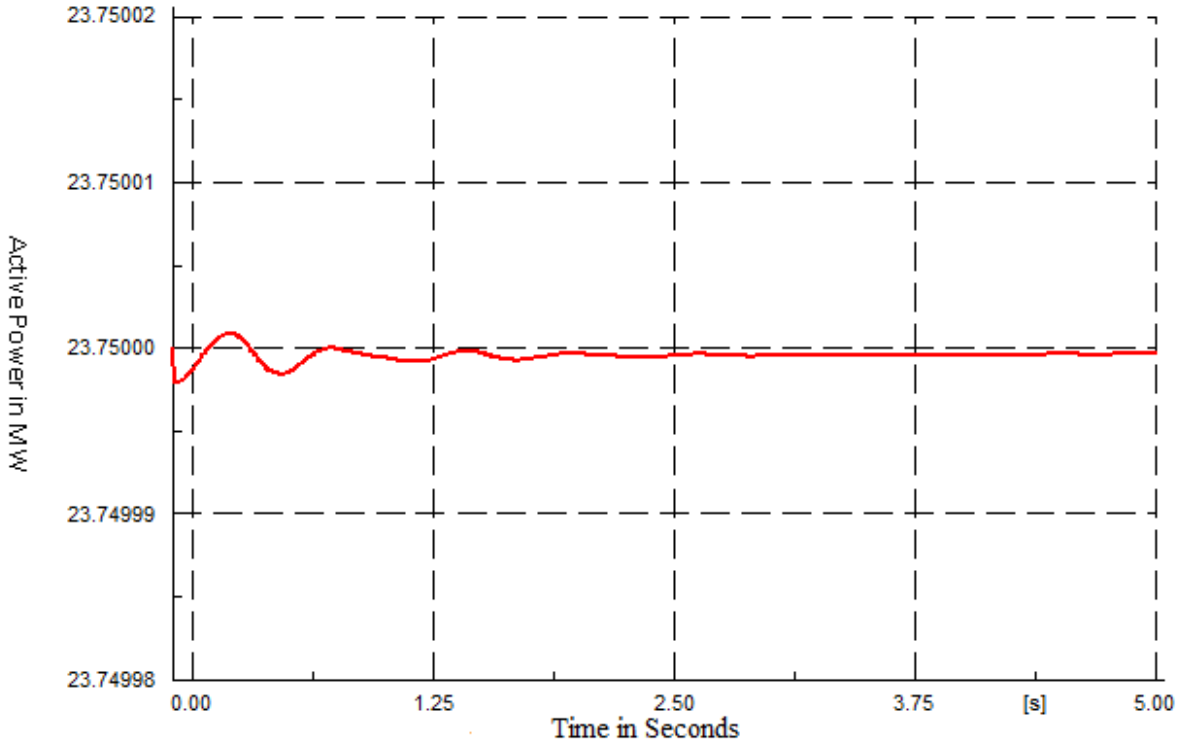

Figure 6. 17: Active power in MW for the generator 5 of the IEEE 14-bus system

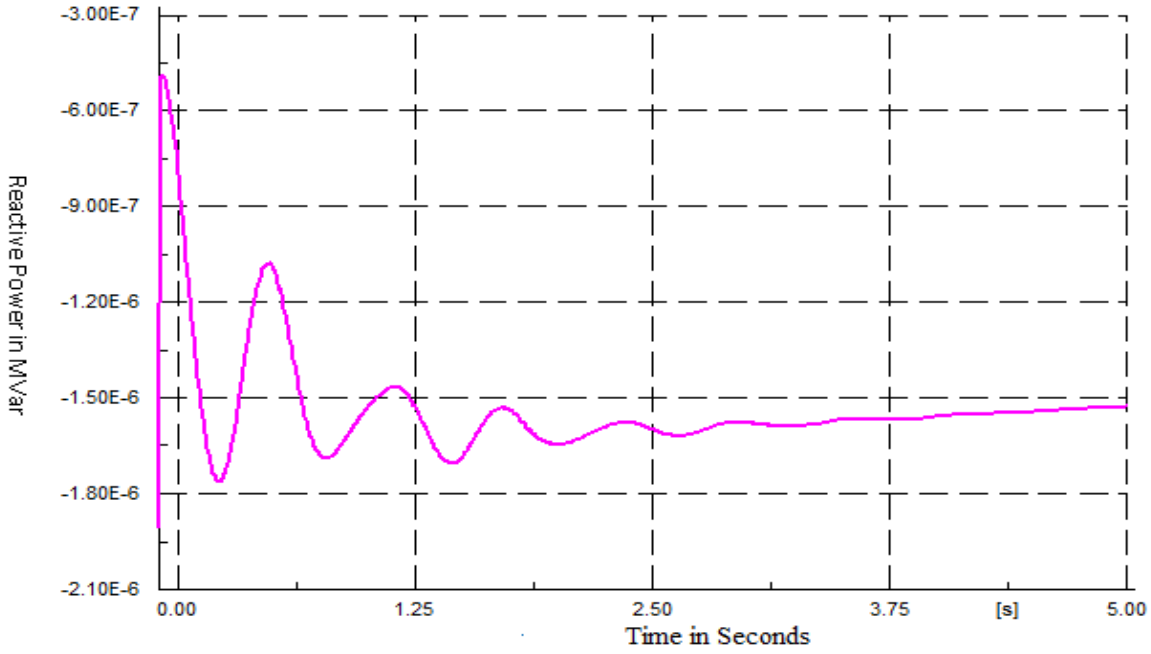

Figure 6. 18: Reactive power in MVar for the generator 5 of the full IEEE 14-bus system

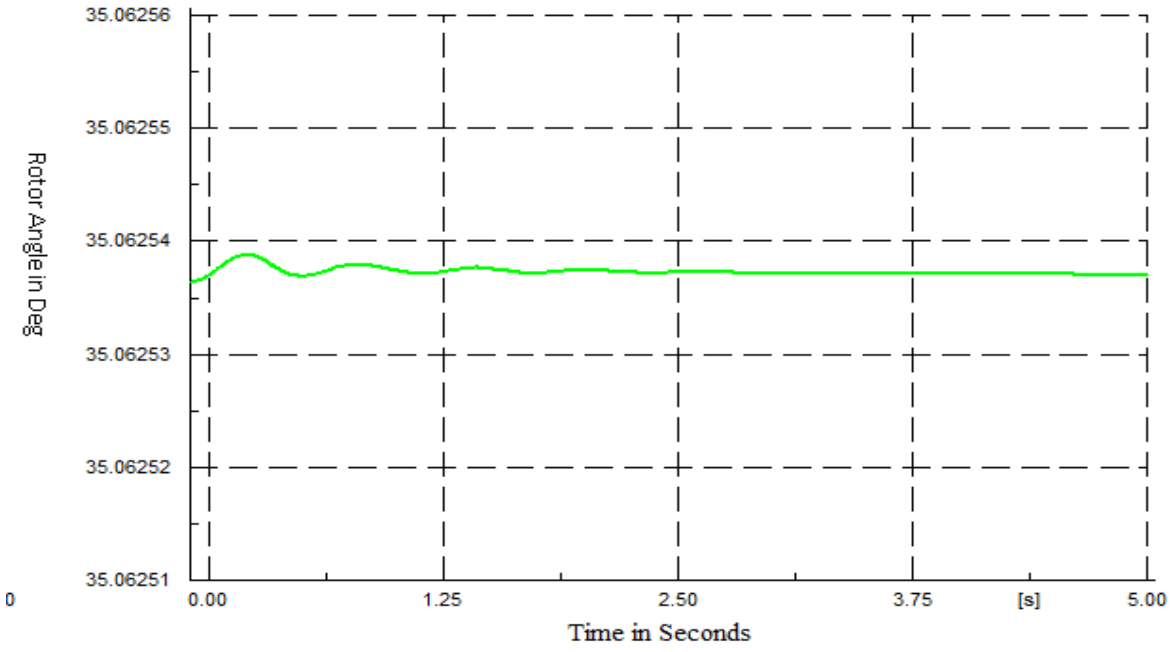

Figure 6. 19: Rotor angle in degrees for the generator 5 of the IEEE 14-bus system

The above dynamic results are for the full model and they will be used for comparison of the full and the reduced system to be developed in the section 6.3.8.

6.3.7 Load buses representation

There are eleven load buses and Equation (4.7) in Chapter 4 is used to represent the loads with the constant admittance. Table 6.3 shows the results obtained from the

computation of the admittances of the load buses, according to Equation (4.8) (Chapter 4). All the load buses parameters are shown in Table 6.3.

Table 6. 3: Constant admittance for the load buses

Load	Active Power [MVar]	Reactive Power [MW]	Voltage [kV]	Admittance [S]
Load 2	21.7	21.7	230	0.0004 - j0.0004
Load 3	94.2	19	230	0.0018 - j0.0004
Load 4	47.8	0	230	0.0009
Load 5	76	1.6	230	0.0014
Load 6	11.2	7.5	230	0.0002 - j0.0001
Load 9	29.5	16.6	230	0.0006 - j0.0003
Load 10	9	5.8	230	0.0002 - j0.0001
Load 11	3.5	1.8	230	0.0001
Load12	6.1	1.6	230	0.0001
Load 13	13.5	5.8	230	0.0003 - j0.0001
Load 14	14.9	5	230	0.0003 - j0.0001

6.3.8 Results from application of the the Kron's method procedure to obtain the reduced model of the Network

The full admittance matrix is with the dimension (11×11) depending on the number of buses of the network. It is reduced by the application of Kron's elimination, Equation (4.19). The reduced matrix obtained is with the dimension (9×9). Further elementary matrix operations are computed, so as to get the reduced admittance matrix. The reduced admittance matrix obtained is as follows:

$$Y_{busR} = \begin{bmatrix} Y_{11} & Y_{(2-3)1} & Y_{41} & Y_{51} & Y_{61} & Y_{71} & Y_{81} & Y_{91} & Y_{E1} \\ Y_{1(2-3)} & Y_{(2-3)(2-3)} & Y_{4(2-3)} & Y_{4(2-3)} & Y_{6(2-3)} & Y_{6(2-3)} & Y_{7(2-3)} & Y_{8(2-3)} & Y_{E(2-3)} \\ Y_{14} & Y_{(2-3)4} & Y_{44} & Y_{44} & Y_{64} & Y_{64} & Y_{74} & Y_{84} & Y_{E4} \\ Y_{15} & Y_{(2-3)5} & Y_{45} & Y_{45} & Y_{65} & Y_{65} & Y_{75} & Y_{85} & Y_{E5} \\ Y_{16} & Y_{(2-3)6} & Y_{46} & Y_{46} & Y_{66} & Y_{66} & Y_{76} & Y_{86} & Y_{E6} \\ Y_{17} & Y_{(2-3)7} & Y_{47} & Y_{47} & Y_{67} & Y_{67} & Y_{77} & Y_{87} & Y_{E7} \\ Y_{18} & Y_{(2-3)8} & Y_{48} & Y_{48} & Y_{68} & Y_{68} & Y_{78} & Y_{88} & Y_{E8} \\ Y_{19} & Y_{(2-3)9} & Y_{49} & Y_{49} & Y_{69} & Y_{69} & Y_{79} & Y_{89} & Y_{E9} \\ Y_{1E} & Y_{(2-3)E} & Y_{4E} & Y_{4E} & Y_{5E} & Y_{6E} & Y_{7E} & Y_{8E} & Y_{EE} \end{bmatrix}$$

The real and imaginary parts of the above matrix are shown below.

Real part

$$\begin{bmatrix}
0.15253 & 0.009454 & 0 & 0.010254 & 0 & 0.01424 & 0 & 0 & 0 \\
0.009454 & 0.02032628 & 0.00725648 & 0.0032158 & 0 & 0 & 0 & 0 & 0 \\
0 & 0.00725648 & 0.28476 & 0.0684 & 0 & 0 & 0 & 0 & 0 \\
0.010254 & 0.0032158 & 0.0684 & 0.097354 & 0 & 0 & 0 & 0 & 0 \\
0 & 0 & 0 & 0 & 0.066 & 0 & 0 & 0 & 0.01955 \\
0.01424 & 0 & 0 & 0 & 0 & 0 & 0 & 0 & 0 \\
0.018809 & 0 & 0 & 0 & 0 & 0 & 0 & 0 & 0 \\
0.0133 & 0 & 0 & 0 & 0 & 0 & 0 & 0.05386 & 0.03902 \\
0 & 0 & 0 & 0 & 0.058005 & 0 & 0 & 0.0026919 & 0.8885
\end{bmatrix}$$

Imaginary part

$$\begin{bmatrix}
-4.9104 & 0 & 0 & -0.0424 & 0 & 0 & 0 & 0 & 0 \\
-0.028858 & -0.0580564 & -0.01898 & -0.0098184 & 0 & 0 & 0 & 0 & 0 \\
0 & -0.01898 & Y44 & -0.02158 & 0 & -0.0478 & 0 & -0.01798 & 0 \\
-0.0424 & -0.0098184 & -0.2158 & -0.34992 & -0.03968 & 0 & 0 & 0 & 0 \\
0 & 0 & 0 & -0.03968 & -4.4746 & 0 & 0 & -0.0909 & -0.044001 \\
0 & 0 & -0.0478 & 0 & 0 & 0 & -0.05677 & 0 & 0 \\
0 & 0 & 0 & 0 & 0 & -0.05677 & -4.36707 & 0 & 0 \\
0 & 0 & -0.01798 & 0 & 0 & -0.0909 & 0 & -0.24282 & -0.005726 \\
0 & 0 & 0 & 0 & -0.044001 & 0 & 0 & -0.005726 & -0.823836
\end{bmatrix}$$

Based on the admittance matrix Y_{busR} the one-line diagram of the reduced model is obtained, Figure 6.20.

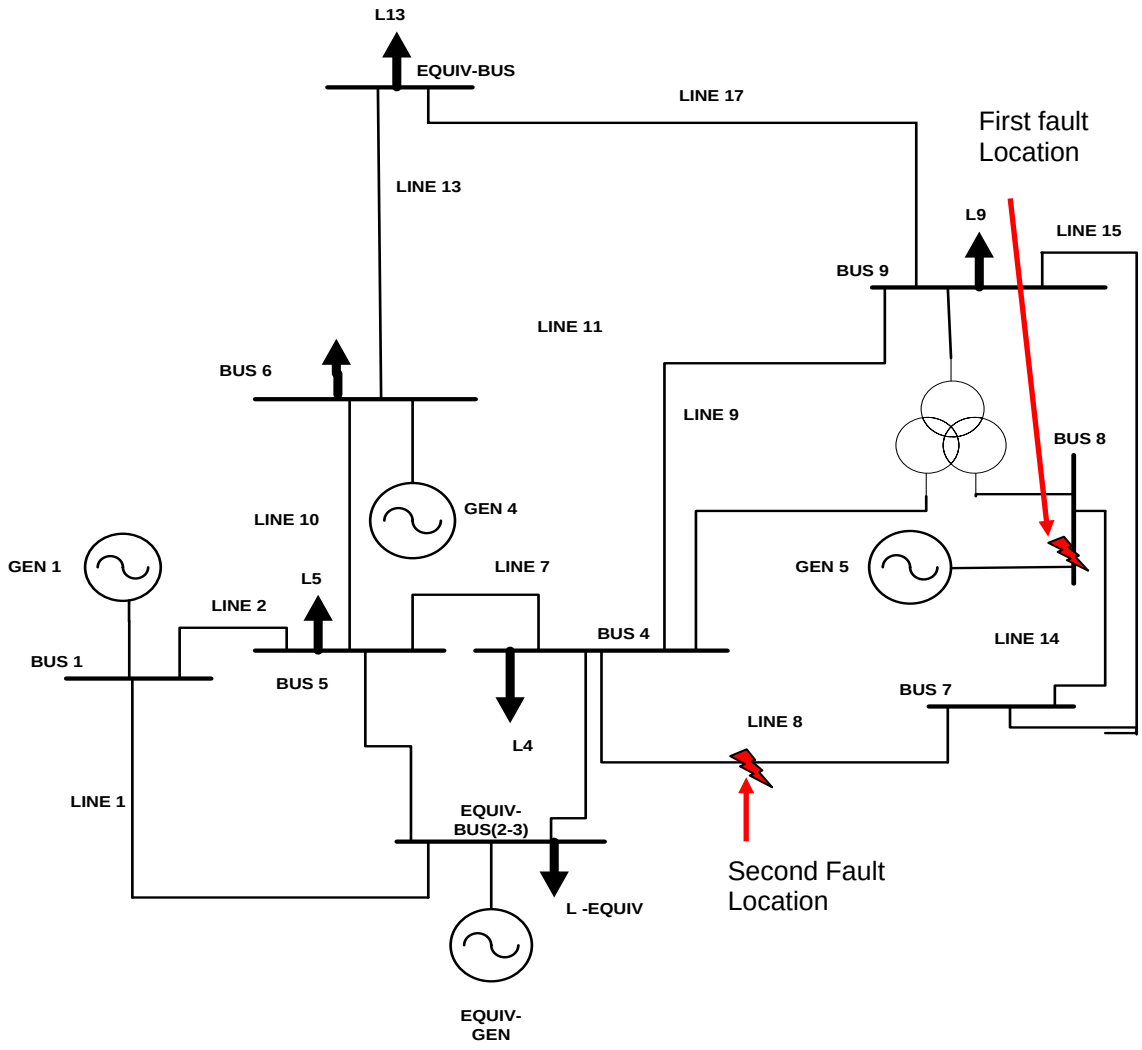

Figure 6. 20: One line diagram of the reduced system in DigSILENT

6.4 Simulation results of the reduced system

Figure (6.20) is built in DigSILENT power Factory software environment, and the load flow computation for the reduced model is performed. Results for the load flow are presented in Table 6.4.

6.4.1 Load flow results of the reduced model

Voltage magnitudes and phase angles of all the buses that are common for both reduced and full models are well depicted in Table 6.4.

Table 6. 4: Load flow results for the full and reduced network

Full Network			Reduced Network		
Bus Number	**Voltage [PU]**	**Phase angle [deg]**	**Bus Number**	**Voltage [PU]**	**Phase angle [deg]**
1	1.040	0	1	1	0
4	1.052	-6.67	4	1.012	-7.34
5	1.025	-5.53	5	1.033	-5.87
6	1.070	-7.43	6	1.07	-5.62
7	1.056	-6.91	7	1.08	-7.67
8	1.044	-6.68	8	1.009	-7.29
9	1.013	-7.17	9	1.006	-7.85

6.5 Comparison of the number of elements in the full and the reduced models

Table 6.5 contains the comparison of the number of buses, number of transmission lines and generators in the full and reduced models.

Table 6. 5: Comparison of the full and reduced models

System	Full model	Reduced model	% Rate of retaining	% Rate of reduction
Number of Buses	14	9	64.286%	35.714%
Number of Lines	20	11	55%	45%
Number of Generators	5	4	80%	20%

Tables 6.6 and 6.7 report and compare values of both the voltage magnitude (in kV) and phasor angle (in degree) for the buses of the two models. The comparison is made based on the boundary buses, buses in the study area and the unreduced buses.

Table 6. 6: Comparison of the full and reduced models bus voltages

Full Network		Reduced Network		e_x
Bus Number	Voltage [PU]	Bus Number	Voltage [PU]	[%]
1	1.040	1	1	-3.846
4	1.052	4	1.012	-3.8023
5	1.025	5	1.033	0.7805
6	1.070	6	1.070	0
7	1.056	7	1.080	2.2727
8	1.044	8	1.009	-3.3525
9	1.013	9	1.006	-0.6910

Table 6. 7: Comparison of the full and the reduced models phase angles

Full Network		Reduced Network		e_x
Bus Number	Phase Angle [Deg]	Bus Number	Phase Angle [Deg]	[%]
1	0	**1**	0	0
4	-6.67	**4**	-7.34	10.044
5	-5.53	**5**	-5.87	6.148
6	**-7.43**	**6**	**-5.62**	**24.36**
7	-6.91	**7**	-7.67	10.99
8	-6.68	**8**	-7.29	9.132
9	-7.17	**9**	-7.85	9.484

6.5.1 Transition behaviour and the comparison of the full and reduced model for the first fault.

Figures (6.21-6.24) show the comparison of the transition behaviour of the generator 5 between the full and the reduced models for the first fault location. Loadflow simulations reports for the full and reduced IEEE 14-bus system are given in Appendix F1 and F4.

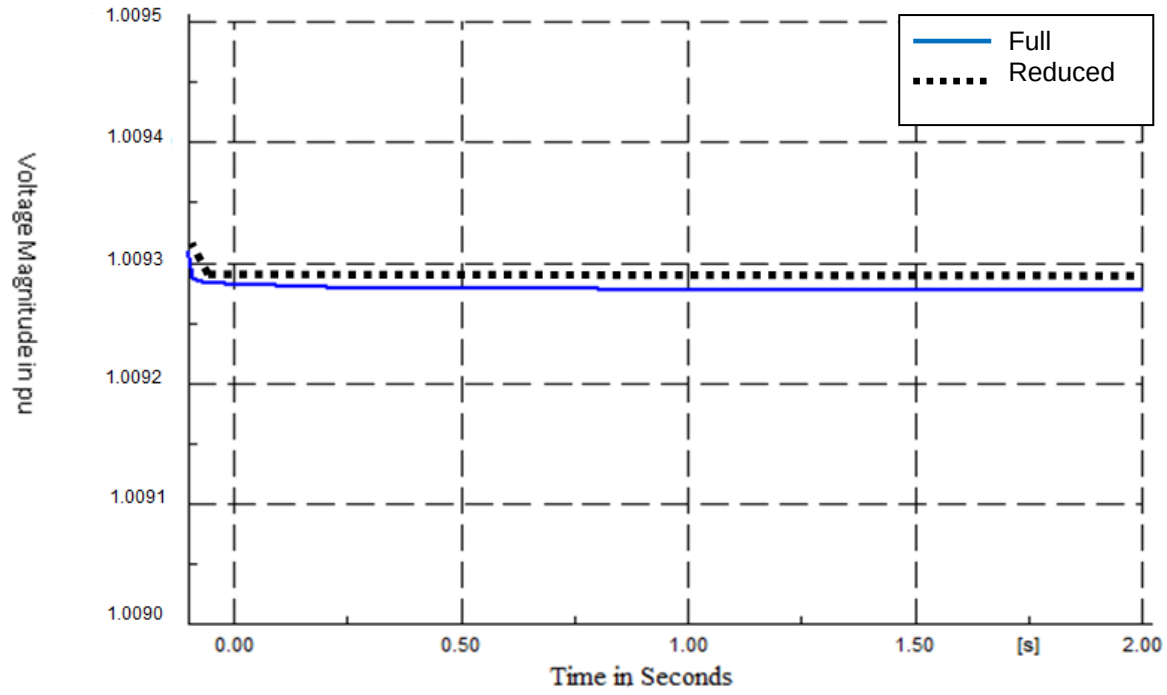

Figure 6. 21: Voltage magnitude of the generator 5 in the reduced and full model for the first fault

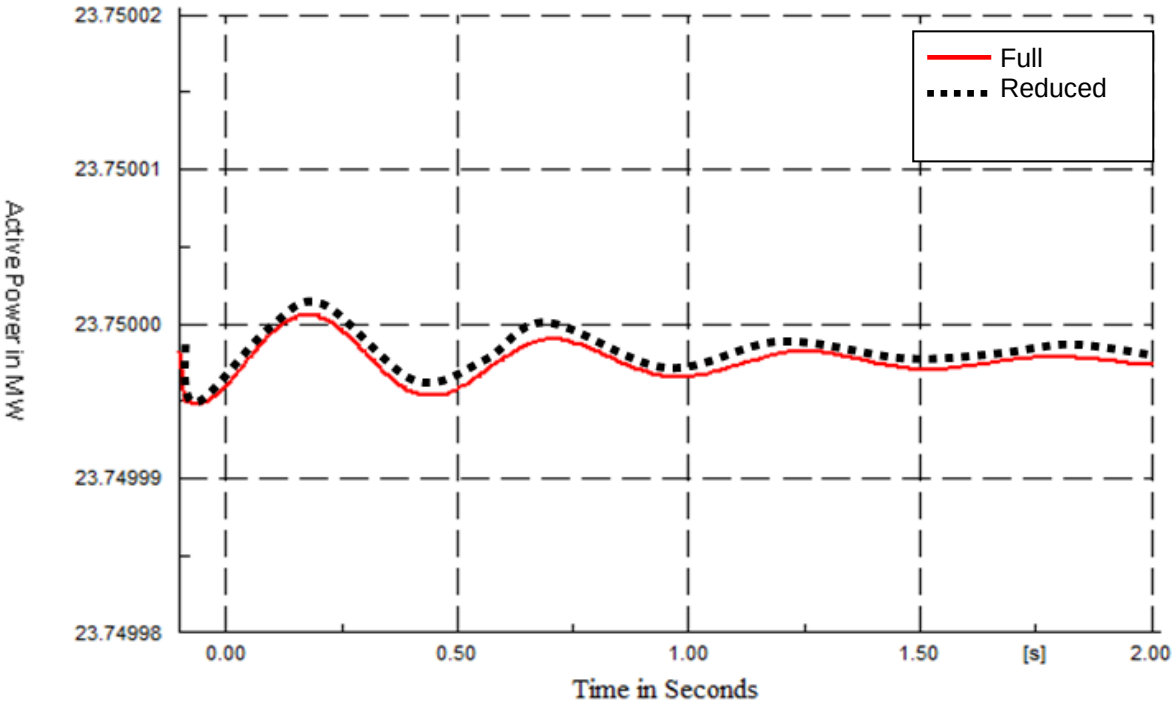

Figure 6. 22: Active power in MW of the generator 5 in the reduced and full models for the first fault

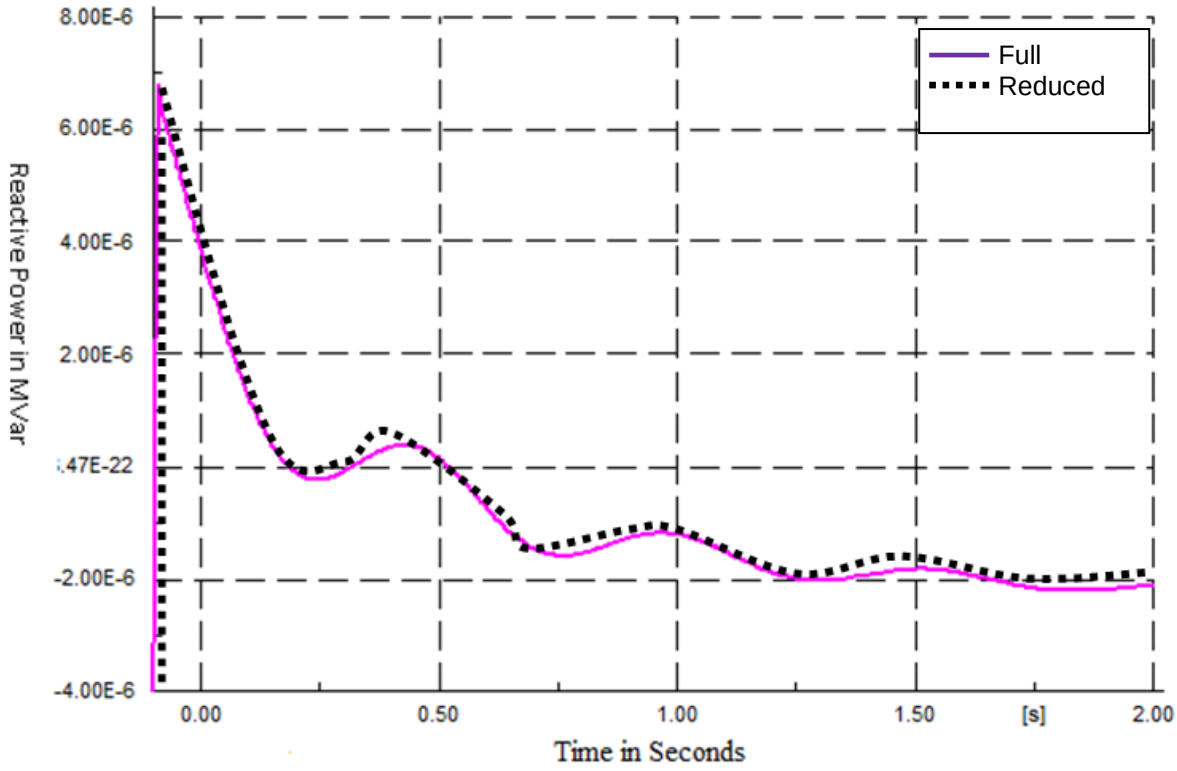

Figure 6. 23: Reactive power in MVar of the generator 5 in the reduced and full models for the first fault

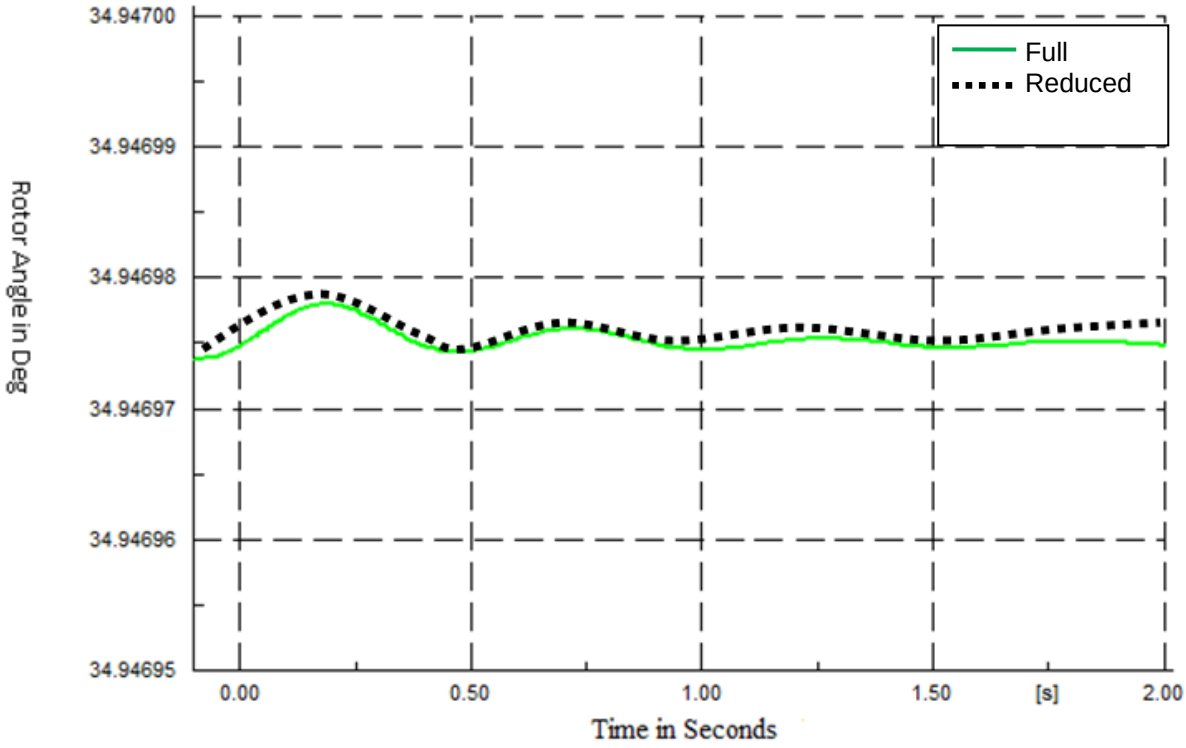

Figure 6. 24: Rotor angle in degrees of the generator 5 in the reduced and full models for the first fault

6.5.2 Transition behaviour and the comparison of the full and reduced model for the second fault

Figures (6.25-6.28) show the comparison between the full and the reduced models transition behaviour of the generator 5 for the second fault location.

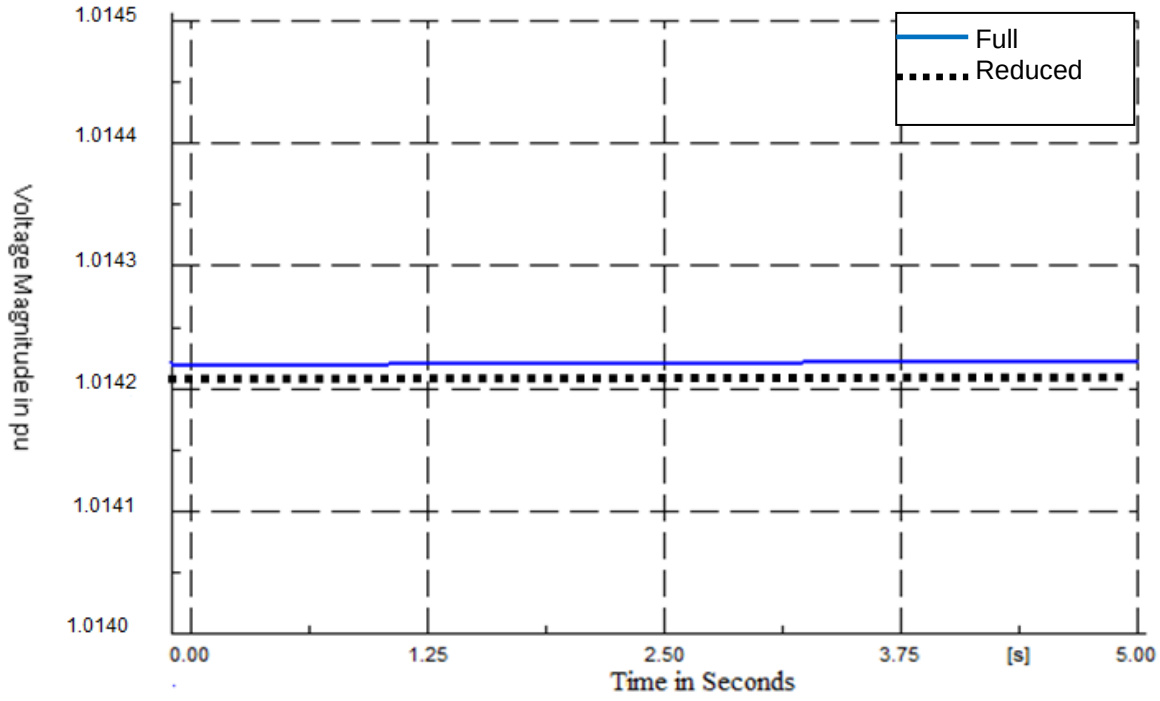

Figure 6. 25: Voltage magnitude in PU of the generator 5 in the reduced and full models for the second fault

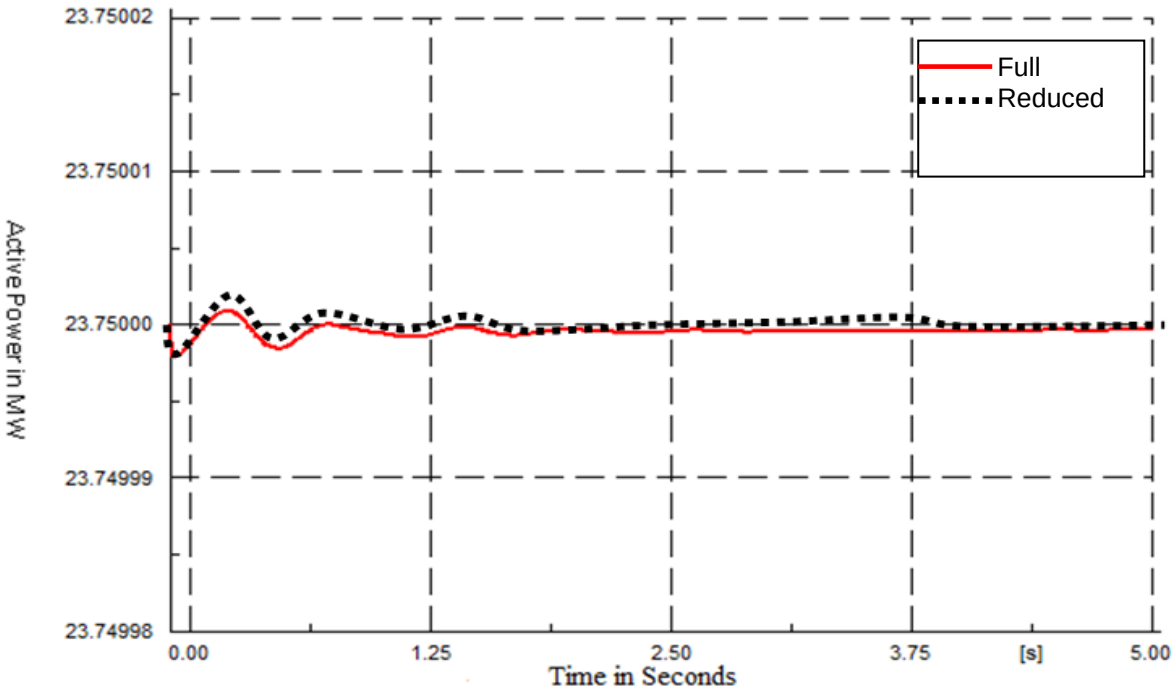

Figure 6. 26: Active power in MW of the generator 5 in the reduced and full models for the second fault

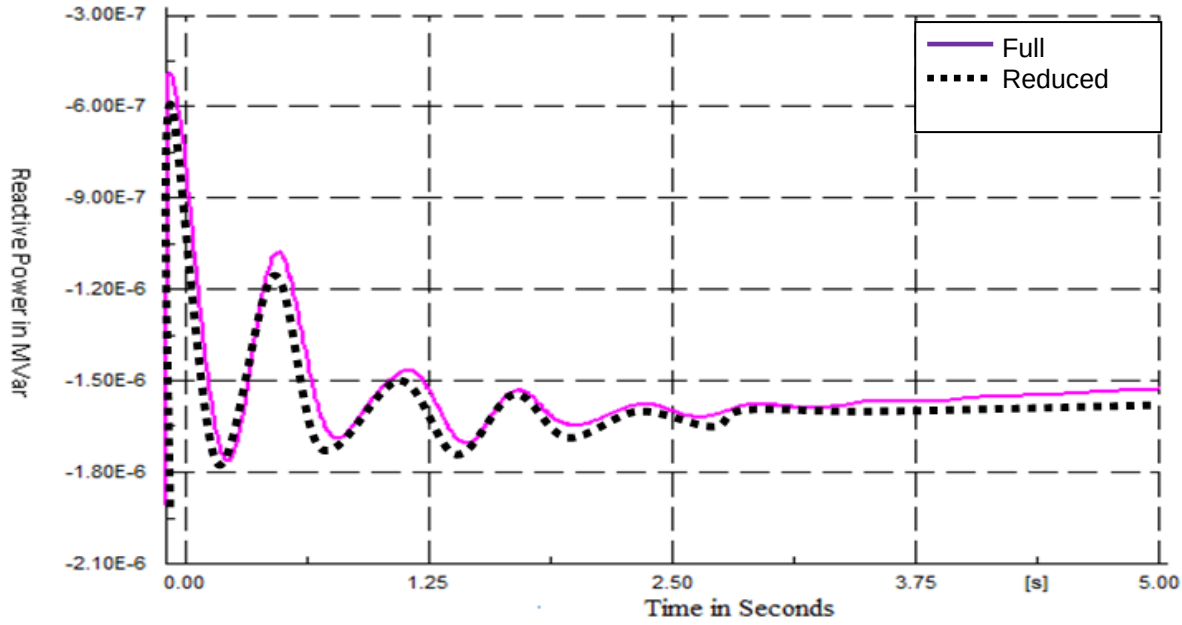

Figure 6. 27: Reactive power in Mvar's of the generator 5 in the reduced and full models for the second fault

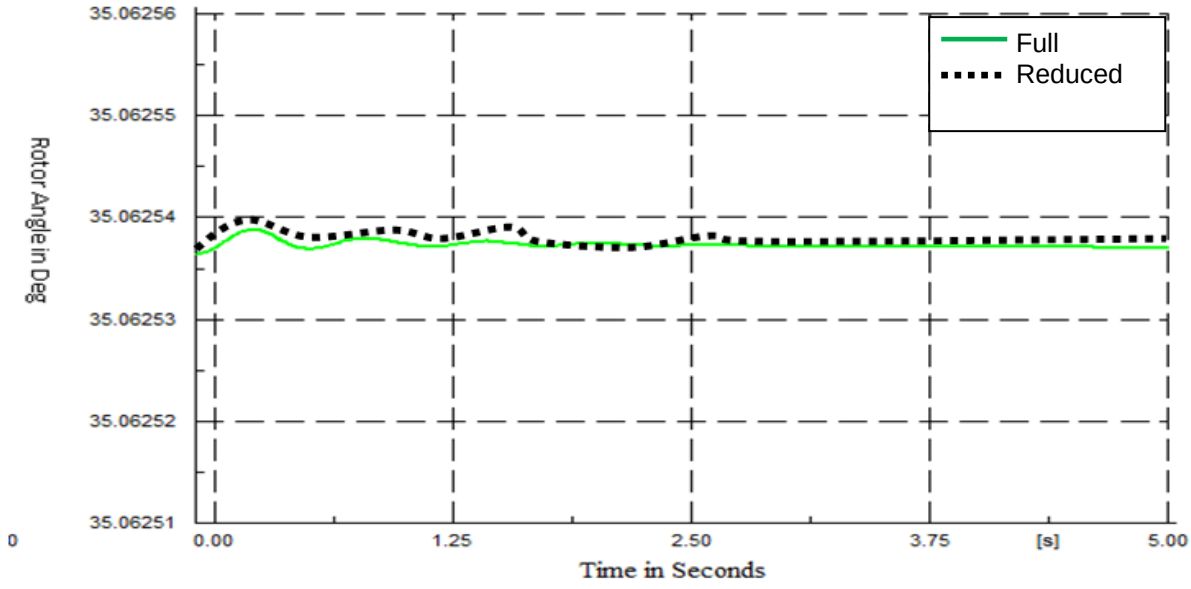

Figure 6. 28: Rotor angle in degrees of the generator 5 in the reduced and full models for the second fault

6.5.3 Comparison of the results for the two faults in the full and the reduced model

The steady state values of the voltages, rotor angles, reactive and active powers obtained after the transition behaviour as responses of the full and the reduced models to the two considered faults in the study area are shown in Tables 6.8 and 6.9 respectifully. Percentage error for the first fault is between **0%** and **0.892 %,** while the one for the second fault is between **0%** and **0.0043%**. Therefore, the results show a good accuracy of the developed reduced model.

Table 6. 8 : Steady state values for the full and reduced models after transition behaviour as a response to the first fault

x	Full model	Reduced model	$e_x\%$
V [PU]	1.014	1.009	0.493
δ [Deg]	35.06253	34.7499	0.892
P [MW]	23.75	23.7499	0.00042
Q [MVAR]	60	60	0

Table 6. 9: Steady state values for the full and reduced models after transition behaviour as a response to the second fault

x	Full model	Reduced model	$e_x\%$
V [PU]	1.014	1.014	0
δ [Deg]	35.06253	35.0624	0.0004
P [MW]	23.75	23.75001	0.00042
Q [MVAR]	60	60	0

6.6 Discussion of results

This chapter developed the equivalent coherent generator and the simulation results obtained are very close to the calculated ones. Table 6.10 depicts the comparison of the calculated and simulation results for the obtained equivalent coherent generator.

Table 6. 10: Comparison of the calculated and simulation results of the equivalent generator

Generator variable	Calculation results	Simulation results	% e_x
Voltage [kV]	232.07	232.1298	0.0258
Rotor angle [Deg]	18.8	18.802	0.0164
Active power [MW]	91	91.000	0
Reactive power[MVAR's]	46.8	45.41	2.991

Comparison of the full and the reduced models for both the voltage magnitude and the angle errors are within the limits. Both the rate of retaintion and reduction are also good. Moreover, percentage error for the steady state valhes for the full and the reduced models after transition behaviour as a response to both the first and the second fault are of good accuracy.

6.7 Conclusions

This chapter extended the developed in Chapter 4 coherency based method and applying it, the IEEE 14-bus system was successfully reduced into 9-bus system. Coherency based method is applied with all its steps including coherent generators aggregation. For the grouping of the coherent generators, inertial algorithm is utilized. The simulation results obtained from both the full system and the reduced order system were compared, and close agreement was obtained. Moreover, the results show that the developed reduced model has good accuracy in representing the dynamic behaviour of the full system.

The coherency based reduced order model has an advantage over the other techniques (such as synchronic modal equivalency, integral modal manifold, e.t.c.), in that the reduced model development retains the basic physical structure of the initial system. The voltage sources of the coherent generators become parallel to each other and are replaced by a single voltage source, which is capable of supplying the active and reactive powers equal to the sum of the active and reactive powers delivered by the generators of the coherent group being replaced. The developed reduced model can be used for electromagnetic transient analysis, on-line dynamic security assessments and system control designs.

Further implementation and assessment of the reduced order model for IEEE 14-bus system will be done in Chapter 7 in real-time simulation environment. RSCAD software is used in order to achieve the objective.

CHAPTER SEVEN
IMPLEMENTATION OF THE COHERENCY METHOD USING RSCAD SOFTWARE ENVIRONMENT FOR THE IEEE 14TEEN BUS SYSTEM

Introduction

In this chapter, the same procedures followed in Chapter 6 for the IEEE 14-bus network are applied in real-time simulation program. The increase in efficiency of an equivalencing algorithm in the real-time environment can be evaluated by expedation in the computation time. However, in this case the equivalent and the full models are both operating in synchronism with a real time clock and have the same calculation times. Instead, a better index for the efficiency would be the comparison of the dynamic behaviour of the synchronous generator 5 for the models built in the two software environments – DigSILENT and RSCAD. As it was stated earlier in this research, synchronous generator 5 is situated in the area of study.

When an RTDS rack is colonized with the latest generation GPC (Giga-Processor Card) from the accessible RTDS inventory, it is competent of solving 66 nodes (22 three phase busses) in one rack. Each rack is usually utilized to model a bunch of network nodes that is secluded from the other nodes in a network by means of transmission line models. Transmission lines do not permit voltages/currents at one end to get to the other faster than the velocity of light in a vacuum (300 000 km or 15 km per 50 μs time step). This enables independent parallel simulations of each of the node clusters. Since most networks are self-similar in configuration, the distribution of clusters and transmission lines is approximately alike in spite of the size. This is an observation borne from practice. Therefore, the size of the simulation hardware needed also scales in line with the network size. The proposed equivalencing algorithm requires only one rack to simulate the detailed internal system and the equivalent external system in real-time.

This Chapter is divided into seven sections. Section 7.1 introduces IEEE 14-bus power network simulations to calculate the load flow. Presentation of bus voltage load flow curves is done in section 7.2. In section 7.3, comparison between the full and the reduced models in RSCAD software for load flow as well as transient stability of the generator 5 is done. Also the simulations of the equivalent generator are done in this section. Section 7.4 deals with the comparison of simulation results obtained from the full and reduced models.

Section 7.5 presents the following parts:

- Comparison between the full and the reduced model load flow results obtained in both RSCAD and DigSILENT software environments.
- Comparison of the generator 5 dynamic simulation results RSCAD for the full and the reduced models.
- Comparison of the generator 5 dynamic behaviour of the reduced model after application of the first fault in both RSCAD and DigSILENT, and
- Comparison of the generator 5 dynamic behaviour of the reduced model after application of the second fault location in both RSCAD and DigSILENT environments.

Finally, sections 7.6 and 7.7 offer the discussions of the results and conclusions respectfully.

7.1 IEEE 14-bus system model in RSCAD software environment

This system consists of five synchronous generators, twenty transmission lines, and eleven loads as depicted on Figure 7.1. The modelling and drawing of the network were done on the draft window of RSCAD. Compiling and load flow computation were successfully conducted, therefore the run time window was utilized to produce graphical results of the system. In the run time window, all the power system components can be monitored according to the choice of the user. For this research, the angle delta, active power, reactive power and the voltage magnitudes are monitored, especially for the components in the selected study area described in Chapter 6.

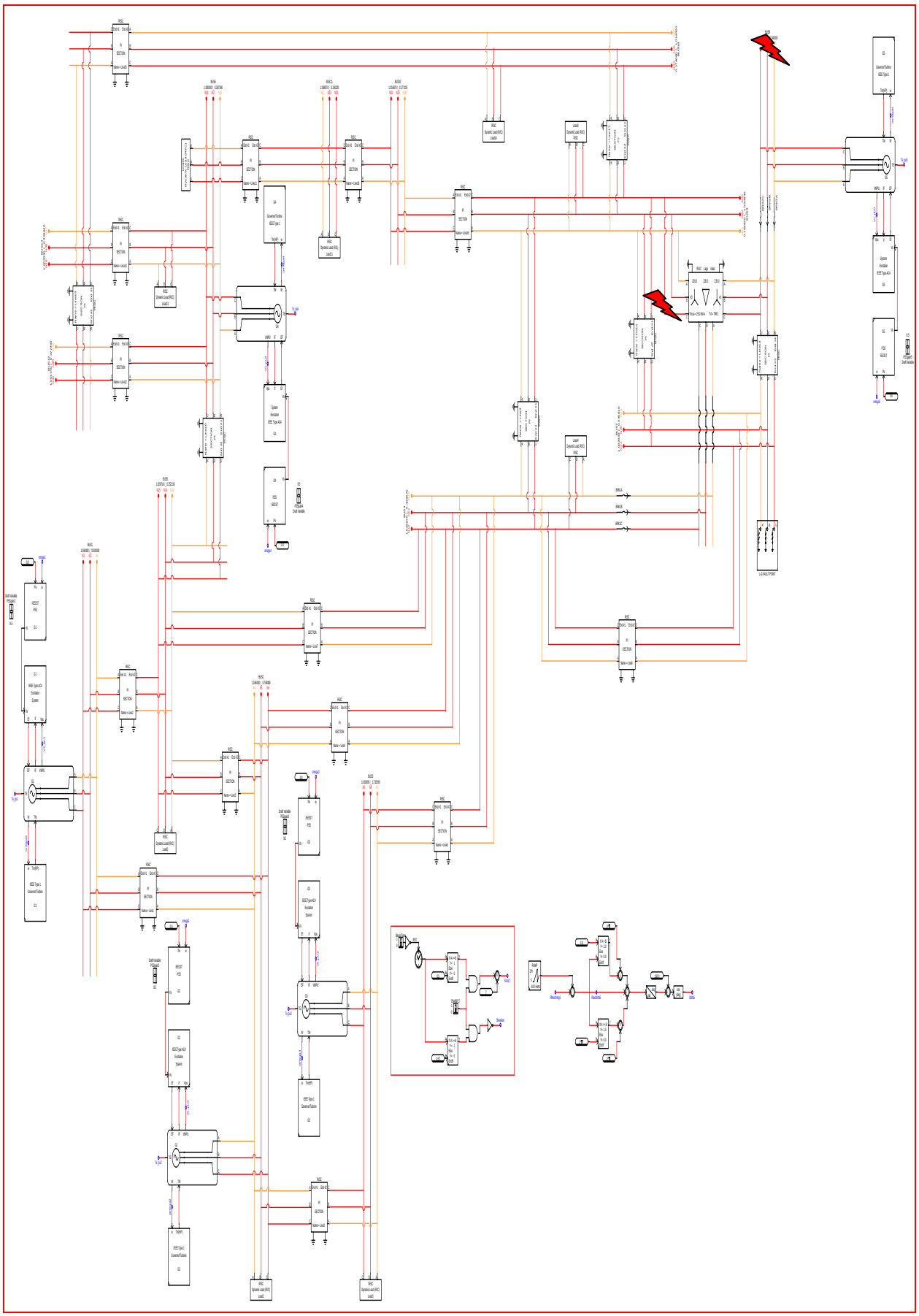

Figure 7. 1: One line diagram of a full IEEE14-bus System.

7.2 Bus voltage load flow curves

Figures (7.2) till Figure (7.6) present the waveforms results of all the 14-buses as shown from the runtime window. Also the three phase RMS (Root-Mean Square) meters were created to measure the values of voltage magnitudes of the buses.

Figure 7.2 shows the wave form of the voltage magnitudes of the buses, 1, 2 and 3.

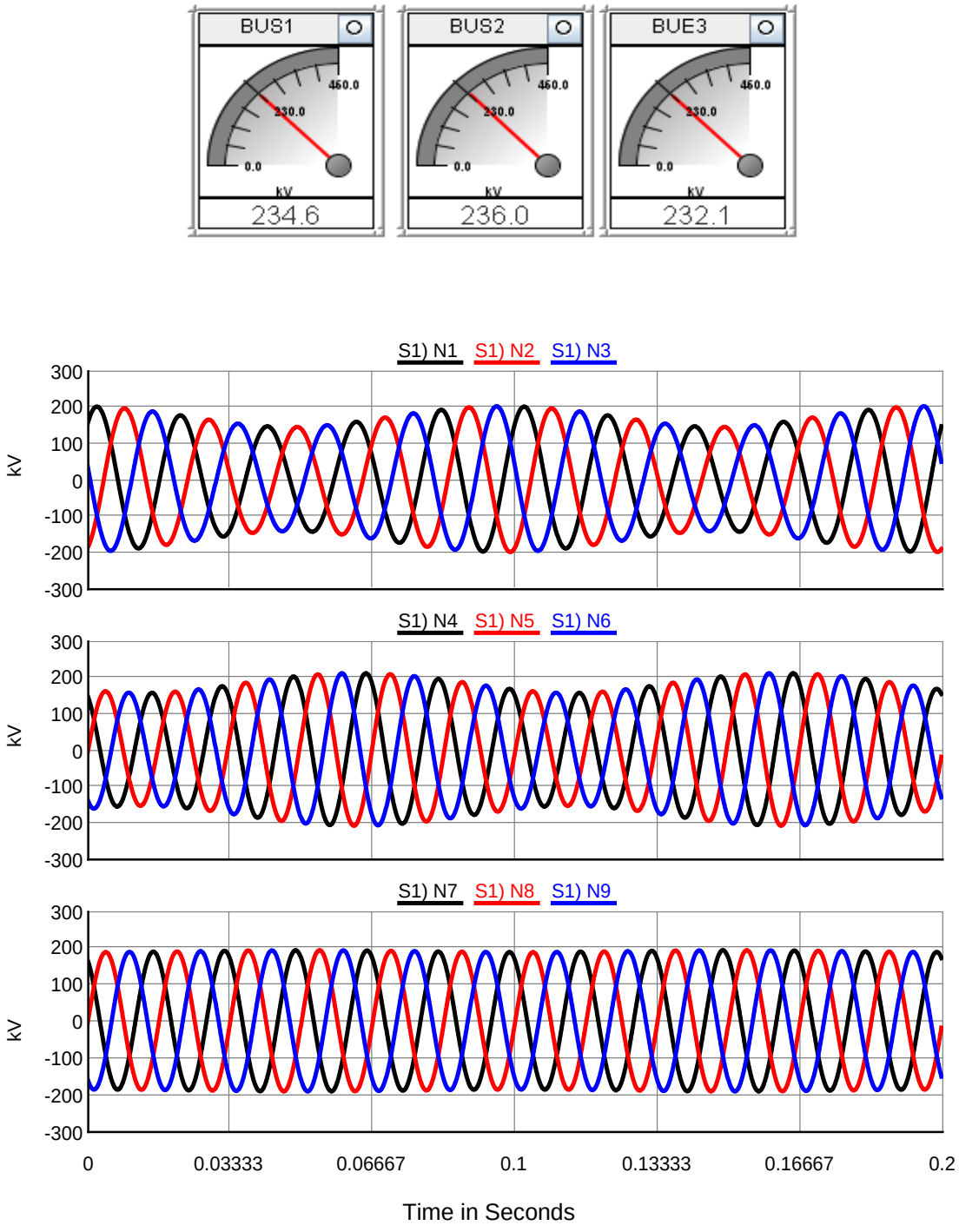

Figure 7. 2: Bus 1 - 3 voltage mgnitudes of the IEEE 14- bus system

Figure 7.3 shows the wave forms of the voltage magnitudes of the buses, 4, 5 and 6.

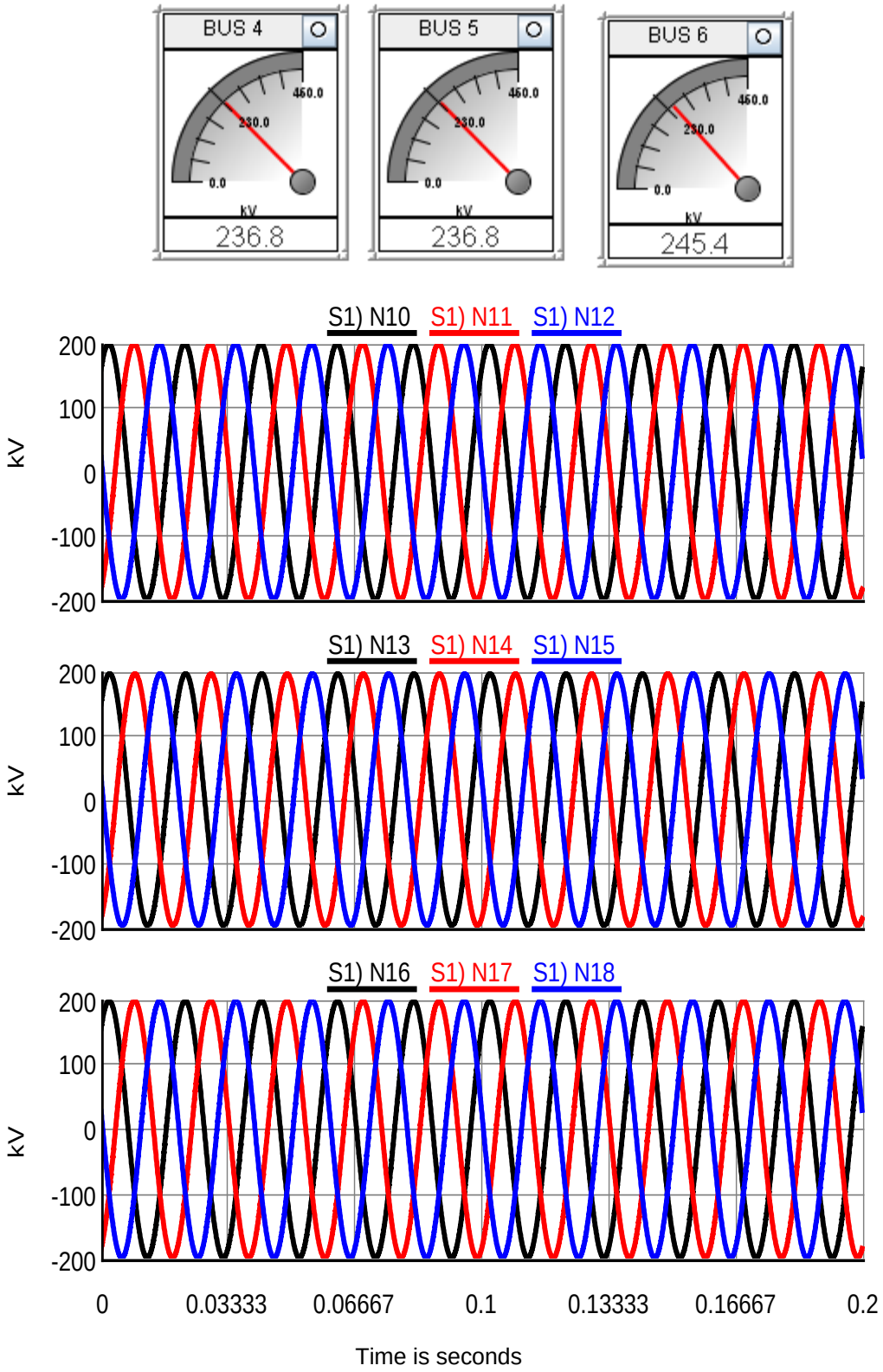

Figure 7. 3: **Bus 4 - 6 voltage magnitudes of the IEEE 14- bus system**

Figure 7.4 shows the wave forms of the voltage magnitudes of the buses, 7, 8 and 9.

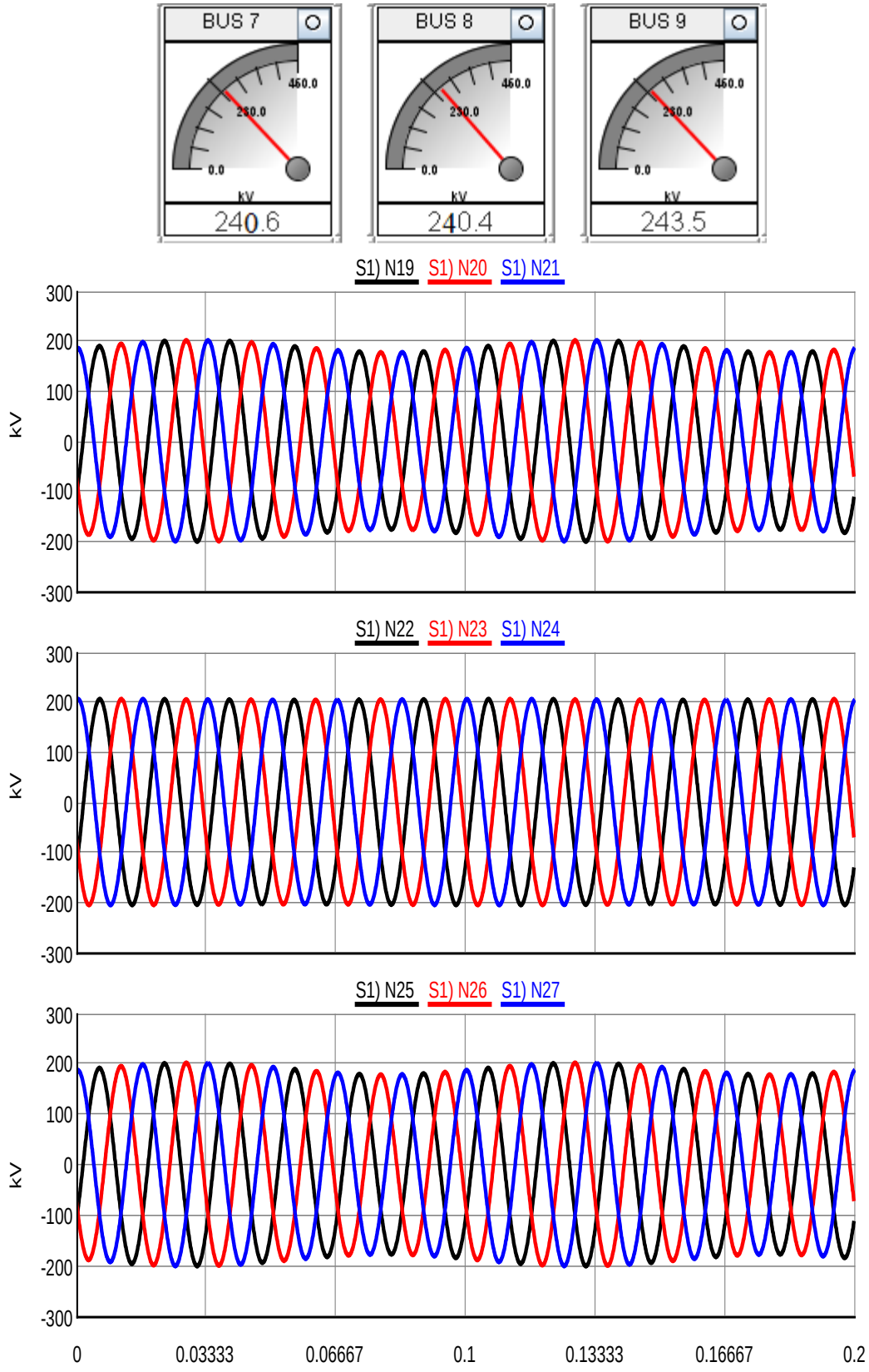

Figure 7. 4: Bus 7 – 9 voltage magnitudes of the IEEE 14- bus system

Figure 7.5 shows the wave forms of the voltage magnitudes of the buses, 10, 11 and 12.

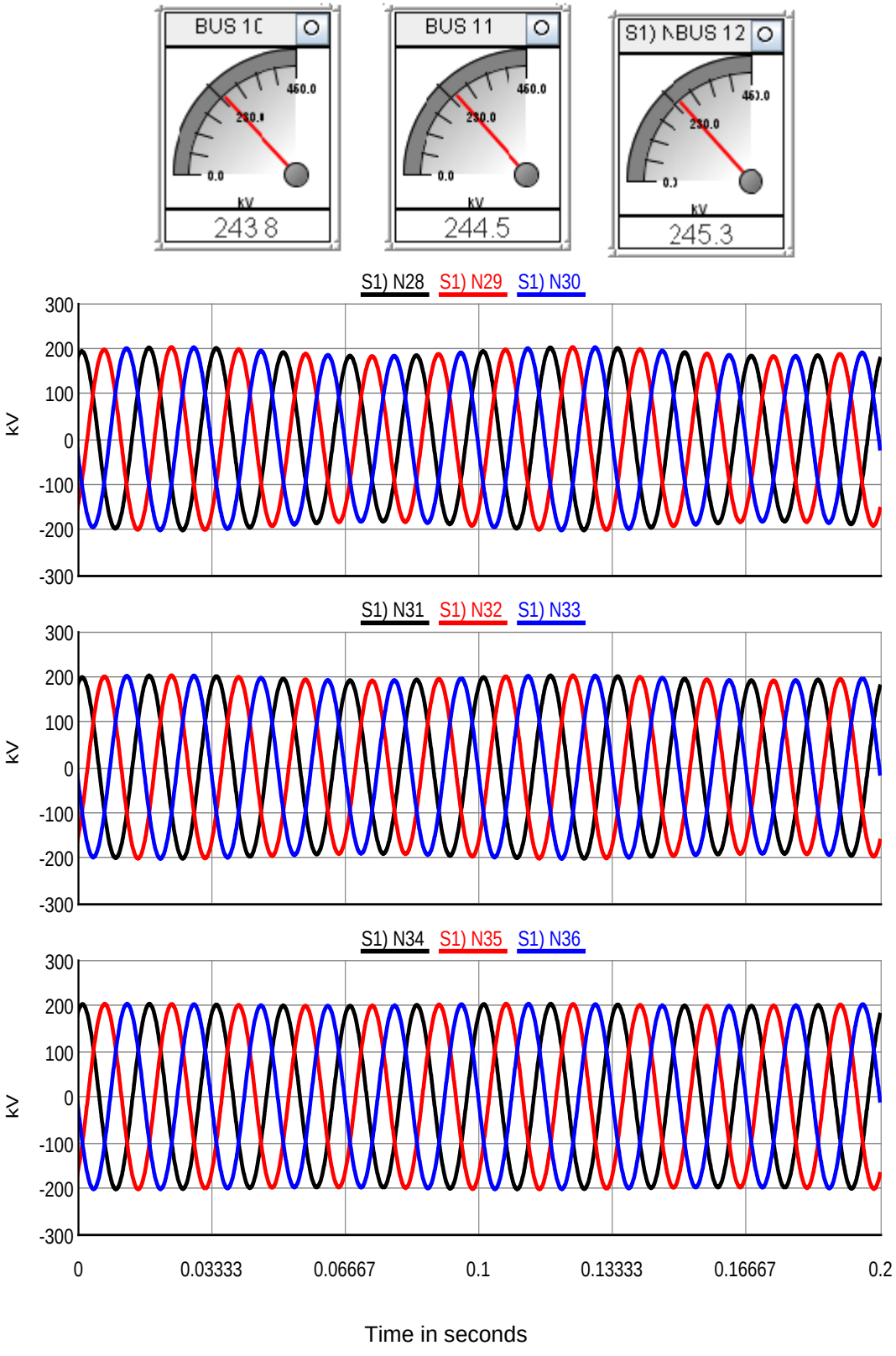

Figure 7. 5: **Bus 10 - 12 voltage magnitudes of the IEEE 14- bus system**

Figure 7.6 shows the wave forms of the voltage magnitudes of the buses, 13 and 14.

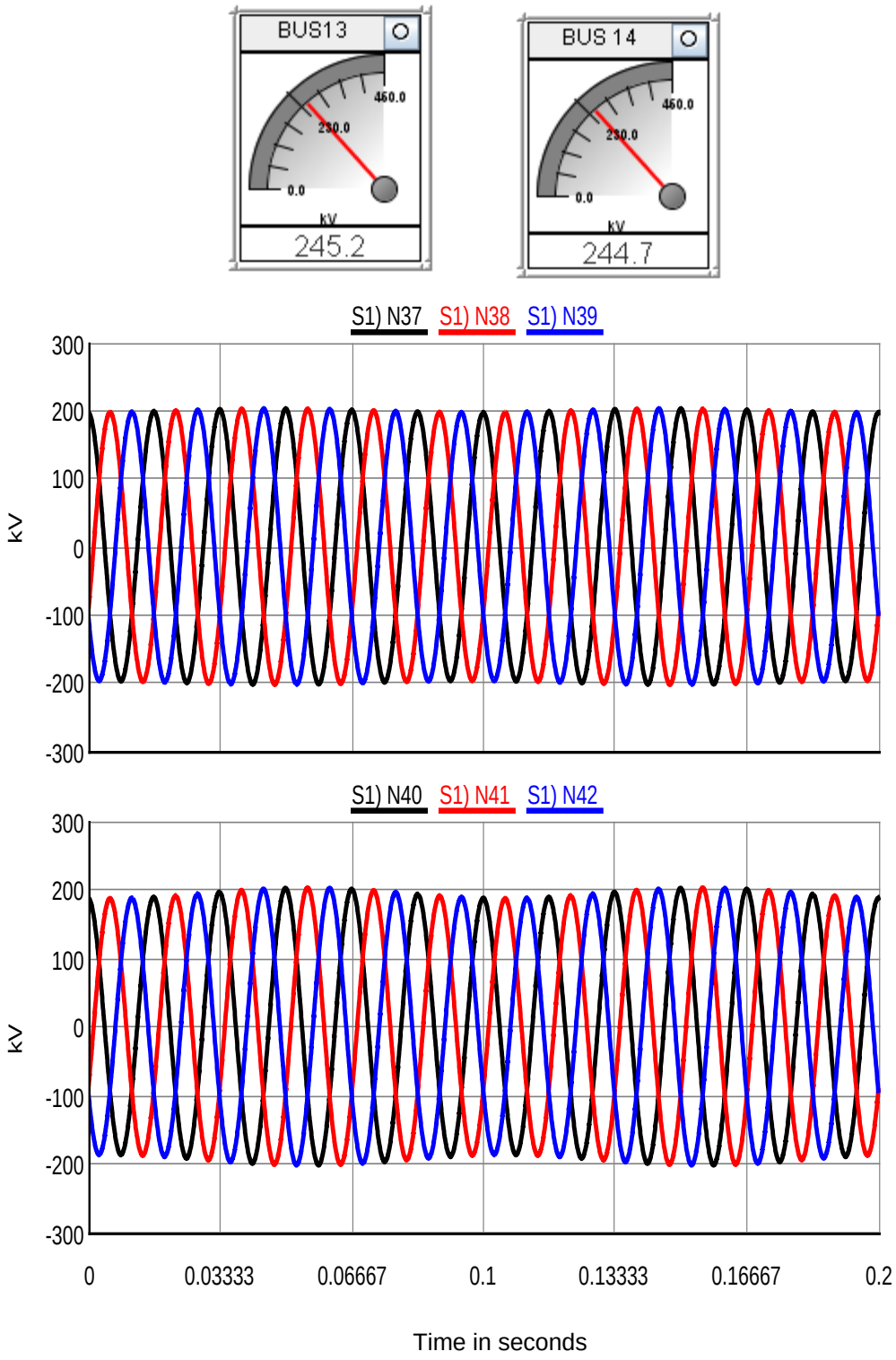

Figure 7. 6: Bus 13 and 14 voltage magnitudes of the IEEE 14- bus system

7.2.1 Comparison of IEEE 14-bus load flow data with the obtained load flow results from simulation in RSCAD real-time software environment

Table 7.1 depicts the results comparison of the IEEE 14-bus system load flow data in per unit values and the load flow results of voltage in per unit values from the RSCAD calculations.

Table 7. 1: Comparison between the IEEE 14-bus system given data and the voltage magnitude load flow results from the RSCAD simulation of the model

Bus	IEEE [P U]	RSCAD [P U]	Percentage deviation [%]
1	1.060	1.050	-0.943
2	1.045	1.045	0
3	1.010	1.01	0
4	1.019	1.02687	0.7723
5	1.020	1.02971	0.95196
6	1.070	1.06696	-0.2841
7	1.062	1.0461	-1.4972
8	1.090	1.0452	-4.11009
9	1.056	1.058696	0.2553
10	1.051	1.06	0.8563
11	1.057	1.06304	0.5714
12	1.055	1.06739	1.1744
13	1.050	1.06609	1.6095
14	1.036	1.06391	2.694

The results have an error percentage in line with the limit ($\pm 5\%$), therefore the model can be used for application of the model order reduction procedures and algorithms.

7.2.2 Dynamic behaviour of the synchronous generator 5 in the full network model

Generator 5 is considered in this chapter as the generator to be retained after the reduction process due to the study area selection and fault location.

Table 7. 2: Steady state behaviour of the full model for the two fault locations

x	First fault	Second fault
V [PU]	0.90736	0.906
δ [Deg]	35.067	35.632
P [MW]	23.2105	23.567
Q [MVAR]	61.5372	61.25

The steady state values of the generator 5 in the full model obtained after the end of the transition behaviour of the model as a response to the two faults located in the study area on bus 8 and on transmission line 8 are shown in Table 7.2

Figure 7.7 shows the graphical results of the dynamic behaviour of synchronous generator 5 after being subjected to the three phase short circuit fault on bus 8. The second fault location is at the transmission line 8.

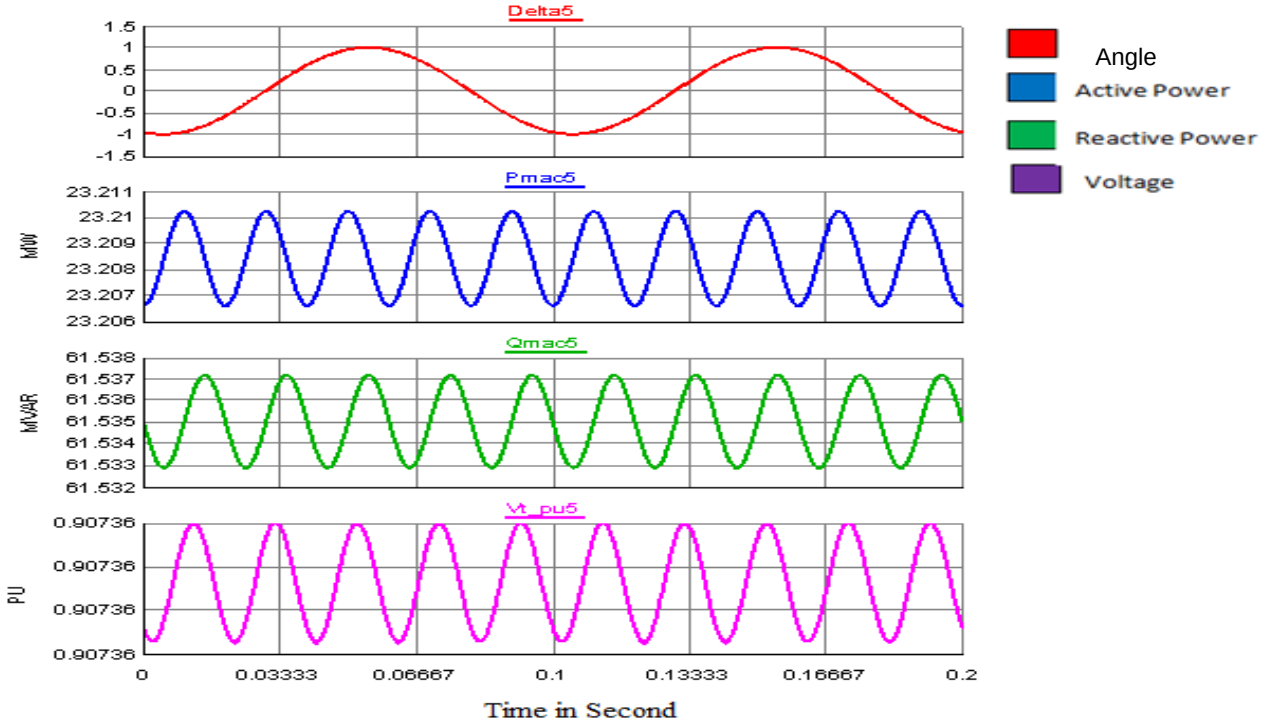

Figure 7. 7: Dynamic behaviour of the synchronous generator 5 in the full network model for the first fault

Figure 7.8 shows the dynamic behaviour of the generator 5 in the full network model for the second fault location.

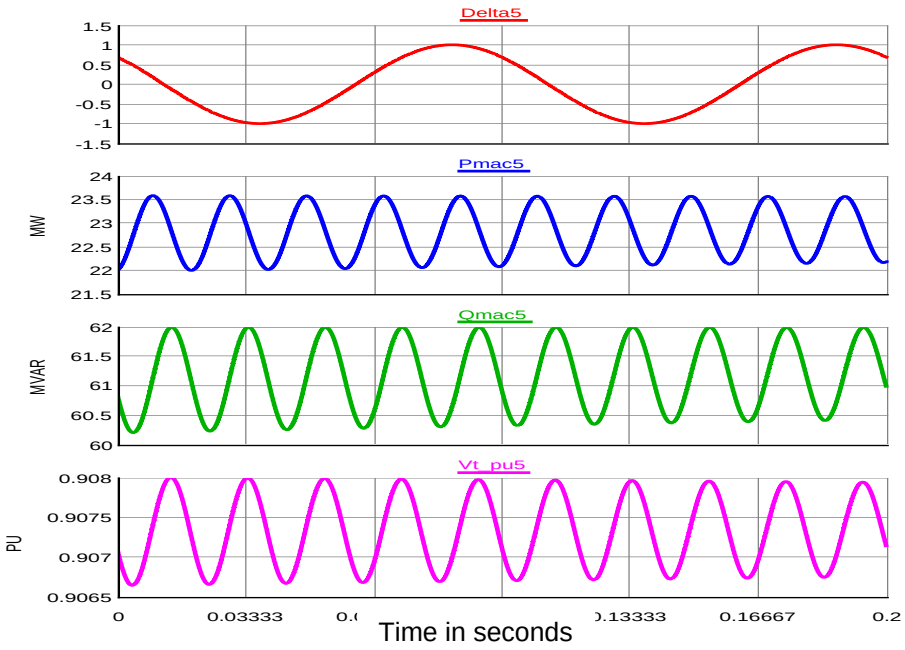

Figure 7. 8: Dynamic behaviour of the synchronous generator 5 in the full network model for the second fault

7.3 Simulation of the reduced model of the IEEE 14-bus system

The same procedures conducted in section 6.3.8 of Chapter 6 to develop and built the reduced network are followed in this chapter. The same obtained reduced admittance matrix is utilized to draw one line diagram of the reduced network in the RSCAD software environment.

Figure 7.9 shows the one line diagram of the reduced system after the process of reduction.

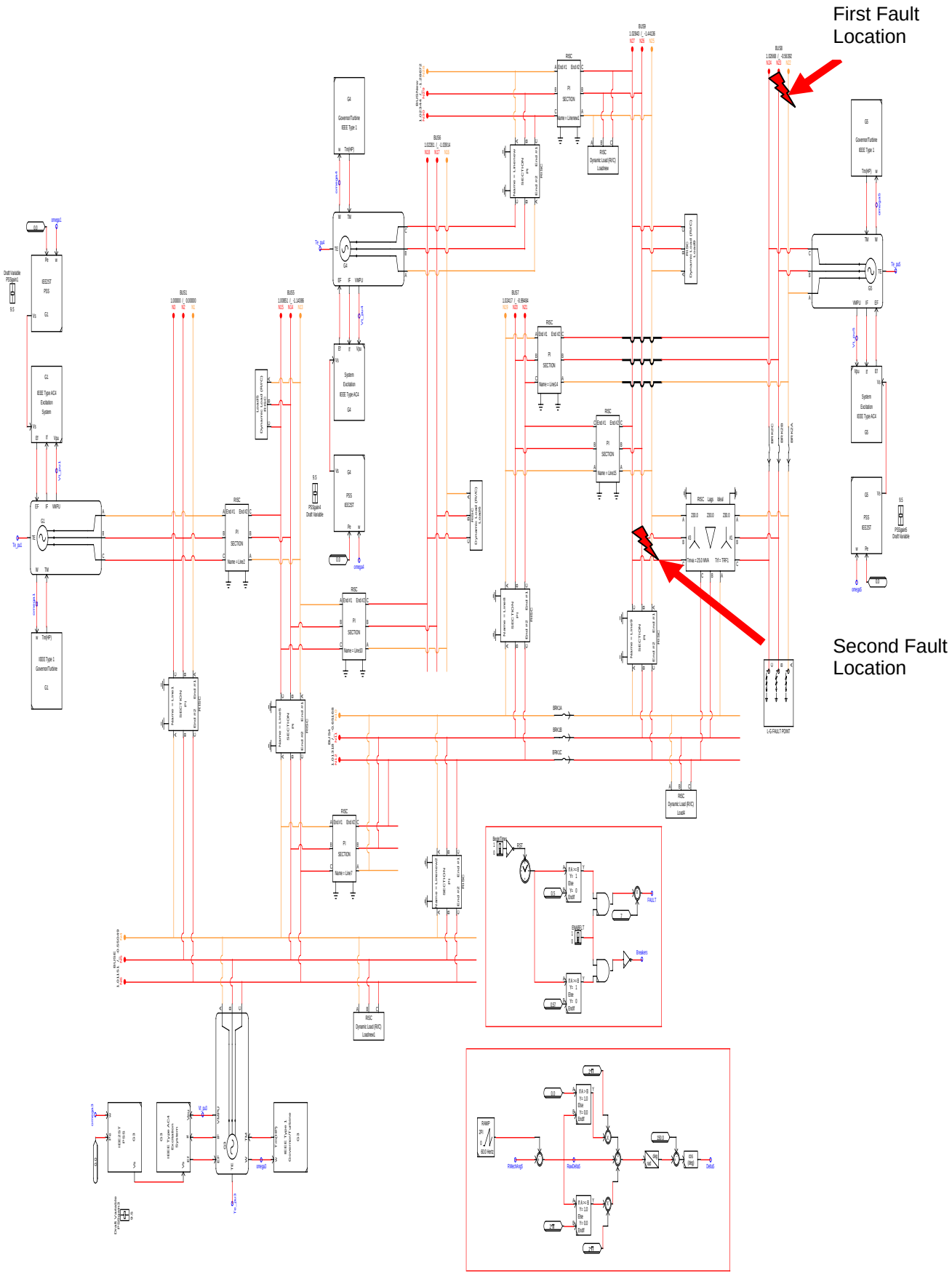

Figure 7. 9: RSCAD one line diagram of the reduced IEEE 14-bus system

7.3.1 Results of the load flow calculation and bus voltage magnitudes for the reduced network

Figure 7.10 shows the wave form of the voltage magnitudes of the bus1, the equivalent of (bus 2 and bus3) and bus 4.

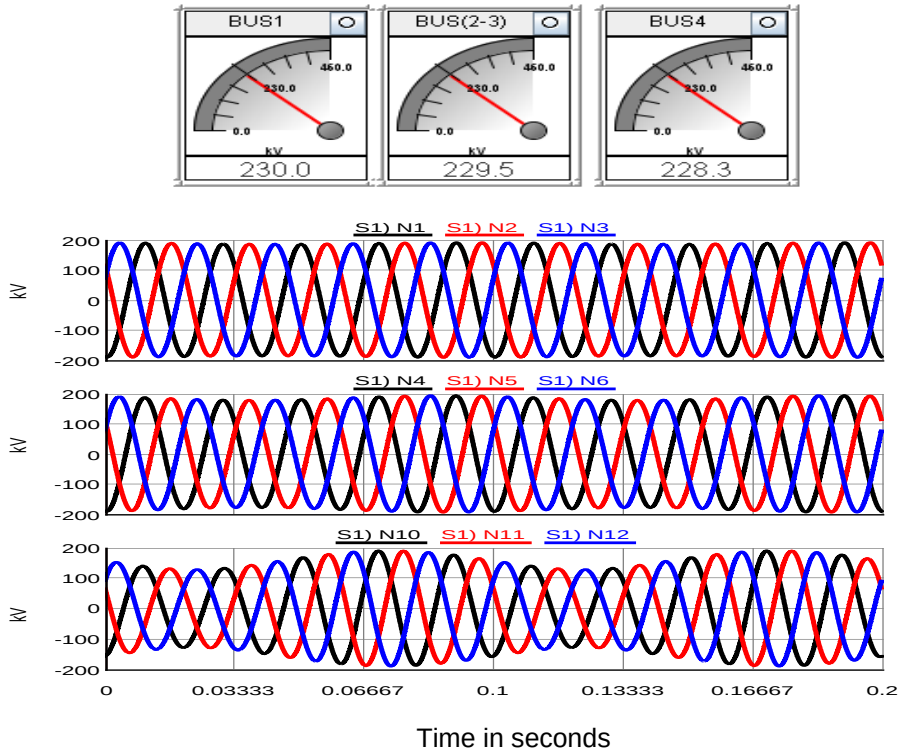

Figure 7. 10: **Voltage waveforms of the the bus 1, the equivalent bus, and the bus 4 of the reduced model**

Figure 7.11 shows the wave forms of the voltage magnitudes of the buses, 5, 6 and 7.

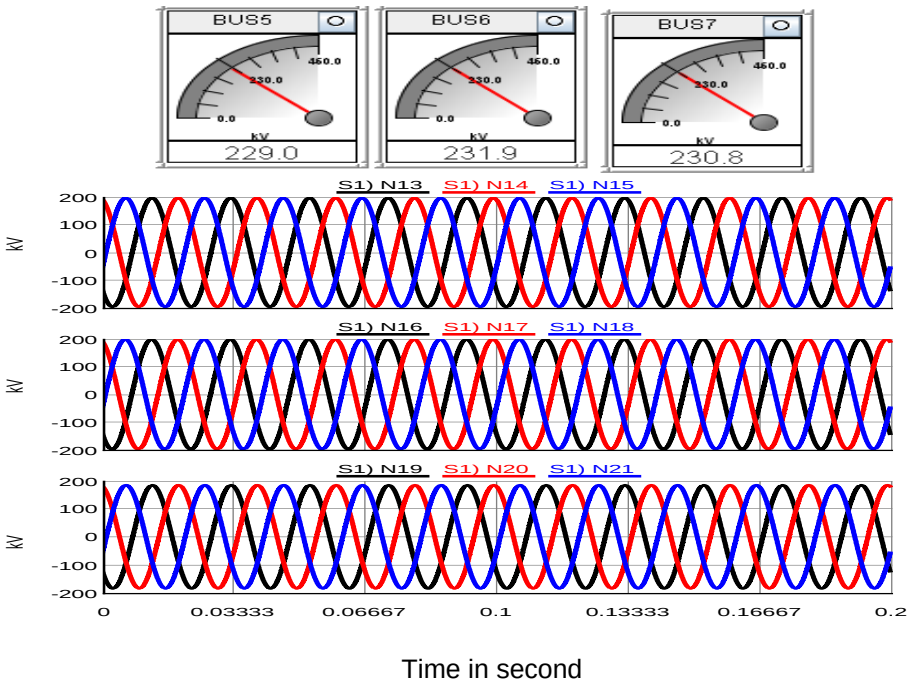

Figure 7. 11: **Voltage waveforms of the bus 5, the bus 6, and the bus 7 of the reduced model**

The main objective in the development of the reduced order power system is to retain both the study area and the boundary buses. For that reason, as it has been reported in previous Chapter that, buses 4, 5, and 9 are a boundary buses. The voltage magnitudes are very much similar to the boundary buses of the full network. Figure 7.12 shows the magnitudes for the boundary buses 9, the equivalent bus (bus 2 and bus 3), and study area bus 8.

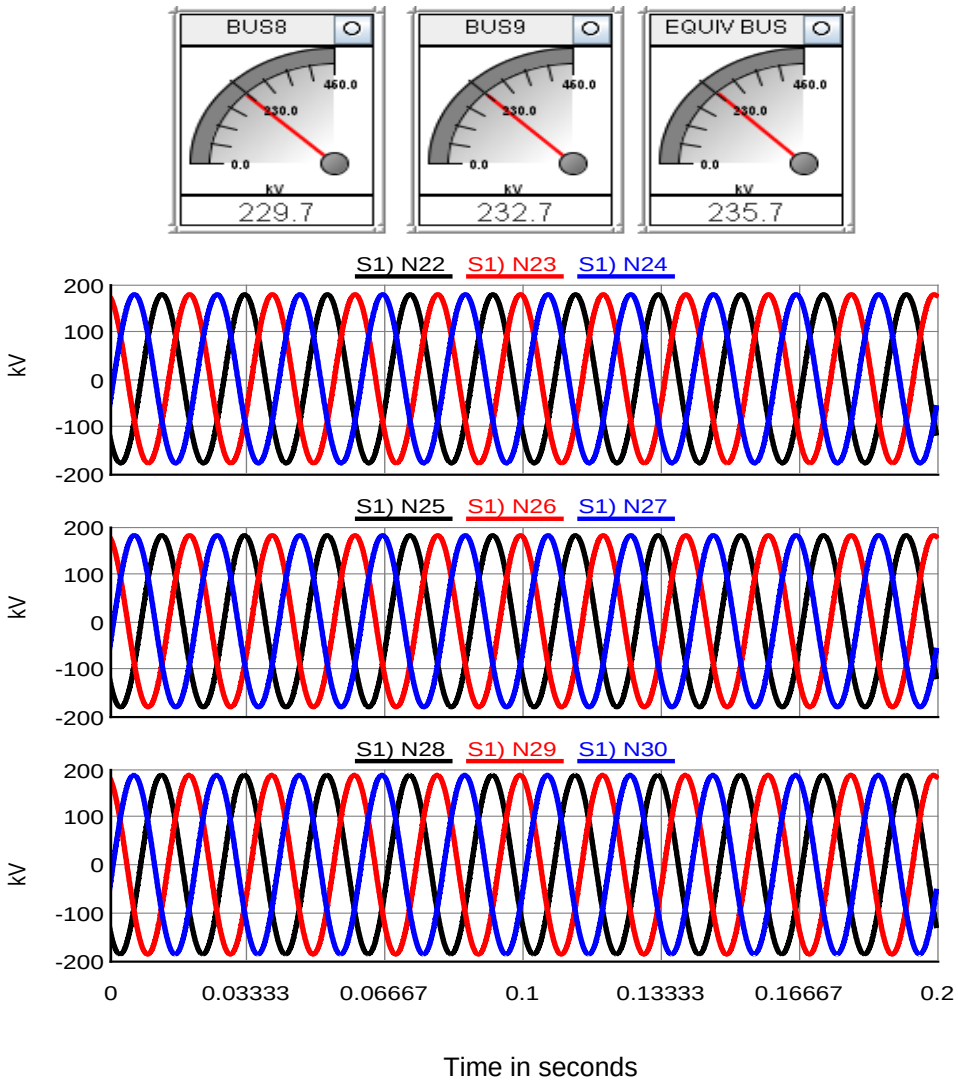

Figure 7. 12: **Voltage waveforms of the bus 8, the bus 9, and the equivalent bus of the reduced model**

7.3.2 Simulation results of the equivalent generator behaviour after the aggregation process

Figure 7.13 shows the dynamic transition behaviour curves of the equivalent generator after the aggregation of the generators 2 and 3 in the external area.

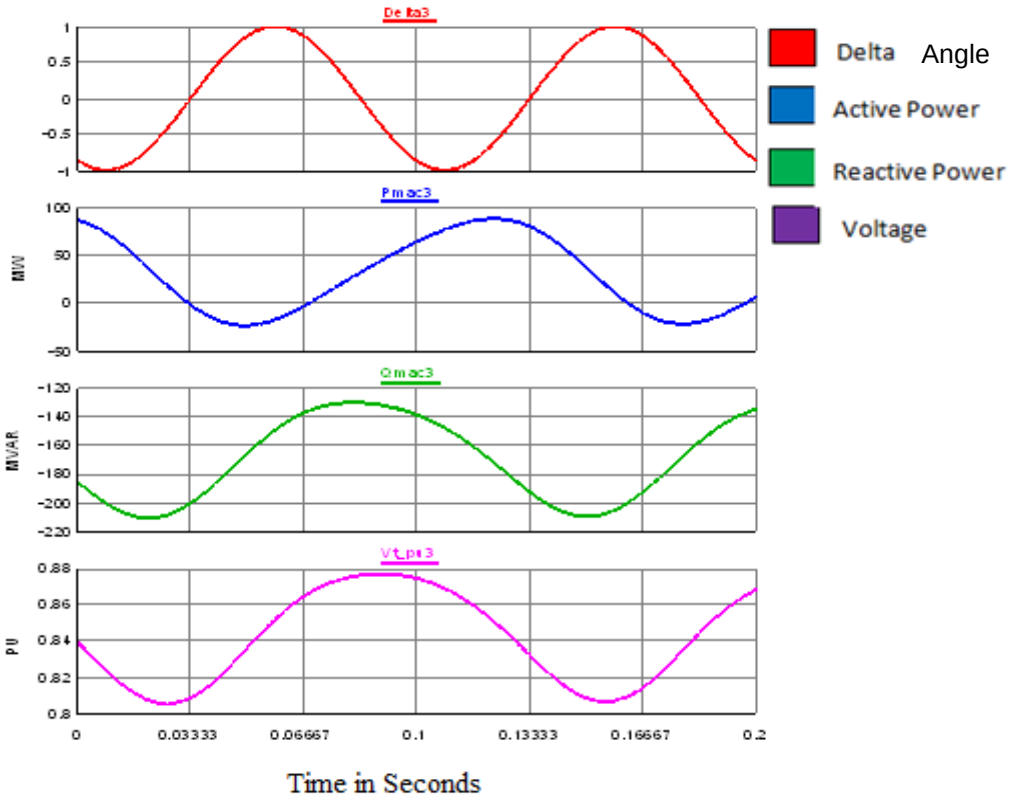

Figure 7. 13: **Dynamic behaviour of the equivalent generator after the aggregation of the generators 2 and 3**

Dynamic transient behaviour curves of the equivalent generator seemed to be good due to the fact that they are very close to the calculation results in the Appendix E.2. Chapter 6, section 6.2.1, presented the Equations (6.1 -6.9) utilized to compute all the equivalent values for the equivalent generator, those values are used to model the equivalent generator. Also section 6.2.2 and 6.3.4 in Chapter 6 described the formation of the equivalent bus.

Two fault locations as shown in Figure (7.9) are used to assess the reduced network obtained. Figure (7.14) depicts the dynamic results of the generator 5 of the study area in the reduced model.

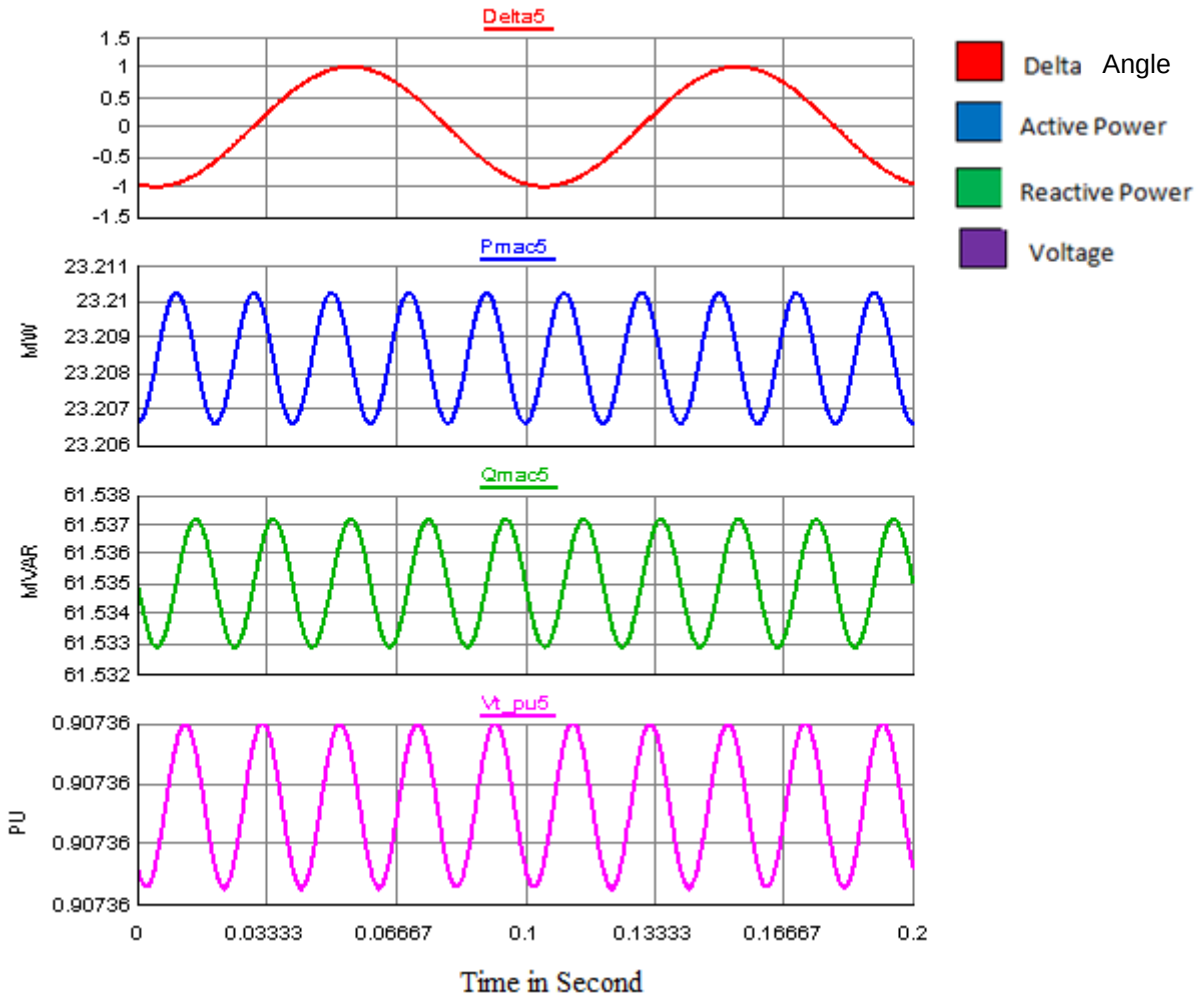

Figure 7. 14: Dynamic results of the generator 5 for the first fault location in the full network

7.3.3 Simulation results of the synchronous generator 5 behaviour for the reduced network

Figure (7.15) and (7.16) show the dynamic behaviour of the generator 5 after being subjected to the first and the second faults in the reduced model respectfully.

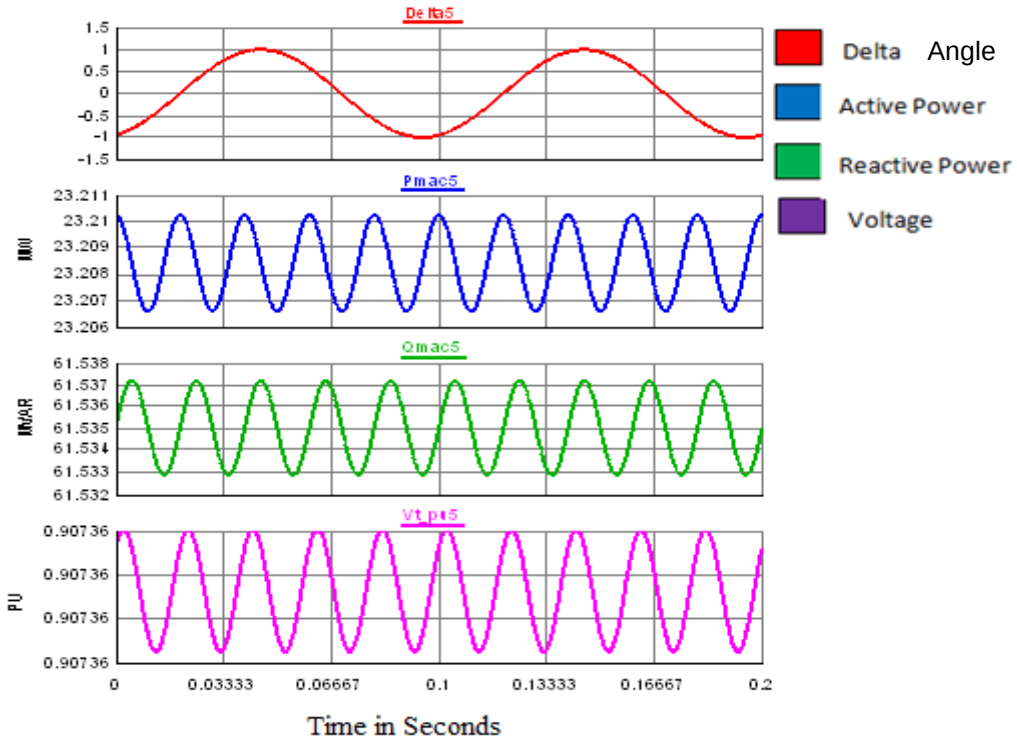

Figure 7. 15: Dynamic behaviour of the generator 5 in the reduced network for the first fault location

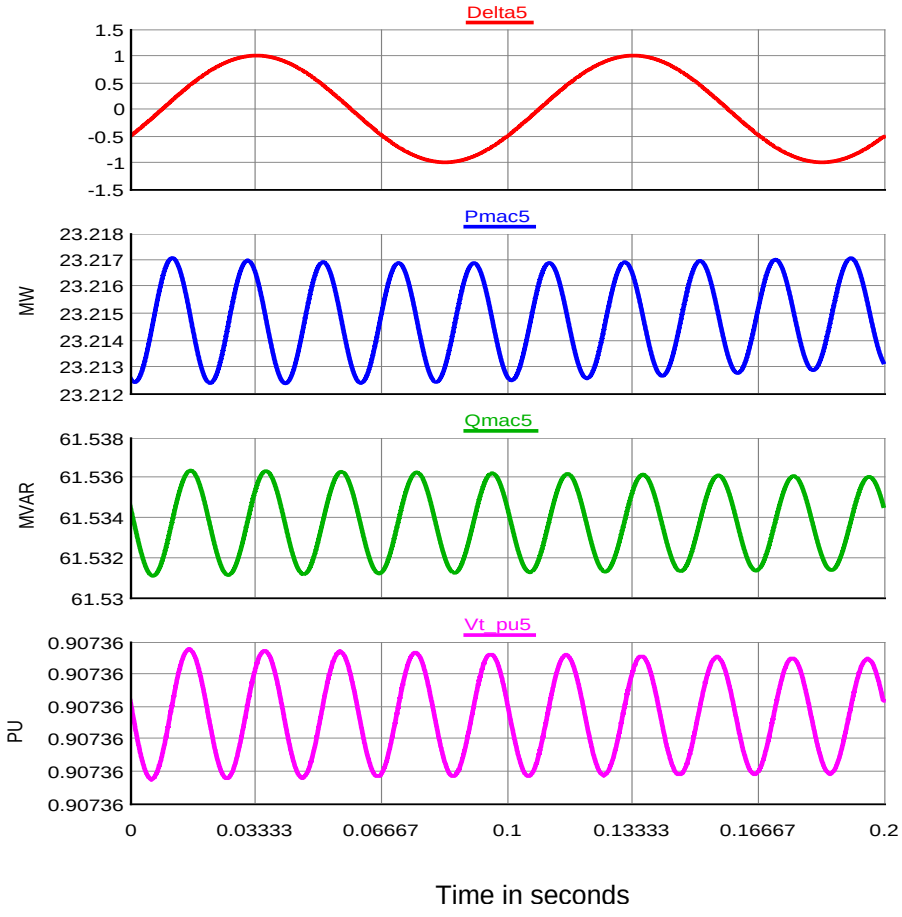

Figure 7. 16: Dynamic behaviour of the generator 5 in the reduced model for the second fault location

7.4 Comparison and discussion of the results

7.4.1 Comparison of the steady state behaviour values after the end of the dynamic behaviour for the generator 5 in the full and the reduced models

Table 7.3 depicts the steady state results values after the end of the dynamic behaviour of the generator 5 in the full and reduced models. Figure (7.17) presents the dynamic results of the generator 5 in both the full and the reduced models.

Table 7. 3: RSCAD steady state results for the generator 5 as a response to the first fault

x	Full model	Reduced model	$e_x\%$
V [PU]	0.90736	0.90738	-0.0022
δ [PU]	1	1	0
P [PU]	23.2105	23.210	0.00215
Q [PU]	61.5372	61.537	0.000325

7.4.2 Comparison of the dynamic behaviour of the full and the reduced model in RSCAD

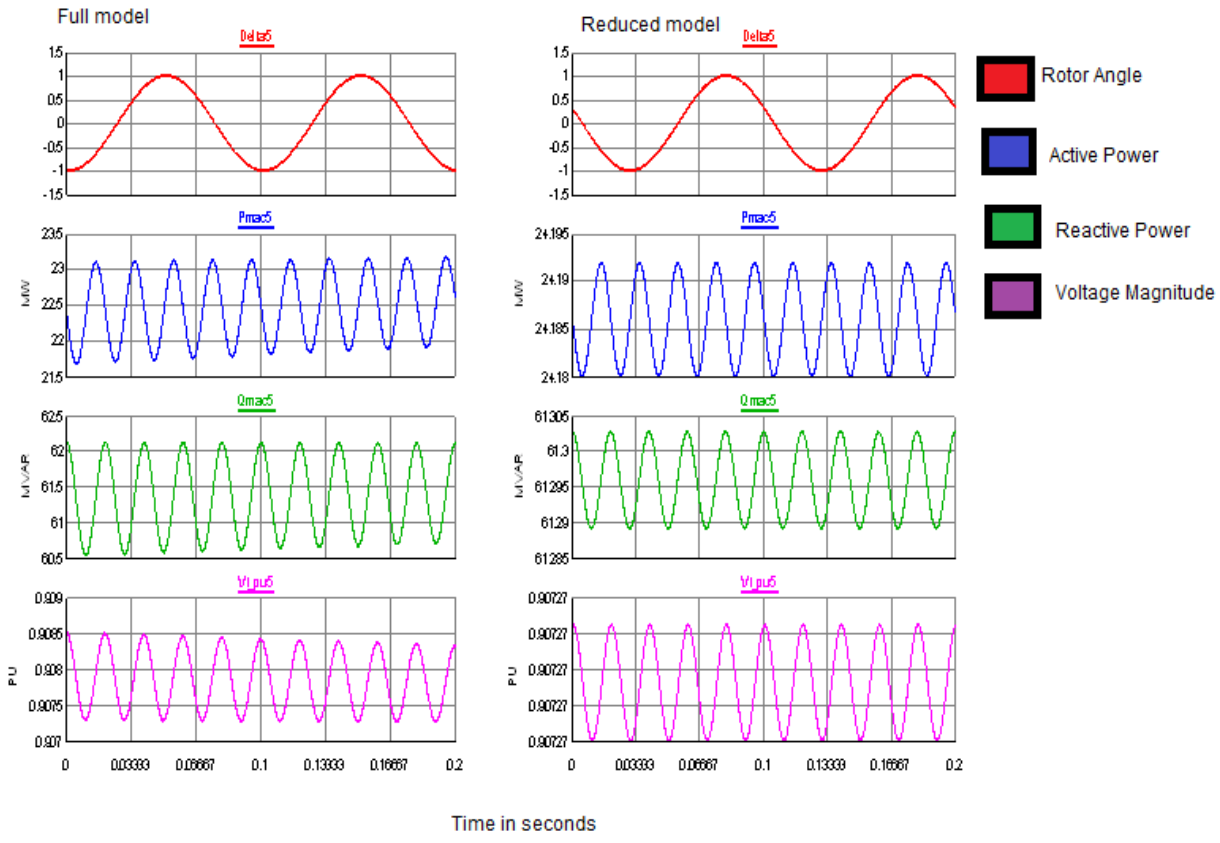

Figure 7. 17: Dynamic behaviour of the generator 5 in the full and the reduced models in RSCAD software environment

7.4.3 Comparison of the steady state behaviour values after the end of the dynamic behaviour of the generator 5 in the full and reduced models for the simulations done in DigSILENT and RSCAD

Table 7.4 shows the comparison of the steady state values of the generator 5 in the full and reduced model for both RSCAD and DigSILENT software environment.

Table 7. 4: Comparison of the steady state values after the end of the dynamic behaviour of the generator 5 using RSCAD and DigSILENT

	RSCAD			DigSILENT		
x	Full model	Reduced model	$e_x\%$	Full model	Reduced model	$e_x\%$
V [PU]	0.90736	0.90738	0.0022	1.014	1.009	0.493
δ [Deg]	35.06	35.06	0	35.063	34.7499	0.892
P [MW]	23.2105	23.210	0.00215	23.75	23.7499	-0.000042
Q [MVAR]	61.5372	61.537	0.000325	60	60	0

7.5 Results Comparison between the full and the reduced networks in RSCAD

Table 7.5 presents the results for voltage magnitudes of both full and reduced networks and their comparison. Bus 6 of the full network is not comparable to the bus 6 of the reduced model because the bus 6 in the reduced model is an equivalent one after the reduction of some buses.

Table 7. 5: Comparison of the load flow bus voltage magnitudes of the full and the reduced networks using RSCAD software

Full network		Reduced network		e_v [%]
Bus number	Voltage [kV]	Bus number	Voltage [kV]	
1	234.6	1	230.0	-1.961
4	236.8	4	228.3	-3.589
5	236.8	5	229.0	-3.294
6	**245.4**	**6**	**258.9**	**-5.501**
7	240.6	7	230.8	-4.073
8	240.4	8	229.7	-4.451
9	243.5	9	232.7	-4.435

7.5.1 Comparison between the IEEE 14-bus system load flow and the load flows of the reduced models received using DigSILENT and RSCAD software

Equation (4.23) in Chapter 4 is utilized to calculate the percentage error between the full and the reduced models based on calculations and the simulations in DigSILENT and RSCAD software. The results are shown in Table 7.6.

Table 7. 6: Comparison of the error percentage between the IEEE 14-bus full model data and the reduced model load flow simulation using both RSCAD and DigSILENT software based.

Bus Number	IEEE full 14-bus model	Reduced Model based on DigSILENT		Reduced Model based on RSCAD	
		Voltages	Errors e_v [%]	Voltages	Errors e_v [%]
1	234.6kV	239.2 kV	-3.846	230.0 kV	-1.961
4	236.8 kV	241.5 kV	-3.8023	228.3 kV	-3.589
5	236.8 kV	235.8 kV	0.7805	229.0 kV	-3.294
7	240.6 kV	242.9 kV	2.2727	230.8 kV	-4.073
8	240.4 kV	240.12 kV	-3.3525	229.7 kV	-4.451
9	243.5 kV	232.99 kV	-0.691	232.7 kV	-4.435

These results are very close to the IEEE load flow data. The error percentage for RSCAD is between (**-1.961** and **-4.451**), while the one for DigSILENT is between (**0.7805** and **2.2727**). Therefore, DigSILENT has smaller errors than RSCAD and gives better reduced model when considered the static load flow simulations.

7.5.2 Comparison of the generator 5 steady state behaviour simulated in DigSILENT for the full and reduced model after a fault application

Table 7.7 depicts achieved steady state behaviour after the end of the dynamic behaviour of the generator 5 as a result of being subjected to two faults. Percentage error for the first fault is between (**0** and **0.892**), while the one for the second fault is between (**-0.000042** and **0**).

Table 7. 7: Comparison of the steady state behaviour after the end of the transition behaviour of the generator 5 after application of the two faults in DigSILENT environment

	First Fault Location			Second Fault Location		
x	Full model	Reduced model	e_x%	Full model	Reduced model	e_x%
V [PU]	1.014	1.009	0.493	1.014	1.014	0
δ [Deg]	35.06253	34.7499	0.892	35.06254	35.0624	0.0004
P [MW]	23.75	23.7499	0.00042	23.75	23.75001	-0.000042
Q [MVAR]	60	60	0	60	60	0

7.5.3 Comparison of the generator 5 steady state values after the end of the dynamic behaviour in RSCAD for the full and reduced model after a fault application

Table 7.8 shows the results obtained after the application of the two fault locations. Percentage error for the first fault is between (**-1** and **0.00215**), while the one for the second fault location is between (**-0.00431** and **0**).

Table 7. 8: Comparison of steady state after the end of the dynamic behaviour of the generator 5 for the applied two faults in the full and reduced model using

	First Fault Location			Second Fault Location		
x	Full model	Reduced model	$e_x\%$	Full model	Reduced model	$e_x\%$
V [PU]	0.90736	0.90738	-0.0022	0.90736	0.90736	0
δ [PU]	1	1.01	-1	1	1	0
P [MW]	23.2105	23.21	0.00215	23.21	23.211	-0.00431
Q [MVAR]	61.5372	61.537	0.000325	61.535	61.536	-0.00163

7.5.4 Comparison of the computation time for the simulation of the full and the reduced models

Figures 7.18 -7.19 depict the time step information of both the full and reduced models to show that, the reduced models take less time for the computation of the system. Map files for simulation of both the full and the reduced models are given in Appendix G.

```
RISC-based Network Solution for Subsystem #1 uses -->
          RPC-GPC Card #1 Processor A
 Network Solution Statistics for 1A:
   Number of nodes on this processor: 48
   Number of G values passed to this proc: 27
   Number of matrix pointers passed to this proc: 0
   Number of columns dynamically decomposed by this proc: 36
   Number of multiply-subtract operations
     for dynamic decomposition on this proc: 902
   Number of clocks pre-T0:      1610
      ( time = 1.610000e+000  uSec. )
   Number of clocks in main:     14032
        ( decomposition:     7287 )
        ( forward-backward:  5348 )
      ( time = 1.403200e+001  uSec. )
   The fill of the decomposed lower matrix is: 355 of 1176 locations.
  Hidden T2 Transfer List
```

Figure 7. 18: Computational time for simulation of the full IEEE 14-bus system

```
RISC-based Network Solution for Subsystem #1 uses -->
          RPC-GPC Card #1 Processor B
 Network Solution Statistics for 1B:
   Number of nodes on this processor: 33
   Number of G values passed to this proc: 18
   Number of matrix pointers passed to this proc: 0
   Number of columns dynamically decomposed by this proc: 27
   Number of multiply-subtract operations
     for dynamic decomposition on this proc: 667
   Number of clocks pre-T0:      1381
      ( time = 1.381000e+000  uSec. )
   Number of clocks in main:     10040
        ( decomposition:     5429 )
        ( forward-backward:  3615 )
      ( time = 1.004000e+001  uSec. )
   The fill of the decomposed lower matrix is: 239 of 561 locations.
```

Figure 7. 19 : Computational time for simulation of the reduced IEEE 14-bus system

7.6 Discussions

Real time simulation is successfully conducted to verify. The real-time simulator seems to produce much better results than a traditional off-line power system simulation. The results obtained for the reduced system are similar to the ones for the full model with the error percentage between (**-4.451** and **-1.961**) %. Also the steady state results seemed to be very close to the original results. The study area components of the full network and the boundary buses were retained in the reduced system. The discrepancy in the error margins from these two softwares is due to the fact that the networks (both the full and the reduced) were modelled using different technique. This is because the computations of the software differ. In the long run of the dynamic simulation RSCAD turned out to be the best, based on the small error margin obtained, as compared to the DigSILENT software. It is therefore suggested that network reduction should be conducted with real-time environment simulation tools.

7.7 Conclusions

Simulations conducted in this Chapter produced capability of the developed procedures and algorithms to successfully reduce the order of power system models. Also the comparisons of both load flow and transient behaviour curves of the full and the reduced models calculated and simulated in RSCAD show small percentage error. Comparison between the IEEE 14-bus system load flow and the load flow of the reduced models received using DigSILENT and RSCAD software environments are done. All the results have the percentage error which is within the limits of $\pm 5\%$. It can be concluded that the transient behaviour of the generator in the study area of the reduced model is almost the same as the corresponding one in the study area of the full model if the faults located in the same study area.

Chapter 8 concludes the overall work conducted for this research. Recommendations for further research are also presented in Chapter 8.

CHAPTER EIGHT
CONCLUSIONS AND RECOMENDATIONS

Introduction

This chapter sums up the most important results obtained in the framework of this project by presenting broad conclusions and discussions on the key findings, the suggestions for applications of the findings, and the future research work. Further work is recommended as possible extensions of this thesis in the areas to be mentioned. The thesis developed and assessed the reduced power system models in order to meet the conditions of the network reduction agreements between the original and the reduced network models. Study of the network equivalency has been the interesting field in power system planning, design and analysis with the objective to retain the load flow and transition behaviour of the study area and the reduced network to be stable.

Power system model reduction is of paramount importance and furtherance of this process is achieved by the application of model reduction techniques based on Coherency method. Moreover, the thesis has applied the network reduction technique of Coherency by development of procedures for implementation of the steps of this technique. The thesis has also reviewed some reduction techniques and power system stability studies. MATLAB software is applied for calculation purposes such as for the Kron's elimination method which is used on the external area of the network topology. Simulations accomplished in both non real-time and real-time software environments using DigSILENT and RSCAD softwares are performed. Two IEEE test bench power systems are utilized as objects for application of the model order reduction method. They are;

- IEEE 9-Bus system
- IEEE 14-Bus system

Section 8.1 expresses the aims and the objectives of the research. Thesis deliverables such as development of coherency based procedures and algorithms, development of the reduced systems for both IEEE 9 and 14 bus test bench power systems, and the assessment of the reduced models developed for both IEEE networks are presented in section 8.2. In section 8.3, applications of the results and the developed softwares are described. Section 8.4 and 8.5 corroborate future research and publications respectfully.

8.1 Aims and objectives of the thesis

The coherency based model reduction methods are widely used in power system management. Coherency means that, for a given remote disturbance, some groups of generators oscillate together and can be represented by a single aggregated generator with an equivalent behaviour and parameters. The standard power system network model order reduction based on the coherency method can be performed in 5 steps (procedures), as follows:

- Power system is being separated into study and external sub-system. The aim of the model order reduction is to preserve the study area and to reduce the external area.
- Identification of the coherency generators in the external area is done with an assumption that there is an abnormal condition inside the study area (fault).
- Coherent generators are aggregated to form a single equivalent generator.
- Reduction of the power system network topology.
- Build the reduced network and compute its parameters.

This research is aimed to develop a variant of the coherency-based method, in order to develop and assess the reduced-order models of large complex power systems. To simulate the full and reduced models after being subject to two faults in the study area in both RSCAD and DigSILENT software environments and to assess the built reduced order models.

The objectives are as follows:

- To conduct literature review on Reduced-Order Models in Power Systems.
- To overview the existing methods for model order reduction in power systems.
- To develop a variant of the model order reduction method based on coherency of the generators.
- To apply the developed model order reduction method based on Coherency.
- To simulate the full and reduced models using DigSILENT software environment.
- To simulate the full and reduced models using RTDS environment.
- To compare the simulation results for both full and reduced models.

8.2 Thesis deliverables

8.2.1 Review of the model reduction techniques in power systems

Literature review of the various existing techniques for model order reduction was written. Total number of 82 papers is reviewed. Comparison of the existing methods was done on a base of the findings outlined in Table 2.1. The analysis of the findings leaded to conclusion that the techniques based on synchronous generators

coherency is the preferred one as the parameters and the structure of the reduced model preserve the physical parameters and structure of the original system.

8.2.2 Development of a variant of a coherency-based method for model order reduction

The coherency-based methods consist of various procedures used to implement the separate steps of the methods. Usually there is more than one procedure to solve the problem at each step. Type of the procedure applied determines how good the obtained solution will be. The thesis developed procedures for reduction of the admittance matrix and for aggregation of the coherent generators.

8.2.3 Development of a reduced system for the IEEE 9-Bus test bench power system

The reduced system from IEEE 9- bus system is successfully developed. It consists of 6-buses, 4-transmission lines and 2 loads. Generator 2, bus-2 and bus-7 are retained in the reduced model because they are in the study area of the network. The percentage of the retained of the full model is about 66.67%. Both the full and the reduced systems are simulated in DigSILENT and RSCAD software packages. External area is reduced by applying Kron's elimination method, and the MATLAB code is given in Appendix B.3 while the MATLAB code for the load conversion to admittance is also in Appendix B.2. All the simulation results for original as well as the equivalent systems obtained by DigSILENT are given in Appendices B.1 and B. 4.

8.2.4 Assessment of the reduced model for IEEE 9-bus power system

The load flow calculations in both DigSILENT and RSCAD software packages for verification and evaluation of the reduced model are done. The reduction rates for the bus-bars and the power lines are 66.67%.The reduced system is further assessed by comparing the dynamic characteristics of the generators to be retained. In this case, generator-2 has been assessed in both the original and the reduced system load flow and transient simulations. On the basis of the analysis of the results from the comparison it can be proven that the developed reduced model is of a good accuracy enough to represent the full models.

8.2.5 Development of a reduced system for the IEEE 14-Bus test bench power system

The same procedures as in point 8.2.3 are followed. The developed method in Chapter 4 is extended with a procedure for coherent generators aggregation. The

reduced model is developed with the well built equivalent coherent generator for the generator-2 and generator-3. The simulations are performed in the same way as the used one for the IEEE 9-bus system. All the relevant results are presented in Appendix E.

8.2.6 Assessment of the reduced model for the IEEE 14-bus power system

The same scenario applied to assess this system as in IEEE 9-bus system. The study area is composed of generator-5, bus 8, bus 9 and bus 7; therefore they are retained in the reduced model. All the results are given in the Appendix F. The retained percentage rate for bus-bars, transmission lines and generators is 64.286%, 55%, and 20% respectively.Appendix G presents the map files of the full and the reduced models for both IEEE 9-bus and 14-bus buildt in RSCAD software for the completion of this research. On the basis of the analysis of the results from the comparison it can be concluded that the developed procedures and algorithms lead to the construction of simplified reduced order models which can represent the full system without loss of any significant characteristic behaviour.

8.2.7 Developed software

Software developed to implement the project aim and objectives is done in MATLAB, DigSILENT and RSCAD software environments. The developed software implements the algorithms of the procedures selected to solve the problems for the various steps of the method of Coherency and to simulate load flow and transition behaviour of the full and reduced models. The list of the developed software is given in Table 8.1.

8.3 Applications of the results

The coherency based technique has the following advantages:

The coherency method does not require any extraordinary interfacing with the internal system model, since the equivalent is in the type of a model of real physical element as utilized in stability investigations.

Test has been done on large systems of 11,028 bus bars and 2,553 generators by applying coherency method (Price at el., 1998; Yuefeng, 2011). And it has been discovered that the coherency-based methods are cost - efficient and realistically precise.

Moreover, engineers have commonly preferred coherency techniques, since the explanations of the coherency equivalents are in the form of the full physical system elements. For this reason, the practitioners can assess the validity of the equivalent and provide an estimated data, if required, for distantly connected utilities by

sketching on earlier period experience. Application of coherency equivalents does not require amendments to present stability programs. More so, nonlinearity can be established in the equivalent generator model, as a consequence this extends the appropriateness of the coherency equivalents for large disturbances.

Nonetheless the coherency method has the following disadvantages:

The conventional coherency technique is a purely experimental method. A theoretical validation for aggregation based on the proposed descriptions of coherency has not been given (Yuefeng, 2011).

The value of the equivalent developed relay on the disturbance selected to establish coherency, and it is difficult to put down instructions for selecting the most suitable perturbation.

It is therefore fault dependent. In order to trounce this drawback, the weak link (WL) and two time scale methods are engaged for the coherency identification (Yusof et al., 1993; Kokovic, 1980; Chaw, 1982; Yuefeng, 2011; Nath et al., 1985). They are based on the linearised state matrix of the power system and hence are fault independent.

The main ares for application of the thesis results are:

- Prevent practical limitations on the size of the computer memory by using reduced models.
- Minimize the excessive computing time needed by the full power system, especially when performing dynamic simulations as well as stability programs.
- Used in the control design to deal with large disturbances.
- Used in the planning analysing and operation of power system networks
- Network topology determination, reliability analysis, and security assessment.
- In dynamic studies of large electric power systems
- For research purpose
- For education of undergraduate and postgraduate students

Table 8. 1: Developed software

Software Environment	Name of the Program	Function of the Program	Appendix Number
MATLAB	1.Load conversion code	Transformation of Load bus	C 2
	2. Kron's Elimination code	Elimination of buses	C 3
DigSILENT	1.Full IEEE 9-Bus Network	Simulations of Load flow, fault application and Stability Analysis	B
	2. Reduced network IEEE of 9-bus		C 4
	1.Full IEEE 14-Bus Network		E
	2. Reduced network IEEE of 14-bus		F
RSCAD	1.Full IEEE 9-Bus Network	Simulations of Load flow, fault application and Stability Analysis	**G**
	2. Reduced network IEEE of 9-bus		
	1.Full IEEE 14-Bus Network		
	2. Reduced network IEEE of 14-bus		

8.4 Future research

Power system networks require solutions that can make them capable to master the complexity of today's generation, transmission, and distribution systems, to keep them in a suitable balance, manage all interfaces, and make power available wherever and whenever it is needed. More research is needed on the real-time monitoring of the network grids conditions, contingency analysis studies, optimization of the grid operating conditions, and assessment of grid stability. Moreover, this research can be extended with more studies on how to find the right balance among various objectives for very large power system networks, such as

- Simulation fidelity
- Computational speed, and
- Modelling flexibility

Specific limitations must be standardized to be utilized on comparing the accuracy of the developed reduced networks. Also the cost must be included as a factor for a good accuracy rate of the network reduction process.

8.5 Publication(s)

Nteka M, R.Tzoneva and C. Kriger*" Development and Assessment of Reduced Order Power System Model"* submitted to Journal of Electrical Engineering and Technology, (2013).

8.6 Conclusions

This chapter expresses the aim and objectives of the thesis and deals with the thesis deliverables for development of the methods, algorithms, and software programs for reduced order model calculation of the large complex power systems. It describes the feasible means of utilazing the developed methods, algorithms and software programs for off-line and real-time simulations of models. The future research direction and list of publications are also given.

BIBLIOGRAPHY

Abd-Aal, M., Abd-El-Rehim., Helal Ain Shams, I.D., Anwar Hassan Omar, M., (2006) "Multi-Machine power system dynamic equivalents using artificial intelligence (ANN). Proc. International Middle East Power Systems Conference; pp. 197-207.

Abdul M. M.,(2006): Dynamic Reduction of Power Systems Using a Simple Equivalent" , Department of Industrial & Electrical Engineering Technology, South Carolina State University, Orangeburg, SC 29117 USA, pp. 1410-1417.

Abido .M. A., (2009).Power System Stability Enhancement Using facts Controllers", Electric Engineering Department, King Fahd University of Petroleum & Minerals, Dhahran 31261, Saudi Arabia or The Arabian Journal for Science and Engineering, Vol. 34, No. 1B, pp.153-172.

Agrawal R, Thukaram D, (2011): Identification of Coherent Synchronous Generators in a Multi- Machine Power System Using Supportm Vector Clustering: IEEE Transaction, pp. 1-6.

Ahmed-Zaid, S., and Awed-Badeeb, O. (1991). On coherency-based dynamic equivalents for large-scale power systems. Presented at the1991 IEEE Dual-Use Technology Conference, IT Utica/Rome, Utica, New York, 20–23 May.

Akoi. M., 1968: Control of large-scale dynamic systems by aggregation: IEEE Transactions on automatic control, vol. AC-13, no.3, pp. 256-253.

Almeida, A.B., Reginatto, R., da Silva R.J.G.C., (2010). A Software Tool for the Determination of Dynamic Equivalents of Power Systems. In IREP Symposium – Bulk Power System Dynamics and Control – VIII (IREP). Rio de Janeiro, Brazil, pp. 1-10.

Alsafih, H. A., and Dunn, R.(2010), Determination of Coherent Clusters in a Multi- Machine Power System Based on Wide-Area Signal Measurements, IEEE, pp.1-8.

Anderson .P.M. and Fouad .A.A., (1994).Power System Control and Stability. IEEE Press,A John Wiley & sons, Inc., Publication.

Annakkage, U. D, Nair N. K. C, Liang Y, Gole A. M, Dinavahi V, Gustavsen B, Noda T, Ghasemi H, Monti A, Matar M, Iravani R, Martinez J. A, (2012): Dynamic System Equivalents: A Survey of Available Techniques: IEEE transactions on power delivery, vol. 27, no. 1, pp.411-419.

Arredondo J.M.R, (1999). Obtaining Dynamic Equivalents through the Minimization of a Line Flows Function, International Journal of Electrical Power and Energy Systems, Vol. 21, No. 5, pp. 365 – 373.

Artenstein, M. and, Giusto, A. (2008). Equivalent model of the Argentinean Electrical power system for stability Analysis of the Uruguayan network. Transmission and Distribution Conference and Exposition, pp.1-5.

Atmaca, E., Serifoglu, N., (1999). A Simple Approach for Identification of Coherent generators in multi-machine Power systems. *International Conference on Electrical and Electronic Engineering*; pp. 258-262.

Avramovic, B., Kokotovic, P. V., R.Winkelman, J., Chow, J. H.,(1980). Area decomposition for electromechanical models of power systems. *Automatica,* vol. 16, no. 6, pp. 637–648.

Badeeb O. M. A, Hazza G.A. W (2004). Application of the slow coherency decomposition method to the Yemeni network, *International Journal of Electrical Engineering Education,* vol.42, no.1 pp. 56-63.

Basu .P, Aishwarya H. (2009). Power system Stability analysis using matlab, from NIT Rourkee, p. 15-16.

Behzad Nouri, Michel S. Nakhla, and Ramachandra Achar, 2013: Efficient Reduced-Order Macromodels of Massively Coupled Interconnect Structures via Clustering: *IEEE Trans. Components, Packaging and Manufacturing Technology,* vol. 3, no. 5, pp. 826-840.

Belhomme. R, Pavella. M, (1991): A composite electromechanical distance approach to transient stability: *IEEE Trans. Power Systems*, vol. 6, no. 2, pp. 622-631.

Bhavikkumar, P. (2011): Transient Stability Analysis of 5-Bus system, National Conference on Recent Trends in Engineering & Technology.

Bose .A. (2003). Power System Stability: New Opportunities for Control. Chapter in Stability and Control of Dynamical Systems and Applications, Derong Liu and Panos J. Antsaklis, editors, Birkhäuser (Boston).

Bruce C. Moore, (1981): Principal Component Analysis in linear systems: Controllability, Observability, and model reduction*: IEEE Trans. On automatic control*, vol.ac-26, no. 1, pp. 17-32.

Brucoli, M. Sbrizzai, R. Torelli, F. Trovato, M. (1983). "Structural Coherency in Interconnected Power Systems", *Large Scale Systems, Theory and Application*, Vol. 5, No. 3, pp. 169 – 178.

Brucoli, M., La Scala, M. Pitrone., N. Trovato, M., (1988). Dynamic Modelling for Retaining Selected Portions of Interconnected Power Networks. *IEE Proceedings on Generation, Transmission and Distribution,* Vol. 135, No. 2, pp. 118 – 123.

Byoung-Kon C., Hsiao-Dong C., Hongbin W., Hua L., David C. Y. 2008: Exciter, Model Reduction and Validation for Large-scale Power System Dynamic Security Assessment, IEEE.

Cai G, Zhang J, Yang D, Chan K.W., Xiao L (2010). The Identification of Coherent Generator Groups via EMD and SSI, *International Conference on Power System Technology*, pp. 1-5.

Cai Y.Q., Wu C.S., (1986). A Novel Algorithm for Aggregating Coherent Generating Units, *IFAC Symposium on Power System and Power Plant Control,* Beijing, China.

Calfe, M. R., Healey, M., (1974). Continued-fraction model-reduction technique for multivariable systems. *Proc.* IEEE; vol. 121, no. 5, pp. 393-395.

Candas, J.E.C. (1996). Optimal reduced order modelling of power systems based on synchronic modal equivalencing. MSC. Dissertation. Dept. Elect. Eng., Massachusetts Institute of Technology

Caprio U.D, (1982). Theoretical and Practical Dynamic Equivalents in Multi-machine Power Systems: Part 1: Construction of Coherency-based Theoretical Equivalent, International Journal of Electrical Power and Energy Systems, Vol. 4, No. 4, pp. 224 – 232.

Caprio U.D., (1981). Conditions for Theoretical Coherency in Multi-machine Power Systems. Automatica, Vol. 17, No. 5, pp. 687 – 701.

Castro R.M.G, Ferreira de Jesus J.M, (1996): A wind park reduced-order model using singular perturbations theory: IEEE Transactions on Energy Conversion, Vol.11, no. 4, and pp.735 741.
Chakrabarti .A. and Halder .S, (2011).Power System Analysis Operation and Control, Third Edition, PHI Learning Private Limted, New Delhi.

Chakrabortty A., (2011). Wide-Area Damping Control of Large Power System Using a Model Reference Approach. *Presented at IEEE Conference on Decision and Control and European Control Conference,* European.

Chakrabortty, A., (2011). Wide-Area Damping Control of Large Power System Using a Model Reference Approach. P*roc. IEEE Conference on Decision and Control and European Control Conference;* pp. 2189-2194.

Chang .B.H, Chooo .J.B and Kwon .S.H, (2000): A Reduced Equivalent Model of Large Power Systems for the Stability Analysis*, Korea Electric Research Institute, Taejon, Korea University, Seoul, 136-701, Korea.*

Chang A, Adibi M.M, (1970): Power System Dynamic Equivalents, *IEEE Transactions on Power Apparatus and Systems,* vol. 89, no. 8, pp. 1737 – 1744.

Chang, B.H. Chooo J.B and Kwon, S.H. (2000). A Reduced Order Equivalent Model of Large Power Systems for the Stability Analysis. *IEEE Korea Electric Research Institute, Taejon, Korea University, Seoul, 136-701, Korea*. Pp.1081-1086.

Chaniotis.D, Pai.M. A, (2005): Model Reduction in Power Systems Using Krylov Subspace Methods: *IEEE transactions on power systems*, vol. 20, no. 2, pp. 888-894.

Chen Y, and Bose A, (1988): Choosing the appropriate boundary for adaptive reduction: IEEE Transactions on Power Systems, vol. 3, no. 2, pp. 747-752.

Chen, S. (2009). Network reduction in power system analyses. Master's Thesis. Department of Electrical Engineering, Centre for Electric Technology (CET) Technical, University of Denmark. Denmark.

Chia-Chi C, Hung-Chi T, Ming-Hong L, (2009). Dynamical Equivalencing of Large-Scale Power Systems Using Second-Order Arnoldi Algorithms: IEEE, pp. 1973-1976.

Chow H. J., Cheung W. Kwok, (1992): A Toolbox for Power System Dynamics and Control Engineering Education and Research: *Transaction on Power Systems*, vol.7, no.4, pp. 1559-1564.

Chow, J.H. Winkelman, J.R. Pai, M.A. Sauer P.W. (1986). Model Reduction and Energy Function Analysis of Power System using Singular Perturbation Techniques, *25th IEEE Conference on Decision and Control*, Athens, Greece, pp. 1206 – 1211.

Chow, J.H. Winkelman, J.R. Pai, M.A. Sauer P.W. (1990). Singular Perturbation Analysis of Large-scale Power Systems, *International Journal of Electrical Power and Energy Systems*, vol. 12, no. 2, pp. 117 – 126.

Chow. J.H, (1982): Time Scale Modelling of Dynamic Networks With Applications to Power Systems, *Lecture Notes in Control and Information Sciences,* Vol. 46, Springer, Berlin, Germany.

Chow. J.H., Cullum. J, Willoughby. R.A and Thomas. J, (1984): A sparsity-Based Technique for Identifying Slow-Coherent Area in Large Power Systems: *IEEE Transactions on Power Apparatus and Systems*, Vol. PAS-103, no. 3, pp. 463-473.

Chow.J. H, Date R. A, Othman.H, Price.W. W, (1990): Slow Coherency Aggregation of Large Power Systems in Eigenanalysis and Frequency Domain Methods for System Dynamic Performance, *IEEE Publications 90TH0292-3-PWR*, pp. 50-60.

Chow.J. H, Galarza.R, Accari.P, Price. W, (1995): Inertial and slow coherency aggregation algorithms for power system dynamic model reduction: *IEEE Trans. Power Syst*., vol. 10, pp. 680–685.

Chow.J. H., (1993): New algorithms for slow coherency aggregation of large power systems, In *Proc. Institute for Mathematics and Its Applications*, pp. 95–115.

Cullum. J., and Willoughby R.A., (1981). Computing eigenvalues of very large symmetric matrices, computational physics, Vol. 44, pp. 329-358.

Date.R.A, Chow.J. H, (1991): Aggregation Properties of Linearized Two-time-scale Power Networks: *IEEE Tmns. Circuits and Systems*, vol. 38, pp. 720-730.

Davodi, Moez, Banejad, Mahdi, Ahmadyfard, Alireza, Buygi, O., Majid, (2008). Coherency Identification Using Hierarchical ClusteringMethod in Power Systems. Faculty of Electrical and Robotics Engineering, Shahrood University of Technology. In Proceedings of the International Conference on Electrical Engineering. Shahrood, Iran.

Da-zhong. F, Chung. T.S, David. A.K, (1994): Fast transient stability estimation using a novel dynamic equivalent reduction: *IEEE Trans. Power Systems*, vol. 9, no. 2, pp. 995-1001.

DeMarco, C. L., Wassner, J. (1995). A generalized eigenvalue perturbation approach to coherency. pp. 611-617.

DeMarco.C.L, Wasser.J, (2005). A Generalized Eigenvalue perturbation Urbation Approach to Coherency. *Proc. IEEE Conference on Control Application*, pp. 605-610.

Djukanovic, M., Sobajic, D.J., Pao Y.H., (1992). “Artificial Neural Network Based Identification of Dynamic Equivalents”, *Electric Power Systems Research*, Vol. 24, No. 1, July, pp. 39 – 48.

Dorsey, J., Schlueter, R.A., (1984). Structural Archetypes for Coherency: A Framework for Comparing Power Systems Equivalents. *Automatica*, Vol. 20, No. 3, pp. 349 – 352.

Dukic, S.D. and Saric, A.T. (2012). Dynamic Model Reduction: An Overview of Available Techniques with Application to Power Systems, *Serbian Journal of Electrical Engineering*, vol. 9, no. 2, pp131-169.

Ebrahimpor, R. Abharian, E. K. Moussavi S.Z., Motie. A. A, (2010). Transient stability assessment of a power system by mixture of expects, *International Journal of Engineering*, vol.4, pp. 643-648.

Eduardo Pires de Souza, J.S. (2008). Identification of Coherent generators considering the electrical proximity for drastic dynamic equivalents. *Electrical Power Systems Research* 78: pp. 1169-1174

Ejigu .A. G, (2009). Implementation of Noord-Holland Grid in RTDS. Faculty of Electrical Engineering, Mathematics and Computer Science, Delft University of Technology.

El-Arini, M.M. and Fathy, (2010). Identification of Coherent generators for large-scale Power Systems using Fuzzy C-Means Clustering Algorithm and Construction of Dynamic Equivalent of Power system. Electrical power and M/C department, Faculty of Engineering, Zagazig

University, pp. 891-896.

El-Arini, M.M. and Fathy, A. (2011) “Identification of Coherent generators for large-scale Power Systems using Fuzzy Algorithm”, *(WSEAS) Transaction on power systems and Control*, Iss 6, vol.6, pp. 229-239.

Erlich, I. Kasztel, Z. and Schegner, P. (2002). Enhanced Model Based Technique for Construction of power systems Dynamic Equivalents. *14th PSCC*, Sevilla: pp.24-28.

Forsyth, P., Kuffel, R., Wierckx, R., Choo, J., Yoon, Y., and Kim, T., (2001). Comparison of Transient Stability Analysis and Large-Scale Real Time Digital Simulation. In *Proceedings of the Power Tech, IEEE Porto*.

Funso K. Ariyo.,(2013):Electrical Network Reduction for Load Flow and Short-Circuit Calculations using PowerFactory Software: Electrical and Electronic Engineering., 3(1): pp.1-7

Gacic.N, Zecevic.A. I. and Siljak.D. D., (1998): Coherency recognition using epsilon decomposition: *IEEE Trans. Power Syst*., vol. 13, pp. 314–319.

Galarza.R.J, Chow.J.H, Price.W.W, Hargrave.A.W, and Hirsch, P.M, (1998): Aggregation of exciter models for constructing power system dynamic equivalent: *IEEE Trans. on Power Systems,* vol. 13, no. 3, pp. 782-788.

Ganapati, P., Sanjay, K.M., and Rasmi R.M. (1996). Adaptive Identification of the Parameters of Nonlinear Systems using Higher Order Statistics. In: *International Conference on Signal Processing Applications and Technology, Boston, MA, USA*, pp. 200 – 204.

Gani, S. and Jayapal, R. (2009). Identification of Coherent generators and Dynamic Equivalent Construction for Multi-Machine Power Sytem. Mathematical and Computational Models Recent trends. Narosa Publishing House. New Delhi India.

Garbow, B.S. et al., (1977): EISPACK Guide Extension - Matrix Eigensystem Routines, *Springer-Verlag, New York.*

Geeves S, (1988): A Modal-coherency Technique for Deriving Dynamic Equivalents: *IEEE Transactions on Power Systems,* Vol. 3, No. 1, pp. 44 – 51.

Germond .A.J., Podmore.R, (1978): Dynamic Aggregation of Generating Unit Models: *IEEE Transactions on Power Apparatus and Systems,* Vol. 97, No. 4, pp. 1060 – 1069.

Ghafouri .A, Gharehpetian .G. B, Milimonfared .J (2012). Fuzzy Coordinated Control of TCSCs to Improve Power System Stability, *International Conference on Renewable Energies and Power Quality*, Santiago de Compostela, spain.

Ghafurian, A. (1979). Modelling Coherent Generators for Multi-Machine Transient Stability Study, Journal of the Franklim Institute Pergarmon Press Ltd, vol.308, no.1, Northorn Ireland, pp. 1-6.

Ghafurian, A., Berg, G.J., Siving, (1982). Coherency-based multi-machine stability study. *Proc. IEEE;* Vol. 129, No. 4, pp. 153-160.

Ghaleh, A.P. Sanaye-Pasand, M. , Saffarian, A, (2011): “Power system stability enhancement using a new combinational load-shedding algorithm, Generation, Transmission & Distribution, IET, Vol.5 , Issue: 5 , pp. 551 - 560.

Gomaringen, (2004).Technical Reference, Dig SILENT Power Factory version 13.1,

Germany.

Gomaringen, (2009). Manual Dig SILENT Power Factory Version 14.0, Dig SILENT GmbH, Germany.

Gomaringen, (2011). Dig SILENT Power Factory User's Manual, tech. rep.

Gugercin S, Antoulas A.C, (2004). A Survey of Model Reduction by Balanced Truncation and Some New Results, *International Journal of Control*, vol. 77, no. 8, pp. 748 – 766.

Hage, J.M., Ayazifar, B., Verghese, G.C., Lesieutre, B.C. (1996). Load bus Partitioning for Synchronic Modal Equivalencing (SME). *28th North American Power Symposium*, pp. 57-61.

Haque, M.H., Rahim, A.H.M.A., (1990).Identification of coherent generators using energy function. In *Proceedings of the IEE*, Vol. 137, Pt. C, No. 4, pp.255-260.

Haque. M. H. and Rahim. A. H. M. A, (1989): Determination of first swing stability limit of multimachine power systems through Taylor series expansion: *IEEE Proceedings - Generation, Transmission and Distribution*, vol. 136, Pt. C, no. 6, pp. 373-379.

Haque.M. H. Rahim.A. H., (1988): An efficient method of identifying coherent generators using Taylor series expansion: *IEEE Trans. Power Syst*., vol. 3, pp. 1112–1118.

Hickin, J. and Sinha, N. K. (1975): Eigenvalue Assignment by Reduced-order models, *Electronics letters 24th*, vol. 11 no. 15, pp.318-319.

Hiyama, T.D.E., (1981).Identification of coherent generators using frequency response. *Proc. IEEE,* Vol. 128, Pt. C, No. 5, pp 262-268.

Hockenberry. J. R, (2000) .Evaluation of Uncertainty in Dynamic, Reduced-Order Model Power System Models, Doctor of Philosophy in Electrical Engineering, Department of Electrical Engineering and Computer Science, Massrchusetts Institute of Technology.

Hsu Y., Wu C., (1991): Experience with dynamic equivalencing of a longitudinal power system, *Electrical Power and Energy systems,* vol.13, no.1, pp. 2-8.

Hussain.M. Y., Rau.V. G., (1993): Coherency identification and construction of dynamic equivalent for large power system, In *Proc. 2nd Int. Conf. Advances Power Syst. Control*, Oper. Manage vol. 2, pp. 887–892.

Ibrahim M.A.H, Mostafa O.M, El-Abiad A.H, (1976): Dynamic Equivalents using Operating Data and Stochastic Modelling: *IEEE Transactions on Power Apparatus and Systems*, Vol. 95, No. 5, pp. 1713 – 1722.

Ishchenko, A. Jokic, Myrzik, J.M.A., and Kling. W.L., (2008). Dynamic Reduction of Distribution Networks with Dispersed Generation," *Technical University Eindhoven*, pp.1-8.

Ishchenko, A., Myrzik, J.M.A., Kling, W.L., (2006). Dynamic Reduction of Distribution Networks with Dispersed Generation. IEEE Power Engineering Society General Meeting; pp. 1-8.

Izugbunam F. I, Okafor E.N.C, Ogbogu S.O.E, (2011). Coherent generator based Transient Stability Analysis of the 16 machines, 330kV Nigeria Power Systems, *Journal of Engineering Trends in Engineering and Applied Sciences*, pp. 456-461.

James D. McCalley, John F. Dorsey, James F. Luini, Mackin R. Peter, Gerardo H. Molina, (1993): Sub transmission reduction for voltage instability analysis: *IEEE Transactions on applied superconductivity*, vol. 3, no.1, pp. 349-356.

Jesko. M. H, (1997) Explorations and Extensions of Synchronic Modal Equivalancing," Master of Science in Electrical Engineering, Department of Electrical Engineering and Computer Science, Massrchusetts Institute of Technology.

Jing, W., Lin, H., (2007). Model Reduction for Classical of Nonlinear Systems. Chinese Control Conference, July 26-31.

Joo S, Liu C, L.E.Jones, Choe J, (2004): Coherency and Aggregation Techniques Incorporating Rotor and Voltage Dynamics: *IEEE Transactions on power systems*, vol. 19, no. 2, pp. 1068-1075.

Joo S.K, Liu C.C, Choe J.W, (2001): Enhancement of Coherency Identification Techniques for Power System Dynamic Equivalents: *IEEE, 0-7803-7173-9/01*, Power Engineering Society Summer Meeting, Dept. Of Electri. Eng., Washington University., Seattle, WA, vol.3, pp. 1811-1816.

Joo.S.K, Liu.C. C., Jones.L. E. and Choe.J. W., (2004): Coherency and aggregation techniques Incorporating rotor and voltage dynamics, vol.19, pp. 1068-1075.

Jung J, Liu C.C, Tanimoto S.L, Vittal V, (2002): Adaptation in load shedding under vulnerable operating conditions: *IEEE Transactions on Power Systems*, pp. 1199-1205.

Kalantar M, Sedighizadeh M (2005). Reduced Order Model for Doubly Output Induction Generator in Wind Park using Integral Manifold Theory, *Iranian Journal of Electrical & Electronic Engineering,* Vol. 1, pp. 41-48.

Kang.Y.I, Zhou.X, Guoen. I. Xie., (1998): Study of Power System Dynamic Equivalents in NETOMAC*, Power Technology*, Vol. 22, No. 5, pp. 21-24.

KaszteZ. L. and Erlich. I., (2001). Consideration of Controllability and Observability of Generators in the Coherency based Dynamic Equivalencing. *IEEE Porto Power Tech Conference 10th -1 3th September, Porto*, Portugal, Vol. 2, 6.

Kayira .S. M., (2009). Power System Dynamic Stability Including Wind Farm Representation, Department of Electronics and Electrical Engineering of the University of Glasgow.

Khan, U.N. and Yan, L. (2008). Power Swing Phenomena and its Detection and Prevention. Phd, Thesis. Faculty of Electrical Engineering. Wroclaw University of Technology. Wroclaw.

Kim.H, Jang.G, Song K, (2004): Dynamic Reduction of the Large-Scale Power Systems Using Relation Factor: *IEEE transactions on power systems*, vol. 19, no. 3, pp. 1696-1699.

Knazkins .V, (2004). Stability of Power Systems with Large Amounts of Distributed Generation. Department of Electrical Engineering, Royal Institute of Technology (KTH), Stockholm, Sweden

Kokotovic, P. V., Allemong, J. J., Winkelman, J. R., Chow, J. H.,(1980). Singular Perturbation and Iterative Separation of Time Scales. *Automatica*, vol. 16, no. 1, pp. 23-33.

Kokotovic, P. V., Avramovic, B., Chow, J. H., Winkelman, J. R., (1982). Coherency based decomposition and aggregation. *Automatica,* vol. 18, no. 1, pp. 47–56.

Kokotovic, P.V. Sauer, P.W, (1989): Intergral Manifold as a tool for reduced-order Modelling of Nonlinear Systems; A Synchronous Machine Case Study: *IEEE Transactions on Circuits and Systems*, Vol. 36, No: 3, pp. 403-410.

Krishnaparandhama T., Elangovan, Kuppurajulu, S. A. (1981): Method for identifying coherent generators, *Electrical Power and Energy systems*, Vol.3, No.2, pp. 85-90.

Kumkratug. P., (2011). Improving Power System Transient Stability with Static Synchronous Series Compensator, 8 (1), pp. 77-81.

Kundur .P. (1994). Power system stability and control. New York McGraw Hill Inc Publication. Kundur.P, Rogers.G.J, Wong.D.Y, Ottevangers.J, Wang L., (1993): Dynamic Reduction, Electric.Power Research Institute, Palo Alto, CA, USA, Technical Report No. 102234, Project 2447-01.

Lawler. J. S., Schlueter. R. A, (1982): Computational algorithms for constructing modal-coherent dynamic equivalents: *IEEE Transactions on Power Apparatus and Systems*, vol. PAS-101, no. 5 pp.1070-1080.

Lawler. J., Schlueter. R.A., Rusche.P, and Hackett.D.L, (1980): Modal-coherent equivalents derived from an RMS coherency measure: *IEEE Transactions on Power Apparatus and Systems,* Vol. 99, No. 4, pp. 1415 – 1425.

Lee B.H., (2009): A Study on Stability Enhancement of Large Scale Systems Using H∞ Control Based on Dynamic Reduction. *IEEE T and D Asia;* pp. 1-4.

Lee. S.T.Y, Schweppe. F.C. (1973): Distance Measures and Coherency Recognition Transient Stability Equivalents: *IEEE Transactions on Power Apparatus and Systems*, Vol. 92, No. 5, pp. 1550 – 1557.

Leffler L.G, Chambliss R.J, Cucchi L A, (1975): Operating reserve and generation risk analysis for the PJM interconnection", *IEEE, transaction Power Apparatus and Systems*, vol. PAS-94, no. 2, pp. 396-407.

Lei X, Povh D, Ruhle O, (2002): Industrial Approaches for Dynamic Equivalents of Large Power Systems: *IEEE Power Engineering Society Winter Meeting*, vol.2, pp. 1036-1042.

Lemon. W.W, Mamundar. K.R.C, and Barcelo W.R, (1989): Transient stability prediction and control in real-time by QUEP: *IEEE Trans. Power Systems*, vol. 4, no. 2, pp. 627-642.

Liang, Y. (2011). An Improved Wide-Band System Equivalent Technique for Real Time Digital Simulators. Doctoral Thesis. Department of Electrical and Computer Engineering, University of Manitoba. Winnipeg, Manitoba.

Lihong, F., (2005): Parameter independent model Order Reduction, Mathematics and Computers in Simulation. 68: pp.221-234.

Lim, W.C. (2003). Dynamic Security Assessment (Generator Aggregation). Degree of Bachelor of Engineering Thesis. School of Information Technology and Electrical Engineering, The University of Queensland, Australia.

Lin, X. (2010). System Equivalent for Real Time Digital Simulator. Doctoral Thesis. Department of Electrical and Computer Engineering, University of Manitoba, Winnipeg. Manitoba.

Liu L, Liu W, Cartes D.A., Chung I. Y, (2007). Slow Coherency and Angle Modulated Particle Swarm Optimization based Islanding of Large power Systems. Advanced Engineering informatics, Neural Network, 2007. (IJCNN) International Joint Conference.

Ma., (2012): Improved Coherency-based Dynamic Equivalents: IEEE Computer Society Conference Publishing Services(CPS).

Ma F, and Vittal V, (2012): A Hybrid Dynamic Equivalent Using ANN-Based Boundary Matching Technique: *IEEE Transactions on Power Systems*, pp.1-9.

Ma F, Vittal V, (2011): Right-sized Power System Dynamic Equivalents for Power System Operation: *IEEE Transactions on Power Systems*, vol. 26, no. 4, pp. 1998 – 2005.

Ma, F., Luo,X., and Vittal, V.(2011), Application of Dynamic Equivalencing in Large-scale Power Systems. IEEE, pp.1-10.

Maas U., Pope S.B., (1992): Simplifying Chemical Kinetics: Intrinsic Low- Dimensional Manifolds in Composition Space. Vol. 88, pp. 239-264.

Machowski J, Bialek J, and Bumby J, (2008). Power System Dynamics: Stability and Control, John Wiley and Sons Publication, Chichester, UK.

Machowski J, Bialek Janusz W and Rlbumby J (1997).Power System Dynamics and Stability. John Wiley & Sons Ltd publishing.

Machowski J, Cichy A, Gubina F, Omahen P, (1988): External Subsystem Equivalent Model for Steady-state and Dynamic Security Assessment*: IEEE Transactions on Power Systems*, vol. 3, no. 4, pp. 1456 – 1463.

Mansour.Y, Vaahedi.E, Chang.A.Y, Coms.B.R, Garrett.B.W, Demaree.K, Athay.T, Cheung K, B.C. (1995): Hydro's On-line Transient Stability Assessment (TSA) Model Development, Analysis, and Post-processing: *IEEE Trans.* vol. PWRS-10, pp. 241-253.

Marinescu B, Mallem B., Rouco L., (2010): Large-Scale Power System Dynamic Equivalents Based on Standard and Border Synchrony: *IEEE transactions on power systems*, vol. 25, no. 4, pp. 1873-1882.

Martins N, Lima L.T.G, Pinto H.J.C.P, (1996): Computing Dominant Poles of Power System Transfer Functions: *IEEE Transactions on Power Systems*, Vol. 11, No. 1, Feb., pp. 162 – 170.

Martins N, Quintao P.E.M, (2003): Computing Dominant Poles of Power System Multivariable Transfer Functions: *IEEE Transactions on Power Systems*, Vol. 18, No. 1, Feb., pp. 152 – 159.

McCalley .J. D, Dorsey .J. F, Luini .J.F, Mackin R. P, Molina .G. H, (1993): Sub transmission reduction for voltage instability analysis: *IEEE Transactions on applied superconductivity*, Vol. 3, No.1, pp.349-356.

McCauley T.M, (1975): Disturbance Dependent Electromechanical Equivalents for Transient Stability Studies, *IEEE Winter Power Meeting*, New York.

McLaren P. G, Kuffel R, Wierckx R, Giesbrecht J, Arendt L, (1992): A Real Time Digital Simulator For Testing Relays: *IEEE Trans on Power Delivery*, vol.7, No.1, pp.207-213.

Miah, A.M., (1998): Simple dynamic equivalent for fast online transient stability assessment: *IEEE Proceedings –Generation, Transmission and Distribution,* vol. 145, no. 1, pp. 49-55.

Milano, F., Srivastava, K., (2009): Dynamic REI equivalents for short circuit and Transient stability analyses. *Electric Power Systems Research*, vol.79, pp. 1-10.

Mitra .P. Venayagamoorthy .G.K., (2010): Wide area control for improving stability of a power system with plug-in electric vehicles, *The Institution of Engineering and Technology*.

Mittlestadt, W.A. (1973). Proposed Algorithms for Approximate Reduced Dynamic Equivalents, Bonneville Power Administration Internal Memorandum.

Mohamed. A Karady .G.G and Yousef .A. M (2005). New Strategy Agents to Improve Power System Transient Stability. *World Academy of Science, Engineering and Technology*.

Moriso .K Wang. L and Kundur .P (2004). Power System Security Assessment*, IEEE power & Energy magazine,* pp.30-39.

Murali .D, and Rajaram .M, (2011). Damping Improvement by Fuzzy Based Power System Stabilizers Applied in Multi-machine Power Systems, *European Journal of Scientific Research*.

Nababhushana.T. N., Veeramanju.K. T., (1998): Coherency identification using growing self organizing feature maps*, Int. Conf. Energy Manage. Power Delivery*, vol. 1, pp. 113–116.

Nahas .E, Ibrahim A., (1983), "Model Reduction Methods Applied to Power Systems" *Open Access Dissertations and Theses Paper 1381.*

Naik, P.K Qureshi, W.A. Nair, N.K-C. (2011). Identification of Coherent Generator Groups in Power System Networks with Wind farms, Department of Electrical and Computer Engineering, University of Auckland WZ, pp. 1-5.

Nath .R, Lamba.S.S, and Prakasa Rao.K.S., (1985): Coherency based system decomposition into study and external areas using weak coupling: *IEEE Trans.,* vol. PAS-104, pp. 1443-1449.

Newell.R.J, Risan.M.D, Allen.L, Rao.K.S, Stuehm D.L, (1985): Utility Experience with Coherency-based Dynamic Equivalents of Very Large Systems*: IEEE Trans*. vol. PAS- 104, pp. 3056-3063.

Nilsson*, O., Rantzer, A., (2009) A novel nonlinear model reduction method applied to automotive controller software. In *Proceeding of the 2009 American Control Conference Hyatt Regency Riverfront,* St. Louis, MO, USA, pp. 4587-4587.

Nishida.S., Takeda.S., (1984): Derivation of equivalents for dynamic security assessment, *Elect. Power Energy Syst*., vol. 6, pp. 15–23.

Oirsouw P.H. van, (1990): A Dynamic Equivalent Using Modal Coherency and Frequency Response: *IEEE Transactions on Power Systems*, Vol. 5, No. 1, pp.289-295.

Olivera.S. D, Massaud.A, (1988): Modal dynamic equivalents for electric power systems. II: Stability simulation tests: IEEE Trans. Power Syst., vol. 3, pp. 1731–1737.

Osorno .B, (2003). Determination of Admittance and Impedance Bus Matrices using Linear Algebra and Matlab in Electric Power Systems .In *Proceedings of the 2003 American Society for Engineering Education Annual Conference & Exposition Copyright 2003*, American.

Ourari, M.L., Dessaint, L.A., Do, V.Q., (2003). Coherency Approach for Dynamic Equivalents of Large Power Systems. *International Conference on Power systems Transients – IPST*, New Orleans, USA.

Pai, M.A., Adgaonkar, R.P, (1984): Electromechanical distance measure for decomposition of power systems. vol.6, no.4, October, pp. 249-254.

Pai, M.A., Adgaonkar, R.P., (1979): Identification of Coherent Generators using Weighted

Eigenvectors, *IEEE Power Engineering Society Winter Meeting*, New York, USA.

Pal .M.K., (1972). Power System Stability: Lecture notes www.scribd.com/doc/92495493, M.K. Pal, "Mathematical Methods in Power System Stability Studies," Ph.D. Thesis, University of Aston in Birmingham.

Panda .S, Patel .R. N (2006). Improving Power System Transient Stability With an off–Centre Location of Shunt Facts Devices, *Journal of Electrical Engineering*, vol. 57, no. 6, pp.365–368

Panda .S. Padhy .N. P. Patel. R. N. (2008) Power-system Stability Improvement by PSO Optimized SSSC-based Damping Controller, *Electric Power Components and Systems*, vol.36 pp.468–490.

Panda.S, Patel .R.N, Padhy .N.P (2006). Power System Stability Improvement by TCSC Controller Employing a Multi-Objective Genetic Algorithm Approach*, International Journal of Electrical and Computer Engineering:* 1-7, pp. 553-560.

Peppas .D, (2008). Development and Analysis of Nordic32 Power System Model in Power Factory, School of Electrical Engineering, *Electric Power Systems, Royal Institute of Technology.*

Perez-Arriaga I. J, Verghese.G. C, Schweppe.F. C, (1982): Selective modal analysis with applications to electric power system. I: Heuristic introduction, *IEEE Trans. Power App. Syst.,* vol. PAS-101, pp. 3117–312.

Peter M. M. B. (1994). Modelling and Identification of flexible wind turbines and factorization Approach to robust control. PhD Thesis. Delft University of technology. Delft.

Podmore .R., Germond.A.,(1977) .Development of Dynamic Equivalents for Transient Stability Studies, *Electric Power Research Institute, Palo Alto*, CA, USA, Technical Report No. EL- 456, Project 763.

Podmore, R., (1979). A Comprehensive Program for Computing Coherency based Dynamic Equivalents. *Power Industry Computer Applications Conference*, pp. 298-306.

Podmore.R, (1977). Development of Dynamic Equivalents for Transient Stability Studies*. EPRI Report EL-456.*

Podmore.R., (1978): Identification of Coherent Generators for Dynamic Equivalents: *IEEE Transactions on Power Apparatus and Systems*, Vol. 97, No. 4, pp. 1344 – 1354.

Price W.W, Ewart D.N, Gulachenski E.M, Silva R.F, (1975): Dynamic Equivalents from On-line Measurements, *IEEE Transactions on Power Apparatus and Systems*, Vol. 94, No. 4, July, pp. 1349 – 1357.

Price W.W, Gulachenski E.M, Kundur P, Lange F.J, Loehr G.C, Roth B.A, Silva R.F, (1978): Testing of the Modal Dynamic Equivalents Technique: *IEEE Transactions on Power Apparatus and Systems,* Vol. 97, No. 4, pp. 1366 – 1372.

Price. W. et al, (1995). Improved Dynamic Equivalencing Software, *GE Power Systems Engineering,* Final Rep, EPRI TR-105 919 Project 2447-02.

Price.W.W, Hargrave.A.W, Hurysz. B.J, Chow.J.H, Hirsch.P.M, (1998): Large-scale System Testing of a Power System Dynamic Equivalencing Program: *IEEE Transactions on Power Systems,* Vol. 13, No. 3, pp. 768 – 774.

Prochaska, M., Oswai., Mathis, B.R. W.,(2005) An approach for reduced order modeling of nonlinear power systems, International Conference on Power Systems Transients IPST'05-098, June 19-17,Montreal, Canada.

Pyo, G.C., Park, J.W., Moon, S.I. (2010): A New Method for Dynamic Reduction of Power System Using PAM Algorithm, School Of Electrical Engineering and Computer Science, Seoul National Univ, Seoul, Korea.

Radhakrishna. C., (2010). Power System Network Reduction Techniques, www.sari-energy.org, Saturday, [19:17hrs, 28th-July-2012].

Ramamoorty M, Balgopal, (1970): Block Diagram Approach to Power System Reliability*: IEEE transactions on Power apparatus and systems*, vol. PAS-89, no. 5/6, pp. 802-811.

Ramaswamy, G. N. (1995). Modal Structures and Model Reduction with Application to Power System Engineering. Doctoral Thesis. Department of Electrical Engineering and Computer Science, Massachusetts Institute of Technology.

Ramaswamy. G.N, Evrard. C, Verghese. G.C, Fillatre, Lesieutre. O. B.B, (1997): Extensions, Simplifications, and Tests of Synchronic Modal Equivalencing (SME), *IEEE Transactions on Power Systems,* Vol. 12, no. 2, pp. 896-905.

Ramaswamy.G. Rouco.N, Fillatre.L.O, Verghese.G.C, Panciatici.P, Lesieutre.B. C, Peltier.D, (1996): Synchronic modal equivalencing (SME) for structure-preserving dynamic equivalents: *IEEE Trans. Power Syst.,* vol. 11, No.1, pp. 19–29.

Ramaswamy.G.N, Verghese.G.C, Rouco.L, Vialas.C, DeMarco.C.L, (1995): Synchrony, Aggregation, and Multi-Area Eigenanalysis, *IEEE PES paper # 95WM192-5-PWRS, PES Winter Power Meeting,* pp. 1986-1993; also, appear, IEEE Trans. on Power Systems.

Ramaswamy.G.N., Verghese.G.C., Rouco.L., Lesieutre.B.C., Fillâtre.O., (1994): Synchronic Modal Equivalencing (SME): A New Framework for Constructing Dynamic Equivalents in Power Systems, North American Power Symposium, Manhattan, KS, USA, 26 – 27 Sept..

Ramaswamy.G.N., Verghese.G.C., Vialas.C., L.DeMarco.C., (1993): Going beyond Coherency: Synchrony as a Basis for Dynamic Equivalencing in power System Models, Proc. North American Power Symposium, , Wash., D.C., pp.579-588.

Ramirez, J.M. and Correa, R.E. (2010). Nutural Strategy for Dynamic equivalencing. IEEE. pp. 1-6.

Rau V. G. and Hussian M. Y. (1998).Coherent Generators. Allied Publishers Limited, New Delhi.

Real-Time Digital Simulator Power System User Manual, (2011).RSCAD Version 2.025.2.

Release Notes for PowerFactory Version 14.1.2, 12.08.2011

Release Notes for PowerFactory Version 14.1.3, 06.12.2011

Rigby .B.S., (2012). Introductory Training Course on Real-Time Simulation Techniques for Hardware-In-Loop Testing of Protective Relay", RTPSS (Real Time Power Systems Studies) Centre.

Rimjhim Agrawal and Thukaram Dhadbanjan, (2013). Zonal Dynamic Equivalents Based on the Concept of Relative Electrical Distance, International Journal of Emerging Electric Power Systems.,pp.1-13

Roosta .A.R., Georges .D. Hadj-Said.N., (2010). Decentralized nonlinear controller design for multi machine power systems via back stepping", Laboratoired 'Automatique de Grenoble *Laboratoired 'Electrotechnique de Grenoble ENSIEG, B.P. 46 - 38402 Saint Martin d'Heres Cedex, France.

Rudnick, H. Patino, R.I. and Brameller A., (1981). Power-system dynamic equivalents: coherency recognition via the rate of change of kinetic energy. Proc. IEE, Vol. 128, Pt. C, No. 6, pp325-333.

Rui, M. G., Castro, J. M. Ferreira de jesus,(1993). A wind park linearised model. Proc.1993 British wind Energy association conf. (BWEA), New York.

Sanaye-Pasand .M, H. Seyedi, H. Lesani and M. R. Dadashzadeh, (2005). Simulation and Analysis of Load Modeling Effects on Power System Transient Stability, Australasian Universities Power Engineering Conference, AUPEC, Hobart, Tasmania, Australia.

Sankaranaraya Nan, Venugopal, V. M, Elango Van, S and Dharma, N. (1983). Coherency Identification and Equivalents for Transient Stability Studies.Electric Power Systems Research. 6, pp-51-60.

Sastry S, Varaiya P, (1981): Coherency for Interconnected power systems", *IEEE Transactions on Automatic Control*, vol.AC-26, no.1, 218-226.

Scherpen J. M. A, Gray W. S, (2000): Minimality and Local State Decomposition of Nonlinear State Space Realization using Energy Functions: *IEEE Trans. Autom. Ctl, AC-45*, 11, pp. 2079-2086.

Schlueter, R.A., and Rusche, P.A., (1987).Dynamic equivalents in rapid analysis of transient stability methods. *Proc. IEEE/PES winter meeting*, New Orleans, USA, pp. 30-36.

Schlueter. R.A., Ahn. U., (1979): Modal analysis equivalents derived based on theorems coherency measure*, IEEE PES Winter Power Meeting*, paper A79061-3.

Schlueter. R.A., Akhtar. H., Modir. H., (1978): An RMS Coherency Measure: A basis for unification of coherency and modal analysis model aggregation techniques, *IEEE PES Summer Power Meeting,* Los Angeles, CA, USA, 16 – 21 July

Schmieg, M.E., Tjong, K.J. and Weber, H.W. (1992). Practical Aspects of the Modal Network Reduction Technique Applied to the Interconnected Power System of Singapore. In *Proceedings of the IFAC Control of Power Plants and Power Systems*, Munich, Germany.

Sedighizadeh M., Rezazadeh A., (2008): A Wind Farm Reduced Order Model Using Integral Manifold Theory, *World Academy of Science, Engineering and Technology* ; 37, pp. 263-267.

Sedighizadeh, M., and, Kalantar, M. (2004). A new Model for double output induction generator with two rotor circuits. In *Proceedings of the International Conference Applied Simulation and Modelling (IASTED),* ASM2004, Rohdes, Greece, June 28-30.

Sedighizadeh, M., Razazadeh, A. (2008). Using Integral Manifolds and Iteration Separation Theory for Decoupling and Reducing Order Model of Double Output Induction Generator, International Journal of Applied Engineering Research.

Senroy N, (2008): Generator Coherency Using the Hilbert-Huang Transforms: *Transaction on IEEE Power systems,* vol.23, no.4, pp. 1701-1708.

Shaker, H. R., Tabatabaeepour, M., Samavat M., Gharaveisi, A. A., (2006). Accuracy and Efficiency Enhancement in Model Order Reduction of Large Circuits. *IEEE*; pp. 266-270.

Shaker, H. R., Tabatabaeepour, M., Samavat, M., Gharaveisi. A. A., (2006). A New Mixed Method for Relative Error Model Order Reduction; pp. 356-360.

Shamash, Y. (1975): Model Reduction using minimal realization algorithms, *Electronics letters 7th* vol. 11, no. 16, and pp.385-387.

Shanshan, L. (2009): Dynamic-Data Driven Real-Time Identification for Electric Power System. Electrical and Computer Engineering.University of Illionois. Urbana, Illionois.

Shivanna. (1986): Stable and Fast algorithm for power system transient stability, IIT, New Delhi.

Shojaei A. A. (2009): Development of generator aggregation technique for power system. Master's Thesis. Faculty of Electrical Engineering, Universiti Teknologi. Malaysia.

Shojaei, A. A., Othman, M.F., Rahmani, R., Frad, M., (2011). Development of generator aggregation technique for power system. *IEEE Student Conference on Research and Development*; pp. 221-224.

Shuqiang.Z, Xianring.C and Yunjiang.P, (1998): A reduced order method for swing mode eigenvalue calculating based on fuzzy coherency recognition, In *Proc. Int. Conf. Power Syst. Technol.,* vol. 2, pp. 1402–1405.

Singh .L.P., (2007). Advance Power system Analysis & Dynamics. p.344, New Age International Pvt Ltd Publishers Amazon

Singh R, Elizondo M, and Lu S. (2011) A Review of Dynamic Generator Reduction Methods for Transient Stability Studies: IEEE, pp. 1-8.

Singhavilai, T., Anaya-Lara, O. Lo K.L. (2009). Identification of the Dynamic Equivalent of a Power System, 44th International Universities Power Engineering Conference (UPEC), Glasgow, UK, pp. 1 – 5.

Smith B.T., et al., (1976): EISPACIK Guide - Matrix Eigensystem Routines, Springer-Verlag, New York.

Stankovic´ M. A, Saric´ T, Miloˇsevic M,(2003): Identification of Nonparametric Dynamic Power System Equivalents With Artificial Neural Networks: *IEEE transactions on power systems*, vol. 18, no. 4, pp. 1478-1486.

Stanton K. Neil, (1969): Reliability Analysis for Power Systems Applications: *IEEE Transactions on Power apparatus and systems,* vol. PAS-88, no. 4, pp. 431-437.

Steindl, A., Troger, H., (2001). Methods for Dimension Reduction and Application in Nonlinear Dynamics, *International Journal of Solids and Structures,* 38, pp. 2131-2147.

Susuki Y. and Mezic I., (2009). Non-linear Koopman modes of Coupled swing Dynamics and Coherency Identification. Department of Mechanical Engineering, University of California, Santa Barbara, US.

Taylor .C. W. and Van Leuven. A. L., (1996): CAPS: Improving Power System Stability Using the Time-Overvoltage Capability of Large Shunt Capacitor Banks: *IEEE Transactions on Power Delivery*, Vol. 11, No. 2, pp.783-792.

Tianqi, L. Jun, W. Xuan, L. Xingyuan, L. (2009). A Fuzzy Clustering Method for Coherent Generator Groups Identification Based on A-K. pp. 1-4.

Troullinos. G. J, Dorsey H. Wong, Myers J, Goodwin. S, (1985): Estimating Order Reduction

for Dynamic Equivalents: *IEEE Transactions on Power Apparatus and Systems,* Vol. 104, No. 12, pp. 3475 – 3481.

Troullinos.G and Dorsey.J. F, (1989): Coherency and model reduction: State space point of view: *IEEE Trans. Power Syst.,* vol. 4, pp. 988–995.

Troullinos.G, Dorsey.J, Wong.H, Myers.J, (1988): Reducing the Order of Very Large Power System Models*: IEEE Trans. vol. PWRS-3*, pp. 127-133.

Trudnowski D.J, (1994): Order Reduction of Large Scale Linear Oscillatory System Models: *IEEE Transactions on Power Systems,* Vol. 9, No. 1, pp. 451 – 458.

Tsai Y, Narasimhamurthi N, Wu F.F, (1982): Structure-preserving Model Reduction with Applications to Power System Dynamic Equivalents: *IEEE Transactions on Circuits and Systems,* Vol. 29, No. 8, pp. 525 – 535.

Tseng, H.C., and Kokotovic, P.V. (1988). Tracking and disturbance rejection in nonlinear systems: the integral manifold approach. In *Proceedings of the 27th IEEE Conference on Decision and Control,* vol.1, pp. 459-463.

Undrill J.M, Casazza J.A, Gulachenski E.M, Kirchmayer L.K, (1971): Electromechanical Equivalents for use in Power System Stability Studies: *IEEE Transactions on Power Apparatus and Systems,* Vol. 90, No. 5, pp. 2060 – 2071.

Undrill J.M, Turner. A.E, (1971): Construction of Power System Electromechanical Equivalents by Modal Analysis: *IEEE Transactions on Power Apparatus and Systems,* vol. 90, no. 5, Sept., pp. 2049 – 2059.

Vasilyev, D., White, J. (2005). A more reliable reduction algorithm for behavioural model extraction. IEEE. Department of Electrical Engineering and Computer Science, Massachusetts Institute of Technology MA 02139. pp. 812-819. 77 Massachusetts Ave., Cambridge.

Verghese, G.C., Péres-Arriaga, J.I., Schweppe, F.C., Tsai, K.W., (1983). Selective Modal Analysis in Power Systems. *Electric Power Research Institute, Palo Alto*, CA, USA, Technical Report No. EL-2830, Project 1764-8.

Verghese.G.C, Perez-Arriaga.I.J., and Schweppe .F.C., (1982): Selective Modal analysis with applications to Electric Power Systems, Part II: The Dynamic Stability Problem: *IEEE Transactions on power apparatus and systems*, vol. PAS-101, no. 5 pp. 3126-3134.

Vittal. V, Kliemann. W, Ni Y, Chapman. D.G, Silk. A.D, Sobajic. D.J, (1998): Determination of generator groupings for an islanding scheme in the Manitoba hydro system using the method of normal forms, *IEEE Transactions on Power Systems 13(4)* pp.1345-1351.

Wang L, Klen.M, Yirga.S, and Kundur.P, (1997): Dynamic Reduction of Large Power Systems for Stability Studies: *IEEE Transactions on Power Systems*, vol. 12, no. 2, pp.889-895.

Wang M.H, Chang H.C, (1994): Novel Clustering Method for Coherency Identification Using an Artificial Neural Network: *IEEE Transaction on Power systems,* vol.9, no.4, pp. 2056-2062.

Wang X., (2005). Slow Coherency grouping based islanding using Minimal Cut-sets and generator coherency index tracing using the Continuation Method. Department of Electrical Engineering, Iowa State University, Ames, Iowa.

Wang, S.C, Huang, P.H, Wu, C.J. and ChuangY.S. (2007) "Direct Coherency Identification of Synchronous Generators on Taiwan Power Systems based on Fizzy C-Means Clustering", IEICE Transaction Fundamentals, vol.E90-A, no.10, pp. 2223-2231.

Wang, X. (2005). Slow Coherency grouping based islanding using Minimal Cut-sets and generator coherency index tracing using the Continuation Method. Department of Electrical Engineering, Iowa State University, Ames, Iowa.

Wang, X., Vttal, V., (2004). System islanding using Minimal Cut-sets with Minimum net Flow. *IEEE PES Power Systems Conference and Exposition*, vol, 1, pp. 379-384.

Wang, X., Yan, Z., Xie, D., (2008). A new kernel-based Clustering algorithm for the multi-machine equivalent of large power systems. *In Proceeding of the International Conference on Electrical Machines and Systems (ICEMS),* pp.3936-3939.

Watson .N. and Arrillaga J., (2003). Power Systems Electromagnetic Transients Simulation," The Institution of Engineering and Technology, London, United Kingdom.

Wehenkel L (1995). A Statistical Approach to the Identification of Electrical Regions in Power Systems. In: *Power Tech, Stockholm*, Sweden, pp. 530 – 535.

Whang. Z.J, Huang, K.W, Chiang, G.M, Lin, S.Y, (1982): A Clustered Dynamical Model for a Class of Linear Autonomous Systems Using Simple Enumerative Sorting: *IEEE Transaction on Circuits and System,* Vol. CAS-29, No. 11, pp. 747-757.

Wilfert, H. H. Voigtlander, K. and Erlich, I. (2001). Dynamic Coherency using self-organising feature maps. *Control Engineering Practice* 9: pp. 769-775.

Winkelman J.R, Chow J.H, Bowler B.C, Avramovic B, Kokotovic P.V, (1981): An analysis of inter-area dynamics of multi-machine systems: *IEEE Transactions on Power Apparatus and Systems,* vol. PAS-100, no. 2, pp. 754-763.

Winkelman.J.R, Chow.J.H, Bowler B.C, Avramovic.B, and Kokotovic.P, (1981): An analysis of interarea dynamics of multi-machine systems: *IEEE Trans.,* vol. PAS-100, pp. 754-763.

Wu, F, Narasimhamurthi N, (1983): Coherency Identification for Power Systems Dynamic Equivalents, *IEEE Transactions on Circuits and Systems*, Vol. 30, No. 3, pp. 140 – 147.

www.archives.ece.iastate.edu [11-07-2013]

www.certs.lbl.gov [11-07-2013]

www.cs.uiuc.edu/class/fa06/cs257/lecture/lecture08.pdf [21-03-2012]

www.eeserver.korea.ac.kr [11-07-2013]

www.egr.msu.edu [10-07-2013]

www.eng.fsu.edu [10-07-2013]

www.ethesis.nitrikl.ac.in [11-07-2013]

www.GE.com [29-03-2011]

www.ijcas.com [11-07-2013]

www.innovexpo.itee.uq.edu.au [11-07-2013]

www.ipst.org [11-07-2013]

www.manchetseruniversitypress.co.uk [11-07-2013]

www.pserc.wisc.edu [11-07-2013]

www.research.att.com [11-07-2013]

www.respository.tudelft.nl [11-07-2013]

www.rtds.com/hardware/hardware.html 12:40PM wednesday [2-03- 2011]

www.waset.org [10-07-2013]

Xu. G., and Vittal. V, (2010): Slow Coherency Based Cutset Determination Algorithm for Large Power Systems: *IEEE transactions on power system*s, vol. 25, no. 2, pp. 877-884.

Yamagishi. Y, Komami. S, (2008): Practical power system Aggregation Considering Dynamic Loads: Engineering Research and Development Centre, Transmission line Team, *IEEJ Transmissions on Power and Energy,* vol.128, pp. 381-387.

Yan W, Lam J, (1999): An Approximate Approach to L_2 Optimal Model Reduction: *IEEE transactions on automatic control,* vol. 44, no. 7, July, pp. 1341-1358.

Yang B., Vittal V., Sen A., and Heydt T. Gerald. (2007). A Novel Slow Coherency Based Graph Theoretic Islanding Strategy. Department of Computer Science & Engineering Arizona State University.

Yang, Z. Yao, D. Buhan, Z. Junfang, L. Kai, W. (2010). Study of Coherency-based Dynamic Equivalent Method for Power System with HVDC. *International Conference on Electrical and Control Engineering,* pp. 2013-2016.

Yang, Z., Kui, W., Buhan, Z., (2011), A Real-time Dynamic Equivalent Solution for Large Interconnected Power Systems, *IEEE,* pp. 871-875.

Yang. B, Vittal, V, Heydt. G. T, (2006): Slow-Coherency-Based Controlled Islanding—A Demonstration of the Approach on the August 14, 2003 Blackout Scenario: *IEEE Transactions on Power Systems,* vol. 21, no. 4, pp. 1840-1847.

Yang. J. P, Cheng. G. H, Xu. Z, (2005): Dynamic Reduction of Large Power System in PSS/E: *IEEE/PES Transmission and Distribution Conference & Exhibition*: Asia and Pacific Dalian, China, pp. 1-4.

You H, Vittal V, Yang Z, (2003): Self-Healing in Power Systems: An Approach Using Islanding and Rate of Frequency Decline-Based Load Shedding: *IEEE transactions on power systems,* vol. 18, no. 1, pp. 174-181.

You. H, Vitta.l V, Wang. X, (2004): Slow Coherency-Based Islanding: *IEEE transactions on power systems,* vol. 19, no. 1, pp. 483-491.

Yu, Y.N, El-Sharkawi M.A, (1981): Estimation of External Dynamic Equivalents of a Thirteen machine System: *IEEE Transactions on Power Apparatus and Systems,* Vol. 100, No. 3, pp. 1324 – 1332.

Yusaf S.B, Rogers G.J, Alden R.T.H, (1993): Slow Coherency based network partitioning including Loads buses: *IEEE Transactions on Power Systems*, vol.8, pp.1375-1382.

Zang, Y. Yu X. and Jia, H. (2005). Theoretical explanation of Hyper- Plane boundary of Dynamic security region. *IEEE*: pp. 1946-1949.

Zhao. Q, Sun. K, Zheng. D, Ma, J, Lu. Q, (2003): A Study of System Splitting Strategies for islanding operation of Power System: a two-phase method based on OBDDs, *IEEE Transactions on Power Systems* 18 (4), pp. 1556-1565.

Zhao, S. (2009): Coherency-based equivalencing Method for Large Wind Farms: *IEEE Power & Energy Society General Meeting,* PES'09, pp. 1-8.

Zhou, H. Q., Song, Z. P., Wang, J. P., Xue, Y. (2011). A Review on Dynamic Equivalent Methods for Large Scale Wind Farms. *IEEE*, pp 1-7.

APPENDICES

APPENDIX A: SIMULATION PROCEDURES IN DIGSILENT SOFTWARE

A.1: Initial Conditions window
A .2: Short circuit calculations window
A.3: Run Simulations window
A.4: Object selection window
A.5: Variable set window
A.6: Steps and flow chart for simulation procedures in RSCAD

Simulation procedures in DigSILENT software

Elements for the single line diagram can be selected from the Drawing Toolbox (Figure A.1) by means of dragging them in the main graphical environment. Every model's data was defined very straightforward by either double-clicking on an object or by accessing the Data Manager through icon in the main toolbar (Chen, 2009; DigSILENT Power Factory, version, 13.1; 2004; DigSILENT Power Factory, Version 14.0, 2009; DigSILENT Power Factory, 2011). The procedures which are used in DigSILENT to build and simulate the full and the reduced models are explained in this Appenix.

Procedure one: Set up the initial conditions

In order for the simulation results to be presented graphically on DigSILENT, there are steps to be followed. These can be explained as follows;
The values of all the variables are calculated based on load flow calculations. Open the calculations of initial conditions window and select the following settings; Figure A.2.

- RMS values (Electromechanical Transients)
- Balanced, Positive Sequence
- Verify Initial Conditions
- Automatic Step size Adaptation.

Procedure two: Perform the simulation after the determination of the initial conditions

After the determination of the initial conditions which is the window shown in Figure A.2, the simulation can be performed and stopped. Three phase short circuit was introduced to the network as shown in the Figures A.3 and A.4.

Procedure three: Creating plots

Several variables are alternating during simulation process, therefore before creating the plots; a selection of the signals essential for the analysis must be performed. This can be achieved by creating result objects for the elements which are essential for the specific studies, such as generators, bus-bars, transmission lines, loads, etc. New result object creation as well as how this is applied to create plots can be better described with an example. The generators are important for the study of network reduction, thus they can be used through a new result object. Firstly select the generator on single line diagram and then right click. Selecting 'Define… → ***variable set (sim)…'***

This will create a new object which is stored in ‘Study Case/All calculations.’ So far the result object does not include any result variables. Result object must be edited by selecting ***‘Data manager*** → ***Study Case*** → ***All calculations’*** and then select ‘edit’ for the element preferred by the user. The following window consists of all the variables contained in generators. Figure A.4 depicts the object selection window utilized. Figure A.5 depicts the variable.

Several variables are available for different types of analysis (Load Flow, RMS-simulation, Harmonic Analysis etc.) For each of the these analyses the variables are grouped in different variable sets such as bus results, Signals, Calculation Parameters, etc. Selecting of a variable is done by double clicking on it’s name which causes the appearance of the variable in the ‘selected variables’ field as shown in Figure A.5. The variables selected in this way are saved in the result object and can be plotted during simulations.

Plots can be inserted via ‘Virtual Instrument Panel’ which is a page where various graphs are stored and displayed. The insertion of a new virtual instrument panel is done and then by selecting virtual instrument panel.

Procedure four: Assign the variables that are of interest into the plots

This is done by double clicking on the variables. A new window will pop up, double click on the ‘element’ will display all the defined results and the user can choose the one that needs to be plotted for the specific study.

The selection of variable is done by double clicking on the ‘variable/ column which will show all the variables contained in this result object. The colour, line style and line width can be adjusted through the other columns More than one variable can be included in the same plot by double clicking on the curve number and by selecting ‘Append Rows’.

A.1: Initial Conditions window

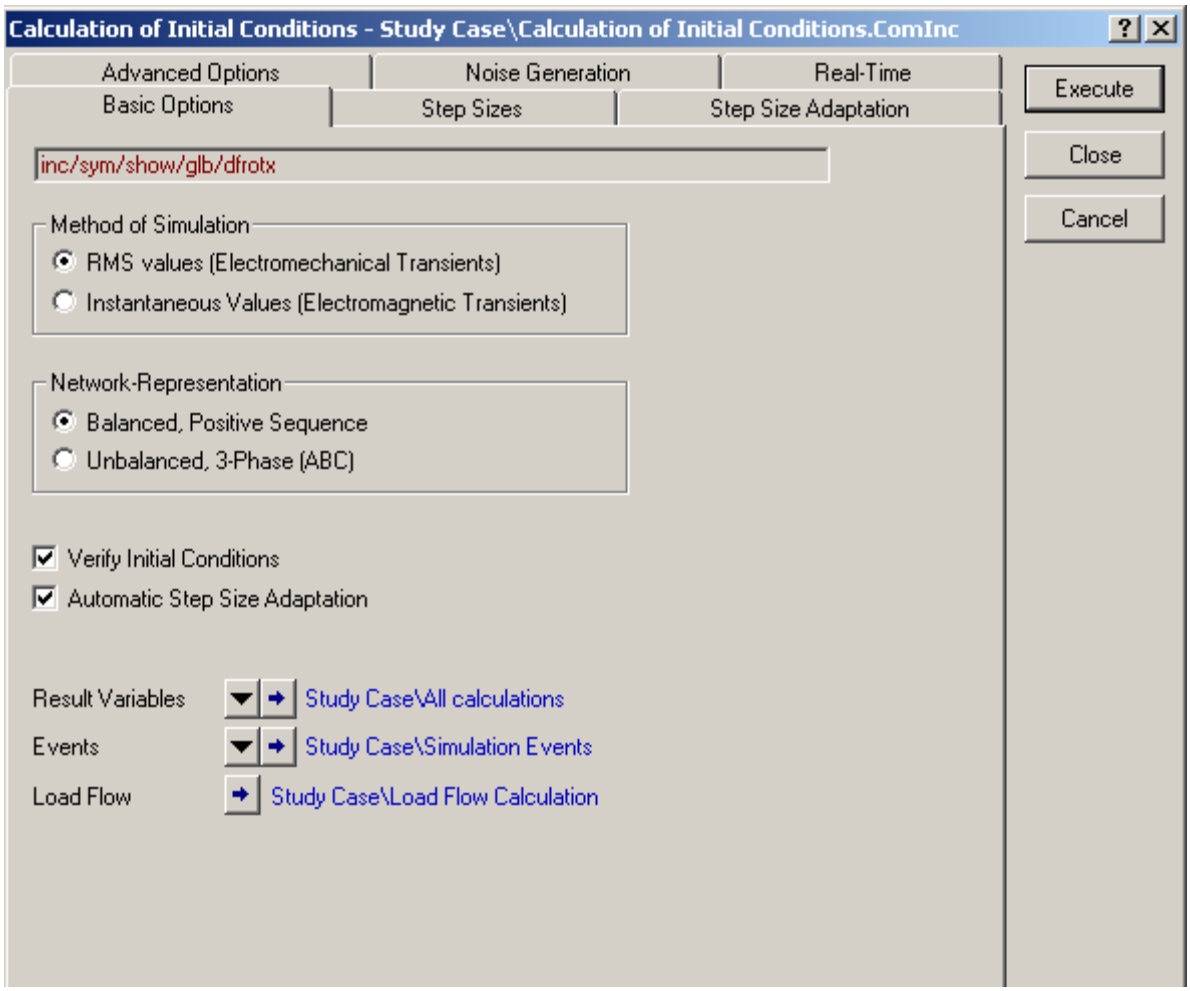

Figure A. 1: Initial Conditions window

A.2: Short circuit calculation window

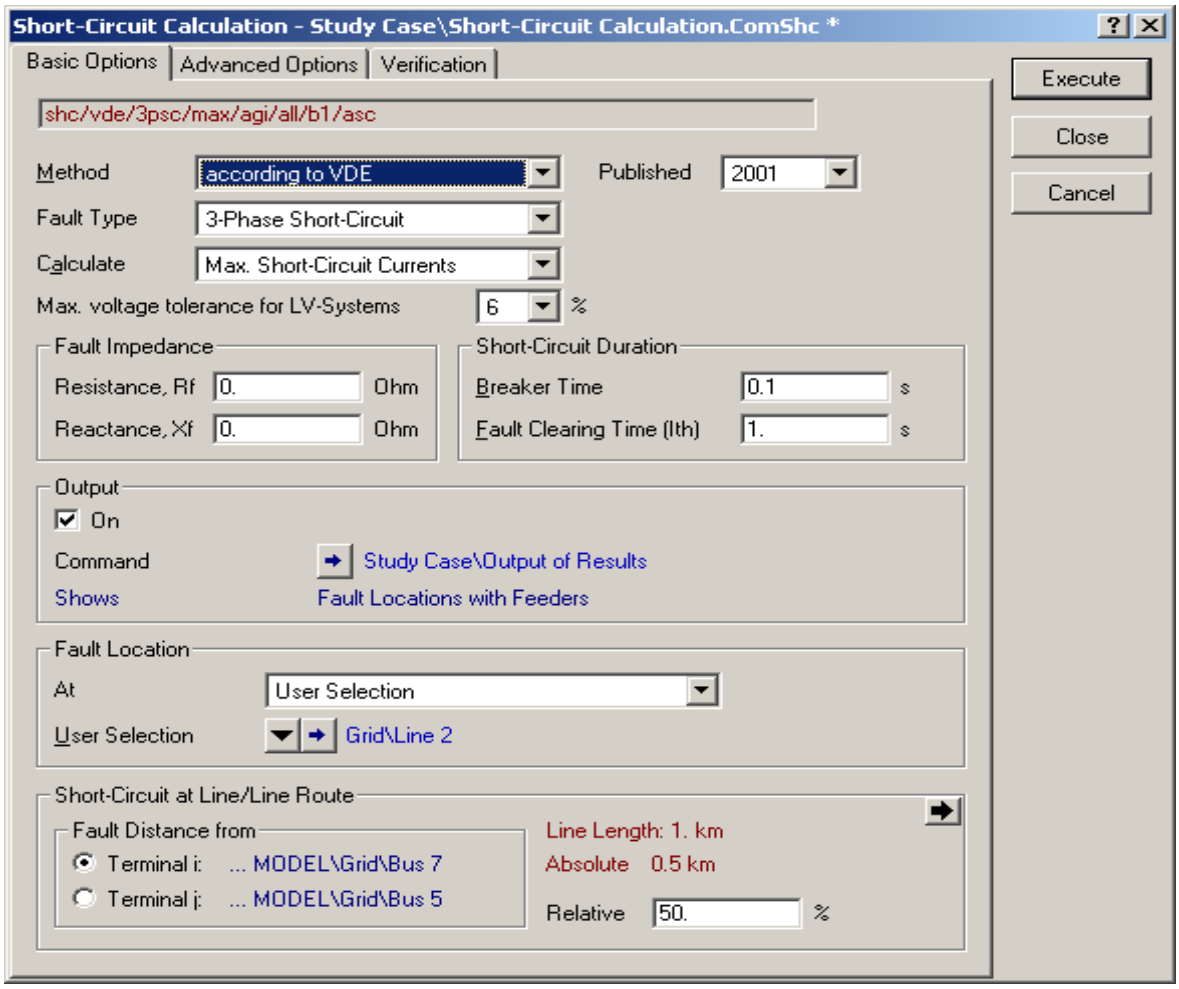

Figure A. 2: Short circuit calculations window

A.3: Run Simulation Window

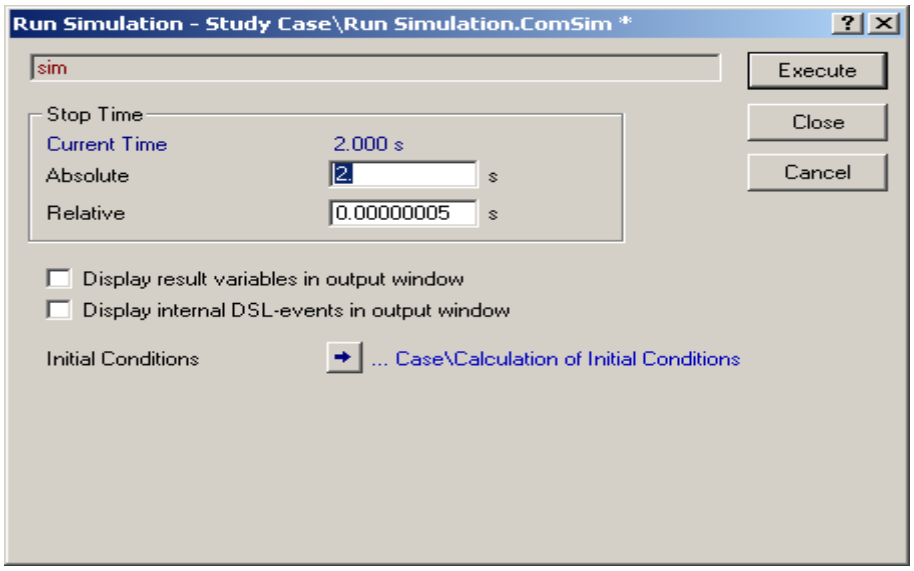

Figure A. 3: Run Simulations window

A.4: Object selection window

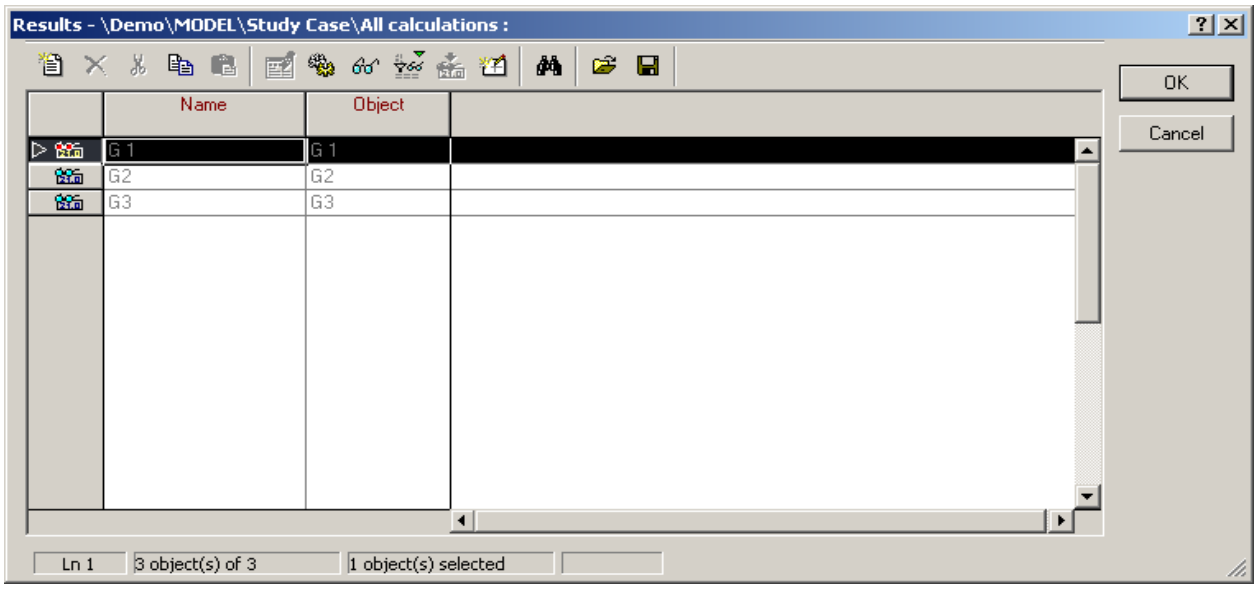

Figure A. 4: Object selection window

A.5: Variable set window

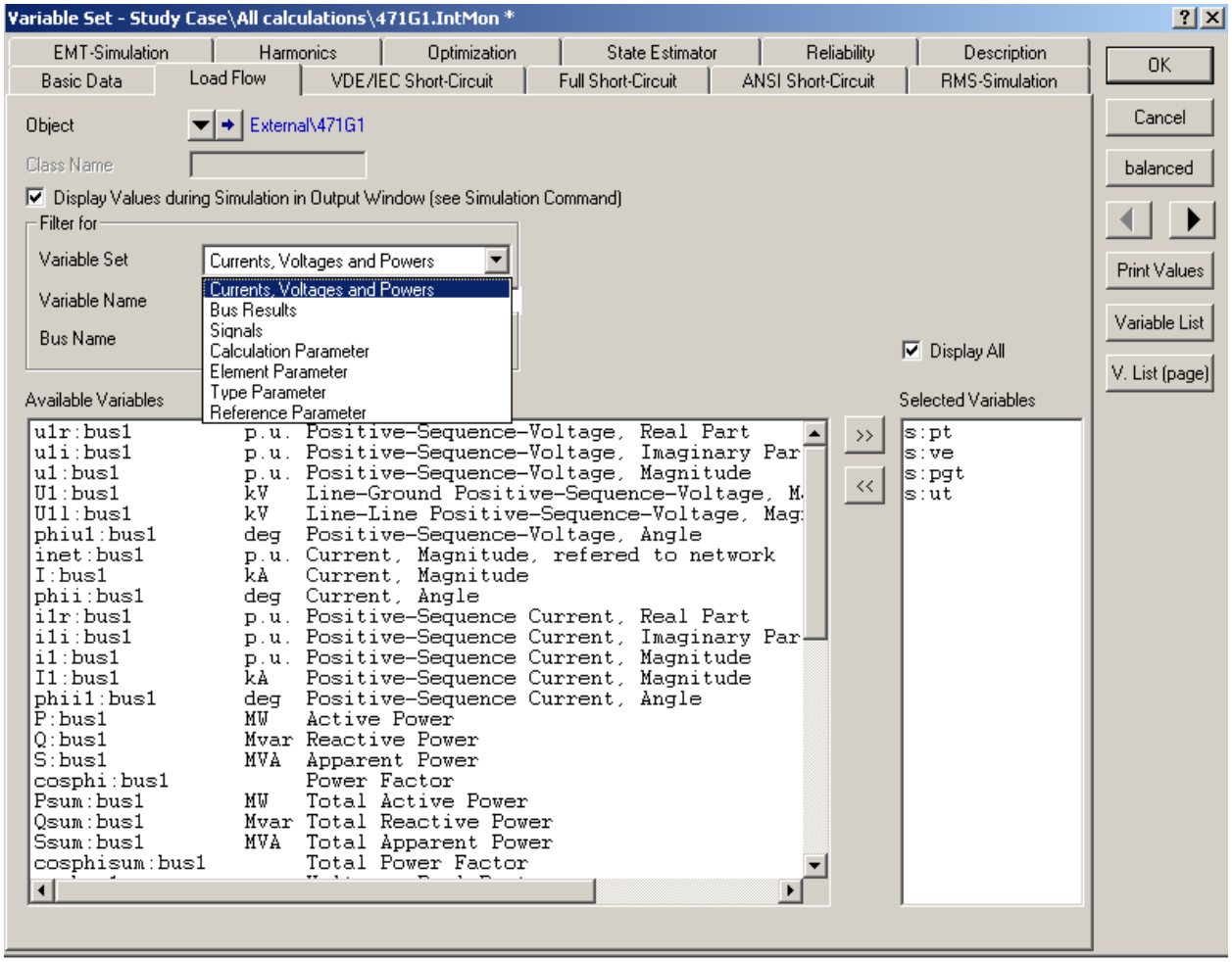

Figure A. 5: Variable set window.

A.6: Steps and flow chart for simulation procedures in RSCAD

Figure A.6 depicts a flow chart of creating and running simulations on RSCAD software. These are the basic procedures followed in order to obtain the load flow results in graphical output. The following steps are considered:

- Open draft window to build one line diagram
- Select the elements from the library to be used.
- Assemble model and save.
- Compile the model.
- Minimize the draft window.
- Open a runtime window.
- Add plots, meters, slider, push buttons, etc and save.
- Start simulation.
- While the simulation is running, refresh plots.
- Update plots and stop the simulations

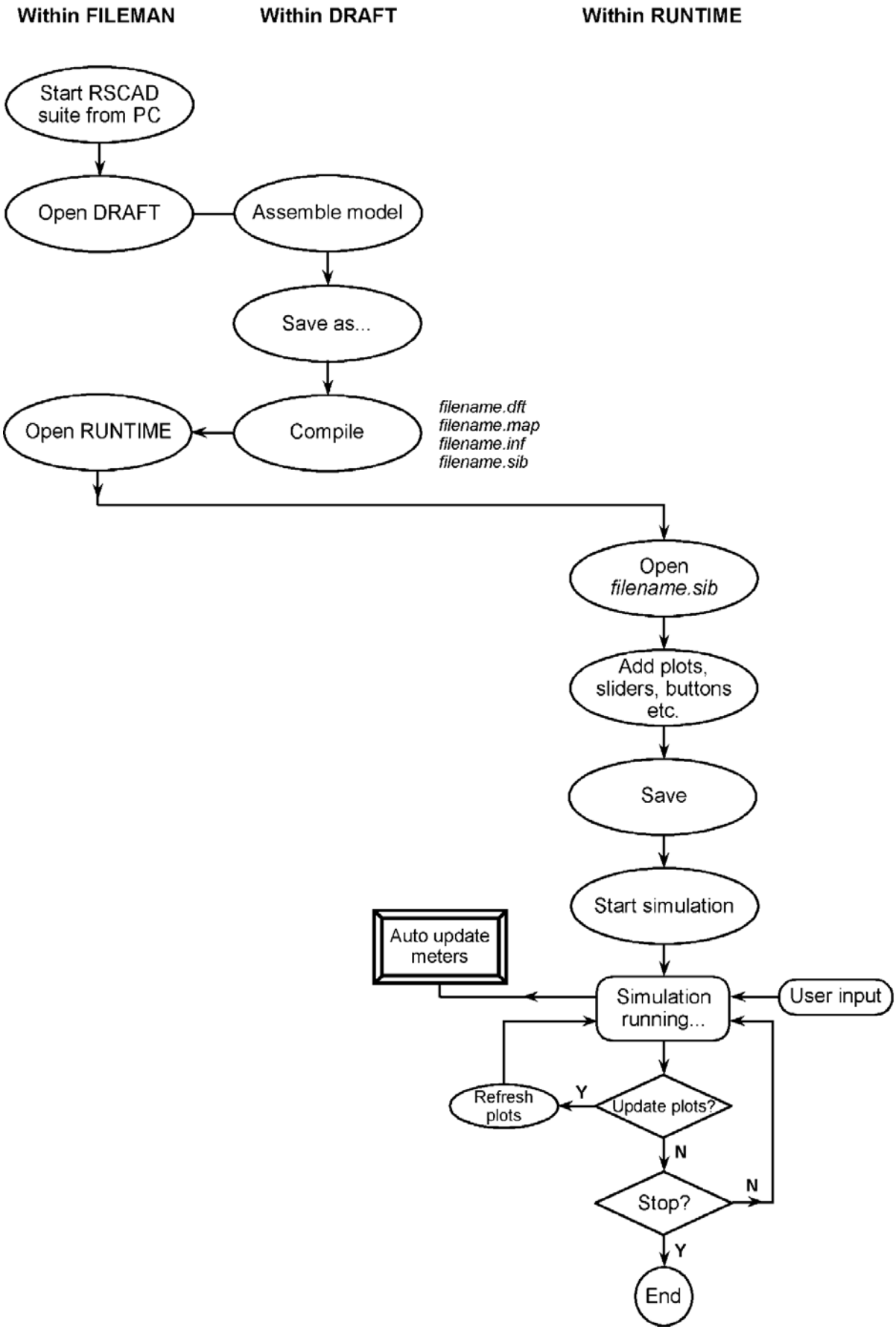

Figure A. 6 : Creating and running a simulation curves in RSCAD (Rigby, 2012)

APPENDIX B: IEEE 9-BUS DATA

B .1: Generator data of 9-bus system
B .2: Preliminary calculations for the 9-bus system
B .3: Additional generator data.

B .1: Generator data of IEEE 9-bus system

Table B.1 ,shows the input data used to model the IEEE 9-busb system. Bas voltage used is 230kV and the MVA base is 100MVA. Therefore, the Z base is obtained as follows;

$V_{base} = 230kV$ and $S_{base} = 100MVA$

$Z_{base} = \frac{V_{base}^2}{S_{base}}$ $Z_{base} = \frac{(230\times10^3)^2}{100\times10^6} = 529\Omega$

Table B. 1: Genarator data of the IEEE 9-bus system (100 MVA bas)

Generator	1	2	3
Rated MVA	247.5	192.0	128.0
kV	16.5	18	13.8
Power Factor	1.0	0.85	0.85
Type	hydro	steam	steam
Speed	180r/min	3600r/min	3600r/min
X_d	0.1460	0.8958	1.3125
$X_{d'}$	0.0608	0.1198	0.1813
X_q	0.0969	0.8645	1.2578
$X_{q'}$	0.0960	0.1969	0.25
Xl	0.0339	0.0521	0.0742
T'_{d0}	8.96	6.00	5.89
T'_{q0}	0	0.535	0.600
Stored energy at rated speed	2346MW.s	640MW.s	301 MW.s

B .2: Preliminary calculations of generators, transmission lines and loads impedances and admittances for the IEEE 9-bus system

Table B.2 depicts the preliminary calculation carried out in order to model the network system. The values are in per unit values.

Table B. 2: Preliminary calculation of the IEEE 9-bus system (100 MVA bas)

	Bus No.	Impedance		Admittance	
		R	X	G	B
Generator					
No.1	1-4	0	0.1184	0	-8.4459
No.2	2-7	0	0.1823	0	-5.4855
No.3	3-9	0	0.2399	0	-4.1684
Transmission lines					
L 1	4-5	0.0100	0.0850	1.3652	-11.6041
L 6	4-6	0.0170	0.0920	1.9422	-10.5107
L 2	5-7	0.0320	0.1610	1.1876	-5.9751
L 5	6-9	0.0390	0.1700	1.2820	-5.5882
L 3	7-8	0.0085	0.0720	1.6171	-13.6980
L 4	8-9	0.0119	0.1008	1.1551	-9.7843
Shunt admittances					
Load A	5-0			1.2610	-0.2643
Load B	6-0			0.8777	-0.0346
Load C	8-0			0.9690	-0.1601
	4-0				0.1670
	7-0				0.2275
	9-0				0.2835

B .3: Additional generator data.

Table B. 3: Additional generator data of the IEEE 9-bus system

QUANTITY	UNIT	GENERATOR 1	GENERATOR 2	GENERATOR 3
H(MW.s/100MVA)	second	23.6400	6.40000	3.0100
$\tau_J = 2h\omega_B$	PU	17824.1400	4825.4863	2269.4865
$x_d - x_d^{'}$	PU	0.0852	0.7760	1.1312
$x_q - x_d^{'}$	PU	0.0361	0.7447	1.0765
$\tau_{q0}^{'}$	second	0	0.5350	0.6000
τ_{q0}	PU	0	210.6900	226.1900
$\tau_{d0}^{'}$	second	8.9600	6.0000	5.8900
τ_{d0}	PU	3377.8404	2261.9467	2220.4777
$E_{q0}^{'}$	PU	-	0.7882	0.7679
$E_{d0}^{'}$	PU	-	-0.6940	-0.6668
I_{q0}	PU	0.6780	0.9320	0.6194
I_{d0}	PU	-0.2872	-1.2902	-0.5615
V_{q0}	PU	1.0392	0.6336	0.6661
V_{d0}	PU	-0.0412	-0.8057	-0.7791
δ_0	Elec deg	2.2717^0	61.0975^0	54.1413^0
$E^{'}$	PU	1.0566	1.0502	1.0170

APPENDIX C: SIMULATION RESULTS FOR THE IEEE 9-BUS NETWORK IN DISILENT

C1: Simulation results for the full model in DigSILENT
C2: Matlab script file – load conversion to addimittance
C3: Matlab script file – Kron's elimination method
C4: Simulation results for the reduced network in DigSILENT

C1: SIMULATION RESULTS FOR FULL NETWORK IN DIGSILENT

Figure C.1: shows the one line diagram in DigSILENT power factory environment.

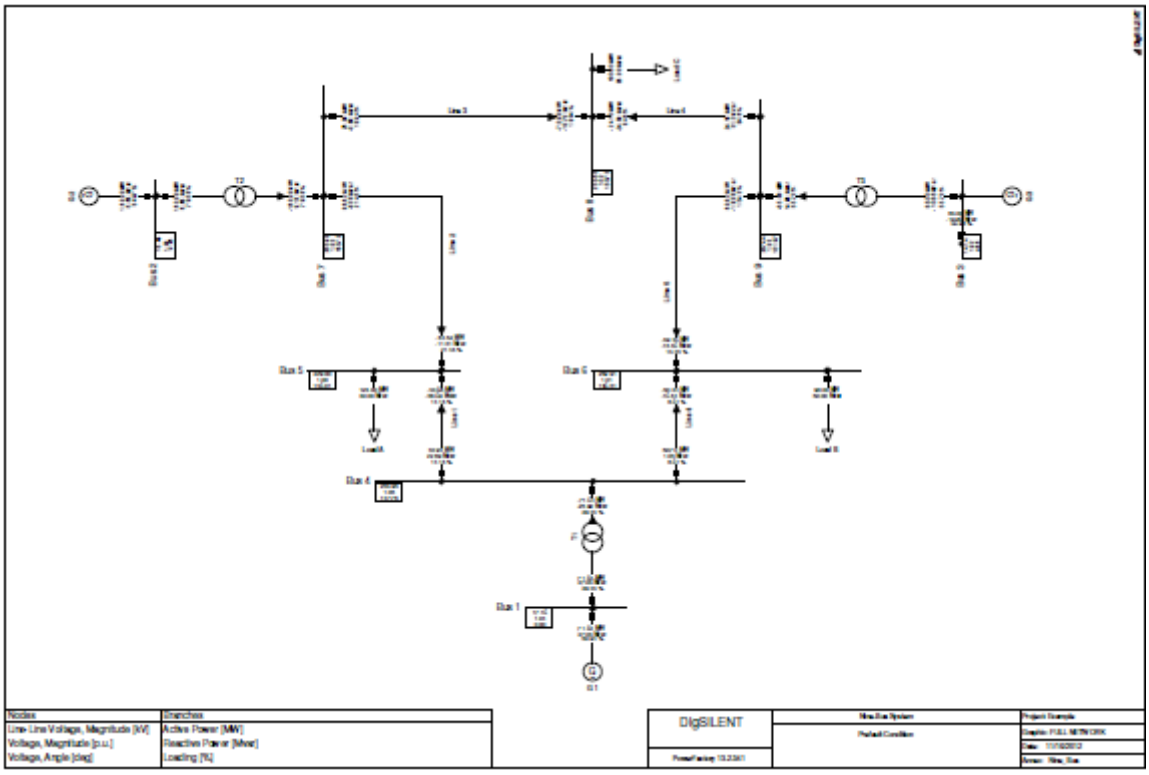

Figure C. 1: Full network of the IEEE 9-bus system

Table C. 1: Load flow results report for the full system

		DIgSILENT PowerFactory 13.2.341	Project:
			Date: 11/16/2012

Load Flow Calculation		Complete System Report: Substations, Voltage Profiles, Area Interchange	
Balanced, positive sequence		Automatic Model Adaptation for Convergency	No
Automatic Tap Adjust of Transformers	No	Max. Acceptable Load Flow Error for	
Consider Reactive Power Limits	No	Nodes	1.00 kVA
		Model Equations	0.10 %

Grid: Nine_Bus	System Stage: System Stage Ma	Study Case: Five-Cycles Fault Mag-A-St	Annex: / 1

	rated Voltage [kV]	Bus-voltage [p.u.]	Bus-voltage [kV]	[deg]	Active Power [MW]	Reactive Power [Mvar]	Power Factor [-]	Current [kA]	Loading [%]	Additional Data
Bus 1	16.50	1.04	17.16	0.00						
Cub_1	/Sym G 1				71.64	27.05	0.94	2.58	30.94	Typ: SL
Cub_2	/Tr2 T1				71.64	27.05	0.94	2.58	29.45	Tap: 0.00 Min: 0 Max: 0
Bus 2	18.00	1.02	18.45	9.28						
Cub_1	/Sym G2				163.00	6.65	1.00	5.10	84.97	Typ: PV
Cub_2	/Tr2 T2				163.00	6.65	1.00	5.10	79.58	Tap: 0.00 Min: 0 Max: 0
Bus 3	13.80	1.02	14.14	4.66						
Cub_1	/Sym G3				85.00	-10.86	0.99	3.50	66.95	Typ: PV
Cub_2	/Tr2 T3				85.00	-10.86	0.99	3.50	55.73	Tap: 0.00 Min: 0 Max: 0
Bus 4	230.00	1.03	235.93	147.78						
Cub_1	/Tr2 T1				-71.64	-23.92	-0.95	0.18	29.45	Tap: 0.00 Min: 0 Max: 0
Cub_2	/Lne Line 1				40.94	22.89	0.87	0.11	14.15	Pv: 257.52 kW cLod: 17.98 Mvar L: 1.00 km
Cub_3	/Lne Line 6				30.70	1.03	1.00	0.08	8.61	Pv: 166.41 kW cLod: 16.41 Mvar L: 1.00 km
Bus 5	230.00	1.00	229.00	146.01						
Cub_2	/Lod Load A				125.00	50.00	0.93	0.34		P10: 125.00 MW Q10: 50.00 Mvar
Cub_1	/Lne Line 1				-40.68	-38.69	-0.72	0.14	14.15	Pv: 257.52 kW cLod: 17.98 Mvar L: 1.00 km
Cub_3	/Lne Line 2				-84.32	-11.31	-0.99	0.21	21.45	Pv: 2299.97 kW cLod: 31.27 Mvar L: 1.00 km
Bus 6	230.00	1.01	232.91	146.31						
Cub_1	/Lod Load B				90.00	30.00	0.95	0.24		P10: 90.00 MW Q10: 30.00 Mvar
Cub_2	/Lne Line 5				-59.46	-13.46	-0.98	0.15	15.43	Pv: 1353.85 kW cLod: 37.43 Mvar L: 1.00 km
Cub_3	/Lne Line 6				-30.54	-16.54	-0.88	0.09	8.61	Pv: 166.41 kW cLod: 16.41 Mvar L: 1.00 km

Grid: Nine_Bus	System Stage: System Stage Ma	Study Case: Five-Cycles Fault Mag-A-St	Annex: / 2

	rated Voltage [kV]	Bus-voltage [p.u.]	Bus-voltage [kV]	[deg]	Active Power [MW]	Reactive Power [Mvar]	Power Factor [-]	Current [kA]	Loading [%]	Additional Data
Bus 7	230.00	1.03	235.93	153.72						
Cub_1	/Lne Line 2				86.62	-8.38	1.00	0.21	21.45	Pv: 2299.97 kW cLod: 31.27 Mvar L: 1.00 km
Cub_2	/Tr2 T2				-163.00	9.18	-1.00	0.40	79.58	Tap: 0.00 Min: 0 Max: 0
Cub_3	/Lne Line 3				76.38	-0.80	1.00	0.19	18.94	Pv: 475.28 kW cLod: 15.53 Mvar L: 1.00 km
Bus 8	230.00	1.02	233.65	150.73						
Cub_2	/Lod Load C				100.00	35.00	0.94	0.26		P10: 100.00 MW Q10: 35.00 Mvar
Cub_1	/Lne Line 3				-75.90	-10.70	-0.99	0.19	18.94	Pv: 475.28 kW cLod: 15.53 Mvar L: 1.00 km
Cub_3	/Lne Line 4				-24.10	-24.30	-0.70	0.08	8.46	Pv: 88.00 kW cLod: 21.92 Mvar L: 1.00 km
Bus 9	230.00	1.03	237.44	151.97						
Cub_1	/Lne Line 4				24.18	3.12	0.99	0.06	8.46	Pv: 88.00 kW cLod: 21.92 Mvar L: 1.00 km
Cub_2	/Tr2 T3				-85.00	14.96	-0.98	0.21	55.73	Tap: 0.00 Min: 0 Max: 0
Cub_3	/Lne Line 5				60.82	-18.08	0.96	0.15	15.43	Pv: 1353.85 kW cLod: 37.43 Mvar L: 1.00 km

Table C.1 continues

		DIgSILENT PowerFactory 13.2.341	Project:
			Date: 11/16/2012

Load Flow Calculation		Complete System Report: Substations, Voltage Profiles, Area Interchange	
Balanced, positive sequence		Automatic Model Adaptation for Convergency	No
Automatic Tap Adjust of Transformers	No	Max. Acceptable Load Flow Error for	
Consider Reactive Power Limits	No	Nodes	1.00 kVA
		Model Equations	0.10 %

Grid: Nine_Bus	System Stage: System Stage Ma	Study Case: Five-Cycles Fault Mag-A-St	Annex: / 3

	rtd.V [kV]	Bus - voltage [p.u.]	[kV]	[deg]	Voltage - Deviation [%] −10 −5 0 +5 +10
Bus 1	16.50	1.040	17.16	0.00	
Bus 2	18.00	1.025	18.45	9.28	
Bus 3	13.80	1.025	14.14	4.66	
Bus 4	230.00	1.026	235.93	147.78	
Bus 5	230.00	0.996	229.00	146.01	
Bus 6	230.00	1.013	232.91	146.31	
Bus 7	230.00	1.026	235.93	153.72	
Bus 8	230.00	1.016	233.65	150.73	
Bus 9	230.00	1.032	237.44	151.97	

		DIgSILENT PowerFactory 13.2.341	Project:
			Date: 11/16/2012

Load Flow Calculation		Complete System Report: Substations, Voltage Profiles, Area Interchange	
Balanced, positive sequence		Automatic Model Adaptation for Convergency	No
Automatic Tap Adjust of Transformers	No	Max. Acceptable Load Flow Error for	
Consider Reactive Power Limits	No	Nodes	1.00 kVA
		Model Equations	0.10 %

Grid: Nine_Bus	System Stage: System Stage Ma	Study Case: Five-Cycles Fault Mag-A-St	Annex: / 4

Volt. Level [kV]	Generation [MW] / [Mvar]	Motor Load [MW] / [Mvar]	Load [MW] / [Mvar]	Compen-sation [MW] / [Mvar]	External Infeed [MW] / [Mvar]	Interchange to	Power Interchange [MW] / [Mvar]	Total Losses [MW] / [Mvar]	Load Losses [MW] / [Mvar]	Noload Losses [MW] / [Mvar]
13.80	85.00	0.00	0.00	0.00	0.00			0.00	0.00	0.00
	-10.86	0.00	0.00	0.00	0.00			0.00	0.00	0.00
						230.00 kV	85.00	-0.00	-0.00	0.00
							-10.86	4.10	4.10	0.00
16.50	71.64	0.00	0.00	0.00	0.00			0.00	0.00	0.00
	27.05	0.00	0.00	0.00	0.00			0.00	0.00	0.00
						230.00 kV	71.64	0.00	0.00	0.00
							27.05	3.12	3.12	0.00
18.00	163.00	0.00	0.00	0.00	0.00			0.00	0.00	0.00
	6.65	0.00	0.00	0.00	0.00			0.00	0.00	0.00
						230.00 kV	163.00	-0.00	-0.00	0.00
							6.65	15.83	15.83	0.00
230.00	0.00	0.00	315.00	0.00	0.00			4.64	4.64	-0.00
	0.00	0.00	115.00	0.00	0.00			-115.21	25.33	-140.54
						13.80 kV	-85.00	-0.00	-0.00	0.00
							14.96	4.10	4.10	0.00
						16.50 kV	-71.64	0.00	0.00	0.00
							-23.92	3.12	3.12	0.00
						18.00 kV	-163.00	-0.00	-0.00	0.00
							9.18	15.83	15.83	0.00
Total:	319.64	0.00	315.00	0.00	0.00		0.00	4.64	4.64	-0.00
	22.84	0.00	115.00	0.00	0.00		0.00	-92.16	48.38	-140.54

Table C.1 continues

		DIgSILENT PowerFactory 13.2.341	Project:
			Date: 11/16/2012

Load Flow Calculation		Complete System Report: Substations, Voltage Profiles, Area Interchange	
Balanced, positive sequence		Automatic Model Adaptation for Convergency	No
Automatic Tap Adjust of Transformers	No	Max. Acceptable Load Flow Error for	
Consider Reactive Power Limits	No	Nodes	1.00 kVA
		Model Equations	0.10 %

Grid: Simulation Output	System Stage: Simulation Outp	Study Case: Five-Cycles Fault Mag-A-St	Annex: / 5

Volt. Level [ ]	Generation [MW]/ [Mvar]	Motor Load [MW]/ [Mvar]	Load [MW]/ [Mvar]	Compen-sation [MW]/ [Mvar]	External Infeed [MW]/ [Mvar]	Interchange to	Power Interchange [MW]/ [Mvar]	Total Losses [MW]/ [Mvar]	Load Losses [MW]/ [Mvar]	Noload Losses [MW]/ [Mvar]
Total:	0.00	0.00	0.00	0.00	0.00		0.00	0.00	0.00	0.00
	0.00	0.00	0.00	0.00	0.00		0.00	0.00	0.00	0.00

		DIgSILENT PowerFactory 13.2.341	Project:
			Date: 11/16/2012

Load Flow Calculation		Complete System Report: Substations, Voltage Profiles, Area Interchange	
Balanced, positive sequence		Automatic Model Adaptation for Convergency	No
Automatic Tap Adjust of Transformers	No	Max. Acceptable Load Flow Error for	
Consider Reactive Power Limits	No	Nodes	1.00 kVA
		Model Equations	0.10 %

Total System Summary	Study Case: Five-Cycles Fault Mag-A-StatAnnex: / 6

	Generation [MW]/ [Mvar]	Motor Load [MW]/ [Mvar]	Load [MW]/ [Mvar]	Compen-sation [MW]/ [Mvar]	External Infeed [MW]/ [Mvar]	Inter Area Flow [MW]/ [Mvar]	Total Losses [MW]/ [Mvar]	Load Losses [MW]/ [Mvar]	Noload Losses [MW]/ [Mvar]
\Demo\Nine Bus System\Nine_Bus									
	319.64	0.00	315.00	0.00	0.00	0.00	4.64	4.64	-0.00
	22.84	0.00	115.00	0.00	0.00	0.00	-92.16	48.38	-140.54
\Demo\Nine Bus System\Simulation Output									
	0.00	0.00	0.00	0.00	0.00	0.00	0.00	0.00	0.00
	0.00	0.00	0.00	0.00	0.00	0.00	0.00	0.00	0.00
Total:									
	319.64	0.00	315.00	0.00	0.00		4.64	4.64	-0.00
	22.84	0.00	115.00	0.00	0.00		-92.16	48.38	-140.54

C2: MATLAB SCRIPT FILE – LOAD CONVERSION TO ADDIMITTANCE

The aim of the code is to convert load buses to admittance values, where the input data are the values of P and Q of the Load. The output is the admittance (y).

```
clear all
clc
P=[ 125 90 100]
Q=i*[50 30 35]
V=[230 230  230]
n=3
```

```
for i=1:n
   y=(P-Q)./abs(V.^2)
end
```

C3: MATLAB SCRIPT FILE – KRON'S ELIMINATION METHOD

This program eliminates the number of buses in the model by using the values of admittance of each bus. The input is the full network admittance matrix dimensions, while the output is the reduced matrix dimensions.

```
% KRON'S ELIMINATION METHOD.
YO = [-8.4459j 0 0 8.4459j 0 0 5.4855j 0
   ;0 -5.4855j 0 0 0 0 5.4855j 0
   ; -2.5475 -2.5475 (-2.5475-4.1684j) -2.5475 -2.5475 -2.5475 -2.5475 -2.5475
   ; 8.4459j 0 0 3.3074-30.3937j -1.3652+11.6041j -1.9422+10.5107j 0 0
   ; 0 0 0 -1.3652+11.6041j 3.8138-17.8426j 0 -1.1876+5.9751j 0
   ; 0 0 0 -1.9422+10.5107j 0 4.1019-16.1335j 0 0 ; 0 5.4855j 0 0 -1.1876+5.9751j 0 2.8047-24.9311j -
1.6171+13.6980j
   ; 0 0 0 0 0 0 -1.6171+3.6980j 3.7412-23.6424j];

Yk3= (4.1019-16.1335j);
for i=1:7
   for j=1:7
YN=YO(i,j)-(YO(i,k)*YO(k,i))/Yk3
   end
end
```

C4: Simulation results for the IEEE 9-bus reduced model in DigSILENT

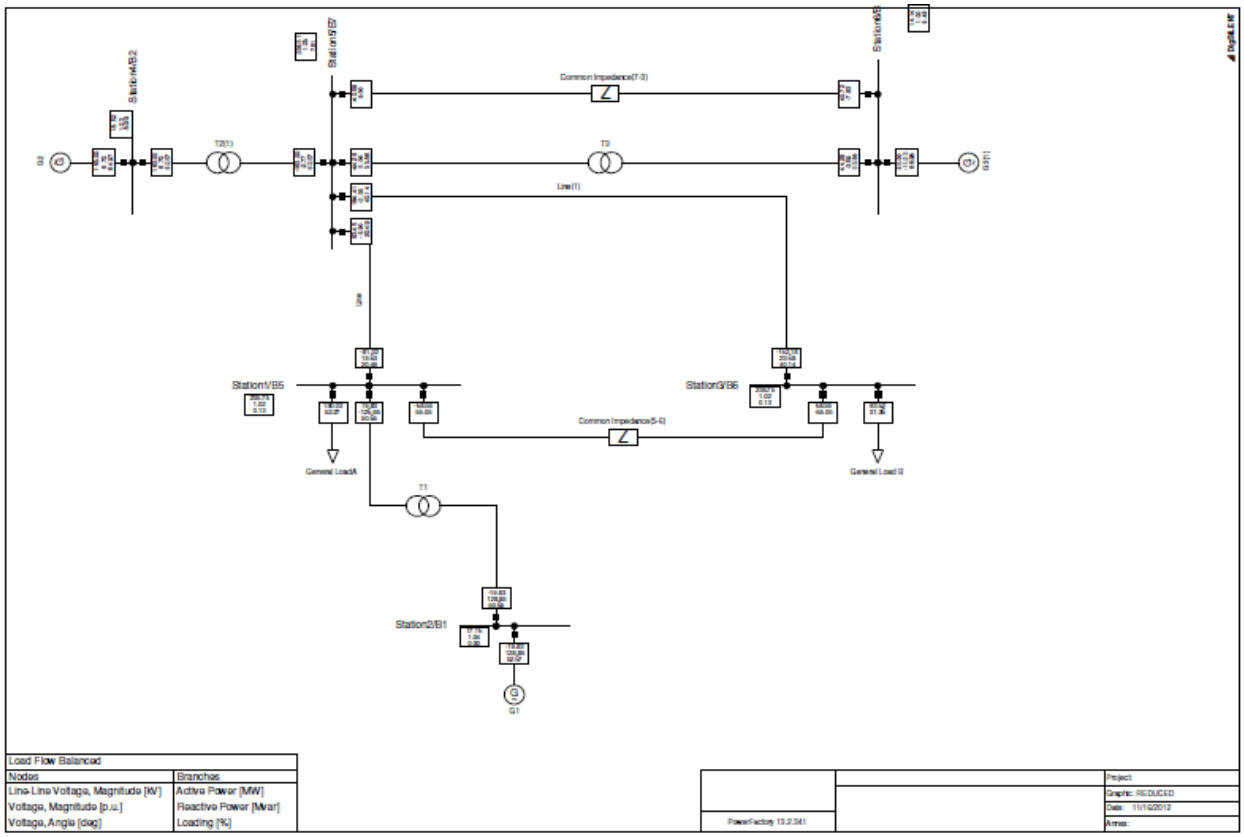

Figure C. 2: Reduced network of the IEEE 9-bus system

Table C.2 presents the report of load flow results of the reduced network under study.

Table C. 2: Load flow results report for the reduced system

Load Flow Calculation			
Balanced, positive sequence			
Automatic Tap Adjust of Transformers	No		
Consider Reactive Power Limits	Yes	Max. Loading of Edge Element	80.00 %
Automatic Model Adaptation for Convergency	No	Lower Limit of Allowed Voltage	0.95 p.u.
		Higher Limit of Allowed Voltage	1.05 p.u.

		DIgSILENT PowerFactory 13.2.341	Project:
			Date: 11/16/2012
Study Case: Study Case			Annex: / 1

Name	Type	Loading [%]	Voltage [p.u.]	Voltage [kV]	Busbar	Apparent Power [MVA]	Current [kA]	Current [p.u.]
T2(1)	Tr2	82.57			Station5/B7	163.02	0.40	0.83
					Station4/B2	163.14	5.09	0.83
G2	Sym	84.97			Station4/B2	163.14	5.09	0.83

		DIgSILENT PowerFactory 13.2.341	Project:
			Date: 11/16/2012

Load Flow Calculation		Complete System Report: Voltage Profiles, Area Interchange	
Balanced, positive sequence		Automatic Model Adaptation for Convergency	No
Automatic Tap Adjust of Transformers	No	Max. Acceptable Load Flow Error for	
Consider Reactive Power Limits	Yes	Nodes	1.00 kVA
		Model Equations	0.10 %

Grid: Grid	System Stage: Grid				Study Case: Study Case	Annex: / 1
	rtd.V [kV]	Bus - voltage [p.u.]	Bus - voltage [kV]	Bus - voltage [deg]	Voltage - Deviation [%] -10 -5 0 +5 +10	
Station1						
B5	230.00	1.025	235.75	0.13		
Station2						
B1	16.50	1.040	17.16	0.00		
Station3						
B6	230.00	1.025	235.75	0.13		
Station4						
B2	18.00	1.029	18.52	8.99		
Station5						
B7	230.00	1.028	236.51	7.61		
Station6						
B3	13.80	1.025	14.14	9.49		

Table C.2 continues

		DIgSILENT PowerFactory 13.2.341	Project:
			Date: 11/16/2012

Load Flow Calculation		Complete System Report: Voltage Profiles, Area Interchange	
Balanced, positive sequence		Automatic Model Adaptation for Convergency	No
Automatic Tap Adjust of Transformers	No	Max. Acceptable Load Flow Error for	
Consider Reactive Power Limits	Yes	Nodes	1.00 kVA
		Model Equations	0.10 %

Grid: Grid	System Stage: Grid	Study Case: Study Case	Annex: / 2

Volt. Level [kV]	Generation [MW] / [Mvar]	Motor Load [MW] / [Mvar]	Load [MW] / [Mvar]	Compensation [MW] / [Mvar]	External Infeed [MW] / [Mvar]	Interchange to	Power Interchange [MW] / [Mvar]	Total Losses [MW] / [Mvar]	Load Losses [MW] / [Mvar]	Noload Losses [MW] / [Mvar]
13.80	85.00	0.00	0.00	0.00	0.00			0.00	0.00	0.00
	-11.23	0.00	0.00	0.00	0.00			0.00	0.00	0.00
						230.00 kV	85.00	0.14	0.14	0.00
							-11.23	2.83	2.83	0.00
16.50	-19.83	0.00	0.00	0.00	0.00			0.00	0.00	0.00
	128.85	0.00	0.00	0.00	0.00			0.00	0.00	0.00
						230.00 kV	-19.83	-0.00	-0.00	0.00
							128.85	1.90	1.90	0.00
18.00	163.00	0.00	0.00	0.00	0.00			0.00	0.00	0.00
	6.70	0.00	0.00	0.00	0.00			0.00	0.00	0.00
						230.00 kV	163.00	-0.00	-0.00	0.00
							6.70	3.93	3.93	0.00
230.00	0.00	0.00	223.66	0.00	0.00			4.36	4.36	0.00
	0.00	0.00	83.63	0.00	0.00			32.03	32.03	0.00
						13.80 kV	-84.86	0.14	0.14	0.00
							14.06	2.83	2.83	0.00
						16.50 kV	19.83	-0.00	-0.00	0.00
							-126.95	1.90	1.90	0.00
						18.00 kV	-163.00	-0.00	-0.00	0.00
							-2.77	3.93	3.93	0.00
Total:	228.17	0.00	223.66	0.00	0.00		0.00	4.51	4.51	0.00
	124.32	0.00	83.63	0.00	0.00		0.00	40.69	40.69	0.00

		DIgSILENT PowerFactory 13.2.341	Project:
			Date: 11/16/2012

Load Flow Calculation		Complete System Report: Voltage Profiles, Area Interchange	
Balanced, positive sequence		Automatic Model Adaptation for Convergency	No
Automatic Tap Adjust of Transformers	No	Max. Acceptable Load Flow Error for	
Consider Reactive Power Limits	Yes	Nodes	1.00 kVA
		Model Equations	0.10 %

Total System Summary	Study Case: Study Case	Annex: / 3

	Generation [MW] / [Mvar]	Motor Load [MW] / [Mvar]	Load [MW] / [Mvar]	Compensation [MW] / [Mvar]	External Infeed [MW] / [Mvar]	Inter Area Flow [MW] / [Mvar]	Total Losses [MW] / [Mvar]	Load Losses [MW] / [Mvar]	Noload Losses [MW] / [Mvar]
\Demo\REDUCED\Grid									
	228.17	0.00	223.66	0.00	0.00	0.00	4.51	4.51	0.00
	124.32	0.00	83.63	0.00	0.00	0.00	40.69	40.69	0.00
Total:									
	228.17	0.00	223.66	0.00	0.00		4.51	4.51	0.00
	124.32	0.00	83.63	0.00	0.00		40.69	40.69	0.00

APPENDIX D: IEEE 14-BUS POWER SYSTEM DATA

D .1: Generator data of the IEEE 14-bus power system

Table D.1 shows the input data for the generator exciter of the 14-bus system.

Table D. 1: Exciter data

Parameters	1	2	3	4	5
K_A	200	20	20	20	20
T_A	0.02	0.02	0.02	0.02	0.02
T_B	0.00	0.00	0.00	0.00	0.00
T_C	0.00	0.00	0.00	0.00	0.00
$V_{R\max}$	7.32	4.38	4.38	6.81	6.81
$V_{R\min}$	0.00	0.00	0.00	1.395	1.395
K_E	1.00	1.00	1.00	1.00	1.00
T_E	0.19	1.98	1.98	0.70	0.70
K_F	0.0012	0.001	0.001	0.001	0.001
T_F	1.0	1.0	1.0	1.0	1.0

Table D.2 shows the input data for the generators of the 14-bus system

Table D. 2: Generator data

Parameter / bus no.	1	2	3	4	5
MVA	615	60	60	25	25
x_l [pu]	0.2396	0.00	0.00	0.134	0.134
x_a [pu]	0.00	0.0031	0.0031	0.0014	0.0014
x_d [pu]	0.8997	1.05	1.05	1.25	1.25
$x_{d'}$ [pu]	0.2995	0.1850	0.1850	0.232	0.232
$x_{d''}$ [pu]	0.23	0.13	0.13	0.12	0.12
T'_{d0}	7.4	6.1	6.1	4.75	4.75
T''_{do}	0.03	0.04	0.04	0.06	0.06
x_g [pu]	0.646	0.98	0.98	1.22	1.22
x'_q [pu]	0.646	0.36	0.36	0.715	0.715
x''_q [pu]	0.4	0.13	0.13	0.12	0.12
T'_{qo}	0.00	0.3	0.3	1.5	1.5
T''_{qo}	0.033	0.099	0.099	0.21	0.21
H	5.148	6.54	6.54	5.06	5.06
D	2	2	2	2	2

Table D.3 shows the input data for the buses of the IEEE 14-bus system and table D.4 shows transmission lines data.

Table D. 3: Bus data

Bus No.	P Generated [pu]	Q Generated [pu]	P Load [pu]	Q Load [pu]	Bus Type*	Q Generated max. [pu]	Q Generated min. [pu]
1	2.32	0.00	0.00	0.00	1	10.0	-10.0
2	0.4	-0.424	0.2170	0.1270	2	0.5	-0.4
3	0.00	0.00	0.9420	0.1900	2	0.4	0.00
4	0.00	0.00	0.4780	0.00	3	0.00	0.00
5	0.00	0.00	0.0760	0.0160	3	0.00	0.00
6	0.00	0.00	0.1120	0.0750	2	0.24	-0.06
7	0.00	0.00	0.00	0.00	3	0.00	0.00
8	0.00	0.00	0.00	0.00	2	0.24	-0.06
9	0.00	0.00	0.2950	0.1660	3	0.00	0.00
10	0.00	0.00	0.0900	0.0580	3	0.00	0.00
11	0.00	0.00	0.0350	0.0180	3	0.00	0.00
12	0.00	0.00	0.0610	0.0160	3	0.00	0.00
13	0.00	0.00	0.1350	0.0580	3	0.00	0.00
14	0.00	0.00	0.1490	0.0500	3	0.00	0.00

*Bus Type: (1) swing bus, (2) generator bus(PV bus), (3) Load bus (PQ bus)

Table D. 4: Line data

From Bus	To Bus	Resistance (p.u)	Reactance (p.u.)	Line charging (p.u.)	Tap ratio
1	2	0.01938	0.05917	0.0528	1
1	5	0.05403	0.22304	0.0492	1
2	3	0.04699	0.19797	0.0438	1
2	4	0.05811	0.17632	0.0374	1
2	5	0.05695	0.17388	0.034	1
3	4	0.06701	0.17103	0.0346	1
4	5	0.01335	0.04211	0.0128	1
4	7	0.00	0.20912	0.00	0.978
4	9	0.00	0.55618	0.00	0.969
5	6	0.00	0.25202	0.00	0.932
6	11	0.09498	0.1989	0.00	1
6	12	0.12291	0.25581	0.00	1
6	13	0.06615	0.13027	0.00	1
7	8	0.00	0.17615	0.00	1
7	9	0.00	0.11001	0.00	1
9	10	0.03181	0.08450	0.00	1
9	14	0.12711	0.27038	0.00	1
10	11	0.08205	0.19207	0.00	1
12	13	0.22092	0.19988	0.00	1
13	14	0.17093	0.34802	0.00	1

APPENDIX E: PRELIMINARY CALCULATIONS FOR THE IEEE 14-BUS SYSTEM

E.1: PRELIMINARY CALCULATIONS FOR THE IEEE 14-BUS SYSTEM

Table E.1 depicts the preliminary calculations done in order to model the IEEE 14-bus network system. The values are in per unit values

Table E. 1 : Preliminary calculations of the IEEE 14-bus system

		Impedance		Admittance	
Generator	Bus No.	R	X	G	B
No.1	1	0	j0.02995	0	-j3.3389
No.2	2	0	j0.1850	0	-j5.4054
No.3	3	0	j0.1850	0	-j5.4054
No.4	6	0	j0.232	0	-j4.3103
No.5	8	0	j0.232	0	-j4.3103
Transmission lines					
L1	(1-2)	1.938	j5.917	0.04999	-j1.526
L2	(1-5)	5.4	j22.304	0.010254	-j0.0424
L3	(2-3)	4.699	j19.797	0.01135	-j0.0478
L4	(2-4)	5.811	j17.632	0.01686	-j0.05116
L5	(2-5)	5.695	j17.388	0.0170	-j0.05194
L6	(4-3)	6.701	j17.103	0.01986	-j0.0507
L7	(4-5)	1.335	j4.211	0.0684	-j0.2158
L8	(4-7)	0	j20.912	0	-j0.0478
L9	(4-9)	0	j55.618	0	-j0.01798
L10	(5-6)	0	j25.202	0	-j0.03968
L11	(6-11)	9.498	j19.89	0.01955	-j0.04094
L12	(6-12)	12.291	j25.581	0.01526	-j0.03176
L13	(6-13)	6.615	j13.027	0.03099	-j0.061
L14	(7-8)	0	j17.615	0	-j0.05677
L15	(7-9)	0	j11.001	0	-j0.0909
L16	(9-10)	3.181	j8.450	0.03902	-j0.10365
L17	(9-14)	12.711	j27.038	0.01424	-j0.03029
L18	(10-11)	8.205	j19.207	0.018809	-j0.04403
L19	(12-13)	22.092	j19.988	0.0133	-j0.02048
L20	(13-14)	17.093	j34.802	0.01137	-j0.02315
Shunt Admittances					
Load 1	2			0.0004	-j0.0004
Load 2	3			0.0018	- j0.0004
Load 3	4				0.0009
Load 4	5				0.0014
Load 5	6			0.0002	- j0.0001
Load 6	9			0.0006	- j0.0003
Load 7	10			0.0002	- j0.0001
Load 8	11				-j0.0001
Load 9	12				-j0.0001
Load 10	13			0.0003	- j0.0001
Load 11	14			0.0003	- j0.0001

E. 2: CALCULATIONS OF THE PARAMETERS OF THE EQUIVALENT GENERATOR TO THE GENERATORS 2 AND 3 PARAMETERS

The parameters of the generators 2 and 3 are given in Table E. 2. The parameters of the equivalent generator are calculated following the Equations (E 1) to (E 13).

Table E. 2 : Parameters of the generators 2 and 3

Parameter	Generator 2	Generator 3
V	238.33kV	232.3 kV
P	40 MW	51 MW
Q	45.41 MVar	15.75 MVar
X_d	0.185Ω	0.185Ω
E	238.361kV	232.43 kV

$$P = VI\cos\theta \tag{E1}$$

$$I_2 = \frac{P}{V_2\cos\theta_2} = \frac{\left(40\times10^6\right)}{\left(\left(238.33\times10^3\right)\times\cos\left(2.78^\circ\right)\right)} = 168.032A \tag{E 2}$$

$$E_2 = V_2 + I_2\times X_{d2} = \left(238.33\times10^3\right) + \left(0.185\times168.032\right) = 238.361kV \tag{E 3}$$

$$I_3 = \frac{P}{V_3\cos\theta_3} = \frac{\left(51\times10^6\right)}{\left(\left(232.30\times10^3\right)\times\cos\left(6.75^\circ\right)\right)} = 221.076A \tag{E 4}$$

$$E_3 = V_3 + I_3\times X_{d3} = \left(232.30\times10^3\right) + \left(0.185\times221.076\right) = 232.34\,kV \tag{E5}$$

$$I_e = \sum_{i=1,2} I_i = \left(221.076 + 168.032\right) = 389.108A \tag{E 6}$$

$$E_e = \sum_{i=1,2}\left(E_i\times I_i\right)/I_e = \frac{\left(238.33\times10^3\times168.038\right) + \left(232.3\times10^3\times221.076\right)}{389.108} = 234.908kV \tag{E7}$$

$$P_e = \sum_{i=1,2} P_i \tag{E8}$$

$$= \left(40\times10^6\right) + \left(51\times10^6\right) = 91\times10^2 = 91MW$$

$$Q_e = \sum_{i=1,2} Q_i \tag{E9}$$

$$= \left(45.41\times10^6\right) + \left(15.75\times10^6\right) = 61.16\times10^2 = 91MVar$$

$$S_T = \sum_{i=1,2} E_i\times I_i \tag{E10}$$

$$= \left[\left(\left(238.33\times10^3\right)\times168.038\right) + \left(\left(232.3\times10^3\right)\times221.076\right)\right]$$

$$= 91.4045\ \ MVA$$

$$X'_{dei} = \left[\frac{\left(E_e - V_i\right)}{E_i - V_i}\right]\times X'_{di} \tag{E11}$$

$$= \left[\frac{\left(234.908\times10^3 - 232.3\times10^3\right)}{\left(238.33\times10^3 - 232.3\times10^3\right)}\right]\times0.185$$

$$= 0.08\Omega$$

$$S_e = E_e\times I_e \tag{E12}$$

$$= \left(234.908\times10^3\right)\times\left(389.108\right) = 91.405\,MVA$$

$$\therefore S_T = S_e \tag{E13}$$

APPENDIX F: SIMULATION RESULTS FOR THE IEEE 14-BUS NETWORK IN DISILENT

Figure F.1 shows the one line diagram of the full network of the IEEE 14-bus system.

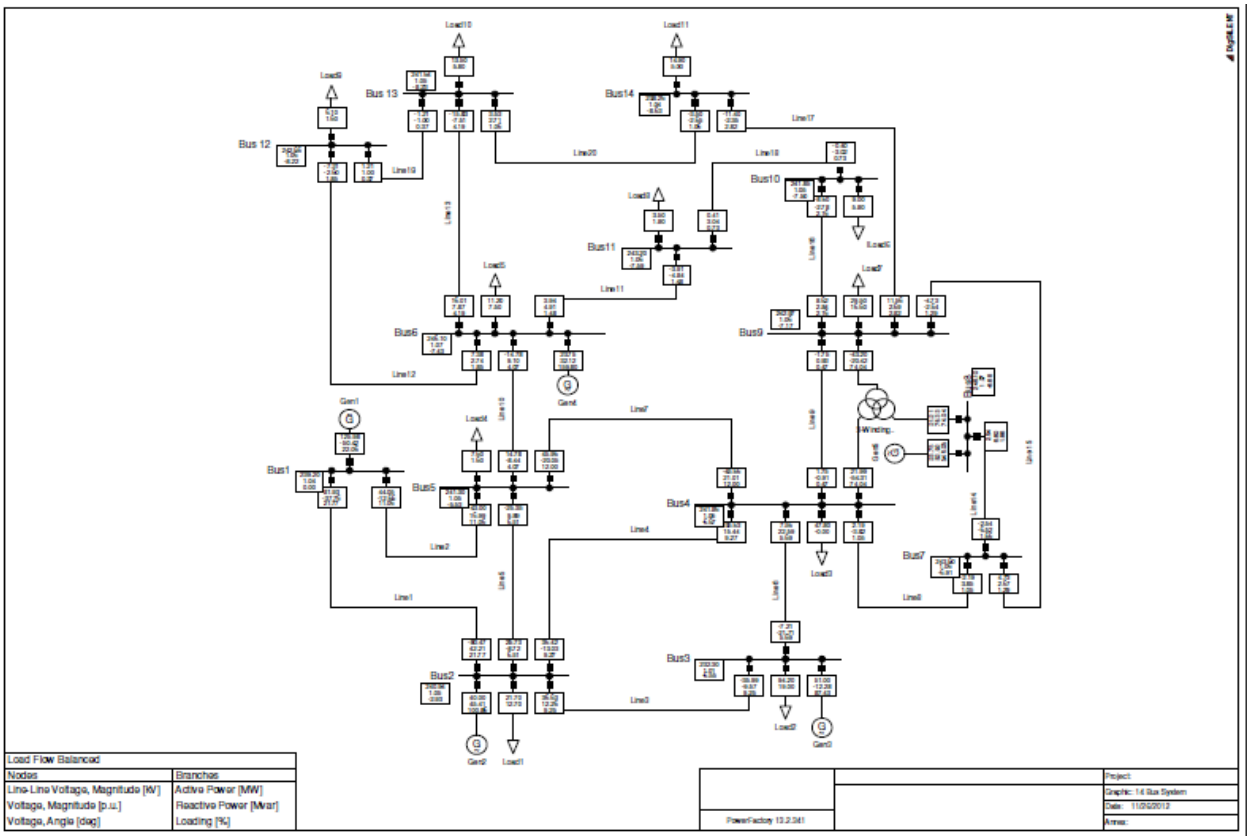

Figure F. 1: One line diagram of the full network of 14-bus system

F .1: Simulation results for full IEEE 14-bus model in DigSILENT software

Table F.1 presents the load flow results of the full model of IEEE 14-Bus system

Table F. 3: Load flow resultsof the full IEEE 14-bus system

		DIgSILENT PowerFactory 13.2.341	Project:
			Date: 11/26/2012

Load Flow Calculation		Complete System Report: Voltage Profiles, Area Interchange	
Balanced, positive sequence		Automatic Model Adaptation for Convergency	No
Automatic Tap Adjust of Transformers	No	Max. Acceptable Load Flow Error for	
Consider Reactive Power Limits	No	Nodes	1.00 kVA
		Model Equations	0.10 %

Grid: 14 Bus System	System Stage: 14 Bus System	Study Case: Study Case	Annex: / 1

	rtd.V [kV]	Bus - voltage [p.u.]	[kV]	[deg]	Voltage - Deviation [%] -10 -5 0 +5 +10
Bus1	230.00	1.040	239.20	0.00	
Bus2	230.00	1.048	240.94	-2.93	
Bus3	230.00	1.010	232.30	-6.55	
Bus4	230.00	1.052	241.86	-6.67	
Bus5	230.00	1.049	241.30	-5.53	
Bus6	230.00	1.070	246.10	-7.43	
Bus8	230.00	1.070	246.10	-6.68	
Bus9	230.00	1.056	242.97	-7.17	
Bus10	230.00	1.052	241.85	-7.50	
Bus11	230.00	1.057	243.20	-7.59	
Bus 13	230.00	1.051	241.64	-8.23	
Bus 12	230.00	1.055	242.66	-8.22	
Bus7	230.00	1.059	243.60	-6.91	
Bus14	230.00	1.036	238.26	-8.63	

		DIgSILENT PowerFactory 13.2.341	Project:
			Date: 11/26/2012

Load Flow Calculation		Complete System Report: Voltage Profiles, Area Interchange	
Balanced, positive sequence		Automatic Model Adaptation for Convergency	No
Automatic Tap Adjust of Transformers	No	Max. Acceptable Load Flow Error for	
Consider Reactive Power Limits	No	Nodes	1.00 kVA
		Model Equations	0.10 %

Grid: 14 Bus System	System Stage: 14 Bus System	Study Case: Study Case	Annex: / 2

Volt. Level [kV]	Generation [MW] / [Mvar]	Motor Load [MW] / [Mvar]	Load [MW] / [Mvar]	Compen-sation [MW] / [Mvar]	External Infeed [MW] / [Mvar]	Interchange to	Power Interchange [MW] / [Mvar]	Total Losses [MW] / [Mvar]	Load Losses [MW] / [Mvar]	Noload Losses [MW] / [Mvar]
230.00	264.48	0.00	259.00	0.00	0.00			5.48	5.48	0.00
	97.76	0.00	77.40	0.00	0.00			20.36	20.36	0.00
Total:	264.48	0.00	259.00	0.00	0.00		0.00	5.48	5.48	0.00
	97.76	0.00	77.40	0.00	0.00		0.00	20.36	20.36	0.00

		DIgSILENT PowerFactory 13.2.341	Project:
			Date: 11/26/2012

Load Flow Calculation		Complete System Report: Voltage Profiles, Area Interchange	
Balanced, positive sequence		Automatic Model Adaptation for Convergency	No
Automatic Tap Adjust of Transformers	No	Max. Acceptable Load Flow Error for	
Consider Reactive Power Limits	No	Nodes	1.00 kVA
		Model Equations	0.10 %

Total System Summary	Study Case: Study Case	Annex: / 3

	Generation [MW] / [Mvar]	Motor Load [MW] / [Mvar]	Load [MW] / [Mvar]	Compen-sation [MW] / [Mvar]	External Infeed [MW] / [Mvar]	Inter Area Flow [MW] / [Mvar]	Total Losses [MW] / [Mvar]	Load Losses [MW] / [Mvar]	Noload Losses [MW] / [Mvar]
\Demo\14 Bus System\14 Bus System	264.48	0.00	259.00	0.00	0.00	0.00	5.48	5.48	0.00
	97.76	0.00	77.40	0.00	0.00	0.00	20.36	20.36	0.00
Total:	264.48	0.00	259.00	0.00	0.00		5.48	5.48	0.00
	97.76	0.00	77.40	0.00	0.00		20.36	20.36	0.00

F. 2: Matlab script file – load conversion to addimittance

This code converts the values of P, Q, and V of the load bus into eqivalent admittance values of the load buses. Therefore, the inputs are P, Q, and V, while y is the output.

```
clear all
clc
P=[ 21.7 94.2 47.8 76 11.2 29.5 9 3.5 6.1 13.5 14.9]
Q=i*[21.7 19 0 1.6 7.5 16.6 5.8 1.8 1.6 5.8 5]
V=[230 230  230 230 230 230 230 230 230 230 230]
n=1

for i=1:n
   y=(P-Q)./abs(V.^2)
end
```

F .3: Matlab script file – kron's elimination method

This code reduce the full model admittance matrix using the values of the admittances of each bus in the model. The input is the full model while the output is the reduced model.

```
YO=[(0.058029-0.04403j) (0) (0) (0) (0);
   (0.018809-0.02048j) (0.038459-0.08497j) (0) (0) (0);
   (0) (0) (0.02866-0.05224j) (0.0133-0.02048j) (0);
   (0) (0) (0.0133-0.02048j) (0.05596-0.10473j) (0.01137-0.02315j);
   (0) (0) (0) (0.01137-0.02315j) (0.02591-0.05354j)]
Ykk=(0.02591-0.05354j);
k=5;
for i=1:4
   for j=1 :4
YN=YO(i,j)-(YO(i,k)*YO(k,i))/Ykk
   end
end

YO=[(0.0580 - 0.0440j) (0) (0) (0) ;
   (0.0188 - 0.0205j) (0.0385 - 0.0850j) (0) (0) ;
   (0) (0) (0.0287 - 0.0522j) (0.0133 - 0.0205j) ;
   (-0.0050 + 0.0100j) (-0.0050 + 0.0100j)  (0.0083 - 0.0105j) (0.0510 - 0.0947j)]
Ykk=(0.0510 - 0.0947i);
k=4;
for i=1:3
   for j=1 :3
YN=YO(i,j)-(YO(i,k)*YO(k,i))/Ykk
   end
end
YO=[(0.0580 - 0.0440j) (0) (0) ;
   (0.0188 - 0.0205j) (0.0385 - 0.0850j) (0)  ;
   (-0.0021 + 0.0022j) (-0.0021 + 0.0022j) (0.0266 - 0.0500j)]
Ykk=(0.0266 - 0.0500i);
k=3;
for i=1:2
   for j=1 :2
YN=YO(i,j)-(YO(i,k)*YO(k,i))/Ykk
   end
end
YO=[(0.0580 - 0.0440j) (0);
   (0.0188 - 0.0205j) (0.0385 - 0.0850j);]
Ykk=(0.0385 - 0.0850j);
k=2;
for i=1:1
```

```
   for j=1 :1
YN=YO(i,j)-(YO(i,k)*YO(k,i))/Ykk
   end
end
```

F .4: Simulation results for the reduced IEEE 14-bus network in DigSILENT

Figure F.4 shows the one line diagram of the reduced network of the IEEE 14-bus system.

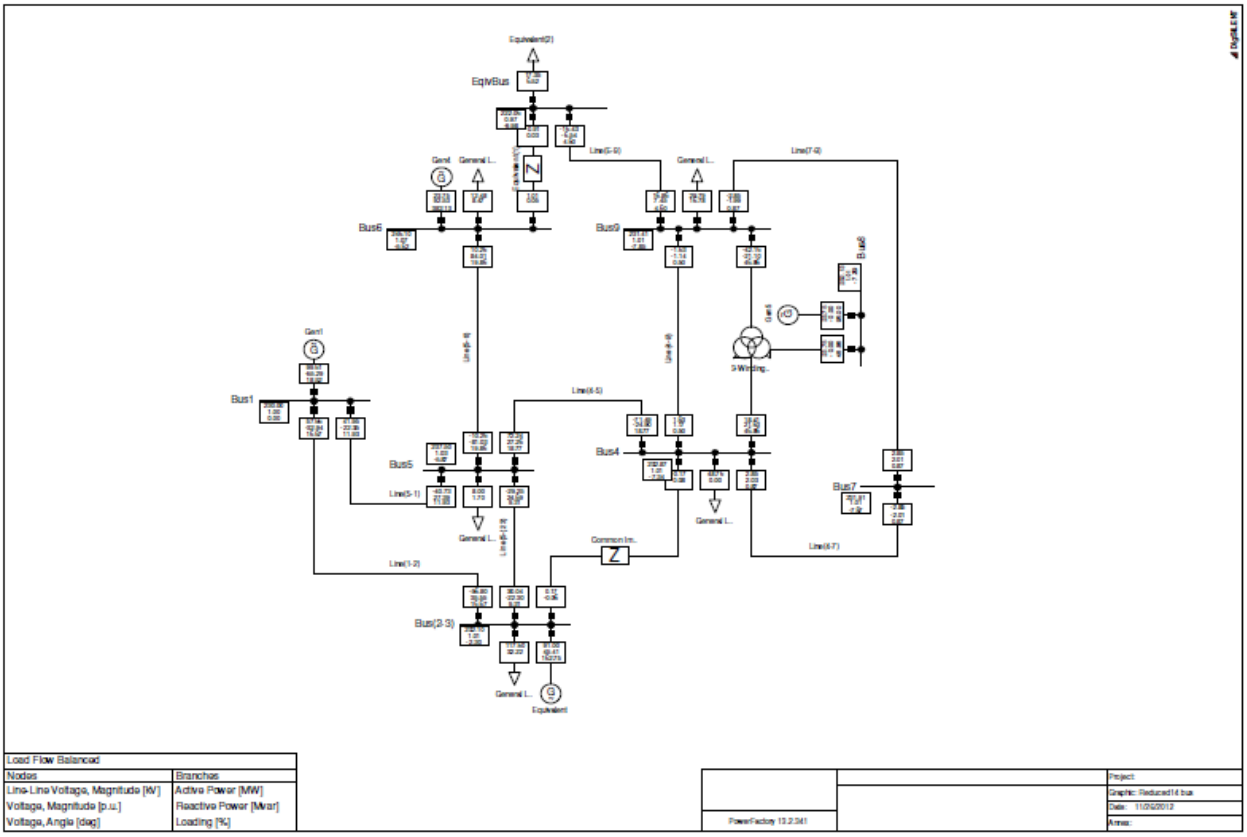

Figure F. 2: Reduced network of the IEEE 14-bus system

Table F.2 depicts the report of the load flow results of the reduced IEEE 14-bus system.

Table F. 4: load flow results of the reduced IEEE 14-bus system

		DIgSILENT PowerFactory 13.2.341	Project:
			Date: 11/26/2012

Load Flow Calculation		Complete System Report: Voltage Profiles, Area Interchange
Balanced, positive sequence		Automatic Model Adaptation for Convergency No
Automatic Tap Adjust of Transformers	No	Max. Acceptable Load Flow Error for
Consider Reactive Power Limits	No	Nodes 1.00 kVA
		Model Equations 0.10 %

Grid: Grid	System Stage: Grid	Study Case: Study Case	Annex: / 1

	rtd.V [kV]	Bus - voltage [p.u.]	[kV]	[deg]	Voltage - Deviation [%] −10 −5 0 +5 +10
EqivBus	230.00	0.965	222.06	-9.98	
Bus6	230.00	1.070	246.10	-5.62	
Bus9	230.00	1.006	231.41	-7.85	
Bus4	230.00	1.012	232.87	-7.34	
Bus5	230.00	1.033	237.50	-5.87	
Bus1	230.00	1.000	230.00	0.00	
Bus7	230.00	1.008	231.91	-7.67	
Bus(2-3)	230.00	1.009	232.10	-2.30	
Bus8	230.00	1.009	232.13	-7.29	

		DIgSILENT PowerFactory 13.2.341	Project:
			Date: 11/26/2012

Load Flow Calculation		Complete System Report: Voltage Profiles, Area Interchange
Balanced, positive sequence		Automatic Model Adaptation for Convergency No
Automatic Tap Adjust of Transformers	No	Max. Acceptable Load Flow Error for
Consider Reactive Power Limits	No	Nodes 1.00 kVA
		Model Equations 0.10 %

Grid: Grid	System Stage: Grid	Study Case: Study Case	Annex: / 2

Volt. Level [kV]	Generation [MW] / [Mvar]	Motor Load [MW] / [Mvar]	Load [MW] / [Mvar]	Compen-sation [MW] / [Mvar]	External Infeed [MW] / [Mvar]	Interchange to	Power Interchange [MW] / [Mvar]	Total Losses [MW] / [Mvar]	Load Losses [MW] / [Mvar]	Noload Losses [MW] / [Mvar]
230.00	238.11	0.00	233.97	0.00	0.00			4.13	4.13	0.00
	82.65	0.00	65.69	0.00	0.00			16.96	16.96	0.00
Total:	238.11	0.00	233.97	0.00	0.00		0.00	4.13	4.13	0.00
	82.65	0.00	65.69	0.00	0.00		0.00	16.96	16.96	0.00

		DIgSILENT PowerFactory 13.2.341	Project:
			Date: 11/26/2012

Load Flow Calculation		Complete System Report: Voltage Profiles, Area Interchange
Balanced, positive sequence		Automatic Model Adaptation for Convergency No
Automatic Tap Adjust of Transformers	No	Max. Acceptable Load Flow Error for
Consider Reactive Power Limits	No	Nodes 1.00 kVA
		Model Equations 0.10 %

Total System Summary	Study Case: Study Case	Annex: / 3

	Generation [MW] / [Mvar]	Motor Load [MW] / [Mvar]	Load [MW] / [Mvar]	Compen-sation [MW] / [Mvar]	External Infeed [MW] / [Mvar]	Inter Area Flow [MW] / [Mvar]	Total Losses [MW] / [Mvar]	Load Losses [MW] / [Mvar]	Noload Losses [MW] / [Mvar]
\Demo\REDUCED14\Grid	238.11	0.00	233.97	0.00	0.00	0.00	4.13	4.13	0.00
	82.65	0.00	65.69	0.00	0.00	0.00	16.96	16.96	0.00
Total:	238.11	0.00	233.97	0.00	0.00		4.13	4.13	0.00
	82.65	0.00	65.69	0.00	0.00		16.96	16.96	0.00

APPENDIX G: SIMULATION DATA FOR BOTH 9-BUS and 14-BUS NETWORK IN RSCAD

G .1: Full and Reduced data for both IEEE 9-bus and 14-Bus models in RSCAD

Table G. 1: IEEE 9-Bus system map files for both the full and the reduced networks

FULL NETWORK	REDUCED NETWORK
CASE: Test Circuit Delt: 50.000000 us Backplane operation set to IEEE mode +----------+ | SUBSYSTEM #01 | | mapped to | | RTDS RACK #01 | +----------+ COMPONENT PROCESSORS ---------- RISC-based MAC_V3 Machine model named: GEN1 in subsystem: #1 is assigned to RPC-GPC Card #3 Processor A RPC-GPC Synchronous Machine model "GEN1" Initial Mechanical Torque required: 1.037158 PU Initial Field Voltage required: 1.194352 NORM D axis circuit parameters ---------- Stator Leakage Reactance: Xs1= 0.033600 pu Stator Resistance: Rs1= 0.033600 pu Field-Damper Mutual Leakage Reactance: X230= 0.000000 pu Unsaturated magnetizing reactance: Xmd0= 0.112400 pu Damper Leakage Reactance: X3d= 0.014303 pu Damper Resistance: R3d= 0.003433 pu Field Leakage Reactance: X2d= 0.036272 pu Field resistance: R2d= 0.000044 pu Q axis circuit parameters ---------- Stator Leakage Reactance: Xs1= 0.033600 pu Stator Resistance: Rs1= 0.033600 pu Magnetizing Reactance: Xmq= 0.066400 pu 2nd Damper Leakage Reactance: X3q= 0.065276 pu 2nd Damper Resistance: R3q= 0.101094 pu 1st damper Leakage Reactance: X2q= 0.681558 pu 1st Damper resistance: R2q= 0.436527 pu RISC-based MAC_V3 Machine model named: GEN2 in subsystem: #1 is assigned to RPC-GPC Card #3 Processor B RPC-GPC Synchronous Machine model "GEN2" Initial Mechanical Torque required: 0.855791 PU Initial Field Voltage required: 1.853426 NORM D axis circuit parameters ---------- Stator Leakage Reactance: Xs1= 0.150000 pu Stator Resistance: Rs1= 0.003000 pu Field-Damper Mutual Leakage Reactance: X230= 0.000000 pu Unsaturated magnetizing reactance: Xmd0= 1.660000 pu Damper Leakage Reactance: X3d= 0.167955 pu Damper Resistance: R3d= 0.027847 pu Field Leakage Reactance: X2d= 0.168248 pu Field resistance: R2d= 0.000617 pu Q axis circuit parameters ---------- Stator Leakage Reactance: Xs1= 0.150000 pu Stator Resistance: Rs1= 0.003000 pu Magnetizing Reactance: Xmq= 1.610000 pu 2nd Damper Leakage Reactance: X3q= 0.122833 pu 2nd Damper Resistance: R3q= 0.021420 pu 1st damper Leakage Reactance: X2q= 0.807938 pu 1st Damper resistance: R2q= 0.007498 pu RISC-based MAC_V3 Machine model named: GEN3 in subsystem: #1 is assigned to RPC-GPC Card #3 Processor A RPC-GPC Synchronous Machine model "GEN3" Initial Mechanical Torque required: 0.857636 PU Initial Field Voltage required: 2.628443 NORM D axis circuit parameters ---------- Stator Leakage Reactance: Xs1= 0.074200 pu Stator Resistance: Rs1= 0.003000 pu Field-Damper Mutual Leakage Reactance: X230= 0.000000 pu Unsaturated magnetizing reactance: Xmd0= 1.238300 pu Damper Leakage Reactance: X3d= 0.136802 pu Damper Resistance: R3d= 0.019887 pu Field Leakage Reactance: X2d= 0.120048 pu Field resistance: R2d= 0.000628 pu Q axis circuit parameters ---------- Stator Leakage Reactance: Xs1= 0.074200 pu Stator Resistance: Rs1= 0.003000 pu Magnetizing Reactance: Xmq= 1.183600 pu	CASE: Test Circuit Delt: 50.000000 us Backplane operation set to IEEE mode +----------+ | SUBSYSTEM #01 | | mapped to | | RTDS RACK #01 | +----------+ COMPONENT PROCESSORS ---------- RISC-based MAC_V3 Machine model named: GEN1 in subsystem: #1 is assigned to RPC-GPC Card #3 Processor A RPC-GPC Synchronous Machine model "GEN1" Initial Mechanical Torque required: -0.693322 PU Initial Field Voltage required: 1.259931 NORM D axis circuit parameters ---------- Stator Leakage Reactance: Xs1= 0.033600 pu Stator Resistance: Rs1= 0.033600 pu Field-Damper Mutual Leakage Reactance: X230= 0.000000 pu Unsaturated magnetizing reactance: Xmd0= 0.112400 pu Damper Leakage Reactance: X3d= 0.014303 pu Damper Resistance: R3d= 0.003433 pu Field Leakage Reactance: X2d= 0.036272 pu Field resistance: R2d= 0.000044 pu Q axis circuit parameters ---------- Stator Leakage Reactance: Xs1= 0.033600 pu Stator Resistance: Rs1= 0.033600 pu Magnetizing Reactance: Xmq= 0.066400 pu 2nd Damper Leakage Reactance: X3q= 0.065276 pu 2nd Damper Resistance: R3q= 0.101094 pu 1st damper Leakage Reactance: X2q= 0.681558 pu 1st Damper resistance: R2q= 0.436527 pu RISC-based MAC_V3 Machine model named: GEN2 in subsystem: #1 is assigned to RPC-GPC Card #3 Processor B RPC-GPC Synchronous Machine model "GEN2" Initial Mechanical Torque required: 0.855842 PU Initial Field Voltage required: 2.371536 NORM D axis circuit parameters ---------- Stator Leakage Reactance: Xs1= 0.150000 pu Stator Resistance: Rs1= 0.003000 pu Field-Damper Mutual Leakage Reactance: X230= 0.000000 pu Unsaturated magnetizing reactance: Xmd0= 1.660000 pu Damper Leakage Reactance: X3d= 0.167955 pu Damper Resistance: R3d= 0.027847 pu Field Leakage Reactance: X2d= 0.168248 pu Field resistance: R2d= 0.000617 pu Q axis circuit parameters ---------- Stator Leakage Reactance: Xs1= 0.150000 pu Stator Resistance: Rs1= 0.003000 pu Magnetizing Reactance: Xmq= 1.610000 pu 2nd Damper Leakage Reactance: X3q= 0.122833 pu 2nd Damper Resistance: R3q= 0.021420 pu 1st damper Leakage Reactance: X2q= 0.807938 pu 1st Damper resistance: R2q= 0.007498 pu RISC-based UDC model srcac2N named: GEN3(E:\RSCAD/BIN/UDC\srcac2N) in subsystem: #1 is assigned to RISC Card #3 Processor A L1 = 0.017460 H R1 = 0.000001 Ohm R2 = 0.000000 Ohm RISC-based UDC model RCDload1 named: LOADA(E:\RSCAD/BIN/UDC\RCDload1) in subsystem: #1 is assigned to RISC Card #3 Processor Dynamic load: R and C in parallel: Pinit = 1.000000 MW (R=52900.000000 ohms) Qinit = 1.000000 MVar (C=0.050143 uF) RISC-based UDC model RCDload1 named: LOADB(E:\RSCAD/BIN/UDC\RCDload1) in subsystem: #1 is assigned to RISC Card #3 Processor A Dynamic load: R and C in parallel: Pinit = 1.000000 MW (R=52900.000000 ohms) Qinit = 1.000000 MVar (C=0.050143 uF) RISC-based UDC model trf3p2wL named: TRF3(E:\RSCAD/BIN/UDC\trf3p2wL) in subsystem: #1 is assigned to RISC Card #3 Processor B RISC-based UDC model pi3 named: LINE1(E:\RSCAD/BIN/UDC\pi3) in subsystem: #1 is assigned to RISC Card #3 Processor A

```
2nd Damper Leakage Reactance:  X3q= 0.251579 pu
2nd Damper Resistance:  R3q= 0.029826 pu
1st damper Leakage Reactance:  X2q= 1.151410 pu
1st Damper resistance:  R2q= 0.006573 pu
RISC-based UDC model RLDload1 named:
LoadA(E:\RSCAD/BIN/UDC\RLDload1)
in subsystem: #1
is assigned to RISC Card #3 Processor B
Dynamic load: R and L in parallel:
Pinit = 1.000000 MW   (R=52900.000000 ohms)
Qinit = 1.000000 MVar (L=140.321608 H)RISC-based UDC model RLDload1
named: LoadB(E:\RSCAD/BIN/UDC\RLDload1)
in subsystem: #1
is assigned to RISC Card #3 Processor B
Dynamic load: R and L in parallel:
Pinit = 1.000000 MW   (R=52900.000000 ohms)
Qinit = 1.000000 MVar (L=140.321608 H)
RISC-based UDC model RLDload1 named:
LoadC(E:\RSCAD/BIN/UDC\RLDload1)
in subsystem: #1
is assigned to RISC Card #3 Processor A
Dynamic load: R and L in parallel:
Pinit = 100.000000 MW   (R=529.000000 ohms)
Qinit = 30.000000 MVar (L=4.677387 H)
RISC-based UDC model pi3 named: LINE1(E:\RSCAD/BIN/UDC\pi3)
in subsystem: #1
is assigned to RISC Card #3 Processor B
RISC-based UDC model pi3 named: LINE2(E:\RSCAD/BIN/UDC\pi3)
in subsystem: #1
is assigned to RISC Card #3 Processor A
RISC-based UDC model pi3 named: LINE3(E:\RSCAD/BIN/UDC\pi3)
in subsystem: #1
is assigned to RISC Card #3 Processor B
RISC-based UDC model pi3 named: LINE4(E:\RSCAD/BIN/UDC\pi3)
in subsystem: #1
is assigned to RISC Card #3 Processor A
RISC-based UDC model pi3 named: LINE5(E:\RSCAD/BIN/UDC\pi3)
in subsystem: #1
is assigned to RISC Card #3 Processor B
RISC-based UDC model pi3 named: LINE6(E:\RSCAD/BIN/UDC\pi3)
in subsystem: #1
is assigned to RISC Card #3 Processor A

RISC CONTROLS COMPONENTS(proc 1) --> RPC-GPC Card #1 Processor B
RISC ARAMP function
RISC sum3_B function
RISC compareX04 function
RISC MULTIPLICATION function
RISC sum3_B function
RISC MULTIPLICATION function
RISC gain_cb function
RISC gain_cb function
RISC gain_cb function
RISC gain_cb function
RISC gain_cb function
RISC gain_cb function
RISC not_cb function
RISC time_cb function
RISC IEE2ST Type Stabilizer (w=376.991118) (next 14 components)
RISC GAIN function (* 0.0027)
RISC Floating Point Summation - +
RISC Real Pole (T= 0.0, G= 9.5000)
RISC GAIN function (* 0.0078)
RISC Real Pole (T= 0.0, G= 0.0000)
RISC Floating Point Summation + +
RISC Wash Out (T= 1.4100, G= 1.0000)
RISC Lead-Lag (T1= 0.1540, T2= 0.0330, G= 1.0000)
RISC Lead-Lag (T1= 0.0000, T2= 0.0010, G= 1.0000)
RISC Lead-Lag (T1= 0.0000, T2= 0.0010, G= 1.0000)
RISC Fixed Limits (UL=0.2000 LL=-0.2000)
RISC GAIN function (* 1.0000)
RISC MULTIPLICATION function
RISC DEGRAD function
RISC compareX03 function
RISC compareX03 function
RISC sum3_B function
RISC logicX01 function
RISC logicX01 function
RISC MULTIPLICATION function
RISC sum3_B function
RISC IEEE Type 1 Governor (w=376.991118) (next 27 components)
RISC GAIN function (* 0.0027)
RISC Floating Point Summation - +
RISC Lead-Lag (T1= 0.0010, T2= 0.0010, G= 25.0000)
RISC Floating Point Summation - - +
RISC GAIN function (* 1.0000)
RISC Fixed Limits (UL=0.1000 LL=-1.0000)
RISC Integrator (T= 1.0000)
RISC Real Pole (T= 0.4000, G= 1.0000)
RISC GAIN function (* 0.3000)
RISC GAIN function (* 0.0000)
RISC Real Pole (T= 9.0000, G= 1.0000)
RISC GAIN function (* 0.4000)
RISC Floating Point Summation + +
RISC GAIN function (* 0.0000)
RISC Floating Point Summation + +
RISC Real Pole (T= 0.5000, G= 1.0000)
RISC GAIN function (* 0.3000)
RISC Floating Point Summation + +
RISC GAIN function (* 0.0000)
RISC Floating Point Summation + +
RISC Real Pole (T= 0.0, G= 1.0000)
RISC GAIN function (* 0.0000)
RISC Floating Point Summation + +
RISC GAIN function (* 0.0000)
```

```
RISC-based UDC model pi3 named: LINE2(E:\RSCAD/BIN/UDC\pi3)
in subsystem: #1
is assigned to RISC Card #3 Processor B
RISC-based UDC model pi3 named: LINE3(E:\RSCAD/BIN/UDC\pi3)
in subsystem: #1
is assigned to RISC Card #3 Processor A
RISC CONTROLS COMPONENTS(proc 1) --> RPC-GPC Card #1 Processor B
RISC ARAMP function
RISC sum3_B function
RISC compareX04 function
RISC MULTIPLICATION function
RISC sum3_B function
RISC not_cb function
RISC MULTIPLICATION function
RISC gain_cb function
RISC gain_cb function
RISC gain_cb function
RISC gain_cb function
RISC DEGRAD function
RISC time_cb function
RISC compareX03 function
RISC logicX01 function
RISC compareX03 function
RISC logicX01 function
RISC MULTIPLICATION function
RISC sum3_B function
RISC sine_cb function
RISC sum3_B function
RISC IEE2ST Type Stabilizer (w=376.991118) (next 15 components)
RISC GAIN function (* 0.0027)
RISC Floating Point Summation - +
RISC Real Pole (T= 0.0, G= 9.5000)
RISC GAIN function (* 0.0052)
RISC Real Pole (T= 0.0, G= 0.0000)
RISC Floating Point Summation + +
RISC Wash Out (T= 1.4100, G= 1.0000)
RISC Lead-Lag (T1= 0.1540, T2= 0.0330, G= 1.0000)
RISC Lead-Lag (T1= 0.0000, T2= 0.0010, G= 1.0000)
RISC Lead-Lag (T1= 0.0000, T2= 0.0010, G= 1.0000)
RISC Fixed Limits (UL=0.2000 LL=-0.2000)
RISC GAIN function (* 1.0000)
RISC MULTIPLICATION function
RISC IEEE Type 1 Governor (w=376.991118) (next 27 components)
RISC GAIN function (* 0.0027)
RISC Floating Point Summation - +
RISC Lead-Lag (T1= 0.0010, T2= 0.0010, G= 25.0000)
RISC Floating Point Summation - - +
RISC GAIN function (* 1.0000)
RISC Fixed Limits (UL=0.1000 LL=-1.0000)
RISC Integrator (T= 1.0000)
RISC Real Pole (T= 0.4000, G= 1.0000)
RISC GAIN function (* 0.3000)
RISC GAIN function (* 0.0000)
RISC Real Pole (T= 9.0000, G= 1.0000)
RISC GAIN function (* 0.4000)
RISC Floating Point Summation + +
RISC GAIN function (* 0.0000)
RISC Floating Point Summation + +
RISC Real Pole (T= 0.5000, G= 1.0000)
RISC GAIN function (* 0.3000)
RISC Floating Point Summation + +
RISC GAIN function (* 0.0000)
RISC Floating Point Summation + +
RISC Real Pole (T= 0.0, G= 1.0000)
RISC GAIN function (* 0.0000)
RISC Floating Point Summation + +
RISC GAIN function (* 0.0000)
RISC Floating Point Summation + +
RISC X/Y Function (dbz)
RISC X/Y Function (dbz)
RISC IEEE Type AC4 Excitation System (next 9 components)
RISC Real Pole (T= 0.0150, G= 1.0000)
RISC Floating Point Summation - + +
RISC Fixed Limits (UL=20.0000 LL=-20.0000)
RISC Lead-Lag (T1= 1.0000, T2= 1.0000, G= 1.0000)
RISC Real Pole (T= 0.0, G= 200.0000)
RISC GAIN function (* 0.0000)
RISC Floating Point Summation - +
RISC Floating Point Summation - +
RISC Dynamic Limits
RISC IEE2ST Type Stabilizer (w=376.991118) (next 14 components)
RISC GAIN function (* 0.0027)
RISC Floating Point Summation - +
RISC Real Pole (T= 0.0, G= 9.5000)
RISC GAIN function (* 0.0040)
RISC Real Pole (T= 0.0, G= 0.0000)
RISC Floating Point Summation + +
RISC Wash Out (T= 1.4100, G= 1.0000)
RISC Lead-Lag (T1= 0.1540, T2= 0.0330, G= 1.0000)
RISC Lead-Lag (T1= 0.0000, T2= 0.0010, G= 1.0000)
RISC Lead-Lag (T1= 0.0000, T2= 0.0010, G= 1.0000)
RISC Fixed Limits (UL=0.2000 LL=-0.2000)
RISC GAIN function (* 1.0000)
RISC MULTIPLICATION function
RISC IEEE Type 1 Governor (w=376.991118) (next 27 components)
RISC GAIN function (* 0.0027)
RISC Floating Point Summation - +
RISC Lead-Lag (T1= 0.0010, T2= 0.0010, G= 25.0000)
RISC Floating Point Summation - - +
RISC GAIN function (* 1.0000)
RISC Fixed Limits (UL=0.1000 LL=-1.0000)
RISC Integrator (T= 1.0000)
RISC Real Pole (T= 0.4000, G= 1.0000)
RISC GAIN function (* 0.3000)
RISC GAIN function (* 0.0000)
```

```
RISC Floating Point Summation + +
RISC X/Y Function (dbz)
RISC X/Y Function (dbz)
RISC IEE2ST Type Stabilizer (w=376.991118) (next 15 components)
RISC GAIN function (* 0.0027)
RISC Floating Point Summation - +
RISC Real Pole (T= 0.0, G= 9.5000)
RISC GAIN function (* 0.0052)
RISC Real Pole (T= 0.0, G= 0.0000)
RISC Floating Point Summation + +
RISC Wash Out (T= 1.4100, G= 1.0000)
RISC Lead-Lag (T1= 0.1540, T2= 0.0330, G= 1.0000)
RISC Lead-Lag (T1= 0.0000, T2= 0.0010, G= 1.0000)
RISC Lead-Lag (T1= 0.0000, T2= 0.0010, G= 1.0000)
RISC Fixed Limits (UL=0.2000 LL=-0.2000)
RISC GAIN function (* 1.0000)
RISC MULTIPLICATION function
RISC IEEE Type AC4 Excitation System (next 9 components)
RISC Real Pole (T= 0.0150, G= 1.0000)
RISC Floating Point Summation - + +
RISC Fixed Limits (UL=20.0000 LL=-20.0000)
RISC Lead-Lag (T1= 1.0000, T2= 1.0000, G= 1.0000)
RISC Real Pole (T= 0.0, G= 200.0000)
RISC GAIN function (* 0.0000)
RISC Floating Point Summation - +
RISC Floating Point Summation - +
RISC Dynamic Limits
RISC IEEE Type 1 Governor (w=376.991118) (next 27 components)
RISC GAIN function (* 0.0027)
RISC Floating Point Summation - +
RISC Lead-Lag (T1= 0.0010, T2= 0.0010, G= 25.0000)
RISC Floating Point Summation - - +
RISC GAIN function (* 1.0000)
RISC Fixed Limits (UL=0.1000 LL=-1.0000)
RISC Integrator (T= 1.0000)
RISC Real Pole (T= 0.4000, G= 1.0000)
RISC GAIN function (* 0.3000)
RISC GAIN function (* 0.0000)
RISC Real Pole (T= 9.0000, G= 1.0000)
RISC GAIN function (* 0.4000)
RISC Floating Point Summation + +
RISC GAIN function (* 0.0000)
RISC Floating Point Summation + +
RISC Real Pole (T= 0.5000, G= 1.0000)
RISC GAIN function (* 0.3000)
RISC Floating Point Summation + +
RISC GAIN function (* 0.0000)
RISC Floating Point Summation + +
RISC Real Pole (T= 0.0, G= 1.0000)
RISC GAIN function (* 0.0000)
RISC Floating Point Summation + +
RISC GAIN function (* 0.0000)
RISC Floating Point Summation + +
RISC X/Y Function (dbz)
RISC X/Y Function (dbz)
RISC IEE2ST Type Stabilizer (w=376.991118) (next 14 components)
RISC GAIN function (* 0.0027)
RISC Floating Point Summation - +
RISC Real Pole (T= 0.0, G= 9.5000)
RISC GAIN function (* 0.0040)
RISC Real Pole (T= 0.0, G= 0.0000)
RISC Floating Point Summation + +
RISC Wash Out (T= 1.4100, G= 1.0000)
RISC Lead-Lag (T1= 0.1540, T2= 0.0330, G= 1.0000)
RISC Lead-Lag (T1= 0.0000, T2= 0.0010, G= 1.0000)
RISC Lead-Lag (T1= 0.0000, T2= 0.0010, G= 1.0000)
RISC Fixed Limits (UL=0.2000 LL=-0.2000)
RISC GAIN function (* 1.0000)
RISC MULTIPLICATION function
RISC IEEE Type AC4 Excitation System (next 9 components)
RISC Real Pole (T= 0.0150, G= 1.0000)
RISC Floating Point Summation - + +
RISC Fixed Limits (UL=20.0000 LL=-20.0000)
RISC Lead-Lag (T1= 1.0000, T2= 1.0000, G= 1.0000)
RISC Real Pole (T= 0.0, G= 200.0000)
RISC GAIN function (* 0.0000)
RISC Floating Point Summation - +
RISC Floating Point Summation - +
RISC Dynamic Limits
RISC IEEE Type 1 Governor (w=376.991118) (next 27 components)
RISC GAIN function (* 0.0027)
RISC Floating Point Summation - +
RISC Lead-Lag (T1= 0.0010, T2= 0.0010, G= 25.0000)
RISC Floating Point Summation - - +
RISC GAIN function (* 1.0000)
RISC Fixed Limits (UL=0.1000 LL=-1.0000)
RISC Integrator (T= 1.0000)
RISC Real Pole (T= 0.4000, G= 1.0000)
RISC GAIN function (* 0.3000)
RISC GAIN function (* 0.0000)
RISC Real Pole (T= 9.0000, G= 1.0000)
RISC GAIN function (* 0.4000)
RISC Floating Point Summation + +
RISC GAIN function (* 0.0000)
RISC Floating Point Summation + +
RISC Real Pole (T= 0.5000, G= 1.0000)
RISC GAIN function (* 0.3000)
RISC Floating Point Summation + +
RISC GAIN function (* 0.0000)
RISC Floating Point Summation + +
RISC Real Pole (T= 0.0, G= 1.0000)
RISC GAIN function (* 0.0000)
RISC Floating Point Summation + +
RISC GAIN function (* 0.0000)
RISC Floating Point Summation + +
RISC Real Pole (T= 9.0000, G= 1.0000)
RISC GAIN function (* 0.4000)
RISC Floating Point Summation + +
RISC GAIN function (* 0.0000)
RISC Floating Point Summation + +
RISC Real Pole (T= 0.5000, G= 1.0000)
RISC GAIN function (* 0.3000)
RISC Floating Point Summation + +
RISC GAIN function (* 0.0000)
RISC Floating Point Summation + +
RISC Real Pole (T= 0.0, G= 1.0000)
RISC GAIN function (* 0.0000)
RISC Floating Point Summation + +
RISC GAIN function (* 0.0000)
RISC Floating Point Summation + +
RISC Real Pole (T= 9.0000, G= 1.0000)
RISC GAIN function (* 0.4000)
RISC Floating Point Summation + +
RISC GAIN function (* 0.0000)
RISC Floating Point Summation + +
RISC Real Pole (T= 0.0, G= 1.0000)
RISC GAIN function (* 0.0000)
RISC Floating Point Summation + +
RISC GAIN function (* 0.0000)
RISC Floating Point Summation + +
RISC Real Pole (T= 0.5000, G= 1.0000)
RISC GAIN function (* 0.3000)
RISC Floating Point Summation + +
RISC GAIN function (* 0.0000)
RISC Floating Point Summation + +
RISC Real Pole (T= 0.0, G= 1.0000)
RISC GAIN function (* 0.0000)
RISC Floating Point Summation + +
RISC GAIN function (* 0.0000)
RISC Floating Point Summation + +
RISC Real Pole (T= 0.0150, G= 1.0000)
RISC GAIN function (* 0.4000)
RISC Floating Point Summation + +
RISC GAIN function (* 0.0000)
RISC Floating Point Summation + +
RISC Real Pole (T= 0.5000, G= 1.0000)
RISC GAIN function (* 0.3000)
RISC Floating Point Summation + +
RISC GAIN function (* 0.0000)
RISC Floating Point Summation + +
RISC Real Pole (T= 0.0, G= 1.0000)
RISC GAIN function (* 0.0000)
RISC Floating Point Summation + +
RISC GAIN function (* 0.0000)
RISC Floating Point Summation + +
RISC Fixed Limits (UL=20.0000 LL=-20.0000)
RISC Lead-Lag (T1= 1.0000, T2= 1.0000, G= 1.0000)
RISC Real Pole (T= 0.0, G= 200.0000)
RISC GAIN function (* 0.0000)
RISC Floating Point Summation - +
RISC Floating Point Summation - +
RISC Dynamic Limits
RISC CONTROLS COMPONENTS(proc 2) --> RPC-GPC Card #2 Processor A
RISC MULTIPLICATION function
RISC compareX04 function
RISC CONTROLS COMPONENTS(proc 7) --> RPC-GPC Card #2 Processor B
RISC not_cb function
RISC-based Network Solution for Subsystem #1 uses -->
RPC-GPC Card #1 Processor A
Network Solution Statistics for 1A:
Number of nodes on this processor: 12
Number of G values passed to this proc: 6
Number of matrix pointers passed to this proc: 0
Number of columns dynamically decomposed by this proc: 9
Number of multiply-subtract operations
for dynamic decomposition on this proc: 120
Number of clocks pre-T0:      667
( time = 6.670000e-001 uSec. )
Number of clocks in main:     2741
( decomposition:     1353 )
( forward-backward:   1016 )
( time = 2.741000e+000 uSec. )
The fill of the decomposed lower matrix is: 59 of 78 locations.

Hidden T2 Transfer List
---------------------------------
BP_Address  Signal_Type      Signal_name
0x13C       named_signal_prc  Te_pu1
0x13D       named_signal_prc  RMechAng1
0x13E       named_signal_prc  P3
0x13F       named_signal_prc  Q3
0x140       named_signal_prc  PmonA
0x141       named_signal_prc  QmonA
0x142       named_signal_prc  PmonB
0x143       named_signal_prc  QmonB
0x144       named_signal_prc  IL31A
0x145       named_signal_prc  IL31B
0x146       named_signal_prc  IL31C
0x147       named_signal_prc  IL32A
0x148       named_signal_prc  IL32B
0x149       named_signal_prc  IL32C
0x14A       named_signal_prc  Iag
0x14B       named_signal_prc  Ibg
0x14C       named_signal_prc  Icg
0x14D       named_signal_prc  Qmac_pu2
0x14E       named_signal_prc  Pmac_pu2
0x14F       named_signal_prc  Pmac_pu1
0x150       named_signal_prc  Qmac_pu1
0x151       named_signal_prc  Delta2
0x152       named_signal_prc  deltaw2
0x153       named_signal_prc  pss_monR
0x154       named_signal_prc  Breakers


                    TIME-STEP INFORMATION
                       SUBSYSTEM 1
   ========================================================
Backplane Communication Speed = 60.000000 ns
T0 communication time 1.8000 us
T2 communication time 3.7200 us
Minimum time-step 9.9999 us
Common Current Injections: 0(local) + 0(xrack)
```

```
RISC X/Y Function (dbz)
RISC X/Y Function (dbz)
RISC IEEE Type AC4 Excitation System (next 9 components)
RISC Real Pole (T= 0.0150, G= 1.0000)
RISC Floating Point Summation - + +
RISC Fixed Limits (UL=20.0000 LL=-20.0000)
RISC Lead-Lag (T1= 1.0000, T2= 1.0000, G= 1.0000)
RISC Real Pole (T= 0.0, G= 200.0000)
RISC GAIN function (* 0.0000)
RISC Floating Point Summation - +
RISC Floating Point Summation - +
RISC Dynamic Limits
RISC CONTROLS COMPONENTS(proc 2) --> RPC-GPC Card #2 Processor A
RISC MULTIPLICATION function
RISC compareX04 function
RISC CONTROLS COMPONENTS(proc 7) --> RPC-GPC Card #2 Processor B
RISC not_cb function
RISC-based Network Solution for Subsystem #1 uses -->
RPC-GPC Card #1 Processor A
Network Solution Statistics for 1A:
Number of nodes on this processor: 24
Number of G values passed to this proc: 9
Number of matrix pointers passed to this proc: 0
Number of columns dynamically decomposed by this proc: 18
Number of multiply-subtract operations
for dynamic decomposition on this proc: 331
Number of clocks pre-T0:      1124
( time = 1.124000e+000 uSec. )
Number of clocks in main:     6175
( decomposition:     3101 )
( forward-backward:  2474 )
( time = 6.175000e+000 uSec. )
The fill of the decomposed lower matrix is: 159 of 300 locations.

Hidden T2 Transfer List
-----------------------------------
BP_Address  Signal_Type      Signal_name
0x162       named_signal_prc  Te_pu1
0x163       named_signal_prc  RMechAng1
0x164       named_signal_prc  Te_pu3
0x165       named_signal_prc  RMechAng3
0x166       named_signal_prc  Iag
0x167       named_signal_prc  Ibg
0x168       named_signal_prc  IBRK1A
0x169       named_signal_prc  IBRK1B
0x16A       named_signal_prc  IBRK1C
0x16B       named_signal_prc  IBRK2A
0x16C       named_signal_prc  IBRK2B
0x16D       named_signal_prc  IBRK2C
0x16E       named_signal_prc  Icg
0x16F       named_signal_prc  omega
0x170       named_signal_prc  Qmac_pu1
0x171       named_signal_prc  Pmac_pu1
0x172       named_signal_prc  Pmac_pu2
0x173       named_signal_prc  Qmac_pu2
0x174       named_signal_prc  Qmac_pu3
0x175       named_signal_prc  Pmac_pu3
0x176       named_signal_prc  Delta2
0x177       named_signal_prc  deltaw2
0x178       named_signal_prc  pss_monR

                    T I M E - S T E P   I N F O R M A T I O N
                              S U B S Y S T E M   1
   ============================================================
Backplane Communication Speed = 60.000000 ns
T0 communication time 2.8800 us
T2 communication time 4.8000 us
Minimum time-step 9.9999 us
Common Current Injections: 0(local) + 0(xrack)
```

Table G. 2: IEEE 14--Bus system Map files for both the full and the reduced networks

FULL NETWORK

```
CASE: Test Circuit
Delt: 50.000000 us
Backplane operation set to IEEE mode

+-----------------------------------------------------------+
|                                                           |
|            S U B S Y S T E M #01                          |
|                                                           |
|                mapped to                                  |
|                                                           |
|             R T D S  R A C K #01                          |
|                                                           |
+-----------------------------------------------------------+


C O M P O N E N T   P R O C E S S O R S
 ----------------------------------------------------------
RISC-based MAC_V3 Machine model named: G1
   in subsystem: #1
   is assigned to RPC-GPC Card #2 Processor A

      RPC-GPC Synchronous Machine model "G1"
      Initial Mechanical Torque required: -0.119017 PU
      Initial Field Voltage required:     1.574944 NORM

      D axis circuit parameters
```

REDUCED NETWORK

```
CASE: Test Circuit
Delt: 50.000000 us
Backplane operation set to IEEE mode

+-----------------------------------------------------------+
|                                                           |
|            S U B S Y S T E M #01                          |
|                                                           |
|                mapped to                                  |
|                                                           |
|             R T D S  R A C K #01                          |
|                                                           |
+-----------------------------------------------------------+


C O M P O N E N T   P R O C E S S O R S
----------------------------------------------------------
RISC-based MAC_V3 Machine model named: G1
   in subsystem: #1
   is assigned to RPC-GPC Card #2 Processor A

      RPC-GPC Synchronous Machine model "G1"
      Initial Mechanical Torque required: 0.147878 PU
      Initial Field Voltage required:     0.912682 NORM

      D axis circuit parameters
```

```
    -------------------------
          Stator Leakage Reactance:  Xs1= 0.010000 pu
               Stator Resistance:  Rs1= 0.003000 pu
 Field-Damper Mutual Leakage Reactance: X230= 0.000000 pu
   Unsaturated magnetizing reactance: Xmd0= 0.887900 pu
          Damper Leakage Reactance:  X3d= 0.916008 pu
               Damper Resistance:  R3d= 0.127654 pu
           Field Leakage Reactance:  X2d= 0.429644 pu
                Field resistance:  R2d= 0.000568 pu

    Q axis circuit parameters
    -------------------------
          Stator Leakage Reactance:  Xs1= 0.010000 pu
               Stator Resistance:  Rs1= 0.003000 pu
             Magnetizing Reactance:  Xmq= 0.636000 pu
        2nd Damper Leakage Reactance:  X3q= 1.910378 pu
             2nd Damper Resistance:  R3q= 0.231057 pu
       1st damper Leakage Reactance:  X2q= 2.135297 pu
            1st Damper resistance:  R2q= 0.008840 pu

RISC-based MAC_V3 Machine model named: G2
  in subsystem: #1
  is assigned to RPC-GPC Card #2 Processor B

    RPC-GPC Synchronous Machine model "G2"
    Initial Mechanical Torque required: 2.744029 PU
    Initial Field Voltage required:     4.856217 NORM

    D axis circuit parameters
    -------------------------
          Stator Leakage Reactance:  Xs1= 0.150000 pu
               Stator Resistance:  Rs1= 0.003000 pu
 Field-Damper Mutual Leakage Reactance: X230= 0.000000 pu
   Unsaturated magnetizing reactance: Xmd0= 1.660000 pu
          Damper Leakage Reactance:  X3d= 0.167955 pu
               Damper Resistance:  R3d= 0.033416 pu
           Field Leakage Reactance:  X2d= 0.168248 pu
                Field resistance:  R2d= 0.000741 pu

    Q axis circuit parameters
    -------------------------
          Stator Leakage Reactance:  Xs1= 0.150000 pu
               Stator Resistance:  Rs1= 0.003000 pu
             Magnetizing Reactance:  Xmq= 1.610000 pu
        2nd Damper Leakage Reactance:  X3q= 0.121570 pu
             2nd Damper Resistance:  R3q= 0.017117 pu
       1st damper Leakage Reactance:  X2q= 0.867163 pu
            1st Damper resistance:  R2q= 0.010148 pu

RISC-based MAC_V3 Machine model named: G3
  in subsystem: #1
  is assigned to RPC-GPC Card #3 Processor A

    RPC-GPC Synchronous Machine model "G3"
    Initial Mechanical Torque required: 2.774279 PU
    Initial Field Voltage required:     6.724356 NORM

    D axis circuit parameters
    -------------------------
          Stator Leakage Reactance:  Xs1= 0.150000 pu
               Stator Resistance:  Rs1= 0.003000 pu
 Field-Damper Mutual Leakage Reactance: X230= 0.000000 pu
   Unsaturated magnetizing reactance: Xmd0= 1.660000 pu
          Damper Leakage Reactance:  X3d= 0.166787 pu
               Damper Resistance:  R3d= 0.024890 pu
           Field Leakage Reactance:  X2d= 0.169436 pu
                Field resistance:  R2d= 0.000746 pu

    Q axis circuit parameters
    -------------------------
          Stator Leakage Reactance:  Xs1= 0.150000 pu
               Stator Resistance:  Rs1= 0.003000 pu
             Magnetizing Reactance:  Xmq= 1.610000 pu
        2nd Damper Leakage Reactance:  X3q= 0.121570 pu
             2nd Damper Resistance:  R3q= 0.017117 pu
       1st damper Leakage Reactance:  X2q= 0.867163 pu
            1st Damper resistance:  R2q= 0.010148 pu

RISC-based MAC_V3 Machine model named: G4
  in subsystem: #1
  is assigned to RPC-GPC Card #3 Processor B

    RPC-GPC Synchronous Machine model "G4"
    Initial Mechanical Torque required: 1.015611 PU
    Initial Field Voltage required:     12.646105 NORM

    D axis circuit parameters
    -------------------------
          Stator Leakage Reactance:  Xs1= 0.134000 pu
               Stator Resistance:  Rs1= 0.003000 pu
 Field-Damper Mutual Leakage Reactance: X230= 0.000000 pu
   Unsaturated magnetizing reactance: Xmd0= 2.856000 pu
          Damper Leakage Reactance:  X3d= 0.189375 pu
               Damper Resistance:  R3d= 0.033669 pu
           Field Leakage Reactance:  X2d= 0.145574 pu
                Field resistance:  R2d= 0.001234 pu

    Q axis circuit parameters
    -------------------------
          Stator Leakage Reactance:  Xs1= 0.134000 pu
               Stator Resistance:  Rs1= 0.003000 pu
             Magnetizing Reactance:  Xmq= 1.656000 pu
        2nd Damper Leakage Reactance:  X3q= 0.147000 pu
             2nd Damper Resistance:  R3q= 0.027238 pu
       1st damper Leakage Reactance:  X2q= 0.823659 pu
    -------------------------
          Stator Leakage Reactance:  Xs1= 0.010000 pu
               Stator Resistance:  Rs1= 0.003000 pu
 Field-Damper Mutual Leakage Reactance: X230= 0.000000 pu
   Unsaturated magnetizing reactance: Xmd0= 0.887900 pu
          Damper Leakage Reactance:  X3d= 0.916008 pu
               Damper Resistance:  R3d= 0.127654 pu
           Field Leakage Reactance:  X2d= 0.429644 pu
                Field resistance:  R2d= 0.000568 pu
    Q axis circuit parameters
    -------------------------
          Stator Leakage Reactance:  Xs1= 0.010000 pu
               Stator Resistance:  Rs1= 0.003000 pu
             Magnetizing Reactance:  Xmq= 0.636000 pu
        2nd Damper Leakage Reactance:  X3q= 1.910378 pu
             2nd Damper Resistance:  R3q= 0.231057 pu
       1st damper Leakage Reactance:  X2q= 2.135297 pu
            1st Damper resistance:  R2q= 0.008840 pu

RISC-based MAC_V3 Machine model named: G3
  in subsystem: #1
  is assigned to RPC-GPC Card #2 Processor B

    RPC-GPC Synchronous Machine model "G3"
    Initial Mechanical Torque required: 1.467483 PU
    Initial Field Voltage required:     3.556720 NORM

    D axis circuit parameters
    -------------------------
          Stator Leakage Reactance:  Xs1= 0.150000 pu
               Stator Resistance:  Rs1= 0.003000 pu
 Field-Damper Mutual Leakage Reactance: X230= 0.000000 pu
   Unsaturated magnetizing reactance: Xmd0= 1.660000 pu
          Damper Leakage Reactance:  X3d= 0.166787 pu
               Damper Resistance:  R3d= 0.024890 pu
           Field Leakage Reactance:  X2d= 0.169436 pu
                Field resistance:  R2d= 0.000746 pu
    Q axis circuit parameters
    -------------------------
          Stator Leakage Reactance:  Xs1= 0.150000 pu
               Stator Resistance:  Rs1= 0.003000 pu
             Magnetizing Reactance:  Xmq= 1.610000 pu
        2nd Damper Leakage Reactance:  X3q= 0.121570 pu
             2nd Damper Resistance:  R3q= 0.017117 pu
       1st damper Leakage Reactance:  X2q= 0.867163 pu
            1st Damper resistance:  R2q= 0.010148 pu
RISC-based MAC_V3 Machine model named: G4
  in subsystem: #1
  is assigned to RPC-GPC Card #3 Processor A
    RPC-GPC Synchronous Machine model "G4"
    Initial Mechanical Torque required: 0.956372 PU
    Initial Field Voltage required:     3.368801 NORM
    D axis circuit parameters
    -------------------------
          Stator Leakage Reactance:  Xs1= 0.134000 pu
               Stator Resistance:  Rs1= 0.003000 pu
 Field-Damper Mutual Leakage Reactance: X230= 0.000000 pu
   Unsaturated magnetizing reactance: Xmd0= 2.856000 pu
          Damper Leakage Reactance:  X3d= 0.189375 pu
               Damper Resistance:  R3d= 0.033669 pu
           Field Leakage Reactance:  X2d= 0.145574 pu
                Field resistance:  R2d= 0.001234 pu
    Q axis circuit parameters
    -------------------------
          Stator Leakage Reactance:  Xs1= 0.134000 pu
               Stator Resistance:  Rs1= 0.003000 pu
             Magnetizing Reactance:  Xmq= 1.656000 pu
        2nd Damper Leakage Reactance:  X3q= 0.147000 pu
             2nd Damper Resistance:  R3q= 0.027238 pu
       1st damper Leakage Reactance:  X2q= 0.823659 pu
            1st Damper resistance:  R2q= 0.009185 pu

RISC-based MAC_V3 Machine model named: G5
  in subsystem: #1
  is assigned to RPC-GPC Card #2 Processor A

    RPC-GPC Synchronous Machine model "G5"
    Initial Mechanical Torque required: 0.956377 PU
    Initial Field Voltage required:     3.362681 NORM

    D axis circuit parameters
    -------------------------
          Stator Leakage Reactance:  Xs1= 0.134000 pu
               Stator Resistance:  Rs1= 0.003000 pu
 Field-Damper Mutual Leakage Reactance: X230= 0.000000 pu
   Unsaturated magnetizing reactance: Xmd0= 2.856000 pu
          Damper Leakage Reactance:  X3d= 0.189375 pu
               Damper Resistance:  R3d= 0.033669 pu
           Field Leakage Reactance:  X2d= 0.145574 pu
                Field resistance:  R2d= 0.001234 pu

    Q axis circuit parameters
    -------------------------
          Stator Leakage Reactance:  Xs1= 0.134000 pu
               Stator Resistance:  Rs1= 0.003000 pu
             Magnetizing Reactance:  Xmq= 1.656000 pu
        2nd Damper Leakage Reactance:  X3q= 0.147000 pu
             2nd Damper Resistance:  R3q= 0.027238 pu
       1st damper Leakage Reactance:  X2q= 0.823659 pu
            1st Damper resistance:  R2q= 0.009185 pu



RISC-based UDC model pi3 named: Line1(E:\RSCAD/BIN/UDC\pi3)
  in subsystem: #1
```

```
            1st Damper resistance:  R2q= 0.009185 pu
RISC-based MAC_V3 Machine model named: G5
  in subsystem: #1
  is assigned to RPC-GPC Card #2 Processor A

    RPC-GPC Synchronous Machine model "G5"
    Initial Mechanical Torque required: 0.003960 PU
    Initial Field Voltage required:     1.289100 NORM

    D axis circuit parameters
    -------------------------
          Stator Leakage Reactance:  Xs1= 0.134000 pu
               Stator Resistance:  Rs1= 0.003000 pu
 Field-Damper Mutual Leakage Reactance: X230= 0.000000 pu
    Unsaturated magnetizing reactance: Xmd0= 2.856000 pu
          Damper Leakage Reactance:  X3d= 0.189375 pu
               Damper Resistance:  R3d= 0.033669 pu
           Field Leakage Reactance:  X2d= 0.145574 pu
                Field resistance:  R2d= 0.001234 pu

    Q axis circuit parameters
    -------------------------
          Stator Leakage Reactance:  Xs1= 0.134000 pu
               Stator Resistance:  Rs1= 0.003000 pu
             Magnetizing Reactance:  Xmq= 1.656000 pu
        2nd Damper Leakage Reactance:  X3q= 0.147000 pu
             2nd Damper Resistance:  R3q= 0.027238 pu
       1st damper Leakage Reactance:  X2q= 0.823659 pu
            1st Damper resistance:  R2q= 0.009185 pu
RISC-based UDC model pi3 named: Line1(E:\RSCAD/BIN/UDC\pi3)
  in subsystem: #1
  is assigned to RISC Card #2 Processor B
RISC-based UDC model pi3 named: Line10(E:\RSCAD/BIN/UDC\pi3)
  in subsystem: #1
  is assigned to RISC Card #3 Processor A
RISC-based UDC model pi3 named: Line11(E:\RSCAD/BIN/UDC\pi3)
  in subsystem: #1
  is assigned to RISC Card #3 Processor B
RISC-based UDC model pi3 named: Line12(E:\RSCAD/BIN/UDC\pi3)
  in subsystem: #1
  is assigned to RISC Card #2 Processor B
RISC-based UDC model pi3 named: Line13(E:\RSCAD/BIN/UDC\pi3)
  in subsystem: #1
  is assigned to RISC Card #3 Processor A
RISC-based UDC model pi3 named: Line14(E:\RSCAD/BIN/UDC\pi3)
  in subsystem: #1
  is assigned to RISC Card #3 Processor B
RISC-based UDC model pi3 named: Line15(E:\RSCAD/BIN/UDC\pi3)
  in subsystem: #1
  is assigned to RISC Card #2 Processor A
RISC-based UDC model pi3 named: Line16(E:\RSCAD/BIN/UDC\pi3)
  in subsystem: #1
  is assigned to RISC Card #2 Processor B
RISC-based UDC model pi3 named: Line17(E:\RSCAD/BIN/UDC\pi3)
  in subsystem: #1
  is assigned to RISC Card #3 Processor A
RISC-based UDC model pi3 named: Line18(E:\RSCAD/BIN/UDC\pi3)
  in subsystem: #1
  is assigned to RISC Card #3 Processor B
RISC-based UDC model pi3 named: Line19(E:\RSCAD/BIN/UDC\pi3)
  in subsystem: #1
  is assigned to RISC Card #2 Processor A
RISC-based UDC model pi3 named: Line2(E:\RSCAD/BIN/UDC\pi3)
  in subsystem: #1
  is assigned to RISC Card #2 Processor B
RISC-based UDC model pi3 named: Line20(E:\RSCAD/BIN/UDC\pi3)
  in subsystem: #1
  is assigned to RISC Card #3 Processor A
RISC-based UDC model pi3 named: Line3(E:\RSCAD/BIN/UDC\pi3)
  in subsystem: #1
  is assigned to RISC Card #3 Processor B
RISC-based UDC model pi3 named: Line4(E:\RSCAD/BIN/UDC\pi3)
  in subsystem: #1
  is assigned to RISC Card #2 Processor A
RISC-based UDC model pi3 named: Line5(E:\RSCAD/BIN/UDC\pi3)
  in subsystem: #1
  is assigned to RISC Card #2 Processor B
RISC-based UDC model pi3 named: Line6(E:\RSCAD/BIN/UDC\pi3)
  in subsystem: #1
  is assigned to RISC Card #3 Processor A
RISC-based UDC model pi3 named: Line7(E:\RSCAD/BIN/UDC\pi3)
  in subsystem: #1
  is assigned to RISC Card #3 Processor B
RISC-based UDC model pi3 named: Line8(E:\RSCAD/BIN/UDC\pi3)
  in subsystem: #1
  is assigned to RISC Card #2 Processor A
RISC-based UDC model pi3 named: Line9(E:\RSCAD/BIN/UDC\pi3)
  in subsystem: #1
  is assigned to RISC Card #2 Processor B



RISC-based UDC model RCDload1 named:
Load13(E:\RSCAD/BIN/UDC\RCDload1)
  in subsystem: #1
  is assigned to RISC Card #3 Processor A
  Dynamic load: R and C in parallel:
              Pinit = 13.500000 MW   (R=3918.518519 ohms)
              Qinit = 5.800000 MVar (C=0.348998 uF)
RISC-based UDC model RCDload1 named:
Load14(E:\RSCAD/BIN/UDC\RCDload1)
  in subsystem: #1
  is assigned to RISC Card #3 Processor B
  Dynamic load: R and C in parallel:
              Pinit = 1.000000 MW   (R=52900.000000 ohms)
  is assigned to RISC Card #2 Processor B


RISC-based UDC model pi3 named: Line10(E:\RSCAD/BIN/UDC\pi3)
  in subsystem: #1
  is assigned to RISC Card #3 Processor A


RISC-based UDC model pi3 named: Line14(E:\RSCAD/BIN/UDC\pi3)
  in subsystem: #1
  is assigned to RISC Card #2 Processor B


RISC-based UDC model pi3 named: Line15(E:\RSCAD/BIN/UDC\pi3)
  in subsystem: #1
  is assigned to RISC Card #3 Processor A


RISC-based UDC model pi3 named: Line2(E:\RSCAD/BIN/UDC\pi3)
  in subsystem: #1
  is assigned to RISC Card #2 Processor A


RISC-based UDC model pi3 named: Line5(E:\RSCAD/BIN/UDC\pi3)
  in subsystem: #1
  is assigned to RISC Card #2 Processor B


RISC-based UDC model pi3 named: Line7(E:\RSCAD/BIN/UDC\pi3)
  in subsystem: #1
  is assigned to RISC Card #3 Processor A


RISC-based UDC model pi3 named: Line8(E:\RSCAD/BIN/UDC\pi3)
  in subsystem: #1
  is assigned to RISC Card #2 Processor A


RISC-based UDC model pi3 named: Line9(E:\RSCAD/BIN/UDC\pi3)
  in subsystem: #1
  is assigned to RISC Card #2 Processor B


RISC-based UDC model pi3 named: Linenew(E:\RSCAD/BIN/UDC\pi3)
  in subsystem: #1
  is assigned to RISC Card #3 Processor A


RISC-based UDC model pi3 named: Linenew1(E:\RSCAD/BIN/UDC\pi3)
  in subsystem: #1
  is assigned to RISC Card #2 Processor A


RISC-based UDC model pi3 named: Linenew2(E:\RSCAD/BIN/UDC\pi3)
  in subsystem: #1
  is assigned to RISC Card #2 Processor B


RISC-based UDC model RCDload1 named:
Load4(E:\RSCAD/BIN/UDC\RCDload1)
  in subsystem: #1
  is assigned to RISC Card #3 Processor A

  Dynamic load: R and C in parallel:
              Pinit = 47.800000 MW   (R=1106.694561 ohms)
              Qinit = 1.000000 MVar (C=0.060172 uF)


RISC-based UDC model RCDload1 named:
Load5(E:\RSCAD/BIN/UDC\RCDload1)
  in subsystem: #1
  is assigned to RISC Card #2 Processor A

  Dynamic load: R and C in parallel:
              Pinit = 76.000000 MW   (R=696.052632 ohms)
              Qinit = 1.600000 MVar (C=0.096275 uF)
RISC-based UDC model RCDload1 named:
Load6(E:\RSCAD/BIN/UDC\RCDload1)
  in subsystem: #1
  is assigned to RISC Card #2 Processor B
  Dynamic load: R and C in parallel:
              Pinit = 11.200000 MW   (R=4723.214286 ohms)
              Qinit = 7.500000 MVar (C=0.451290 uF)
RISC-based UDC model RCDload1 named:
Load9(E:\RSCAD/BIN/UDC\RCDload1)
  in subsystem: #1
  is assigned to RISC Card #3 Processor A
  Dynamic load: R and C in parallel:
              Pinit = 1.000000 MW   (R=52900.000000 ohms)
              Qinit = 16.600000 MVar (C=0.998855 uF)
RISC-based UDC model RCDload1 named:
Loadnew(E:\RSCAD/BIN/UDC\RCDload1)
  in subsystem: #1
```

```
            Qinit = 5.000000 MVar (C=0.300860 uF)
RISC-based UDC model RCDload1 named:
Load2(E:\RSCAD/BIN/UDC\RCDload1)
  in subsystem: #1
  is assigned to RISC Card #2 Processor A
  Dynamic load: R and C in parallel:
            Pinit = 21.700000 MW   (R=2437.788018 ohms)
            Qinit = 12.700000 MVar (C=0.764184 uF)
RISC-based UDC model RCDload1 named:
Load3(E:\RSCAD/BIN/UDC\RCDload1)
  in subsystem: #1
  is assigned to RISC Card #2 Processor B
Dynamic load: R and C in parallel:
            Pinit = 94.200000 MW   (R=561.571125 ohms)
            Qinit = 19.000000 MVar (C=1.143268 uF)
RISC-based UDC model RCDload1 named:
Load4(E:\RSCAD/BIN/UDC\RCDload1)
  in subsystem: #1
  is assigned to RISC Card #3 Processor A
  Dynamic load: R and C in parallel:
            Pinit = 47.800000 MW   (R=1106.694561 ohms)
            Qinit = 1.000000 MVar (C=0.060172 uF)
RISC-based UDC model RCDload1 named:
Load5(E:\RSCAD/BIN/UDC\RCDload1)
  in subsystem: #1
  is assigned to RISC Card #3 Processor B
  Dynamic load: R and C in parallel:
            Pinit = 76.000000 MW   (R=696.052632 ohms)
            Qinit = 1.600000 MVar (C=0.096275 uF)
RISC-based UDC model RCDload1 named:
Load6(E:\RSCAD/BIN/UDC\RCDload1)
  in subsystem: #1
  is assigned to RISC Card #2 Processor A
  Dynamic load: R and C in parallel:
            Pinit = 11.200000 MW   (R=4723.214286 ohms)
            Qinit = 7.500000 MVar (C=0.451290 uF)
RISC-based UDC model RCDload1 named:
Load9(E:\RSCAD/BIN/UDC\RCDload1)
  in subsystem: #1
  is assigned to RISC Card #2 Processor B
  Dynamic load: R and C in parallel:
            Pinit = 1.000000 MW   (R=52900.000000 ohms)
            Qinit = 16.600000 MVar (C=0.998855 uF)
RISC-based MUDC model trf3p3wS named: TRF1
                        E:\RSCAD/BIN/UDC\trf1p3wl
                        E:\RSCAD/BIN/UDC\trf1p3wl
                        E:\RSCAD/BIN/UDC\trf1p3wl
  in subsystem: #1
  is assigned to RISC Card #3 Processor A
RISC-based UDC model RLDload1 named:
Load11(E:\RSCAD/BIN/UDC\RLDload1)
  in subsystem: #1
  is assigned to RISC Card #3 Processor B
  Dynamic load: R and L in parallel:
            Pinit = 3.500000 MW   (R=15114.285714 ohms)
            Qinit = 1.800000 MVar (L=93.547739 H)
RISC CONTROLS COMPONENTS(proc 1) --> RPC-GPC Card #1 Processor B
            RISC ARAMP function
            RISC sum3_B function
            RISC compareX04 function
            RISC MULTIPLICATION function
            RISC compareX04 function
            RISC MULTIPLICATION function
            RISC sum3_B function
            RISC not_cb function
            RISC DEGRAD function
            RISC time_cb function
            RISC compareX03 function
            RISC logicX01 function
            RISC compareX03 function
            RISC logicX01 function
            RISC MULTIPLICATION function
            RISC not_cb function
            RISC sum3_B function
            RISC IEEE Type 1 Governor (w=314.159265) (next 27
components)
            RISC GAIN function (* 0.0032)
            RISC Floating Point Summation - +
            RISC Lead-Lag (T1= 0.0010, T2= 0.0010, G= 5.0000)
            RISC Floating Point Summation - - +
            RISC GAIN function (* 1.0000)
            RISC Fixed Limits (UL=0.1000 LL=-1.0000)
            RISC Integrator (T= 1.0000)
            RISC Real Pole (T= 0.4000, G= 1.0000)
            RISC GAIN function (* 0.3000)
            RISC GAIN function (* 0.0000)
            RISC Real Pole (T= 9.0000, G= 1.0000)
            RISC GAIN function (* 0.4000)
            RISC Floating Point Summation + +
            RISC GAIN function (* 0.0000)
            RISC Floating Point Summation + +
            RISC Real Pole (T= 0.5000, G= 1.0000)
            RISC GAIN function (* 0.3000)
            RISC Floating Point Summation + +
            RISC GAIN function (* 0.0000)
            RISC Floating Point Summation + +
            RISC Real Pole (T= 0.0, G= 1.0000)
            RISC GAIN function (* 0.0000)
            RISC Floating Point Summation + +
            RISC GAIN function (* 0.0000)
            RISC Floating Point Summation + +
            RISC X/Y Function (dbz)
            RISC X/Y Function (dbz)
            RISC IEE2ST Type Stabilizer (w=314.159265) (next 14
components)
  is assigned to RISC Card #2 Processor A
  Dynamic load: R and C in parallel:
            Pinit = 47.000000 MW   (R=1125.531915 ohms)
            Qinit = 20.000000 MVar (C=1.203440 uF)
RISC-based UDC model RCDload1 named:
Loadnew1(E:\RSCAD/BIN/UDC\RCDload1)
  in subsystem: #1
  is assigned to RISC Card #2 Processor B
  Dynamic load: R and C in parallel:
            Pinit = 91.000000 MW   (R=581.318681 ohms)
            Qinit = 45.410000 MVar (C=2.732411 uF)
RISC-based MUDC model trf3p3wS named: TRF1
                        E:\RSCAD/BIN/UDC\trf1p3wl
                        E:\RSCAD/BIN/UDC\trf1p3wl
                        E:\RSCAD/BIN/UDC\trf1p3wl
  in subsystem: #1
  is assigned to RISC Card #3 Processor A
RISC CONTROLS COMPONENTS(proc 1) --> RPC-GPC Card #1 Processor A
            RISC ARAMP function
            RISC sum3_B function
            RISC compareX04 function
            RISC MULTIPLICATION function
            RISC compareX04 function
            RISC MULTIPLICATION function
            RISC sum3_B function
            RISC not_cb function
            RISC DEGRAD function
            RISC time_cb function
            RISC compareX03 function
            RISC logicX01 function
            RISC compareX03 function
            RISC logicX01 function
            RISC MULTIPLICATION function
            RISC not_cb function
            RISC sum3_B function
            RISC sine_cb function
            RISC IEE2ST Type Stabilizer (w=314.159265) (next 14
components)
            RISC GAIN function (* 0.0032)
            RISC Floating Point Summation - +
            RISC Real Pole (T= 0.0, G= 9.5000)
            RISC GAIN function (* 0.0016)
            RISC Real Pole (T= 0.0, G= 0.0000)
            RISC Floating Point Summation + +
            RISC Wash Out (T= 1.4100, G= 1.0000)
            RISC Lead-Lag (T1= 0.1540, T2= 0.0330, G= 1.0000)
            RISC Lead-Lag (T1= 0.0000, T2= 0.0010, G= 1.0000)
            RISC Lead-Lag (T1= 0.0000, T2= 0.0010, G= 1.0000)
            RISC Fixed Limits (UL=0.2000 LL=-0.2000)
            RISC GAIN function (* 1.0000)
            RISC MULTIPLICATION function
            RISC IEEE Type 1 Governor (w=314.159265) (next 27
components)
            RISC GAIN function (* 0.0032)
            RISC Floating Point Summation - +
            RISC Lead-Lag (T1= 0.0010, T2= 0.0010, G= 5.0000)
            RISC Floating Point Summation - - +
            RISC GAIN function (* 1.0000)
            RISC Fixed Limits (UL=0.1000 LL=-1.0000)
            RISC Integrator (T= 1.0000)
            RISC Real Pole (T= 0.4000, G= 1.0000)
            RISC GAIN function (* 0.3000)
            RISC GAIN function (* 0.0000)
            RISC Real Pole (T= 9.0000, G= 1.0000)
            RISC GAIN function (* 0.4000)
            RISC Floating Point Summation + +
            RISC GAIN function (* 0.0000)
            RISC Floating Point Summation + +
            RISC Real Pole (T= 0.5000, G= 1.0000)
            RISC GAIN function (* 0.3000)
            RISC Floating Point Summation + +
            RISC GAIN function (* 0.0000)
            RISC Floating Point Summation + +
            RISC Real Pole (T= 0.0, G= 1.0000)
            RISC GAIN function (* 0.0000)
            RISC Floating Point Summation + +
            RISC GAIN function (* 0.0000)
            RISC Floating Point Summation + +
            RISC X/Y Function (dbz)
            RISC X/Y Function (dbz)
            RISC IEEE Type AC4 Excitation System (next 9 components)
            RISC Real Pole (T= 0.0150, G= 1.0000)
            RISC Floating Point Summation - + +
            RISC Fixed Limits (UL=40.0000 LL=-40.0000)
            RISC Lead-Lag (T1= 1.0000, T2= 1.0000, G= 1.0000)
            RISC Real Pole (T= 0.0, G= 200.0000)
            RISC GAIN function (* 0.0000)
            RISC Floating Point Summation - +
            RISC Floating Point Summation - +
            RISC Dynamic Limits
            RISC IEEE Type 1 Governor (w=314.159265) (next 27
components)
            RISC GAIN function (* 0.0032)
            RISC Floating Point Summation - +
            RISC Lead-Lag (T1= 0.0010, T2= 0.0010, G= 5.0000)
            RISC Floating Point Summation - - +
            RISC GAIN function (* 1.0000)
            RISC Fixed Limits (UL=0.1000 LL=-1.0000)
            RISC Integrator (T= 1.0000)
            RISC Real Pole (T= 0.4000, G= 1.0000)
            RISC GAIN function (* 0.3000)
            RISC GAIN function (* 0.0000)
            RISC Real Pole (T= 9.0000, G= 1.0000)
            RISC GAIN function (* 0.4000)
            RISC Floating Point Summation + +
```

RISC GAIN function (* 0.0032)
RISC Floating Point Summation - +
RISC Real Pole (T= 0.0, G= 9.5000)
RISC GAIN function (* 0.0016)
RISC Real Pole (T= 0.0, G= 0.0000)
RISC Floating Point Summation + +
RISC Wash Out (T= 1.4100, G= 1.0000)
RISC Lead-Lag (T1= 0.1540, T2= 0.0330, G= 1.0000)
RISC Lead-Lag (T1= 0.0000, T2= 0.0010, G= 1.0000)
RISC Lead-Lag (T1= 0.0000, T2= 0.0010, G= 1.0000)
RISC Fixed Limits (UL=0.2000 LL=-0.2000)
RISC GAIN function (* 1.0000)
RISC MULTIPLICATION function
RISC IEEE Type AC4 Excitation System (next 9 components)
RISC Real Pole (T= 0.0150, G= 1.0000)
RISC Floating Point Summation - + +
RISC Fixed Limits (UL=40.0000 LL=-40.0000)
RISC Lead-Lag (T1= 1.0000, T2= 1.0000, G= 1.0000)
RISC Real Pole (T= 0.0, G= 200.0000)
RISC GAIN function (* 0.0000)
RISC Floating Point Summation - +
RISC Floating Point Summation - +
RISC Dynamic Limits
RISC IEEE Type 1 Governor (w=314.159265) (next 27 components)
RISC GAIN function (* 0.0032)
RISC Floating Point Summation - +
RISC Lead-Lag (T1= 0.0010, T2= 0.0010, G= 5.0000)
RISC Floating Point Summation - - +
RISC GAIN function (* 1.0000)
RISC Fixed Limits (UL=0.1000 LL=-1.0000)
RISC Integrator (T= 1.0000)
RISC Real Pole (T= 0.4000, G= 1.0000)
RISC GAIN function (* 0.3000)
RISC GAIN function (* 0.0000)
RISC Real Pole (T= 9.0000, G= 1.0000)
RISC GAIN function (* 0.4000)
RISC Floating Point Summation + +
RISC GAIN function (* 0.0000)
RISC Floating Point Summation + +
RISC Real Pole (T= 0.5000, G= 1.0000)
RISC GAIN function (* 0.3000)
RISC Floating Point Summation + +
RISC GAIN function (* 0.0000)
RISC Floating Point Summation + +
RISC Real Pole (T= 0.0, G= 1.0000)
RISC GAIN function (* 0.0000)
RISC Floating Point Summation + +
RISC GAIN function (* 0.0000)
RISC Floating Point Summation + +
RISC X/Y Function (dbz)
RISC X/Y Function (dbz)
RISC IEE2ST Type Stabilizer (w=314.159265) (next 14 components)
RISC GAIN function (* 0.0032)
RISC Floating Point Summation - +
RISC Real Pole (T= 0.0, G= 9.5000)
RISC GAIN function (* 0.0200)
RISC Real Pole (T= 0.0, G= 0.0000)
RISC Floating Point Summation + +
RISC Wash Out (T= 1.4100, G= 1.0000)
RISC Lead-Lag (T1= 0.1540, T2= 0.0330, G= 1.0000)
RISC Lead-Lag (T1= 0.0000, T2= 0.0010, G= 1.0000)
RISC Lead-Lag (T1= 0.0000, T2= 0.0010, G= 1.0000)
RISC Fixed Limits (UL=0.2000 LL=-0.2000)
RISC GAIN function (* 1.0000)
RISC MULTIPLICATION function
RISC IEEE Type AC4 Excitation System (next 9 components)
RISC Real Pole (T= 0.0150, G= 1.0000)
RISC Floating Point Summation - + +
RISC Fixed Limits (UL=40.0000 LL=-40.0000)
RISC Lead-Lag (T1= 1.0000, T2= 1.0000, G= 1.0000)
RISC Real Pole (T= 0.0, G= 200.0000)
RISC GAIN function (* 0.0000)
RISC Floating Point Summation - +
RISC Floating Point Summation - +
RISC Dynamic Limits
RISC IEEE Type 1 Governor (w=314.159265) (next 27 components)
RISC GAIN function (* 0.0032)
RISC Floating Point Summation - +
RISC Lead-Lag (T1= 0.0010, T2= 0.0010, G= 5.0000)
RISC Floating Point Summation - - +
RISC GAIN function (* 1.0000)
RISC Fixed Limits (UL=0.1000 LL=-1.0000)
RISC Integrator (T= 1.0000)
RISC Real Pole (T= 0.4000, G= 1.0000)
RISC GAIN function (* 0.3000)
RISC GAIN function (* 0.0000)
RISC Real Pole (T= 9.0000, G= 1.0000)
RISC GAIN function (* 0.4000)
RISC Floating Point Summation + +
RISC GAIN function (* 0.0000)
RISC Floating Point Summation + +
RISC Real Pole (T= 0.5000, G= 1.0000)
RISC GAIN function (* 0.3000)
RISC Floating Point Summation + +
RISC GAIN function (* 0.0000)
RISC Floating Point Summation + +
RISC Real Pole (T= 0.0, G= 1.0000)
RISC GAIN function (* 0.0000)
RISC Floating Point Summation + +
RISC GAIN function (* 0.0000)
RISC Floating Point Summation + +
RISC X/Y Function (dbz)
RISC X/Y Function (dbz)
RISC IEE2ST Type Stabilizer (w=314.159265) (next 14 components)
RISC GAIN function (* 0.0032)
RISC Floating Point Summation - +
RISC Real Pole (T= 0.0, G= 9.5000)
RISC GAIN function (* 0.0400)
RISC Real Pole (T= 0.0, G= 0.0000)
RISC Floating Point Summation + +
RISC Wash Out (T= 1.4100, G= 1.0000)
RISC Lead-Lag (T1= 0.1540, T2= 0.0330, G= 1.0000)
RISC Lead-Lag (T1= 0.0000, T2= 0.0010, G= 1.0000)
RISC Lead-Lag (T1= 0.0000, T2= 0.0010, G= 1.0000)
RISC Fixed Limits (UL=0.2000 LL=-0.2000)
RISC GAIN function (* 1.0000)
RISC MULTIPLICATION function
RISC IEEE Type AC4 Excitation System (next 9 components)
RISC Real Pole (T= 0.0150, G= 1.0000)
RISC Floating Point Summation - + +
RISC Fixed Limits (UL=20.0000 LL=-20.0000)
RISC Lead-Lag (T1= 1.0000, T2= 1.0000, G= 1.0000)
RISC Real Pole (T= 0.0, G= 300.0000)
RISC GAIN function (* 0.0000)
RISC Floating Point Summation - +
RISC Floating Point Summation - +
RISC Dynamic Limits
RISC IEEE Type 1 Governor (w=314.159265) (next 27 components)
RISC GAIN function (* 0.0032)
RISC Floating Point Summation - +
RISC Lead-Lag (T1= 0.0010, T2= 0.0010, G= 5.0000)
RISC Floating Point Summation - - +
RISC GAIN function (* 1.0000)
RISC Fixed Limits (UL=0.1000 LL=-1.0000)
RISC Integrator (T= 1.0000)
RISC Real Pole (T= 0.4000, G= 1.0000)
RISC GAIN function (* 0.3000)
RISC GAIN function (* 0.0000)
RISC Real Pole (T= 9.0000, G= 1.0000)
RISC GAIN function (* 0.4000)
RISC Floating Point Summation + +
RISC GAIN function (* 0.0000)
RISC Floating Point Summation + +
RISC Real Pole (T= 0.5000, G= 1.0000)
RISC GAIN function (* 0.3000)
RISC Floating Point Summation + +
RISC GAIN function (* 0.0000)
RISC Floating Point Summation + +
RISC Real Pole (T= 0.0, G= 1.0000)
RISC GAIN function (* 0.0000)
RISC Floating Point Summation + +
RISC GAIN function (* 0.0000)
RISC Floating Point Summation + +
RISC X/Y Function (dbz)
RISC X/Y Function (dbz)
RISC IEE2ST Type Stabilizer (w=314.159265) (next 15 components)
RISC GAIN function (* 0.0032)
RISC Floating Point Summation - +
RISC Real Pole (T= 0.0, G= 9.5000)
RISC GAIN function (* 0.0200)
RISC Real Pole (T= 0.0, G= 0.0000)
RISC Floating Point Summation + +
RISC Wash Out (T= 1.4100, G= 1.0000)
RISC Lead-Lag (T1= 0.1540, T2= 0.0330, G= 1.0000)
RISC Lead-Lag (T1= 0.0000, T2= 0.0010, G= 1.0000)
RISC Lead-Lag (T1= 0.0000, T2= 0.0010, G= 1.0000)
RISC Fixed Limits (UL=0.2000 LL=-0.2000)
RISC GAIN function (* 1.0000)
RISC MULTIPLICATION function
RISC IEEE Type AC4 Excitation System (next 9 components)
RISC Real Pole (T= 0.0150, G= 1.0000)
RISC Floating Point Summation - + +
RISC Fixed Limits (UL=40.0000 LL=-40.0000)
RISC Lead-Lag (T1= 1.0000, T2= 1.0000, G= 1.0000)
RISC Real Pole (T= 0.0, G= 200.0000)
RISC GAIN function (* 0.0000)
RISC Floating Point Summation - +
RISC Floating Point Summation - +
RISC Dynamic Limits
RISC IEE2ST Type Stabilizer (w=314.159265) (next 14 components)
RISC GAIN function (* 0.0032)
RISC Floating Point Summation - +
RISC Real Pole (T= 0.0, G= 9.5000)
RISC GAIN function (* 0.0400)
RISC Real Pole (T= 0.0, G= 0.0000)
RISC Floating Point Summation + +
RISC Wash Out (T= 1.4100, G= 1.0000)
RISC Lead-Lag (T1= 0.1540, T2= 0.0330, G= 1.0000)
RISC Lead-Lag (T1= 0.0000, T2= 0.0010, G= 1.0000)
RISC Lead-Lag (T1= 0.0000, T2= 0.0010, G= 1.0000)

RISC X/Y Function (dbz)
RISC IEE2ST Type Stabilizer (w=314.159265) (next 14 components)
RISC GAIN function (* 0.0032)
RISC Floating Point Summation - +
RISC Real Pole (T= 0.0, G= 9.5000)
RISC GAIN function (* 0.0200)
RISC Real Pole (T= 0.0, G= 0.0000)
RISC Floating Point Summation + +
RISC Wash Out (T= 1.4100, G= 1.0000)
RISC Lead-Lag (T1= 0.1540, T2= 0.0330, G= 1.0000)
RISC Lead-Lag (T1= 0.0000, T2= 0.0010, G= 1.0000)
RISC Lead-Lag (T1= 0.0000, T2= 0.0010, G= 1.0000)
RISC Fixed Limits (UL=0.2000 LL=-0.2000)
RISC GAIN function (* 1.0000)
RISC MULTIPLICATION function
RISC IEEE Type AC4 Excitation System (next 9 components)
RISC Real Pole (T= 0.0150, G= 1.0000)
RISC Floating Point Summation - + +
RISC Fixed Limits (UL=40.0000 LL=-40.0000)
RISC Lead-Lag (T1= 1.0000, T2= 1.0000, G= 1.0000)
RISC Real Pole (T= 0.0, G= 200.0000)
RISC GAIN function (* 0.0000)
RISC Floating Point Summation - +
RISC Floating Point Summation - +
RISC Dynamic Limits
RISC IEE2ST Type Stabilizer (w=314.159265) (next 14 components)
RISC GAIN function (* 0.0032)
RISC Floating Point Summation - +
RISC Real Pole (T= 0.0, G= 9.5000)
RISC GAIN function (* 0.0400)
RISC Real Pole (T= 0.0, G= 0.0000)
RISC Floating Point Summation + +
RISC Wash Out (T= 1.4100, G= 1.0000)
RISC Lead-Lag (T1= 0.1540, T2= 0.0330, G= 1.0000)
RISC Lead-Lag (T1= 0.0000, T2= 0.0010, G= 1.0000)
RISC Lead-Lag (T1= 0.0000, T2= 0.0010, G= 1.0000)
RISC Fixed Limits (UL=0.2000 LL=-0.2000)
RISC GAIN function (* 1.0000)
RISC MULTIPLICATION function
RISC IEEE Type AC4 Excitation System (next 9 components)
RISC Real Pole (T= 0.0150, G= 1.0000)
RISC Floating Point Summation - + +
RISC Fixed Limits (UL=20.0000 LL=-20.0000)
RISC Lead-Lag (T1= 1.0000, T2= 1.0000, G= 1.0000)
RISC Real Pole (T= 0.0, G= 300.0000)
RISC GAIN function (* 0.0000)
RISC Floating Point Summation - +
RISC Floating Point Summation - +
RISC Dynamic Limits
RISC IEEE Type 1 Governor (w=314.159265) (next 27 components)
RISC GAIN function (* 0.0032)
RISC Floating Point Summation - +
RISC Lead-Lag (T1= 0.0010, T2= 0.0010, G= 5.0000)
RISC Floating Point Summation - - +
RISC GAIN function (* 1.0000)
RISC Fixed Limits (UL=0.1000 LL=-1.0000)
RISC Integrator (T= 1.0000)
RISC Real Pole (T= 0.4000, G= 1.0000)
RISC GAIN function (* 0.3000)
RISC GAIN function (* 0.0000)
RISC Real Pole (T= 9.0000, G= 1.0000)
RISC GAIN function (* 0.4000)
RISC Floating Point Summation + +
RISC GAIN function (* 0.0000)
RISC Floating Point Summation + +
RISC Real Pole (T= 0.5000, G= 1.0000)
RISC GAIN function (* 0.3000)
RISC Floating Point Summation + +
RISC GAIN function (* 0.0000)
RISC Floating Point Summation + +
RISC Real Pole (T= 0.0, G= 1.0000)
RISC GAIN function (* 0.0000)
RISC Floating Point Summation + +
RISC GAIN function (* 0.0000)
RISC Floating Point Summation + +
RISC X/Y Function (dbz)
RISC X/Y Function (dbz)
RISC IEE2ST Type Stabilizer (w=314.159265) (next 15 components)
RISC GAIN function (* 0.0032)
RISC Floating Point Summation - +
RISC Real Pole (T= 0.0, G= 9.5000)
RISC GAIN function (* 0.0400)
RISC Real Pole (T= 0.0, G= 0.0000)
RISC Floating Point Summation + +
RISC Wash Out (T= 1.4100, G= 1.0000)
RISC Lead-Lag (T1= 0.1540, T2= 0.0330, G= 1.0000)
RISC Lead-Lag (T1= 0.0000, T2= 0.0010, G= 1.0000)
RISC Lead-Lag (T1= 0.0000, T2= 0.0010, G= 1.0000)
RISC Fixed Limits (UL=0.2000 LL=-0.2000)
RISC GAIN function (* 1.0000)
RISC MULTIPLICATION function
RISC IEEE Type AC4 Excitation System (next 9 components)
RISC Real Pole (T= 0.0150, G= 1.0000)
RISC Floating Point Summation - + +
RISC Fixed Limits (UL=20.0000 LL=-20.0000)
RISC Lead-Lag (T1= 1.0000, T2= 1.0000, G= 1.0000)
RISC Real Pole (T= 0.0, G= 300.0000)
RISC GAIN function (* 0.0000)
RISC Floating Point Summation - +
RISC Floating Point Summation - +
RISC Dynamic Limits
RISC Fixed Limits (UL=0.2000 LL=-0.2000)
RISC GAIN function (* 1.0000)
RISC MULTIPLICATION function
RISC IEEE Type AC4 Excitation System (next 9 components)
RISC Real Pole (T= 0.0150, G= 1.0000)
RISC Floating Point Summation - + +
RISC Fixed Limits (UL=20.0000 LL=-20.0000)
RISC Lead-Lag (T1= 1.0000, T2= 1.0000, G= 1.0000)
RISC Real Pole (T= 0.0, G= 300.0000)
RISC GAIN function (* 0.0000)
RISC Floating Point Summation - +
RISC Floating Point Summation - +
RISC Dynamic Limits
RISC IEEE Type 1 Governor (w=314.159265) (next 27 components)
RISC GAIN function (* 0.0032)
RISC Floating Point Summation - +
RISC Lead-Lag (T1= 0.0010, T2= 0.0010, G= 5.0000)
RISC Floating Point Summation - - +
RISC GAIN function (* 1.0000)
RISC Fixed Limits (UL=0.1000 LL=-1.0000)
RISC Integrator (T= 1.0000)
RISC Real Pole (T= 0.4000, G= 1.0000)
RISC GAIN function (* 0.3000)
RISC GAIN function (* 0.0000)
RISC Real Pole (T= 9.0000, G= 1.0000)
RISC GAIN function (* 0.4000)
RISC Floating Point Summation + +
RISC GAIN function (* 0.0000)
RISC Floating Point Summation + +
RISC Real Pole (T= 0.5000, G= 1.0000)
RISC GAIN function (* 0.3000)
RISC Floating Point Summation + +
RISC GAIN function (* 0.0000)
RISC Floating Point Summation + +
RISC Real Pole (T= 0.0, G= 1.0000)
RISC GAIN function (* 0.0000)
RISC Floating Point Summation + +
RISC GAIN function (* 0.0000)
RISC Floating Point Summation + +
RISC X/Y Function (dbz)
RISC X/Y Function (dbz)

RISC-based Network Solution for Subsystem #1 uses -->
RPC-GPC Card #1 Processor B
Network Solution Statistics for 1B:
Number of nodes on this processor: 33
Number of G values passed to this proc: 18
Number of matrix pointers passed to this proc: 0
Number of columns dynamically decomposed by this proc: 27
Number of multiply-subtract operations
for dynamic decomposition on this proc: 667
Number of clocks pre-T0: 1381
(time = 1.381000e+000 uSec.)
Number of clocks in main: 10040
(decomposition: 5429)
(forward-backward: 3615)
(time = 1.004000e+001 uSec.)
The fill of the decomposed lower matrix is: 239 of 561 locations.
Hidden T2 Transfer List

BP_Address	Signal_Type	Signal_name
0x195	named_signal_prc	Te_pu1
0x196	named_signal_prc	Pmac1
0x197	named_signal_prc	Qmac1
0x198	named_signal_prc	RMechAng1
0x199	named_signal_prc	Te_pu3
0x19A	named_signal_prc	Pmac3
0x19B	named_signal_prc	Qmac3
0x19C	named_signal_prc	RMechAng3
0x19D	named_signal_prc	Te_pu4
0x19E	named_signal_prc	Pmac4
0x19F	named_signal_prc	Qmac4
0x1A0	named_signal_prc	RMechAng4
0x1A1	named_signal_prc	Te_pu5
0x1A2	named_signal_prc	Pmac5
0x1A3	named_signal_prc	Qmac5
0x1A4	named_signal_prc	Iag
0x1A5	named_signal_prc	Ibg
0x1A6	named_signal_prc	IBRK1A
0x1A7	named_signal_prc	IBRK1B
0x1A8	named_signal_prc	IBRK1C
0x1A9	named_signal_prc	IBRK2A
0x1AA	named_signal_prc	IBRK2B
0x1AB	named_signal_prc	IBRK2C
0x1AC	named_signal_prc	Icg
0x1AD	named_signal_prc	RawDelta5
0x1AE	named_signal_prc	Delta5
0x1AF	named_signal_prc	pss_monR

T I M E - S T E P I N F O R M A T I O N
S U B S Y S T E M 1
==
Backplane Communication Speed = 60.000000 ns
T0 communication time 5.7600 us
T2 communication time 5.2200 us
Minimum time-step 12.9800 us
Common Current Injections: 0(local) + 0(xrack)

```
                RISC IEEE Type 1 Governor (w=314.159265) (next 27
components)
                RISC GAIN function (* 0.0032)
                RISC Floating Point Summation - +
                RISC Lead-Lag (T1= 0.0010, T2= 0.0010, G= 5.0000)
                RISC Floating Point Summation - - +
                RISC GAIN function (* 1.0000)
                RISC Fixed Limits (UL=0.1000 LL=-1.0000)
                RISC Integrator (T= 1.0000)
                RISC Real Pole (T= 0.4000, G= 1.0000)
                RISC GAIN function (* 0.3000)
                RISC GAIN function (* 0.0000)
                RISC Real Pole (T= 9.0000, G= 1.0000)
                RISC GAIN function (* 0.4000)
                RISC Floating Point Summation + +
                RISC GAIN function (* 0.0000)
                RISC Floating Point Summation + +
                RISC Real Pole (T= 0.5000, G= 1.0000)
                RISC GAIN function (* 0.3000)
                RISC Floating Point Summation + +
                RISC GAIN function (* 0.0000)
                RISC Floating Point Summation + +
                RISC Real Pole (T= 0.0, G= 1.0000)
                RISC GAIN function (* 0.0000)
                RISC Floating Point Summation + +
                RISC GAIN function (* 0.0000)
                RISC Floating Point Summation + +
                RISC X/Y Function (dbz)
                RISC X/Y Function (dbz)

RISC-based Network Solution for Subsystem #1 uses -->
             RPC-GPC Card #1 Processor A
  Network Solution Statistics for 1A:
    Number of nodes on this processor: 48
    Number of G values passed to this proc: 27
    Number of matrix pointers passed to this proc: 0
    Number of columns dynamically decomposed by this proc: 36
    Number of multiply-subtract operations
       for dynamic decomposition on this proc: 902
    Number of clocks pre-T0:      1610
         ( time = 1.610000e+000 uSec. )
    Number of clocks in main:     14032
           ( decomposition:     7287 )
           ( forward-backward:  5348 )
         ( time = 1.403200e+001 uSec. )
    The fill of the decomposed lower matrix is: 355 of 1176 locations.
    Hidden T2 Transfer List
---------------------------------
BP_Address  Signal_Type      Signal_name
0x1D6       named_signal_prc  Te_pu1
0x1D7       named_signal_prc  Pmac1
0x1D8       named_signal_prc  Qmac1
0x1D9       named_signal_prc  RMechAng1
0x1DA       named_signal_prc  Te_pu2
0x1DB       named_signal_prc  Pmac2
0x1DC       named_signal_prc  Qmac2
0x1DD       named_signal_prc  RMechAng2
0x1DE       named_signal_prc  Te_pu3
0x1DF       named_signal_prc  Pmac3
0x1E0       named_signal_prc  Qmac3
0x1E1       named_signal_prc  RMechAng3
0x1E2       named_signal_prc  Te_pu4
0x1E3       named_signal_prc  Pmac4
0x1E4       named_signal_prc  Qmac4
0x1E5       named_signal_prc  RMechAng4
0x1E6       named_signal_prc  Te_pu5
0x1E7       named_signal_prc  Pmac5
0x1E8       named_signal_prc  Qmac5
0x1E9       named_signal_prc  Iag
0x1EA       named_signal_prc  Ibg
0x1EB       named_signal_prc  IBRK1A
0x1EC       named_signal_prc  IBRK1B
0x1ED       named_signal_prc  IBRK1C
0x1EE       named_signal_prc  IBRK2A
0x1EF       named_signal_prc  IBRK2B
0x1F0       named_signal_prc  IBRK2C
0x1F1       named_signal_prc  Icg
0x1F2       named_signal_prc  RawDelta5
0x1F3       named_signal_prc  Delta5
0x1F4       named_signal_prc  pss_monR

     T I M E - S T E P   I N F O R M A T I O N
           S U B S Y S T E M   1
 ============================================================
  Backplane Communication Speed = 60.000000 ns
  T0 communication time 8.4600 us
  T2 communication time 6.6600 us
  Minimum time-step 17.1200 us
                Common Current Injections: 0(local) + 0(xrack)
```

APPENDIX H: MATLAB CODE TO GENERATE BAR GRAPH FOR NUMBER OF PUBLICATIONS USED IN THESIS

H .1: Matlab code to generate bar graph to represent the number of publications versus year used in thesis

H .1: Matlab code to generate bar graph to represent the number of publications versus year used in thesis

```
function Number_of_Publications_versus_year(Number_of_Publications)
figure1 = figure;
% Create axes
axes1 = axes('Parent',figure1);
% Uncomment the following line to preserve the X-limits of the axes
xlim(axes1,[0 47]);
% Uncomment the following line to preserve the Y-limits of the axes
ylim(axes1,[0 14]);
%box(axes1,'on');
hold(axes1,'all');
Number_of_Publications=[1  1   2   2   1   2   1   5   2   3  4   3   3   9
9    4   4   4   3   1   8   4   4   4   4  7  5  7  6   5  9  3  3  4  4
6  7  8  6  3  12  9  12  12  3  3];
% Create bar
bar(Number_of_Publications);

% Create title
title('Number of Publications versus Year','FontSize',20);

% Create xlabel
xlabel('Year','FontSize',20);

% Create ylabel
ylabel(' Number of Publications','FontSize',20);

% Create text
text('Parent',axes1,'String','1968','Rotation',90,'Position',[1 1.1 0]);

% Create text
text('Parent',axes1,'String','1969','Rotation',90,'Position',[2 1.1 0]);

% Create text
text('Parent',axes1,'String','1970','Rotation',90,'Position',[3 2.1 0]);

% Create text
text('Parent',axes1,'String','1971','Rotation',90,'Position',[4 2.1 0]);

% Create text
text('Parent',axes1,'String','1972','Rotation',90,'Position',[5 1.1 0]);

% Create text
text('Parent',axes1,'String','1973','Rotation',90,'Position',[6 2.1 0]);

% Create text
text('Parent',axes1,'String','1974','Rotation',90,'Position',[7 1.1 0]);

% Create text
text('Parent',axes1,'String','1975','Rotation',90,'Position',[8 5.1 0]);

% Create text
text('Parent',axes1,'String','1976','Rotation',90,'Position',[9 2.1 0]);

% Create text
text('Parent',axes1,'String','1977','Rotation',90,'Position',[10 3.1 0]);

% Create text
```

```
text('Parent',axes1,'String','1978','Rotation',90,'Position',[11 4.1 0]);

% Create text
text('Parent',axes1,'String','1979','Rotation',90,'Position',[12 3.1 0]);

% Create text
text('Parent',axes1,'String','1980','Rotation',90,'Position',[13 3.1 0]);

% Create text
text('Parent',axes1,'String','1981','Rotation',90,'Position',[14 9.1 0]);

% Create text
text('Parent',axes1,'String','1982','Rotation',90,'Position',[15 9.1 0]);

% Create text
text('Parent',axes1,'String','1983','Rotation',90,'Position',[16 4.1 0]);

% Create text
text('Parent',axes1,'String','1984','Rotation',90,'Position',[17 4.1 0]);

% Create text
text('Parent',axes1,'String','1985','Rotation',90,'Position',[18 4.1 0]);

% Create text
text('Parent',axes1,'String','1986','Rotation',90,'Position',[19 3.1 0]);

% Create text
text('Parent',axes1,'String','1987','Rotation',90,'Position',[20 1.1 0]);

% Create text
text('Parent',axes1,'String','1988','Rotation',90,'Position',[21 8.1 0]);

% Create text
text('Parent',axes1,'String','1989','Rotation',90,'Position',[22 4.1 0]);

% Create text
text('Parent',axes1,'String','1990','Rotation',90,'Position',[23 4.1 0]);

% Create text
text('Parent',axes1,'String','1991','Rotation',90,'Position',[24 4.1 0]);

% Create text
text('Parent',axes1,'String','1992','Rotation',90,'Position',[25 4.1 0]);

% Create text
text('Parent',axes1,'String','1993','Rotation',90,'Position',[26 7.1 0]);

% Create text
text('Parent',axes1,'String','1994','Rotation',90,'Position',[27 5.1 0]);

% Create text
text('Parent',axes1,'String','1995','Rotation',90,'Position',[28 7.1 0]);

% Create text
text('Parent',axes1,'String','1996','Rotation',90,'Position',[29 6.1 0]);

% Create text
text('Parent',axes1,'String','1997','Rotation',90,'Position',[30 5.1 0]);

% Create text
```

```
text('Parent',axes1,'String','1998','Rotation',90,'Position',[31 9.1 0]);

% Create text
text('Parent',axes1,'String','1999','Rotation',90,'Position',[32 3.1 0]);

% Create text
text('Parent',axes1,'String','2000','Rotation',90,'Position',[33 3.1 0]);

% Create text
text('Parent',axes1,'String','2001','Rotation',90,'Position',[34 4.1 0]);

% Create text
text('Parent',axes1,'String','2002','Rotation',90,'Position',[35 4 0]);

% Create text
text('Parent',axes1,'String','2003','Rotation',90,'Position',[36 6.1 0]);

% Create text
text('Parent',axes1,'String','2004','Rotation',90,'Position',[37 7.1 0]);

% Create text
text('Parent',axes1,'String','2005','Rotation',90,'Position',[38 8.1 0]);

% Create text
text('Parent',axes1,'String','2006','Rotation',90,'Position',[39 6.1 0]);

% Create text
text('Parent',axes1,'String','2007','Rotation',90,'Position',[40 3.1 0]);

% Create text
text('Parent',axes1,'String','2008','Rotation',90,'Position',[41 12.1 0]);

% Create text
text('Parent',axes1,'String','2009','Rotation',90,'Position',[42 9.1 0]);

% Create text
text('Parent',axes1,'String','2010','Rotation',90,'Position',[43 12.1 0]);

% Create text
text('Parent',axes1,'String','2011','Rotation',90,'Position',[44 12.1 0]);

% Create text
text('Parent',axes1,'String','2012','Rotation',90,'Position',[45 3.1 0]);

% Create text
text('Parent',axes1,'String','2013','Rotation',90,'Position',[46 3.1 0]);
```